Winter 12-15-2016

Novel regulation of the nonsense-mediated RNA decay pathway

Andrew Keith Nickless
Washington University in St. Louis

WASHINGTON UNIVERSITY IN ST. LOUIS

Division of Biology and Biomedical Sciences
Molecular Genetics and Genomics

Dissertation Examination Committee:
Zhongsheng You, Chairperson
Sergej Djuranovic
Joseph Dougherty
Qin Liu
Barry Sleckman
Jason Weber

Novel Regulation of the Nonsense-Mediated RNA Decay Pathway

by
Andrew Nickless

A dissertation presented to
The Graduate School
of Washington University in
partial fulfillment of the
requirements for the degree
of Doctor of Philosophy

December 2016
St. Louis, Missouri

Table of Contents

List of Figures

Chapter 1: Introduction

Chapter 2: Regulation of NMD by intracellular calcium

Chapter 3: Regulation of NMD by persistent DNA damage

Chapter 4: Conclusion and future directions

List of Tables

List of Abbreviations

AS, alternative splicing

ARE, AU-rich element

CBC, cap binding complex

CBG, click beetle green

CBR, click beetle red

CG, cardiac glycoside

CPT, camptothecin

DDR, DNA damage response

DMEM, Dulbecco's Modified Eagle's Medium

eIF2α, eukaryotic translation initiation factor 2 alpha

ER, endoplasmic reticulum

EJC, exon-junction complex

ESC, embryonic stem cell

FBS, fetile bovine serum

FISH, fluorescence in situ hybridization

IR, ionizing radiation

KCl, potassium chloride

MKK6-CA, constitutively active MKK6

mRNP, messenger ribonucleoprotein

NMD, nonsense-mediated decay

PTC, premature termination codon

uORF, upstream open reading frame

UPF, up-frameshift protein

ROI, region of interest

SA-β-Gal, senescence-associated β-galactosidase

SASP, senescence associated secretory phenotype

SMD, Staufen-mediated decay

SMG, suppressor with morphological effect on genitalia

TCR, T cell receptor

WT, wild type

γH2AX, phosphorylated histone variant H2AX

Acknowledgments

As I sit writing this dissertation, I cannot help but reflect on the immeasurable contributions of my colleagues and friends to my personal and scientific growth. As a graduate student, I have experienced the unambiguous and enthusiastic support of so many groups and individuals that made my work possible.

I would be remiss if I did not begin by expressing my gratitude to Zhongsheng You. When rotating in his lab five years ago, Zhongsheng's undeniable passion for science impressed me as much as his scientific aptitude, and I remain in awe to this day at his unwavering love of scientific discovery. Zhongsheng's passion extends to his mentorship, and his steadfast belief in me was an essential source of support when I needed it most.

I am grateful to my thesis committee—Barry Sleckman, Jason Weber, Joseph Dougherty, Sergej Djuranovic, and Qin Liu—for their support, advice, and feedback. I benefitted immensely from their expertise and unique scientific perspectives.

The members of the You Lab were always kind, gracious, and extremely helpful. Their input during lab meetings and scientific discussions were invaluable, and their company was invariably pleasant. Special thanks to Abby Cheruiyot who joined me on the RNA side of the lab; her intelligence and thoughtfulness made discussions with her incredibly fruitful.

I am so fortunate to have worked with a number of fantastic collaborators both at Washington University and elsewhere. In particular, I must thank David Piwnica-Worms whose direction in the early portion of my graduate career was instrumental to my success. I must also thank Sheila Stewart and her lab. Very few people sat through more of my presentations than

Sheila, and her feedback was consistently helpful and thought-provoking. The willingness of the Stewart lab to share expertise and reagents was much needed, and I am greatly appreciative.

Thanks to the Cell Biology and Physiology department for administrative support and for fostering a collegial atmosphere among a great group of people. I would have never successfully submitted a grant were it not for the administrative staff, and the happy hours and retreats were much needed respites from the stresses of lab.

Many thanks to the Molecular Genetics and Genomics graduate program. In addition to being top-notch scientists, Jim Skeath and Tim Schedl are two of the most approachable, thoughtful, and caring mentors I have encountered. And of course, thanks to Melanie Relich whose hard work and great personality keeps the MGG program running smoothly.

I am grateful to Siteman Cancer Center for two years of funding and for constantly reminding me why science is important—because it improves lives.

I want to thank all of my friends and family who have supported me, endured my rambling complaints and crazy ideas, and forced me to maintain some semblance of a life outside of lab these last five years. I am forever grateful to my parents who instilled in me a lifelong love of learning. Thank you to my in-laws, Steve and Lucina, whose company is always a welcome diversion from science and who raised my favorite person in the world. Finally, I want to thank to my wife Colleen. Whether my day in lab was good or bad, it never really mattered because I spent my nights with her. I could not have done this without her.

Dedicated to my beautiful wife Colleen and our furry friends Martin and Trouble

ABSTRACT OF THE DISSERTATION

Novel Regulation of the Nonsense-Mediated RNA Decay Pathway

Andrew Nickless

Doctor of Philosophy in Biology and Biomedical Sciences

Molecular Genetics and Genomics

Washington University in St. Louis, 2016

Dr. Zhongsheng You, Chairperson

The nonsense-mediated RNA decay (NMD) pathway maintains the integrity of cellular RNAs and controls gene expression. NMD is essential for vertebrate development, and defects in NMD are associated with a variety of cancers and neurodevelopmental disorders. NMD activity is tightly regulated and is altered in response to environmental and developmental signals. To better study this dynamic pathway and to identify clinically relevant regulators of its activity, we developed a dual-color bioluminescent NMD reporter that rapidly and accurately quantifies NMD activity in mammalian cells. Using this reporter, we performed a chemical screen for small-molecule modulators of NMD activity and identified the cardiac glycosides (CGs) as potent repressors of NMD activity. Further studies on the mechanism of action of these drugs led to the finding that cytoplasmic calcium, a key cellular signaling molecule, regulates NMD, with increases in cytoplasmic calcium repressing NMD. The regulation of NMD by calcium may be exploited to treat certain genetic diseases and cancers.

Regulation of NMD is particularly important to the cellular stress response. Stresses such as hypoxia, amino acid deprivation, and ER stress induce a reduction in NMD activity that

promotes the expression of genes that help cells cope with these environmental insults. We investigated the regulation of NMD and its role in the cellular response to DNA damage. We found that NMD is suppressed by persistent, but not transient, DNA damage. Persistent DNA damages arises from a variety of physiologic sources and profoundly influences tumorigenesis. The inhibition of NMD by persistent DNA damage is mediated in part by p38 MAP kinase signaling and stabilizes the mRNAs of ATF3, a transcription factor that stifles tumorigenesis by promoting senescence but also engenders a favorable tumor microenvironment by altering expression of secreted factors, thereby contributing to its augmented expression in cells harboring persistent DNA damage. These results reveal a novel p38-dependent pathway that regulates NMD activity in response to persistent DNA damage and contributes to gene expression changes in damaged cells.

Chapter 1: Introduction

In this introductory chapter, I begin with a brief summary of my thesis work and its goals. I then provide a general overview of NMD: its basic functions, the factors involved, how they work together to identify target mRNAs, and what distinguishes target mRNAs from non-targets. I go on to discuss topics more specifically relevant to my work in sections 1.3-1.6. In these sections, I expound upon the functions of NMD, its dynamic regulation, its physiological consequences, its connection to disease, and how the pathway is studied.

1.1 Aim and scope of the dissertation

In this dissertation, I describe my work developing and validating a bioluminescent NMD reporter that overcomes many of the obstacles of previous reporter systems and is amenable to high-throughput screening. I expound upon my finding, made with this reporter, that the clinically relevant cardiac glycosides (CGs) repress NMD activity by inhibiting their canonical target, the Na^+/K^+-ATPase, and subsequent work implicating cytoplasmic calcium as an inhibitor of NMD. I also describe my work demonstrating the regulation of NMD by the p38 MAP kinase in response to persistent DNA damage. I present models which place these findings in appropriate biological contexts and emphasize their clinical and physiological significance. Finally, I build upon these models to propose natural extensions of this research.

1.2 The molecular mechanism of nonsense-mediated RNA decay

Nonsense-mediated RNA decay (NMD) is a conserved cellular quality control and gene regulatory mechanism essential for viability in vertebrates[1-10]. NMD dutifully eliminates transcripts harboring a premature termination codon (PTC), thereby preserving the quality of the transcriptome and maintaining cellular homeostasis. PTCs arise in numerous ways: many result from errors in nucleic acid metabolism, such as genetic mutations or transcriptional aberrations,

while others are components of normal gene structures. Many diverse physiological processes depend on NMD, and its dysregulation can cause a myriad of health problems, illustrating the importance of regulating nonsense transcripts.

1.2.1 Detecting Nonsense: How and where are nonsense transcripts identified?

The ability to accurately distinguish premature termination codons from their wild type counterparts lies at the heart of proper NMD. This distinction is made by a "second signal," which denotes the status of a stop codon. The presence of a second signal downstream of a stop codon induces nonsense-mediated decay. The second signal of lower eukaryotes consists of a loosely defined downstream sequence element or an exceedingly long 3' UTR while the mammalian second signal is deposited as a result of pre-mRNA splicing[11-16]. Consequently, naturally intron-less mammalian genes are unaffected by the activity of NMD[17,18]. Since the vast majority of normal stop codons lie in the final exon, most non-mutant transcripts exist unperturbed by NMD[19].

For years, although the reliance upon pre-mRNA splicing was well established, the molecular nature of the mammalian second signal remained mysterious. It wasn't until the discovery of the exon-junction complex (EJC), a large multi-protein assembly deposited upstream of exon-exon junctions as a result of pre-mRNA splicing, that a suitable molecular candidate for the second signal became apparent[20]. Analysis of EJC components revealed that proteins involved in nuclear export, translation initiation, and NMD factors are associated with this complex, and mechanistic studies demonstrated that many EJC components are necessary for robust NMD[21-31]. These observations support the hypothesis that exon-exon junctions,

through their associated EJCs, facilitate NMD factor activity and initiate NMD when located downstream of a stop codon.

Inherently, NMD depends upon the translation machinery for the identification of stop codons. However, it would be detrimental to cellular vitality if multiple rounds of translation produced aberrantly expressed or truncated proteins before transcript degradation. Therefore, many researchers suspected that NMD degrades PTC-bearing transcripts during an initial "pioneer" round of translation to prevent the accumulation of harmful protein products. This supposition has garnered much interest throughout the years, and multiple lines of evidence suggest its veracity.

Curiously, the first evidence for the notion that PTC-containing mRNAs are eliminated early in their existence stemmed from studies demonstrating a significant decrease of these transcripts in nuclear fractions[32,33]. This observation is difficult to reconcile with the reliance of NMD on translation, which overwhelmingly occurs in the cytoplasm, and with the trafficking of NMD factors through specialized cytoplasmic RNA processing regions known as p-bodies[34,35]. Nevertheless, the effects of NMD on mRNAs that fractionate with the nucleus suggest that NMD acts on nascent transcripts that have not yet disassociated from the nucleus.

Biochemical approaches that identified proteins associated with NMD-target transcripts provided more direct evidence for the pioneer round hypothesis. This work exploited the sequential binding pattern of various proteins to the 5' cap of mRNAs. Nascent transcripts are bound by a cap binding complex (CBC), consisting of CBP80 and CBP20, which promotes mRNA maturation by fostering pre-mRNA splicing and nuclear export[36-40]. After splicing, CBP80 and CBP20 accompany the transcript to the cytoplasm where they are eventually

displaced by the translation initiation factor eIF4E[41]. Interestingly, several NMD factors exclusively reside on the nascent CBC-bound mRNAs[40]. This differential occupancy has functional consequences as PTC-containing transcripts bound to the CBC are degraded while identical transcripts associated with eIF4E are not[41]. Additionally, the moving ribosome actively displaces EJC components that promote NMD[42]. Together, these data suggest that NMD occurs during the initial round of translation before critical NMD factors are ejected from the transcript.

Where NMD occurs is another fundamental aspect of NMD currently under intense scrutiny. Nonsense transcripts are depleted in the nuclear fraction of cells. However, NMD depends upon translation, which occurs overwhelmingly in the cytoplasm, and NMD is inhibited by dominant negative peptides only when localized to the cytoplasm[29]. Many resolve this paradox by subscribing to the model that NMD occurs during or immediately following nuclear export, where nonsense RNAs are still associated with the nuclear fraction[43]. Fluorescence in situ hybridization (FISH) studies designed to observe the locations of single NMD-target mRNAs support this model as the majority of transcripts are degraded near the nuclear membrane—likely during nuclear export[44]. However, contradictory results were obtained by a second group—also using FISH to address this question, albeit without single-molecule resolution—that observed decay of NMD substrates in the nucleus that was dependent upon translation[45]. A second point of contention concerns whether NMD occurs in p-bodies. NMD factors have been observed within these RNA-processing regions after inhibition of NMD[34,35]. In contrast, prevention of p-body body formation fails to influence the efficiency of NMD[46,47]. Many argue that the localization of NMD factors to p-bodies is an artifact of inhibiting late-stage events of NMD. A more complete

understanding of the NMD factors and their properties is needed to resolve this contentious issue.

1.2.2 The Targets: What RNAs are degraded by NMD?

As discussed in the previous section, the presence of an exon-junction complex (EJC) downstream of a stop codon elicits NMD. Mechanistic studies determined that an EJC must be greater than 50-55 bases downstream of a stop codon to destabilize mRNAs, lest it be ejected from the transcript by the translocating ribosome before NMD can occur [48]. Multiple processes, both normal and aberrant, generate RNAs with a stop codon positioned greater than 50 bases upstream of an EJC and therefore trigger NMD (Fig. 1).

The earliest NMD-sensitive transcripts identified arose from genetic mutations that introduced a PTC. Disease-causing mutations, such as those causing β-thalessemia, were particularly noticeable[49,50]. In addition to mutations in the DNA, other sources of PTCs include inaccurate transcription and faulty splicing. Indeed, abolition of NMD activity increases expression of the low-abundance PTC-containing transcripts that result from mis-splicing[51]. However, inaccurate transcription is relatively rare, and fewer than 0.5% transcripts from a given gene are predicted to contain such errors[52]. Furthermore, new studies suggest that the vast majority of transcripts targeted by NMD are non-mutant mRNAs[53,54].

Normal, as opposed to aberrant, physiological processes generate NMD target transcripts to regulate gene expression. For example, widespread alternative transcription initiation and splicing ensures that most genes produce multiple mRNA isoforms, many of which alter the coding sequence and place a stop codon upstream of a splice junction[19,55]. There are many examples of programmed alternative splicing being coupled to NMD (discussed in section 1.3).

Programmed ribosomal frameshifting can also sensitize transcripts to degradation via NMD. Computational analyses predict that 8-12% of genes contain signals that induce programmed ribosomal frameshifting, most commonly switching translation into the -1 reading frame[56]. The stop codon in this new reading frame often resides > 50 bases upstream of a splice junction and will trigger mRNA degradation via NMD[57-59]. Consequently, the prevalence of these frameshifting events for a given gene will influence its expression.

Many transcripts naturally contain features that make them susceptible to NMD. Below are descriptions of common NMD-inducing features.

3' UTR introns

A subset of normal gene structures place a stop codon upstream of a splice junction residing in the 3' UTR and so predispose their mRNAs to NMD. The stop codons for about 4% of genes are located >50 bases upstream of the final exon and are thus potentially susceptible to degradation via NMD[19].

Upstream open reading frames (uORFs)

The primary coding region for nearly 50% of transcripts is preceded by an uORF that begins within the 5' UTR and either terminates there or overlaps with the canonical coding sequence[60]. uORFs commonly place stop codons upstream of splice junctions and are capable of eliciting NMD if translated[61].

Selenocysteine insertion sequences

Transcripts encoding selenoproteins comprise an interesting class of NMD targets. In high selenium environments, a sequence element in the 3' UTR of these mRNAs facilitates the incorporation of a selenocysteine into the peptide at certain UGA codons rather than terminating

translation[62]. For some selenoprotein-encoding mRNAs, this UGA is predicted to elicit NMD if it initiates translation, and indeed a subset of these transcripts are sensitive to NMD inhibition and are unstable in the absence of selenium[63,64].

Long 3' UTRs

mRNAs with long 3' UTRs are also susceptible to NMD in an EJC-independent manner (see section 1.2.3 for mechanism), and transcriptome-wide analysis indicates that long 3' UTRs are the most common feature of NMD targets[13,54,65].

1.2.3 The Factors

Two classes of NMD factors were identified through genetic screens in *S. cerevisea* and *C. elegans*[66-69]. The UPF enzymes, identified in yeast, are the fundamental NMD components whose importance is reflected by their conservation throughout all organisms with an intact NMD response[70]. The SMG proteins are not present in yeast but are conserved from *C. elegans* to humans[70]. In mammals, the UPF and SMG proteins act in concert to detect transcripts harboring premature termination codons (PTCs) and initiate their degradation (Figure 2).

The UPF proteins are essential to NMD in human cells. Notably, reporter mRNAs are effectively destabilized by tethering Upf1, Upf2, UPF3b, or—to a lesser extent—UPF3a to their 3' UTRs[71]. This effect is contingent on the proteins being tethered downstream of the stop codon, implying that they function at this position under physiological conditions. Contrasting this gain-of-function approach, knock-down or expression of dominant negative mutants of UPF enzymes stabilize nonsense mRNAs, and mutations in these factors are associated with decreased NMD[72-74]. The biochemical and biological properties of these crucial enzymes provide wonderful insight into the mechanism of NMD.

The most functionally complex of the UPF proteins is Upf1, a phosphoprotein with ATP-dependent helicase activity and RNA-dependent ATPase activity[75-81]. Upf1 promiscuously interacts with numerous protein factors and associates with at least two distinct protein complexes during NMD: one containing the kinase SMG1 as well as the translation release factors eRF1 and eRF3 and a second including members of the exon-junction complex (EJC) and other NMD factors[75-78]. These interactions alone provide many insights into the mechanistic function of Upf1 in NMD. For instance, the association with translation release factors implies that Upf1 is recruited to mRNAs as a member of the translation termination complex. The primarily cytoplasmic localization of Upf1 also supports the notion that Upf1 associates with mRNAs after their export from the nucleus[71,78].

The ability of release factors to recruit NMD components to the ribosome before it successfully terminates translation is a critical determinant of whether a transcript will undergo NMD. Indeed, experimental manipulations that promote efficient translation termination block decay of NMD substrates. For example, tethering PolyA-binding protein1 (PABPC1), whose interaction with the cap-associated protein eIF4G promotes mRNA circularization and efficient translation termination, near a PTC stabilizes nonsense transcripts[82-88]. Consistent with the notion that the PABCP1:eIF4G complex stimulates termination and suppresses NMD, a subset of nonsense mutations near the 5' end of mRNAs, where eIF4G resides, are known to evade NMD[89-91]. Conversely, barriers to efficient termination—such as long 3' UTRs whose great physical distance between the stop codon and the polyA tail diminishes the ability of PABPC1 to effectively engage with the terminating ribosome—sensitize transcripts to NMD[54,61,86,92-95]. UPF1 binds nonspecifically to RNAs and primarily resides within the 3' UTR of mRNAs where

it is not ejected by translocating ribosomes[61,96-98]. For transcripts with exceedingly long 3' UTRs, the combination of inefficient termination and an abundance of localized UPF1 elicits decay even when no EJC resides downstream. However, 3' UTR length itself is often not predictive of whether a transcript will undergo NMD as certain elements within 3' UTRs, such as internal A-rich stretches capable of recruiting PABPC1, allow RNAs to evade degradation[61,86,94,99].

The observation that Upf1 is a phosphoprotein prompted the discovery that SMG1 phosphorylates Upf1 at multiple positions and that these modifications are necessary for proper NMD activity[79]. Further work revealed an intricate cycle of Upf1 phosphorylation and dephosphorylation coordinated by the SMG proteins that facilitates NMD. The cycle begins with the phosphorylation of Upf1 by SMG1[79]. Phosphorylated Upf1 then inhibits further translation initiation of the RNA[100]. It also recruits SMG5-7 which, in turn, initiate RNA destabilization and decay[75,76,101-103]. These factors then induce Upf1 dephosphorylation by recruiting the phosphatase PP2A, thus replenishing unmodified Upf1 for future rounds of NMD[75,104,105]. This cycle is a critical regulatory step in the NMD process and delays in NMD cause UPF1 hyperphosphorylation which enhances its affinity for its binding partners, thereby ensuring the timely decay of NMD target transcripts[106].

Both the helicase and ATPase activity of Upf1 are important for NMD[71,80]. Indeed, Upf1 disassembles messenger ribonucleoprotein (mRNP) complexes undergoing NMD in a manner dependent upon its ATPase activity[80]. Another RNA helicase, MOV10, also dissassembles the mRNP for decay[107]. Whether these factors function redundantly or have distinct roles in mRNP clearance is not known, but ablating either of their helicase activities causes the accumulation of decay products, indicating an inability to complete mRNA degradation[80,81,107]. Additionally,

helicase-defective Upf1 mutants less effectively initiate mRNA degradation when tethered to reporter transcripts[71]. The critical nature of these activities necessitates tight regulation, which is provided in part by the remaining UPF enzymes— Upf2 and Upf3.

The multiple biochemical activities of Upf1 lie in stark contrast to those of Upf2 which functions largely as an adapter protein, facilitating complex formation. Consistent with this function, Upf2 possesses binding sites for both Upf1 and Upf3[78,108,109]. Upon formation of these interactions, Upf2 and Upf3 stimulate the helicase and ATPase activities of Upf1, permitting mRNP disassociation only after appropriate complex formation[108,110]. The role of Upf2 in mediating complex formation during NMD may extend to the RNA itself although the significance of this result remains in question[109,111]. The concomitant interaction of Upf2 with both Upf1 and Upf3 brings together NMD factors associated with the translation termination complex and the second signal EJC complex, providing the physical connection that initiates NMD.

The paralogs Upf3a and Upf3b comprise the final core NMD components in mammals. Upf3 resides predominantly in the nucleus where it associates with EJC components; however, UPF3 remains associated with RNAs after their exit into the cytoplasm where it likely meets Upf2 which exhibits robust perinuclear localization[71,78,111]. Its association with the EJC makes UPF3 the principle second signal component whose presence on an RNA determines the status of a stop codon.

Possessing two Upf3 genes is a uniquely vertebrate aspect of NMD: all other organisms have only one[112]. The reason for having paralogous NMD genes is unknown. Until recently, most believed that Upf3a acts redundantly to Upf3b, which resides on the X-chromosome and may be

subject to silencing during spermatogenesis. Indeed, early studies demonstrated that both proteins induce mRNA decay when tethered to the 3' UTR of reporter transcripts, although the ability of UPF3a to initiate decay is weak[71,113]. However, recent evidence suggests that UPF3a actually functions as a negative regulator of NMD for most transcripts, although it does promote NMD of others, and UPF3a deficient cells exhibit extremely robust NMD[7]. This lead to a more complicated model of NMD in which the relative expression of these two genes to one another influences NMD activity, with additional complexity stemming from the fact that Upf3b negatively regulates the protein stability of Upf3a[112]. Despite their antagonistic influences on NMD activity, these proteins have similar binding partners as each binds Upf2 and associates with the core EJC components[71,78,112,113].

The suppressor with morphological effect on genitalia (SMG) genes constitute the second major class of NMD genes. This family is comprised of six genes, four of which were identified in mammals through their homology to essential NMD genes in *C. elegans*[66,75,79,104,105]. These proteins collectively coordinate the biochemical events of NMD in a temporally distinct manner, largely through the regulation of Upf1 phosphorylation and dephosphorylation.

The PI3K-like kinase SMG1 phosphorylates Upf1 at multiple residues[79]. These modifications act as docking sites for other NMD factors and stimulate Upf1's ability to inhibit further translation initiation on nonsense transcripts[75,76,100]. Consistent with the importance of these functions, abrogation of SMG-1 kinase activity severely impairs the NMD response[79]. The tight regulation of SMG1 kinase activity by at least 6 other NMD factors (SMG8, SMG9, DHX34, MARVELD1, RUVBL1 and RUVBL2) speaks to the significance of this molecular action[114-119]. SMG8 and SMG9 restrict SMG1 kinase activity until after the full NMD complex

has formed on the EJC, thus preventing the aberrant phosphorylation of Upf1 which could drastically disrupt NMD and translation[114-116]. Subsequently, RUVBL1 and RUVBL2 facilitate complex formation and DHX34 binds both SMG1 and UPF1 and acts as a scaffold to promote UPF1 phosphorylation and proper NMD[117,118]. MARVELD1 is a relatively understudied negative regulator of UPF1 phosphorylation which appears to disrupt the interaction between SMG1 and UPF1[119].

Following Upf1 phosphorylation, the remaining SMG factors (SMG5, SMG6, and SMG7) join the UPF proteins on the RNA[75,76]. Recruitment of the SMG-5:SMG-7 heterodimer is mediated by the ability of SMG-7 to recognize and bind Upf1 via phosphorylated serine 1,096 while SMG-6 directly interacts with the EJC through multiple conserved EJC-binding motifs and also recognizes phosphorylated Upf1 at threonine 28[76,120]. All three proteins antagonize the earlier activity of SMG-1 by recruiting the phosphatase PP2A to remove phosphate groups from Upf1[75,104]. The significance of this action rivals that of the initial phosphorylation events in importance as genetic ablation of these factors results in a hyperphosphorylated Upf1 and decreased NMD activity[75,104].

SMG6 and SMG7 further function as the terminal effectors of NMD by destabilizing the nonsense transcripts, yet they employ distinct means of initiating decay[101-103]. SMG7 promotes RNA decapping and deadenylation events that expose the transcript ends to cellular exonucleases —identical to the mechanism originally discovered in yeast[101,122-124]. Mammalian NMD targets also undergo increased deadenylation, and genetic ablation of decapping/deadenylation enzymes stabilizes nonsense transcripts[125-129]. In addition to SMG5 and SMG7, PNRC2 associates with phosphorylated UPF1 and recruits the decapping factor DCP1a[130,131]. Alternatively, SMG6,

which has endonuclease activity, cleaves transcripts near the PTC, generating two unprotected RNA ends that are summarily targeted by cellular nucleases—a mechanism absent in yeast but prominently utilized in *Drosophila*[102,103].

Although recent evidence indicates SMG6-mediated endonucleolytic cleavage is quite widespread and may represent the primary mammalian decay initiating mechanism**,** the presence of two distinct mammalian decay mechanisms raises a number of questions—especially given that simultaneous binding of the SMG5:7 heterodimer and SMG6 to Upf1 appears necessary for NMD[76,132,133]. What decides which mechanism to employ? Do transcript-, developmental stage-, or tissue-specific preferences exist and, if so, how does this regulation occur? Answering questions such as these will provide insight into the relevance of having two RNA decay mechanisms and further illuminate the role of NMD in cells.

Most of the NMD factors discussed above (Table 1) were discovered in forward genetic screens in lower eukaryotes. Recently, two more NMD factors, GNL2 and SEC13, were identified in an siRNA screen in *C. elegans* although their role in the pathway remains unclear[134]. However, major differences exist between mammals and lower eukaryotes in the mechanisms responsible for detecting PTCs and degrading NMD targets. These differences imply the possible existence of additional human genes. There is precedent for this as SMG8 and SMG9 were discovered through their association with SMG1 in HeLa cells[115]. High-throughput reverse genetic techniques must be employed to effectively discover new mammalian NMD factors.

1.3 Constitutive functions of NMD

The canonical function of nonsense-mediated decay is to prevent the expression of potentially deleterious truncated protein products that result from errors in nucleic acid

metabolism. Indeed, the ability of NMD to target mutant genes is well documented, and disruption of NMD activity causes an increase in low-abundance PTC-containing transcripts that result from erroneous splicing[51]. However, decades of research have revealed that—by removing aberrant transcripts and by regulating gene expression—NMD contributes significantly to organismal development and many essential physiological processes.

The role of NMD in immune development and health is well established. Developing B- and T-lymphocytes undergo a series of programmed genomic rearrangements to assemble their immunoglobin and T-cell receptor (TCR) genes respectively. Two-thirds of these rearrangements yield unproductive gene products harboring a PTC and are strong NMD substrates[5,135,136]. Conditional ablation of NMD in T-cells significantly reduced the number of mature T-lymphocytes and increased the amount of apoptotic cells[5]. An increase in the abundance of nonsense TCR transcripts accompanied the reduced cell viability. Similar effects on viability are obtained when NMD is abrogated in hematopoetic progenitor cells[5]. Interestingly, viability can be restored by introducing a complete TCRβ sequence that prevents the accumulation of nonsense counterparts, implying that NMD is acting in its canonical role and not controlling gene expression[136].

Incidentally, while exploring the downregulation of aberrant TCRβ, an alternative Upf3-independent NMD pathway was discovered[137]. This work gave credence to earlier findings that nonsense transcripts can be degraded in a Upf2- or EJC-independent manner[95,138]. Just as possessing multiple mechanisms of RNA decay raises questions, having alternative NMD pathways does as well. Exploring the significance of each pathway and understanding their regulation will be a major focus of future NMD research.

A burgeoning facet of NMD research concerns its promotion of neuronal health, development, and function. Interest in this area skyrocketed after a number of studies demonstrated an association between aberrant NMD and mental disorders, including autism and schizophrenia, or developmental abnormalities of nervous system[1, 10, 139-144]. To uncover the molecular basis of these phenotypes, researchers employed a variety of model systems to probe the role of NMD in neurons and found that in *Drosophila* NMD influences both synaptic morphology and transmission, while in mammalian cells the ablation of the EJC factor eIF4AIII, an effector of NMD which preferentially associates with dendritic mRNAs in neurons, results in increased synaptic strength[145,146]. Furthermore, in commissural neurons, NMD limits expression of Robo 3.2 to ensure proper axonal migration and, in mature neurons, activity-dependent alternative splicing coupled to NMD controls expression of many synaptic proteins as neuronal activity induces the retentention of cryptic exons that elicit degradation via NMD[147,148]. These results highlight the significance of NMD to the nervous system, which is only beginning to be understood.

Outside of the nervous system, NMD similarly influences the expression of multiple families of splicing regulators including the SR splicing activators and the HNRNP splicing repressors[149-153]. These factors regulate the splicing of many mRNAs—including their own—and alternative splicing of SR and HNRNP protein transcripts induce NMD. As a result, NMD is critical to ensuring proper expression of the splicing machinery, which explains observations that abrogation of NMD causes a drastic restructuring of the transcriptome characterized by widespread alternative splicing[51].

Strong NMD actvity is also necessary for differentiation of murine embryonic stem cells (ESCs). Knockout of SMG6 in these cells prevents differentiation[6]. Proper differentiation is restored by expressing wild type SMG6 but not mutant versions that specifcally abrogate its function in the NMD pathway, demonstrating that reduced NMD activity—not alternative effects of SMG6 abrogation—is responsible for the failure to differentiate[6]. Further supporting this conclusion are results demonstrating that knockdown of other NMD factors causes the same phenotype. Prolonged, elevated expression of NMD-regulated pluropotency genes, such as c-Myc, underlie the inability of NMD-incompetent ESCs to differentiate[6]. This result is particularly significant because it provides intriguing evidence that NMD-mediated gene regulation—as opposed to general RNA surveillance—plays a crucial role in an essential developmental process and bolsters the argument that NMD's primary and most essential function is regulating the expression of non-mutant genes.

One of the major challenges in characterizing the physiological significance of NMD is distinguishing between its quality control and gene regulatory roles. An outstanding attempt at this was published by the Metzstein lab; to determine why NMD is essential to *Drosophila* viability they performed a suppressor screen to identify regions of the genome that sensitize *Drosophila* embryos to death in the absence of NMD[154,155]. They found that loss-of-function mutations in the NMD-target GADD45 gene partially restore viability of NMD-deficient mutants, suggesting that the embryonic lethality of NMD-deficient embryos is due to an accumulation of GADD45, which induces widespread apoptosis[155]. Thus, at least in *Drosophila*, NMD is essential because it regulates gene expression, not because of its suppression of aberrant truncated protein expression.

The quality control and gene regulatory functions of NMD are well established, but recent studies reveal other functions of the pathway that open future avenues for future research. An exciting and potentially significant new function of NMD is the regulation of long non-coding RNAs (lncRNAs). Although only about 2% of the genome codes for proteins, the majority is transcribed into RNA[156,157]. lncRNAs are a prominent class of RNA molecules produced by this widespread transcription and have important functions modifying chromatin, regulating transcription, altering mRNA stability, and influencing translation[158,159]. For many years the prevailing notion was that these transcripts were not translated despite possessing 5' caps and poly-A tails—two features that facilitate translation of mRNAs—but observations that lncRNAs associate with the translation machinery challenged this assertion[160-163]. In 2014, Smith et al. demonstrated that not only are a subset of lncRNAs translated—sometimes producing detectable micropeptides—but about 17% of lncRNAs are degraded by NMD in both yeast and human cells[164]. A year later researchers from the Morillon lab observed similar decay of lncRNAs by NMD unless they possess a dsRNA structure that prevents NMD[165]. With so many uncharacterized lncRNAs and their profound influence on development and disease, the study of lncRNAs seems poised for many interesting discoveries. The fact that so many of these transcripts are regulated by NMD all but ensures that NMD will play a prominent role in future lncRNA and micropeptide research.

1.4 Dynamic regulation of NMD

For many years, it was assumed that NMD activity was constitutive, as periods of low NMD activity would permit the accumulation of potentially disruptive mutants. As scientists began to appreciate the full scope and significance of NMD's capacity to regulate normal genes,

the notion of constitutive NMD activity was challenged: if quality control is not the most important function of NMD, or if compensatory mechanisms exist that allow cells to cope with aberrant mRNAs and proteins for short periods, cells may not require high levels of NMD activity at all times. Studies applying whole-transcriptome analyses to cells deficient in essential NMD proteins opened the eyes of many to just how pervasive NMD-mediated gene regulation is, because these studies invariably found that NMD directly controls the expression of between 3-10% of genes[166-169]. In a seminal paper, Mendell et al. knocked-down Upf1 and observed a widespread upregulation of transcripts with NMD-inducing features including 3' introns, upstream open-reading frames (uORFS), and splice variants containing a PTC[167]. Many of the upregulated gene products function in amino acid metabolism. This is significant, because they found that amino acid deprivation reduces NMD activity, allowing for the expression of proteins that respond to this environmental insult[167]. This finding introduced a new dimension to the study of nonsense-mediated decay, and researchers have since identified large numbers of NMD targets and demonstrated that NMD-dependent transcript regulation coordinates the response to multiple cellular stresses[167,170-175].

Mechanistically, phosphorylation of the translation initiation factor eIF2α during amino acid deprivation is likely necessary for NMD repression during amino acid deprivation, although exactly how this influences the NMD process remains unknown[175]. This mechanism appears to be widespread as other stresses which induce eIF2α phosphorylation—such as endoplasmic reticulum (ER) stress and hypoxia—also repress NMD[170,171,173-175]. Similar to the response to amino acid deprivation, hypoxia- and ER-stress-induced NMD repression facilitates the stabilization and increased expression of critical stress response factors such as ATF4, ATF3, and

CHOP and IRE1α respectively[170,171,173]. In hypoxic cells, these NMD target mRNAs associate with polysomes and are efficiently translated, suggesting that eIF2α phosphorylation diminishes NMD activity in a translation-independent manner[176,177]. Furthering this conclusion are the observations that NMD does not require robust translation to efficiently degrade transcripts as it occurs during early rounds of translation and that the pioneer round of translation transpires even under conditions which diminish general translation[178-180].

The functions of NMD in the stress response extend beyond promoting survival and recovery. Occasionally, environmental insults are so great that cells trigger programmed cell death via apoptosis and here too NMD contributes. Recent work by the Maquat lab revealed that an early event during apoptosis is the cleavage of UPF1, the primary NMD factor, by multiple caspases[181]. This cleavage generates a dominant negative peptide fragment that stifles NMD activity[181]. The resulting reduction in NMD activity allows for the upregulation of several pro-apoptotic genes including GADD45α, GADD45β, BAK1, GAS5, DAP3, and DUSTP2. This finding is also relevant to cancer biology as they found that the chemical inhibition of NMD sensitizes tumor cell lines to chemotherapeutics by promoting apoptosis[181].

In the prenominate examples, stressed cells autonomously repress NMD to promote appropriate cellular stress responses. Interestingly, viruses possess mechanisms to control NMD efficiency and co-opt cellular stress responses for their own benefit. Indeed, robust NMD activity targets genomic and full-length viral RNAs, thereby suppressing expression of viral proteins and reducing viral titer in both plants and animals[182,183]. The suppressive effects of NMD on viral function are immediate and constitutive. Since this form of antiviral immunity does not require activation by the virus or depend upon outside signals, it is one of the first threats to successful

replication that viruses encounter. Consequently, some viruses have developed mechanisms to suppress NMD. The Human T-cell Leukemia Virus Type-1 encodes RNA binding proteins called Tax and Rex which stabilize not only viral RNAs but also host NMD target mRNAs and enhance viral replication[184,185]. Furthermore, an element in the 3' UTR of the Rous sarcoma virus renders the viral RNA insensitive to host NMD, possibly by limiting the capacity of UPF1 to initiate decay[186,187].

The observation that NMD is suppressed during periods of stress and development raises the question of how aberrant RNAs with PTCs are dealt with during intervals of reduced NMD activity. One explanation is that NMD inhibition is only restricted to brief temporal windows of inactivation during development or to periods of severe cellular stress where the cellular insults are so great that the benefits—expression of stress response genes—outweigh the risks posed by truncated proteins. However, this is an unsatisfying, albeit potentially correct, response that raises many additional questions. Why antagonistically link the stress response to the repression of a pathway whose constitutive activation promotes homeostasis? Is the quality control function of NMD really essential?

Work done in the Maquat lab delivers an alternative explanation. They found that STAU1, a factor essential for the Staufen-mediated decay (SMD) pathway, competes for a binding site on UPF1 with UPF2, a core NMD component[188]. As a result of this competition, the upregulation of STAU1 during myoblast differentiation significantly reduces the ability of UPF2 to bind UPF1[188]. Notably, this diminishes the activity of the UPF2-dependent branch of NMD but actually stimulates an alternative branch. The specific repression of only the UPF2-dependent branch permits the upregulation of myogenin, which is required for myogensis, while alternative

branches maintain their capacity to prevent expression of aberrant proteins[188]. Thus the multiple branches of NMD allay the tension between the two primary functions of NMD—quality control and gene regulation.

Cells also cope with reduced NMD activity by activating compensatory mechanisms, such as autophagy, which also prevent expression of abnormal proteins. Indeed, NMD inhibition is sufficient to induce autophagy—likely a result of increased ATF4 expression in NMD deficient cells[189]. eIF2α phosphorylation also links the two pathways as it not only inhibits NMD but is also necessary for initiating autophagy[189]. The Gardner lab, which discovered this regulation, believes that the induction of autophagy by NMD inhibition purges cells of mutated, misfolded, and aggregated proteins that accumulate in NMD-deficient cells. Supporting this notion is data demonstrating that the loss of NMD in autophagy-deficient cells augments cell death while NMD enhancement rescues viability[189]. While inconclusive, this is consistent with their model that autophagy clears harmful proteins from cells when NMD is inactive. Additionally, the stimulation of autophagy increases the free amino acid concentration within cells, which bolsters the response to amino acid deprivation.

Since NMD is an essential process responsible for regulating the expression numerous genes, the precise regulation of this pathway is critical. Considering this, it is perhaps unsurprising that an autoregulatory loop exists whereby the transcripts of many NMD factors are themselves susceptible to NMD, thus facilitating expression of NMD components during intervals of low NMD activity while suppressing their expression to some extent when the pathway is active[54,92,190]. This autoregulation may be critical to restoring NMD activity to appropriate levels after adjustments.

In summation, NMD functions to maintain cellular homeostasis by degrading both mutant and non-mutant transcripts harboring PTCs. NMD activity is dynamic and varies depending upon cell type, developmental stage, and environmental inputs[24,65,167,170,171,173,174,181,184,185,188,191,192]. NMD contributes to multifarious developmental and stress response programs by regulating mRNAs possessing NMD-inducing features, and the modulation of NMD activity in these settings alters expression of relevant genes. Our current understanding of how NMD is dynamically regulated is limited to a small number of mechanisms: phosphorylation of eIF2α by stress-activated kinases (how this diminishes NMD function remains to be elucidated), upregulation of miRNAs that target NMD factors, UPF1 cleavage during apoptosis, viral expression of NMD-inhibiting proteins, and the activation of competing RNA decay pathways like SMD[65,167,170,171,173,181,184,185,188,193,194]. These mechanisms are not yet fully understood and other mechanisms—such as transcriptional regulation of NMD factors—may be utilized. Determining how, when, where, and why NMD efficiency is modified are major challenges facing NMD researchers today. Indeed, novel biological roles for NMD, such as its ability to survey mRNAs for proper transcription start site usage, are being discovered regularly—demonstrating the promising future of NMD research[55].

1.5 NMD and human disease

The activity of nonsense-mediated decay affects the manifestation of numerous diseases of both simple and complex causes. Interestingly, many disease phenotypes are exacerbated by the effects of NMD while others are suppressed by them. Because of this, NMD acts as a "double-edged sword" regarding human health.

β-thalassemia is a genetic disorder characterized by ineffective hemoglobin production deriving from mutations in the β-globin gene. Most recessive forms of β-thalassemia result from nonsense mutations in either the first or second exon, and these transcripts elicit degradation by NMD. In these cases, expression of the unaffected allele is able to compensate for the mutated copy. However, mutations in the final exon evade degradation and are translated normally, resulting in the expression of truncated proteins[195]. Often, these proteins act as dominant negatives and interfere with normal hemoglobin production. In this manner, the inheritance pattern of simple genetic disorders can be influenced by whether the mutation is recognized by the NMD machinery[195,196].

The relevance of NMD to human maladies extends beyond simple Mendelian disorders. As mentioned previously, mutations in the NMD factor UPF3b are associated with multiple forms of mental retardation and autism[139-144]. NMD is also emerging as a prominent modulator of tumorigenesis due to its role in controlling the expression levels of oncogenes and tumor suppressor genes with PTCs[197,198]. For example, 80% of cancer-associated mutations in the E-cadherin tumor suppressor gene generate a PTC and are downregulated by NMD. Here, NMD promotes degradation of a tumor suppressor gene, making NMD activity detrimental to the individual. As a result, patients with NMD-sensitive mutations develop cancer at an earlier age than patients with NMD insensitive truncation mutations[197]. NMD factors are also mutated or overexpressed in a variety of human cancers: the newly discovered NMD factor Nbas is overexpressed in pediatric neuroblastomas, and UPF1 is commonly mutated in pancreatic adenosquamous carcinoma as well as inflammatory myofibroblastic tumors[199-203].

Comprehending how NMD dsyregulation affects such vital events as tumorigenesis and metastisis will have enormous implications for clinical therapeutics.

The protective capacity of NMD under stress conditions, while generally salubrious, can unfortunately be co-opted by cancer cells to promote tumor growth. For many tumors, harsh microenvironments fostered by chaotic vascularity limit valuable nutrients and oxygen and impede growth[175]. To overcome this impediment, tumor cells enact cellular responses that allow them to adapt and thrive in these unfavorable conditions. One such response is the inhibition of NMD. Indeed, NMD is repressed in an eIF2α-dependent manner in stressed tumor cells, and restoration of NMD activity by UPF1 overexpression significantly arrests tumor growth[171]. The profound influence that NMD wields on tumorigenesis in harsh cellular environments bespeaks an important role for NMD in coordinating the cellular stress response and makes it a promising target for the treatment of cancer.

Given its relevance to human health, NMD is an attractive target for treatment of many human diseases. Inhibiting NMD may alleviate the symptoms of certain genetic diseases caused by PTCs in a single gene—such as cystic fibrosis, β-thalassemia, Hurler's syndrome, and Duchenne muscular dystrophy—if the truncated protein products are functional or partially functional[195]. However, although nearly 30% of genetic disorders are caused by nonsense mutations, this therapeutic strategy is severely limited by its reliance on the truncated proteins retaining their functionality without disrupting cellular metabolism. To address this limitation, the Bedwell lab combined chemical NMD inhibitors, which stabilize nonsense transcripts and augment nonsense mRNA expression, with stop-codon read-through drugs, which promote read-through of the aberrant nonsense codon, partially restoring expression of full-length proteins

encoded by mutant alleles. They demonstrated the efficacy of this strategy in models of cystic fibrosis and Hurler's syndrome[204,205]. Furthering this work, Lawrence Gardner's group revealed that this strategy can be employed to restore p53 expression in cancer cells with nonsense mutations in the p53 gene, suggesting that this treatment strategy also represents a potential means of treating cancers driven by nonsense mutations in tumor suppressor genes[206].

Inhibition of NMD also represents a promising cancer therapeutic strategy for cancers whose transforming mutations don't elicit NMD. Cancer cells may have an elevated dependency on NMD for survival since they produce more nonsense RNAs as a result of their intrinsic genomic instability. As such, inhibiting NMD may lead to preferential killing of cancer cells. Furthermore, abrogation of NMD may result in the synthesis of novel, tumor-specific antigens on the surface of cancer cells which induce anti-tumor immune responses[207]. However, as mentioned previously, certain tumors actually thrive when NMD activity is low due to increased expression of stress-response genes[171]. Clearly the role of NMD in cancer biology is complex and highly context-dependent. More knowledge of how NMD contributes to cancer and other diseases will facilitate the targeting of NMD for therapeutic purposes and, for this reason, small-molecule inhibitors of NMD hold great promise for the treatment of genetic diseases including cancer. Moreover, such inhibitors may serve as chemical biology tools for probing the NMD process.

Many groups have searched for chemical inhibitors of NMD. When the Ohno group identified the PI3K-like kinase SMG1 as an NMD factor, they realized that classic inhibitors of this kinase family, such as wortmannin and caffeine, will inhibit NMD[79]. Indeed they do; however, these drugs have wide-ranging effects on cells and the concentrations required to

repress NMD are too toxic for clinical use. Years later, another inhibitor termed NMDI1 was identified in a screen for chemicals that disrupt the activity of certain splicing proteins[34]. NMDI1 blocks NMD by preventing the interaction between SMG5 and UPF1 and is a promising clinical candidate as no cellular toxicity is observed even at concentrations 25 times greater are required for substantial NMD inhibition[34]. In 2014, NMDI14, a potentially more promising chemical inhibitor of NMD, was identified in a computational screen for molecules that physically prevent the interaction of SMG7 with UPF1. NMDI14 works at nanomolar concentrations and exhibits minimal cellular toxicity[206]. However, given the low percentage of drugs that thrive in a clinical setting, the identification of more small-molecule NMD inhibitors will better the odds of successfully treating diseases by modulating NMD activity.

NMD has also proven useful in the identification of disease genes. Many disease alleles harbor nonsense mutations that are recognized by the NMD machinery. By charting the gene expression changes following NMD inhibition in diseased tissue, a list of candidates can be assembled[208]. In this manner, disease genes associated with colon, prostate, and breast cancers have already been identified[209-212]. With this advancement in methodology, the functional consequences of NMD serve as a critical diagnostic tool.

1.6 Methods of studying NMD

As we come to appreciate the physiological and clinical significance of NMD, it becomes increasingly necessary to possess tools capable of rapidly and accurately assessing NMD activity to expedite drug development and to fully characterize the mechanism and regulation of NMD. However, NMD research has often been hindered by low-throughput or poorly controlled methods of assessing NMD. In the early days of NMD research, scientists assessed the stability

of endogenous transcripts with pulse-chase experiments and northern blotting[49]. While still widely used today, this method lacks perfect controls and is inherently low-throughput. Over the next couple decades, a number of reporter genes were developed with known, characterized mutations (for example see ref 196). This greatly expanded the ability to mechanistically dissect the NMD pathway and allowed for much more controlled experiments but still relied on low-throughput RNA-based methods of assessing NMD—northern blot or qPCR. In the early 2000s, two groups tried to address the throughput issue by tethering reporter genes to fluorophores or luciferases[213,214]. However, these two reporters are limited by the lack of proper internal controls in the same cell. Recently, a new fluorescent reporter with better, although imperfect, controls capable of assessing NMD activity in single cells was introduced[215]. So for nearly 4 decades of NMD research, scientists have relied on low-throughput NMD assessment strategies that often lacked great controls and that precluded live cell or animal studies. In chapter 2, I describe a dual-color bioluminescent reporter that overcomes these obstacles.

1.7 Figures

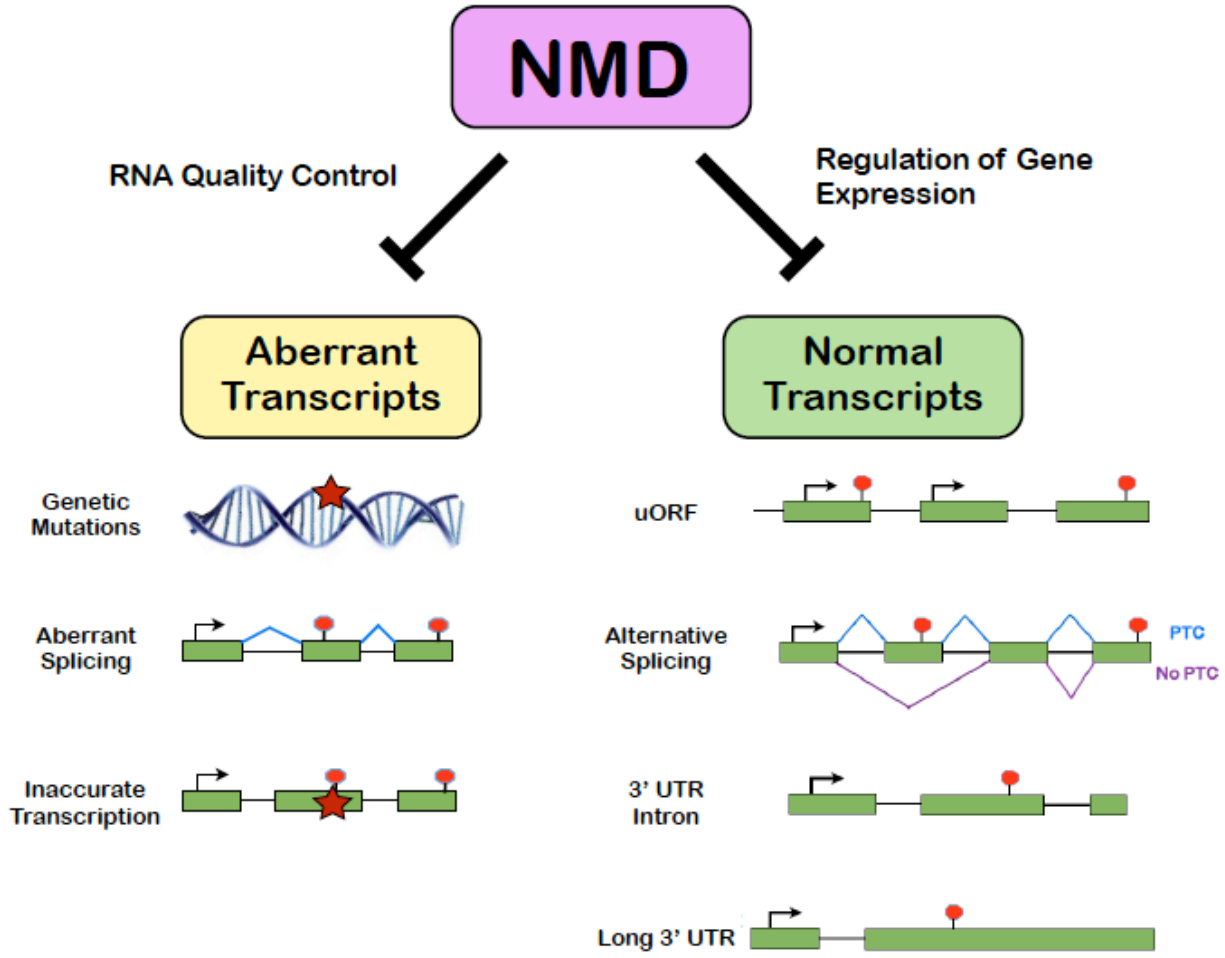

Figure 1: NMD Substrates.

NMD eliminates transcripts harboring premature termination codons (PTCs), thereby preserving the quality of the transcriptome and maintaining cellular homeostasis. PTCs arise in numerous ways—often from errors in nucleic acid metabolism including genetic mutations, aberrant splicing, and transcriptional aberrations. In addition to preventing expression of abnormal truncated proteins, NMD also represses expression of many normal genes whose mRNAs contain features recognizable to the NMD machinery.

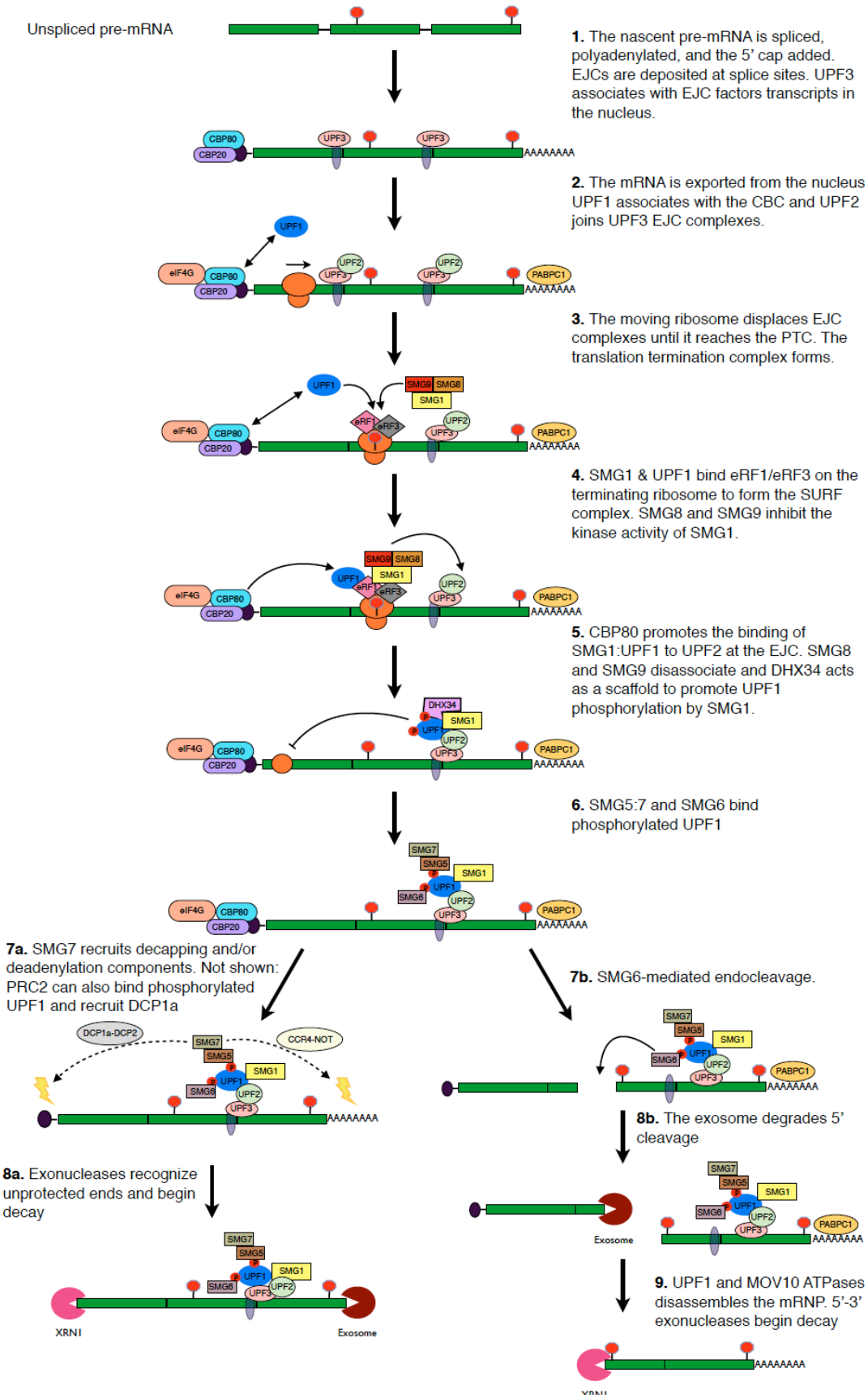
Unspliced pre-mRNA
1. The nascent pre-mRNA is spliced, polyadenylated, and the 5' cap added. EJCs are deposited at splice sites. UPF3 associates with EJC factors transcripts in the nucleus.
2. The mRNA is exported from the nucleus UPF1 associates with the CBC and UPF2 joins UPF3 EJC complexes.
3. The moving ribosome displaces EJC complexes until it reaches the PTC. The translation termination complex forms.
4. SMG1 & UPF1 bind eRF1/eRF3 on the terminating ribosome to form the SURF complex. SMG8 and SMG9 inhibit the kinase activity of SMG1.
5. CBP80 promotes the binding of SMG1:UPF1 to UPF2 at the EJC. SMG8 and SMG9 disassociate and DHX34 acts as a scaffold to promote UPF1 phosphorylation by SMG1.
6. SMG5:7 and SMG6 bind phosphorylated UPF1
7a. SMG7 recruits decapping and/or deadenylation components. Not shown: PRC2 can also bind phosphorylated UPF1 and recruit DCP1a
7b. SMG6-mediated endocleavage.
8a. Exonucleases recognize unprotected ends and begin decay
8b. The exosome degrades 5' cleavage
9. UPF1 and MOV10 ATPases disassembles the mRNP. 5'-3' exonucleases begin decay
CBP80
CBP20
UPF1
UPF2
UPF3
eIF4G
PABPC1
AAAAAAAA
SMG1
SMG5
SMG6
SMG7
SMG8
SMG9
eRF1
eRF3
DHX34
DCP1a-DCP2
CCR4-NOT
XRN1
Exosome

Figure 2: NMD mechanism.

NMD substrates are recognized and degraded through a series of biochemical events involving SMG proteins, UPF proteins, EJC proteins, and general RNA decay factors.

1.8 Tables

Table 1 **NMD factors and their functions**

Protein	Cellular Localization	Properties and Functions
Upf1	Primarily Cytoplasmic	Phosphorylated by SMG1; Recruits SMG5-7; Inhibits translation initiation; dissassembles mRNP
Upf2	Cytoplasmic (perinuclear)	Binds Upf1, Upf3, and RNA; Activates Upf1 helicase and ATPase activity.
Upf3a	Mainly Nuclear; Shuttles to cytoplasm	Binds EJC and later Upf2; Activates Upf1 helicase and ATPase activity. Weak inducer of NMD
Upf3b	Mainly Nuclear; Shuttles to cytoplasm	Binds EJC and later Upf2; Activates Upf1 helicase and ATPase activity. Destabilizes Upf3a protein.
SMG1	Cytoplasmic	Phosphorylates Upf1 at multiple residues;
SMG5	Mainly cytoplasmic, some in nucleus	Forms heterodimer with SMG7; binds Upf1; recruits phosphatase PP2A to dephosphorylate Upf1
SMG6	Mainly cytoplasmic, some in nucleus	Binds Upf1; Recruits phosphatase PP2A to dephosphorylate Upf1; Cleaves transcripts near PTC
SMG7	Mainly cytoplasmic, some in nucleus	Forms heterodimer with SMG5; recruits PP2A to dephosphorylate Upf1; Initiates decapping/deadenylation
SMG8	Cytoplasmic; may be in nucleus as well	Inhibits SMG1 kinase activity
SMG9	Cytoplasmic; may be in nucleus as well	Inhibits SMG1 kinase activity
NBAS	Unknown	Unknown
Dhx34	Cytoplasmic	Promotes phosphorylation of UPF1 by SMG1
GNL2	Nuclear	Unknown
SEC13	Nuclear membrane	Component of nuclear pore complex
Mov10	Cytosplasmic	RNA helicase; removes proteins and secondary structure from mRNP for decay
RUVBL1	Cytoplasmic	Promotes SMG1 kinase activity
RUVBL2	Cytosplasmic	Promotes SMG1 kinase activity
PNRC2	Cytoplasmic	Interacts with UPF1, promotes mRNA decapping by recruiting DCP1a
MARVELD1	Cytoplasmic	Negative regulator of SMG1 kinase activity

1.9 References

1) Mcllwain, D.R., Pan, Q., Reilly, P.T., Elia, A.J., McCracken, S., Wakeham, A.C., Itie-Youten, A., Blencowe, B.J. & Mak, T.W. Smg1 is required for embryogenesis and regulates diverse genes via alternative splicing coupled to nonsense-mediated mRNA decay. Proc Natl Acad Sci U S A 107, 12186-12191 (2010).

2) Medghalchi, S.M., Frischmeyer, P.A., Mendell, J.T., Kelly, A.G., Lawler, A.M. & Dietz, H.C. Rent1, a trans-effector of nonsense-mediated mRNA decay, is essential for mammalian embryonic viability. Hum Mol Genet. 10, 99–105 (2001).

3) Roberts, T.L., Ho, U., Luff, J., Lee C.S., Apte, S.H., MacDonald, K.P., Raggat, L.J., Pettit, A.R., Morrow, C.A., Waters, M.J., Chen, P., Woods, R.G., Thomas, G.P., St Pierre, L., Farah, C.S., Clarke, R.A., Brown, J.A. & Lavin, M.F. Smg1 haploinsufficiency predisposes to tumor formation and inflammation. Proc Natl Acad Sci U S A. 110, E285-294 (2013).

4) Thoren, L.A., Nørgaard, G.A., Weischenfeldt, J., Waage, J., Jakobsen, J.S., Damgaard, I., Bergström, F.C., Blom, A.M., Borup, R., Bisgaard, H.C. & Porse, B.T. UPF2 is a critical regulator of liver development, function and regeneration. PLoS One. e11650 (2010).

5) Weischenfeldt, J., Damgaard, I., Bryder, D., Theilgaard-Monch, K., Thoren, L.A., Nielsen, F.C., Jacobsen, S.E., Nerlov, C. & Porse, B.T. NMD is essential for hematopoietic stem and progenitor cells and for eliminating by-products of programmed DNA rearrangements. Genes Dev. 22, 1381-1396 (2008).

6) Li, T., Shi, Y., Wang, P., Guachalla, L.M., Sun, B., Joerss, T., Chen, Y.S., Groth, M., Krueger, A., Platzer, M., Yang, Y.G., Rudolph, K.L. & Wang, Z.Q. Smg6/Est1 licenses embryonic stem cell differentiation via nonsense-mediated mRNA decay. EMBO J. 34, 1630-1647 (2015).

7) Shum, E.Y., Jones, S.H., Shao, A., Dumdie, J., Krause, M.D., Chan, W.K., Lou, C.H., Espinoza, J.L., Song, H.W., Phan, M.H., Ramaiah, M., Huang, L., McCarrey, J.R., Peterson, K.J., De Rooij, D.G., Cook-Andersen, H. & Wilkinson, M.F. The antagonistic gene paralogs Upf3a and Upf3b govern nonsense-mediated RNA decay. Cell. 165, 382-395 (2016).

8) Longman, D., Plasterk, R.H., Johnstone, I.L. & Caceres, J.F. Mechanistic insights and identification of two novel factors in the C. elegans NMD pathway. Genes Dev. 21, 1075-1085 (2007).

9) Anastasaki, C., Longman, D., Capper, A., Patton E.E. & Caceres, J.F. Dhx34 and Nbas function in the NMD pathway and are required for embryonic development in zebrafish. Nucleic Acids Res. 39, 3686-3694 (2011).

10) Wittkopp, N., Huntzinger, E., Weiler, C., Saulière, J., Schmidt, S., Sonawane, M. & Izaurralde, E. Nonsense-mediated mRNA decay effectors are essential for zebrafish embryonic development and survival. Mol Cell Biol. 29, 3517-3528 (2009).

11) Zhang, S., Ruizechevarria, M.J., Quan, Y. & Peltz, S.W. Identification and characterization of a sequence motif involved in nonsense-mediated messenger RNA decay. Mol. Cell. Biol. 15, 2231–2244 (1995).

12) Gonzalez, C.I., Ruiz-Echevarria, M.J., Vasudevan, S., Henry, M.F. & Peltz, S.W. The yeast hnRNP-like protein Hrp1/Nab4 marks a transcript for nonsense-mediated mRNA decay. Mol. Cell 5, 489–499 (2000).

13) Muhlrad, D. & Parker, R. Aberrant mRNAs with extended 3' UTRs are substrates for rapid degradation by mRNA surveillance. RNA 5, 1299–1307 (1999).

14) Zhang, J., Sun, X.L., Qian, Y.M., LaDuca, J.P. & Maquat, L.E. At least one intron is required for the nonsense-mediated decay of triosephosphate isomerase mRNA: a possible link between nuclear splicing and cytoplasmic translation. Mol. Cell. Biol. 18, 5272–5283 (1998).

15) Carter, M.S., Li, S.L. & Wilkinson, M.F. A splicing dependent regulatory mechanism that detects translation signals. EMBO J. 15, 5965–5975 (1996).

16) Thermann, R., Neu-Yilik, G., Deters, A., Frede, U., Wehr, K., Hagemeier, C., Hentze, M.W. & Kulozic, A.E. Binary specification of nonsense codons by splicing and cytoplasmic translation. EMBO J. 17, 3484–3494 (1998).

17) The human intronless melanocortin 4-receptor gene is NMD insensitive. Hum. Mol. Genet. 11, 331–335 (2002).

18) Maquat, L.E. & Li, X. Mammalian heat shock p70 and histone H4 transcripts, which derive from naturally intronless genes, are immune to nonsense-mediated decay. RNA. 7, 445-456 (2001).

19) Lewis, B.P., Green, R.E. & Brenner, S.E. Evidence for the widespread coupling of alternative splicing and nonsense-mediated mRNA decay in humans. Proc Natl Acad Sci U S A. 100, 189-192 (2003).

20) Le Hir, H., Izaurralde, E., Maquat, L.E., and Moore, M.J. The spliceosome deposits multiple proteins 20-24 nucleotides upstream of mRNA exon-exon junctions. EMBO J. 19, 6860–6869 (2000).

21) Steckelberg, A., Boehm, V., Gromadzka, A.M. & Gehring, N.H. CWC22 connects pre-mRNA splicing and exon junction complex assembly. Cell Reports. 2, 454-461 (2012).

22) Le Hir, H., Gatfield, D., Izaurralde, E. & Moore, M.J. The exon-exon junction complex provides a binding platform for factors involved in mRNA export and nonsense-mediated mRNA decay. EMBO J. 20, 4987–4997 (2001).

23) Gehring, N.H., Neu-Yilik, G., Schell, T., Hentze, M.W. & Kulozik, A.E. Y14 and hUpf3b form an NMD-activating complex. Mol Cell 11, 939-949 (2003).

24) Viegas, M.H., Gehring, N.H., Breit, S., Hentze, M.W. & Kulozik, A.E. The abundance of RNPS1, a protein component of the exon junction complex, can determine the variability in efficiency of the nonsense mediated decay pathway. Nucleic Acids Res 35, 4542-4551 (2007).

25) Singh, K.K., Wachsmuth, L., Kulozik, A.E. & Gehring, N.H. Two mammalian MAGOH genes contribute to exon junction complex composition and nonsense-mediated decay. RNA Biol 10, 1291-1298 (2013).

26) Kim, V.K., Yong, J., Kataoka, N., Abel, L., Diem, M.D. & Dreyfuss, G. The Y14 protein communicates to the cytoplasm the position of exon-exon junctions. EMBO J 20, 2062-2068 (2001).

27) Dang, Y., Low, W.K., Xu, J., Gehring, N.H., Dietz, H.C., Romo, D. & Liu, J.O. Inhibition of nonsense-mediated mRNA decay by the natural product pateamine A through eukaryotic initiation factor 4AIII. J Biol Chem 284, 23613-23621 (2009).

28) Palacios, I.M., Gatfield, D., St Johnston, D. & Izaurralde, E. An eIF4AIII-containing complex required for mRNA localization and nonsense-mediated mRNA decay. Nature 427, 737-757 (2004).

29) Singh, G., Jakob, S., Kleedehn, M.G. & Lykke-Andersen, J. Communication with the exon-junction complex and activation of nonsense-mediated decay by human Upf proteins occur in the cytoplasm. Mol Cell. 27, 780-792 (2007).

30) Bono, F., Ebert, J., Unterholzner, L., Güttler, T., Izaurralde, E. & Conti, E. Molecular insights into the interaction of PYM with the Mago-Y14 core of the exon junction complex. EMBO Rep 5, 304-310 (2004).

31) Lykke-Andersen, J., Mei-Di, S. & Steitz, J.A. Communication of the position of exon-exon junctions to the mRNA surveillance machinery by the protein RNPS1. Science. 293, 1836-1839 (2001).

32) Takeshita, K., Forget, B.G., Scarpa, A. & Benz, E.J. Intranuclear defect in beta-globin mRNA accumulation due to a premature translation termination codon. Blood. 64, 13-22 (1984).

33) Cheng, J. & Maquat, L.E. Nonsense codons can reduce the abundance of nuclear mRNA without affecting the abundance of pre-mRNA or the half-life of cytoplamsic mRNA. Mol Cell Biol. 13, 1892-1902 (1993).

34) Durand, S., Cougot, N., Mahuteau-Betzer, F., Nguyen, C.H., Grierson, D.S., Bertrand, E., Tazi, J. & Lejeune, F. Inhibition of nonsense-mediated mRNA decay (NMD) by a new chemical molecule reveals the dynamic of NMD factors in P-bodies. J Cell Biol. 178, 1145-1160 (2007).

35) Sheth, U. & Parker, R. Targeting of aberrant mRNAs to cytoplasmic processing bodies. Cell. 125, 1095-1109 (2006).

36) Visa, N., Izaurralde, E., Ferreira, J., Daneholt, B. & Mattaj, I.W. A nuclear cap-binding complex binds Balbiani ring pre-mRNA cotranscriptionally and accompanies the ribonucleoprotein particle during nuclear export. J Cell Biol. 133, 5-14 (1996).

37) Izaurralde, E. Lewis, J., Gamberi, C., Jarmolowski, A., McGuigan, C. Mattaj, I.W. A cap-binding protein complex mediating U snRNA export. Nature. 376, 709-712 (1995).

38) Izaurralde, E., Lewis, J., McGuigan, C., Jankowska, M., Darzynkiewicz, E. & Mattaj, I.W. A nuclear cap binding protein complex involved in pre-mRNA splicing. Cell. 78, 657-668 (1994).

39) Lewis, J., Izaurralde, E., Jarmolowski, A., McGuigan, C. & Mattaj, I.W. A nuclear cap-binding complex facilitates association of U1 snRNP with the cap-proximal 5' splice site. Genes Dev. 10, 1683-1698 (1996).

40) Lejeune, F., Ishigaki, Y., Li, X. & Maquat, L.E. The exon junction complex is detected on CBP80-bound but not eIF4E-bound mRNA in mammalian cells: dynamics of mRNP remodeling. EMBO J. 21, 3536-3545 (2002).

41) Ishigaki, Y., Li, X., Serin, G. & Maquat, L.E. Evidence for a pioneer round of mRNA translation: mRNAs subject to nonsense-mediated decay in mammalian cells are bound by CBP80 and CBP20. Cell. 106, 607-617 (2001).

42) Dostie, J. & Dreyfuss, G. Translation is required to remove Y14 from mRNAs in the cytoplasm. Curr Biol. 12, 1060-1067 (2002).

43) Stephenson, L.S. & Maquat, L.E. Cytoplasmic mRNA for human triosephosphate isomerase is immune to nonsense-mediated decay despite forming polysomes. Biochemie. 78, 1043-1047 (1996).

44) Trcek, T., Sato, H., Singer, R.H. & Maquat, L.E. Temporal and spatial characterization of nonsense-mediated mRNA decay. Genes Dev. 27, 541-551 (2013).

45) Baboo, S., Bhushan, B., Jiang, H., Grovenor, C.R., Pierre, P., Davis, B.G. & Cook, P.R. Most human proteins made in both nucleus and cytoplasm turn over within minutes. PLoS One. 9, e99346 (2014).

46) Stalder, L. & Muhlemann, O. Processing bodies are not required for mammalian nonsense-mediated mRNA decay. RNA. 15, 1265-1273 (2009).

47) Eulalio, A., Behm-Ansmant, I., Schweizer, D. & Izaurralde, E. P-body formation is a consequence, not the cause, of RNA-mediated gene silencing. Mol Cell Biol. 27, 3970-3981 (2007).

48) Nagy, E. & Maquat, L. E. A rule for termination-codon position within intron-containing genes: when nonsense affects RNA abundance. Trends Biochem Sci. 23, 198–199 (1998).

49) Maquat, L.E., Kinniburgh, A.J., Rachmilewitz, E.A. & Ross, J. Unstable β-globin mRNA in mRNA-deficient β0 thalassemia. Cell 27, 543–553 (1981).

50) Frischmeyer, P.A. & Dietz, H.C. Nonsense-mediated mRNA decay in health and disease. Hum Mol Genet. 8, 1893-1900 (1999).

51) Weischenfeldt, J., Waage, J., Tian, G., Zhao, J., Damgaard, I., Jakobsen, J.S., Kristiansen, K., Krough, A., Wang, J. & Porse, B.T. Mammalian tissues defective in nonsense-mediated mRNA decay display highly aberrant splicing patterns. Genome Biol. 13, R35 (2012).

52) Sydow, J.F. & Cramer, P. RNA polymerase fidelity and transcriptional proofreading. Curr Opin Struct Biol. 19, 732–739 (2009).

53) Chapin, A., Hu, H., Rynearson, S.G., Hollien, J., Yandell, M. & Metzstein, M.M. In vivo determination of direct targets of the nonsense-mediated decay pathway in Drosophila. G3. 4, 485–96 (2014).

54) Yepiskoposyan, H., Aescimann, F., Nilsson, D., Okoniewski, M. & Mühlemann. Autoregulation of the nonsense-mediated mRNA decay pathway in human cells. RNA. 17, 2108-2118 (2011).

55) Malabat, C., Feuerbach, F., Ma, L., Saveanu, C. & Jacquier, A. Quality control of transcription start site selection by nonsense-mediated-mRNA decay. eLife 4, e06722 (2015).

56) Belew, A.T., Hepler, N.L., Jacobs, J.L. & Dinman, J.D. PRFdb: a database of computationally predicted eukaryotic programmed −1 ribosomal frameshift signals. BMC Genomics. 9, 339 (2008).

57) Belew, A.T., Advani, V.M. & Dinman, J.D. Endogenous ribosomal frameshift signals operate as mRNA destabilizing elements through at least two molecular pathways in yeast. Nucleic Acids Res. 39, 2799–2808 (2011).

58) Belew, A.T., Meskauskas, A., Musalgaonkar, S., Advani, V.M., Sulima, S.O., Kasprzak, W.K., Shapiro, B.A. & Dinman, J.D. Ribosomal frameshifting in the CCR5 mRNA is regulated by miRNAs and the NMD pathway. Nature. 512, 265-269 (2014).

59) Advani VM, Belew AT, Dinman JD. Yeast telomere maintenance is globally controlled by programmed ribosomal frameshifting and the nonsense-mediated mRNA decay pathway. Translation.1:e24418 (2013).

60) Barbosa, C., Peixeiro, I. & Romão, L. Gene expression regulation by upstream open reading frames and human disease. PLoS Genet. 9, e1003529 (2013).

61) Hurt, J. A., Robertson, A. D. & Burge, C. B. Global analyses of UPF1 binding and function reveal expanded scope of nonsense-mediated mRNA decay. Genome Res. 23, 1636–1650 (2013).

62) Shetty, S. P. & Copeland, P. R. Selenocysteine incorporation: a trump card in the game of mRNA decay. Biochimie 114, 97–101 (2015).

63) Seyedali, A. & Berry, M. J. Nonsense-mediated decay factors are involved in the regulation of selenoprotein mRNA levels during selenium deficiency. RNA 20, 1248–1256 (2014).

64) Usuki, F., Yamashita, A. & Fujimura, M. Post-transcriptional defects of antioxidant selenoenzymes cause oxidative stress under methylmercury exposure. J. Biol. Chem. 286,6641–6649 (2011).

65) Bruno, I.G., Karam, R., Huang, L., Bhardwaj, A., Lou, C.H., Shum, E.Y., Song. H.W., Corbett, M.A., Gifford, W.D., Gecz, J., Pfaff, S.L. & Wilkinson, M.F. Identification of a microRNA that activates gene expression by repressing nonsense-mediated RNA decay. Mol Cell. 42, 500-510 (2011).

66) Pulak, R. & Anderson, P. mRNA surveillance by the Caenorbaditis elegans smg genes. Genes Dev. 7, 1885-1897 (1993).

67) Leeds, P., Wood, J.M., Lee, B.S. & Culbertson, M.R. Gene products that promote mRNA turnover in Saccharomyces cerevisiae. Mol Cell Biol. 12, 2165-2177 (1992).

68) Leeds, P., Peltz, S.W., Jacobson, A. & Culbertson, M.R. The product of the yeast UPF1 gene is required for rapid turnover of mRNAs containing a premature translation termination codon. Genes Dev. 5, 2303-2314 (1991).

69) He, F. & Jacobson, A. Identification of a novel component of the nonsense-mediated mRNA decay pathway by use of an interacting protein screen. Genes Dev. 9, 437-454 (1995).

70) Hwang, J. & Maquat, L.E. Nonsense-mediated mRNA decay (NMD) in animal embryogenesis: to die or not to die, that is the question. Curr Opin Genet Dev. 21, 422-430 (2011).

71) Lykke-Andersen, J., Shu, M.D. & Steitz, J.A. Human Upf proteins target an mRNA for NMD when bound downstream of a termination codon. Cell. 103, 1121-1131 (2000).

72) Kim, Y.K., Furic, L., Desgroseillers, L. & Maquat, L.E. Mammalian Staufen1 recruits Upf1 to specific mRNA 3'UTRs so as to elicit mRNA decay. Cell. 120, 195-208 (2005).

73) Mendell, J.T., Rhys, C.M. & Dietz, H.C. Separable roles for rent1/hUpf1 in altered splicing and decay of nonsense transcripts. Science. 298, 419-422 (2005).

74) Sun, X., Perlick, H.A., Dietz, H.C. & Maquat, L.E. A mutated human homologue to yeast Upf1 protein has a dominant-negative effect on the decay of nonsense-containing mRNAs in mammalian cells. Proc Natl Acad Sci USA. 95, 10009-10014 (1998).

75) Ohnishi, T., Yamashita, A., Kashima, I., Schell, T., Anders, K.R., Grimson, A., Hachiya, T., Hentze, M.W., Anderson, P. & Ohno, S. Phosphorylation of hUPF1 induces formation of mRNA surveillance complexes containing hSMG-5 and hSMG-7. Mol. Cell. 12, 1187-1200 (2003).

76) Okada-Katsuhata, Y., Yamashita, A., Kutsuzawa, K., Izumi, N., Hirahara, F. & Ohno, S. N- and C-terminal Upf1 phosphorylations create binding platforms for SMG-6 and SMG-5:SMG-7 during NMD. Nuc Acids Res. 40, 1251-1266 (2012).

77) Kashima, I. Yamashita, A., Izumi, N., Kataoka, N., Morishita, R., Hoshino, S., Ohno, M., Dreyfuss, G. & Ohno, S. Binding of a novel SMG-1-UPF1-eRF1-eRF3 complex (SURF) to the exon junction complex triggers UPF1 phosphorylation and nonsense-mediated mRNA decay. Genes Dev. 20, 355-367 (2006).

78) Serin, G., Gersappe, A., Black, J., Aronoff, R. & Maquat, L.E. Identification and characterization of human orthologues to Saccharomyces cerevisiae Upf2 protein and Upf3 protein (caenorhabditis elegancs SMG-4). Mol Cell Biol. 21, 209-223 (2001).

79) Yamashita, A., Ohnishi, T., Kashima, I., Taya, Y. & Ohno, S. Human SMG-1, a novel phosphatidylinositol 3-kinase-related protein kinase, associates with components of the mRNA surveillance complex and is involved in the regulation of nonsense-mediated decay. Genes Dev. 15, 2215-2228 (2001).

80) Franks, T.M., Singh, G. & Lykke-Andersen, J. Upf1 ATPase-dependent mRNP dissassembly is required for completion of nonsense-mediated mRNA decay. Cell. 143, 938-950 (2011).

81) Bhattacharya, A., Czaplinski, K., Trifillis, P., He, F., Jacobson, A. & Peltz, S.W. Characterization of the biochemical properties of the human Upf1 gene product that is involved in nonsense-mediated mRNA decay. RNA. 6, 1226-1235 (2000).

82) Lejeune, F., Ranganathan, A.C. & Maquat, L.E. eIF4G is required for the pioneer round of translation in mammalian cells. Nat Struct Mol Biol. 11, 992-1000 (2004).

83) Ivanov, P. V., Gehring, N. H., Kunz, J. B., Hentze, M. W. & Kulozik, A. E. Interactions between UPF1, eRFs, PABP and the exon junction complex suggest an integrated model for mammalian NMD pathways. EMBO J. 27, 736–747 (2008).

84) Behm-Ansmant, I., Gatfield, D., Rehwinkel, J., Hilgers, V. & Izaurralde, E. A conserved role for cytoplasmic poly(A)-binding protein 1 (PABPC1) in nonsense-mediated mRNA decay. EMBO J. 26, 1591–1601 (2007).

85) Silva, A. L., Ribeiro, P., Inacio, A., Liebhaber, S. A. & Romao, L. Proximity of the poly(A)-binding protein to a premature termination codon inhibits mammalian nonsense-mediated mRNA decay. RNA 14, 563–576 (2008).

86) Singh, G., Rebbapragada, I. & Lykke-Andersen, J. A competition between stimulators and antagonists of Upf complex recruitment governs human nonsense-mediated mRNA decay. PLoS Biol. 6, e111 (2008).

87) Fatscher, T., Boehm, V., Weiche, B. & Gehring, N. H. The interaction of cytoplasmic poly (A)-binding protein with eukaryotic initiation factor 4G suppresses nonsense-mediated mRNA decay. RNA 20, 1579–1592 (2014).

88) Joncourt, R., Eberle, A. B., Rufener, S. C. & Muhlemann, O. Eukaryotic initiation factor 4G suppresses nonsense-mediated mRNA decay by two genetically separable mechanisms. PLoS ONE 9, e104391 (2014).

89) Inacio, A., Silva, A.L., Pinto, J., Ji, X., Morgado, A., Almeida, F., Faustino, P., Lavinha, J., Liebhaber,S.A. & Romão, L. Nonsense mutations in close proximity to the initiation codon fail to trigger full nonsense-mediated mRNA decay. J. Biol. Chem. 279, 32170–32180 (2004).

90) Neu-Yilik, G., Amthor, B., Gehring, N.H., Bahri, S., Paidassi, H., Hentze, M.W. & Kulozik, A.E. Mechanism of escape from nonsense-mediated mRNA decay of human β-globin transcripts with nonsense mutations in the first exon. RNA 17, 843–854 (2011).

91) Peixeiro, I., Inácio, Â., Barbosa, C., Silva, A.L., Liebhaber, S.A. & Romão, L. Interaction of PABPC1 with the translation initiation complex is critical to the NMD resistance of AUG-proximal nonsense mutations. Nucleic Acids Res. 40,1160–1173 (2012).

92) Huang, L., Lou, C.H., Chan, W., Shum, E.Y., Shao, A., Stone, E., Karam, R., Song, H.W. & Wilkinson, M.F. RNA homeostasis governed by cell type-specific and branched feedback loops acting on NMD. Mol. Cell 43, 950–961 (2011).

93) Hogg, J. R. & Goff, S. P. Upf1 senses 3′ UTR length to potentiate mRNA decay. Cell 143,379–389 (2010).

94) Eberle, A. B., Stalder, L., Mathys, H., Orozco, R. Z. & Muhlemann, O. Posttranscriptional gene regulation by spatial rearrangement of the 3′ untranslated region. PLoS Biol. 6, e92 (2008).

95) Buhler, M., Steiner, S., Mohn, F., Paillusson, A. & Muhlemann, O. EJC-independent degradation of nonsense immunoglobulin-μ mRNA depends on 3′ UTR length. Nat. Struct. Mol. Biol. 13, 462–464 (2006).

96) Kurosaki, T. & Maquat, L. E. Rules that govern UPF1 binding to mRNA 3′ UTRs. Proc. Natl Acad. Sci. USA 110, 3357–3362 (2013).

97) Zund, D., Gruber, A.R., Zavolan, M. & Muhlemann, O. Translation-dependent displacement of UPF1 from coding sequences causes its enrichment in 3' UTRs. Nat Struct Mol Biol 20, 936–943 (2013).

98) Kurosaki, T., Li, W., Hoque, M., Popp, M.W., Ermolenko, D.N., Tian, B. & Maquat, L.E. A post-translational regulatory switch on UPF1 controls targeted mRNA degradation. Genes Dev. 28, 1900–1916 (2014).

99) Toma, K. G., Rebbapragada, I., Durand, S. & Lykke-Andersen, J. Identification of elements in human long 3′ UTRs that inhibit nonsense-mediated decay. RNA 21, 887–897 (2015).

100) Isken, O., Kim, Y.K., Hosoda, N., Mayeur, G.L., Hershey, J. & Maquat, L.E. Upf1 phosphorylation triggers translational repression during nonsense-mediated mRNA decay. Cell. 133, 314-327 (2008).

101) Unterholzner, L. & Izaurralde, E. SMG7 acts as a molecular link between mRNA surveillance and mRNA decay. Mol Cell. 16, 587-596 (2004).

102) Huntzinger, E. & Kashima, I., Fauser, M., Sauliere, J. & Izaurralde, E. SMG6 is the catalytic endonuclease that cleaves mRNAs containing nonsense codons in metazoans. RNA. 14, 2609-2917 (2008).

103) Eberle, A.B., Lykke-Andersen, S., Muhlemann, O. & Jensen, T.H. SMG6 promotes endonucleolytic cleavage of nonsense mRNA in human cells. Nat Struct Mol Biol. 16, 49-55 (2009).

104) Chia, S., Serin, G., Ohara, O. & Maquat, L.E. Characterization of human Smg5/7a: A protein with similarities to Caenorhabditis elegans SMG5 and SMG7 that functions in the dephosphorylation of Upf1. RNA. 9: 77-87 (2003).

105) Anders, K. R., Grimson, A. & Anderson, P. SMG-5, required for C. elegans nonsense-mediated mRNA decay, associates with SMG-2 and protein phosphatase 2A. EMBO J. 22: 641–650 (2003).

106) Durand, S., Franks, T.M. & Lykke-Andersen, J. Hyperphosphorylation amplifies UPF1 activity to resolve stalls in nonsense-mediated mRNA decay (2016).

107) Gregersen, L.H., Schueler, M., Munschauer, M., Mastrobuoni, G., Chen, W., Kempa, S., Dieterich, C. & Landthaler, M. MOV10 is a 5’ to 3’ RNA helicase contributing to UPF1 mRNA target degradation by translocating along 3’ UTRs. Mol Cell. 54, 573-585 (2014).

108) Chamieh, H., Ballut, L., Bonneau, F. & Le Hir, H. NMD factors UPF2 and UPF3 bridge UPF1 to the exon junction complex and stimulate its RNA helicase activity. Nat Struct Mol Biol. 15, 85-93 (2008).

109) Kadlec, J., Izaurralde, E. & Cusack, S. The structural basis for the interaction between nonsense-mediated mRNA decay factors UPF2 and UPF3. Nat Struct Mol Biol. 11, 330-337 (2004).

110) Chakrabarti, S., Jayachandran, U., Bonneau, F., Fiorini, F., Basquin, C., Domcke, S., Le Hir, H. & Conti, E. Molecular mechanisms for the RNA-dependent ATPase activity of Upf1 and its regulation by Upf2. Mol. Cell 41, 693–703 (2011).

111) Tatsuno, T., Nakamura, Y., Ma, S., Tomosugi, N. & Ishigaki, Y. Nonsense-mediated mRNA decay factor Upf2 exists in both the nucleoplasm and the cytoplasm. Mol Med Rep 14, 655-660 (2016).

112) Chan, W.K., Bhalla, A.D., Le Hir, H., Nguyen, L.S., Huang, L., Gecz, J. & Wilkinson, M.F. A UPF3-mediated regulatory switch that maintains RNA surveillance. Nat Struct Mol Biol. 16, 747-753 (2009).

113) Kunz, J.B., Neu-Yilik, G., Hentze, M.W., Kulozik, A.E. & Gehring, N.H. Functions of hUpf3a and hUpf3b in nonsense-mediated mRNA decay and translation. RNA. 12, 1015-1022 (2006).

114) Arias-Palomo, E. Yamashita, A., Fernandez, I.S., Nunez-Ramirez, R., Bamba, Y., Ohno, S. & Llorca, O. The nonsense-mediated mRNA decay SMG-1 kinase is regulated by large-scale conformational changes controlled by SMG-8. Genes Dev. 25, 153-164 (2011).

115) Yamashita, A., Izumi, N., Kashima, I., Ohnishi, T., Saari, B., Katsuhata, Y., Muramatsu, R., Morita, T., Iwamatsu, A., Hachiya, T., Kurata, R., Hirano, H., Anderson, P. & Ohno, S. SMG-8 and SMG-9, two novel subunits of the SMG-1 complex, regulate remodeling of the mRNA surveillance complex during nonsense-mediated mRNA decay. Genes Dev. 23, 1091-1105 (2009).

116) Deniaud, A., Karuppasamy, M., Bock, T., Masiulis, S., Huard, K., Garzoni, F., Kerschgens, K., Hentze, M.W., Kulozik, A.E., Beck, M., Neu-Yilik, G. & Schaffitzel, C. A network of SMG-8, SMG-9 and SMG-1 C-terminal insertion domain regulates UPF1 substrate recruitment and phosphorylation. Nucleic Acids Res. 43, 7600-7611 (2015).

117) Izumi, N., Yamashita, A., Iwamatsu, A., Kurata, R., Nakamura, H., Saari, B., Hirano, H., Anderson, P. & Ohno, S. AAA+ proteins RUVBL1 and RUVBL2 coordinate PIKK activity and function in nonsense-mediated mRNA decay. Sci Signal. 3, ra27 (2010).

118) Melero, R., Hug, N., López-Perrote, A., Yamashita, A., Cáceres, J.F. & Llorca, O. The RNA helicase DHX34 functions as a scaffold for SMG1-mediated UPF1 phosphorylation. Nat Commun. 7, 10585 doi: 10.1038/ncomms10585 (2016).

119) Hu, J., Li, Y. & Li, P. MARVELD1 inhibits nonsense-mediated RNA decay by repressing serine phosphorylation of UPF1. PLoS One. 8, e68291 (2013).

120) Kashima, I., Jonas, S., Jayachandran, U., Buchwald, G., Conti, E., Lupas, A.N. & Izaurralde, E. SMG6 interacts with the exon junction complex via two conserved EJC-binding motifs (EBMs) required for nonsense-mediated mRNA decay. Genes Dev. 24, 2440-2450 (2010).

121) Cao, D. & Parker, R. Computational modeling and experimental analysis of nonsense-mediated decay in yeast. Cell. 113, 533-45 (2003).

122) Muhlrad, D. & Parker, R. Premature translational termination triggers mRNA decapping. Nature. 370, 578-81 (2004).

123) Mitchell, P. & Tollervey, D. An NMD pathway in yeast involving accelerated deadenylation and exosome-mediated 3' → 5' degradation. Mol Cell. 11, 1405-13 (2003).

124) Takahashi, S., Araki, Y., Sakuno, T. & Katada, T. Interaction between Ski7p and Upf1p is required for nonsense-mediated 3'-to-5' mRNA decay in yeast. EMBO J. 22, 3951-9 (2003).

125) Lejeune, F., Li, X. & Maquat, L.E. Nonsense-mediated mRNA decay in mammalian cells involves decapping, deadenylation, and exonucleolytic activities. Mol Cell. 12, 675-687 (2003).

126) Lykke-Andersen J. Identification of a human decapping complex associated with the hUpf proteins in nonsense-mediated decay. Mol. Cell. Biol. 22, 8114-8121 (2002).

127) Chen, C.Y. & Shyu, A.B. Rapid deadenylation triggered by a nonsense codon precedes decay of the RNA body in a mammalian cytoplasmic nonsense-mediated decay pathway. Mol Cell Biol. 23, 4805-4813 (2003).

128) Coullet, P. & Grange, T. Premature termination codons enhance mRNA decapping in human cells. Nucleic Acids Res. 32, 488-494 (2004).

129) Yamashita, A., Chang, T.C., Yamashita, Y., Zhu, W., Zhong, Z., Chen, C.Y. & Shyu, A.B. Concerted action of poly(A) nucleases and decapping enzyme in mammalian mRNA turnover. Nat Struct Mol Biol. 12, 1054-1063 (2005).

130) Cho H., Kim K.M., Kim Y.K. Human proline-rich nuclear receptor coregulatory protein 2 mediates an interaction between mRNA surveillance machinery and decapping complex. Mol Cell. 33, 75-86 (2009).

131) Lai T., Cho H., Liu Z., Bowler M.W., Piao S., Parker R., Kim Y.K., Song H. Structural basis of the PNRC2-mediated link between mrna surveillance and decapping. Structure.20, 2025-2037 (2012).

132) Lykke-Andersen, S., Chen, Y., Ardal, B.R., Lilje, B., Waage, J., Sandelin, A. & Jensen, T.H. Human nonsense-mediated RNA decay initiates widely by endonucleolysis and targets snoRNA host genes. Genes Dev. 28, 2498-2517 (2014).

133) Schmidt, S.A., Foley, P.L., Jeong, D.H., Rymarquis, L.A., Doyle, F., Tenenbaum, S.A., Belasco, J.G. & Green, P.J. Identification of SMG6 cleavage sites and a preferred RNA cleavage motif by global analysis of endogenous NMD targets in human cells. Nucleic Acids Res. 43, 309-323 (2015).

134) Casadia, A., Longman, D., Hug, N., Delavaine, L., Vallejos Baier, R., Alonso, C.R. & Cáceres, J.F. Identification and characterization of novel factors that act in the nonsense-mediated mRNA decay pathway in nematodes, flies and mammals. EMBO Rep. 16, 71-78 (2015).

135) Gudikote, J.P. & Wilkinson, M.F. T-cell Receptor Sequences that elicit Strong Downregulation of Premature Termination Codon-bearing Transcripts. EMBO Journal 21, 125-134 (2002).

136) Frischmeyer-Guerrerio, P.A., Montgomery, R.A., Warren, D.S., Cooke, S.K., Lutz, J., Sonnenday, C.J., Guerrerio, A.L. & Dietz, H.C. Perturbation of thymocyte development in nonsense-mediated decay (NMD)-deficient mice. Proc Natl Acad Sci U S A. 108, 10638-10643 (2011).

137) Chan, W., Huang, L., Gudikote, J.P., Chang, Y., Imam, J.S., MacLean II, J.A. & Wilkinson, M.F. An alternative branch of the nonsense-mediated decay pathway. EMBO J. 26, 1820-1830 (2007).

138) Gehring, N.H., Kunz, J.B., Neu-Yilik, G., Breit, S., Viegas, M.H., Hentze, M.W. & Kulozik A.E. Exon-junction complex components specify distinct routes of nonsense-mediated mRNA decay with differential cofactor requirements. Mol Cell 20, 65–75 (2005).

139) Tarpey, P.S., Raymond, F.L., Nguyen, L.S., Rodriguez, J., Hackett, A., Vandeleur, L., Smith, R., Shoulbridge, C., Edkins, S., Stevens, C., O'Meara, S., Tofts, C., Barthorpe, S., Buck, G., Cole, J., Halliday, K., Hills, K., Jones, D., Mironenko, T., Perry, J., Varian, J., West, S., Widaa, S., Teague, J., Dicks, E., Butler, A., Menzies, A., Richardson, D., Jenkinson, A., Shepherd, R., Raine, K., Moon, J., Luo, Y., Parnau, J., Bhat, S., Gardner, A., Corbett, M., Brooks, D., Thomas, P., Parkinson-Lawrence, E., Porteous, M., Warner, J., Sanderson, T., Pearson, P., Simensen, R., Skinner, C., Hoganson, G., Superneau, D., Wooster, R., Bobrow, M., Turner, G., Stevenson, R., Schwartz, C., Futreal, P., Srivastava, A., Stratton, M. & Gecz, J. Mutations in UPF3B, a member of the nonsense-mediated mRNA decay complex, cause syndromic and nonsyndromic mental retardation. Nat Genet. 39, 1127-1133 (2007).

140) Nguyen, L.S., Kim, H.G., Rosenfeld, J.A., Shen, Y., Gusella, J.F., Lacassie, Y., Layman, L.C., Shaffer, L.G. & Gécz, J. Contribution of copy number variants involving nonsense-mediated mRNA decay pathway genes to neuro-developmental disorders. Hum Mol Genet. 22, 1816-1825 (2013).

141) Addington, A.M., Gauthier, J., Piton, A., Hamdan, F.F., Raymond, A., Gogtay, N., Miller, R., Tossell, J., Bakalar, J., Inoff-Germain, G., Gochman, P., Long, R., Rapoport, J.L. & Rouleau, G.A. A novel frameshift mutation in UPF3B identified in brothers affected with

childhood onset schizophrenia and autism spectrum disorders. Mol Psychiatry. 16, 238-239 (2011).

142) Laumonnier, F., Shoubridge, C., Antar, C., Nguyen, L.S., Van Esch, H., Kleefstra, T., Briault, S., Fryns, J.P., Hamel, B., Chelly, J., Ropers, H.H., Ronce, N., Blesson, S., Moraine, C., Gécz, J. & Raynaud, M. Mutations of the UPF3B gene, which encodes a protein widely expressed in neurons, are associated with nonspecific mental retardation with or without autism. Mol Psychiatry. 15, 767-776 (2010).

143) Jolly, L.A., Homan, C.C., Jacob, R., Barry, S. & Gécz, J. The UPF3B gene, implicated in intellectual disability, autism, ADHD and childhood onset schizophrenia regulates neural progenitor cell behaviour and neuronal outgrowth. Hum Mol Genet. 22, 4673-4687 (2013).

144) Xu, X., Zhang, L., Tong, P., Xun, G., Su, W., Xiong, Z., Zhu, T., Zheng, Y., Luo, S., Pan, Y., Xia, K. & Hu, Z. Exome sequencing identifies UPF3B as the causative gene for a Chinese non-syndrome mental retardation pedigree. Clin Genet. 83, 560–564 (2013).

145) Long, A.A., Mahapatra, C.T., Woodruff, E.A., Rohrbough, J., Leung, H.T., Shino, S., An, L., Doerge, R.W., Metzstein, M.M., Pak, W.L. & Broadie, K. The nonsense-mediated decay pathway maintains synapse architecture and synaptic vesicle cycle efficacy. J Cell Sci. 123, 3303-3315 (2010).

146) Giorgi, C., Yeo, G.W., Stone, M.E., Katz, D.B., Burge, C., Turrigiano, G. & Moore, M.J. The EJC factor eIF4AIII modulates synaptic strength and neuronal protein expression. Cell. 130, 179-191 (2007).

147) Colak, D., Ji, S.J., Porse, B.T. & Jaffrey, S.R. Regulation of axon guidance by compartmentalized nonsense-mediated mRNA decay. Cell. 153, 1252-1265 (2013).

148) Eom, T., Zhang, C., Wang, H., Lay, K., Fak, J., Noebels, J.L. & Darnell, R.B. NOVA-dependent regulation of cryptic NMD exons controls synaptic protein levels after seizure. Elife. 2, e00178 (2013).

149) Ni, J.Z., Grate, L., Donohue, J.P., Preston, C., Nobida, N., O'Brien, G., Shiue, L., Clark, T.A., Blume, J.E. & Ares, M. Jr. Ultraconserved elements are associated with homeostatic control of splicing regulators by alternative splicing and nonsense-mediated decay. Genes Dev. 21, 708-718 (2007).

150) Lareau, L.F., Inada, M., Green, R.E., Wengrod, J.C. & Brenner, S.E. Unproductive splicing of SR genes associated with high conserved and ultraconserved DNA elements. Nature. 446, 926-929 (2007).

151) Saltzman, A. L., Kim, Y.K., Pan, Q., Fagnani, M.M., Maquat, L.E. & Blencowe, B.J. Regulation of multiple core spliceosomal proteins by alternative splicing-coupled nonsense-mediated mRNA decay. Mol. Cell. Biol. 28, 4320–4330 (2008).

152) Sureau, A., Gattoni, R., Dooghe, Y., Stevenin, J. & Soret, J. SC35 autoregulates its expression by promoting splicing events that destabilize its mRNAs. EMBO J. 20,1785–1796 (2001).

153) Wollerton, M. C., Gooding, C., Wagner, E. J., Garcia-Blanco, M. A. & Smith, C. W. Autoregulation of polypyrimidine tract binding protein by alternative splicing leading to nonsense-mediated decay. Mol. Cell 13, 91–100 (2004).

154) Avery, P., Vicente-Crespo, M., Francis, D., Nashchekina, O., Alonso, C.R. & Palacios, I.M. Drosophila Upf1 and Upf2 loss of function inhibits cell growth and causes animal death in a Upf3-independent manner. RNA. 17, 624-638 (2011).

155) Nelson, J.O., Moore, K.A., Chapin, A., Hollien, J. & Metzstein, M.M. Degradation of Gadd45 mRNA by nonsense-mediated decay is essential for viability. Elife. 5, e12876 (2016).

156) Taft, R.J., Pheasant, M. & Mattick, J.S. The relationship between non-protein-coding DNA and eukaryotic complexity. BioEssays. 29, 288–299 (2007).

157) Djebali, S., Davis, C.A., Merkel, A., Dobin, A., Lassmann, T., Mortazavi, A., Tanzer, A., Lagarde, J., Lin, W., Schlesinger, F., Xue, C., Marinov, G.K., Khatun, J., Williams, B.A., Zaleski, C., Rozowsky, J., Röder, M., Kokocinski, F., Abdelhamid, R.F., Alioto, T., Antoshechkin, I., Baer, M.T., Bar, N.S., Batut, P., Bell, K., Bell, I., Chakrabortty, S., Chen, X., Chrast, J., Curado, J., Derrien, T., Drenkow, J., Dumais, E., Dumais, J., Duttagupta, R., Falconnet, E., Fastuca, M., Fejes-Toth, K., Ferreira, P., Foissac, S., Fullwood, M.J., Gao, H., Gonzalez, D., Gordon, A., Gunawardena, H., Howald, C., Jha, S., Johnson, R., Kapranov, P., King, B., Kingswood, C., Luo, O.J., Park, E., Persaud, K., Preall, J.B., Ribeca, P., Risk, B., Robyr, D., Sammeth, M., Schaffer, L., See, L.H., Shahab, A., Skancke, J., Suzuki, A.M., Takahashi, H., Tilgner, H., Trout, D., Walters, N., Wang, H., Wrobel, J., Yu, Y., Ruan, X., Hayashizaki, Y., Harrow, J., Gerstein, M., Hubbard, T., Reymond, A., Antonarakis, S.E., Hannon, G., Giddings, M.C., Ruan, Y., Wold, B., Carninci, P., Guigó, R. & Gingeras, T.R. Landscape of transcription in human cells. Nature. 489, 101–108 (2012).

158) Batista, P.J. & Chang, H.Y. Long noncoding RNAs: cellular address codes in development and disease. Cell. 152, 1298–1307 (2013).

159) Guttman, M., Amit, I., Garber, M., French, C., Lin, M.F., Feldser, D., Huarte, M., Zuk, O., Carey, B.W., Cassady, J.P., Cabili, M.N., Jaenisch, R., Mikkelsen, T.S., Jacks, T., Hacohen,

N., Bernstein, B.E., Kellis, M., Regev, A., Rinn, J.L. & Lander, E.S. Chromatin signature reveals over a thousand highly conserved large non-coding RNAs in mammals. Nature. 458, 223–227 (2009).

160) Ingolia, N.T., Lareau, L.F. & Weissman, J.S. Ribosome profiling of mouse embryonic stem cells reveals the complexity and dynamics of mammalian proteomes. Cell. 147, 789–802 (2011).

161) Brar, G.A., Yassour, M., Friedman, N., Regev, A., Ingolia, N.T., and Weissman, J.S. High-resolution view of the yeast meiotic program revealed by ribosome profiling. Science. 335, 552–557 (2012).

162) Chew, G.-L., Pauli, A., Rinn, J.L., Regev, A., Schier, A.F. & Valen, E. Ribosome profiling reveals resemblance between long non-coding RNAs and 5' leaders of coding RNAs. Development. 140, 2828–2834 (2013).

163) van Heesch, S., van Iterson, M., Jacobi, J., Boymans, S., Essers, P.B., de Bruijn, E., Hao, W., Macinnes, A.W., Cuppen, E., and Simonis, M. Extensive localization of long noncoding RNAs to the cytosol and mono and polyribosomal complexes. Genome Biol. 15, R6 (2014).

164) Smith, J.E., Alvarez-Dominguez, J.R., Kline, N., Huynh, N.J., Geisler, S., Hu, W., Coller, J. & Baker, K.E. Translation of small open reading frames within unannotated RNA transcripts in Saccharomyces cerevisiae. Cell Rep. 7, 1858-1866 (2014).

165) Wery, M., Descrimes, M., Vogt, N., Dallongeville, A.S., Gautheret, D. & Morillon, A. Nonsense-mediated decay restricts lncRNA levels in yeast unless blocked by double-stranded RNA structure. Mol Cell. 61, 379-392 (2016).

166) Lelivelt, M.J. & Culbertson, M.R. Yeast Upf proteins required for RNA surveillance affect global expression of the yeast transcriptome. Mol Cell Biol. 19, 6710-6719 (1999).

167) Mendell, J.T., Sharifi, N.A., Meyers, J.L., Matinez-Murillo, R. & Dietz, H.C. Nonsense surveillance regulates expression of diverse classes of mammalian transcripts and mutes genomic noise. Nat Genet. 36, 1073-1078 (2004).

168) Wittmann, J., Hol, E.M. & Hans-Martin, J. hUPF2 silencing identifies physiologic substrates of mammalian nonsense-mediated mRNA decay. Mol Cell Biol. 26, 1272-1287 (2006).

169) Tani, H., Imamachi, N., Salam, K.A., Mizutani, R., Ijiri, K., Irie, T., Yada, T., Suzuki, Y. & Akimitsu, N. Identification of hundreds of novel UPF1 target transcripts by direct determination of whole transcriptome stability.

170) Gardner, L.B. Hypoxic inhibition of nonsense-mediated RNA decay regulates gene expression and the integrated stress response. Mol Cell Biol. 28, 3729-3741 (2008).

171) Wang, D., Zavadil, J., Martin, L., Parisi, F., Friedman, E., Levy, D., Harding, H., Ron, D. & Gardner, L.B. Inhibition of nonsense-mediated RNA decay by the tumor microenvironment promotes tumorigenesis. Mol Cell Biol. 31, 3670-3680 (2011).

172) Martin, L. & Gardner, L.B. Stress-induced inhibition of nonsense-mediated RNA decay regulates intracellular cystine transport and intracellular glutathione through regulation of the cystine/glutamate exchanger SLC7A11. Oncogene. 34, 4211-4218 (2015).

173) Karam, R., Lou, C.H., Kroeger, H., Huang, L., Lin, J.H. & Wilkinson, M.F. The unfolded protein response is shaped by the NMD pathway. EMBO Rep 16, 599-609 (2015).

174) Oren, Y.S., McClure, M.L., Rowe, S.M., Sorcher, E.J., Bester, A.C., Manor, M., Kerem, E., Rivlin, J., Zahdeh, F., Mann, M., Geiger, T. & Kerem, B. The unfolded protein response affects readthrough of premature termination codons. EMBO Mol Med 6, 685-701 (2014).

175) Gardner, L.B. Nonsense-mediated RNA decay regulation by cellular stress: implications for tumorigenesis. Mol Cancer Res. 8, 295-308 (2010).

176) Blais, J. D., Filipenko, V., Bi, M., Harding, H. P., Ron, D., Koumenis, C., Wouters, B. G. & Bell, J.C. Activating transcription factor 4 is translationally regulated by hypoxic stress. Mol Cell Biol. 24, 7469–7482 (2004).

177) Nemetski, S. M. & Gardner, L. B. Hypoxic regulation of Id-1 and activation of the unfolded protein response are aberrant in neuroblastoma. J Biol Chem. 282, 240–248 (2007).

178) Buzina, A. & Shulman, M. J. Infrequent translation of a nonsense codon is sufficient to decrease mRNA level. Mol Biol Cell. 10, 515–524 (1999).

179) Marin-Vinader, L., van Genesen, S. T. & Lubsen, N. H. mRNA made during heat shock enters the first round of translation. Biochim Biophys Acta. 1759, 535–542 (2006).

180) Oh, N., Kim, K. M., Cho, H., Choe, J. & Kim, Y. K. Pioneer round of translation occurs during serum starvation. Biochem Biophys Res Commun. 362, 145–151 (2007).

181) Popp, M.W. & Maquat, L.E. Attenuation of nonsense-mediated mRNA decay facilitates the response to chemotherapeutics. Nat Commun. 6, 6632 (2015).

182) Balistreri, G., Horvath, P., Schweingruber, C., Zünd, D., Mclnerney, G., Merits, A., Mühlemann, O., Azzalin, C. & Helenius, A. The host nonsense-mediated mRNA decay pathway restricts mammalian RNA virus replication. Cell Host Microbe. 16, 403-411 (2014).

183) Garcia, D., Garcia, S. & Voinnet, O. Nonsense-mediated decay serves as a general viral restriction mechanism in plants. Cell Host Microbe. 16, 391-402 (2014).

184) Mocquet V., Neusiedler J., Rende F., Cluet D., Robin J.-P., Terme J.-M.,Duc Dodon M., Wittmann J., Morris C., Le Hir H., Ciminale, V. & Jalinot, P. The human T-lymphotropic virus type 1 tax protein inhibits nonsense-mediated mRNA decay by interacting with INT6/ EIF3E and UPF1. J. Virol. 86, 7530-7543 (2012).

185) Nakano K., Ando T., Yamagishi M., Yokoyama K., Ishida T., Ohsugi T., TanakaY., Brighty D.W., Watanabe T. Viral interference with host mRNA surveillance, the nonsense-mediated mRNA decay (NMD) pathway, through a new function of HTLV-1 Rex: implications for retroviral replication. Microbes Infect. 15, 491-505 (2013).

186) Weil J.E., Beemon K.L. A 3′ UTR sequence stabilizes termination codons in the unspliced RNA of Rous sarcoma virus. RNA. 12, 102-110 (2006).

187) Quek B.L., Beemon K. Retroviral strategy to stabilize viral RNA. Curr. Opin. Microbiol. 18, 78-82 (2014).

188) Gong, C., Kim, Y.K., Woeller, C.F., Tang, Y. & Maquat, L.E. SMD and NMD are competitive pathways that contribute to myogenesis: effects on PAX3 and myogenin mRNAs. Genes Dev. 23, 54-66 (2009).

189) Wengrod, J., Martin, L., Wang, D., Frischmeyer-Guerrerio, P., Dietz, H.C. & Gardner, L.B. Inhibition of nonsense-mediated RNA decay activates autophagy. Mol Cell Biol. 33, 2128-2135 (2013).

190) Longman D, Hug N, Keith M, Anastasaki C, Patton, E.E., Grimes, G. & Cáceres, J.F. DHX34 and NBAS form part of an autoregulatory NMD circuit that regulates endogenous RNA targets in human cells, zebrafish and Caenorhabditis elegans.Nucleic Acids Res. 41, 8319–8331 (2013).

191) Linde, L., Boelz, S., Neu-Yilik, G., Kulozik, A.E. & Kerem, B. The efficiency of nonsense-mediated mRNA decay is an inherent character and varies among different cells. Eur J Hum Genet 15, 1156-1162 (2007)

192) Linde, L., Boelz, S., Nissim-Rafinia, M., Oren, Y.S., Wilschanski, M., Yaacov, Y., Virgilis, D., Neu-Yilik, G., Kulozik, A.E., Kerem, E. & Kerem, B. Nonsense-mediated mRNA decay affects nonsense transcript levels and governs response of cystic fibrosis patients to gentamicin. J Clin Invest 117, 683-692 (2007)

193) Jin, Y., Zhang, F., Ma, Z. & Ren Z. MicroRNA 433 regulates nonsense-mediated mRNA decay by targeting SMG5 mRNA. BMC Mol Biol. 17, 17 (2016).

194) Wang, G., Jiang, B., Jia, C., Chai, B. & Liang, A. MicroRNA 125 represses nonsense-mediated mRNA decay by regulating SMG1 expression. Biochem Biophys Res Commun. 435, 16-20 (2013).

195) Holbrook, J.A., Neu-Yilik, G., Hentze, M.W. & Kulozik, A.E. Nonsense-mediated decay approaches the clinic. Nat Genet. 36, 801-808 (2004).

196) Zhang, J., Sun, X., Qian, Y. & Maquat, L.E. Intron function in the nonsense-mediated decay of beta-globin mRNA: indications that pre-mRNA splicing in the nucleus can influence mRNA translation in the cytoplasm. RNA. 4, 801-815 (1998).

197) Karam, R., Carvalho, J., Bruno, I., Graziadio, C., Senz, J., Huntsman, D., Carneiro, F., Seruca, R., Wilkinson, M.F. & Oliveira, C. The NMD mRNA surveillance pathway downregulates aberrant E-cadherin transcripts in gastric cancer cells and in CDH1 mutation carriers. Oncogene. 27, 4255-4260 (2008).

198) De Rosa, M., Morelli, G., Cesaro, E., Duraturo, F., Turano, M., Rossi, G.B., Delrio, P. & Izzo, P. Alternative splicing and nonsense-mediated mRNA decay in the regulation of a new adenomatous polyposis coli transcript. Gene. 395, 8-14 (2007).

199) El-Bchiri, J., Guilloux, A., Dartigues, P., Loire, E., Mercier, D., Buhard, O., Sobhani, I., de la Grange, P., Auboeuf, D., Praz, F., Flejou, J. & Duval, A. Nonsense-mediated mRNA decay impacts MSI-driven carcinogenesis and anti-tumor immunity in colorectal cancers. PLoS One. 3, e2583 (2008).

200) George, R.E., Kenyon, R., McGuckin, A.G., Kohl, N., Kogner, P., Christiansen, H., Pearson, A.D. & Lunec, J. Analysis of candidate gene co-amplification with MYCN in neuroblastoma. Eur J Cancer. 33, 2037-2042 (1997).

201) Beheshti, B., Braude, I., Marrano, P., Throner, P., Zielenska, M. & Squire, J.A. Chromosomal localization of DNA amplifications in neuroblastoma tumors using cDNA microarray comparative genomic hybridization. Neoplasia. 5, 53-62 (2003).

202) Liu, C., Karam, R., Zhou, Y., Su, F., Ji, Y., Li, G., Xu, G., Lu, L., Wang, C., Song, M., Zhu, J., Wang, Y., Zhao, Y., Foo, W.C., Zuo, M., Valasek, M.A., Javle, M., Wilkinson, M.F. & Lu, Y. The UPF1 RNA surveillance gene is commonly mutated in pancreatic adenosquamaous carcinoma. Nat Med. 20, 596-598 (2014).

203) Lu, J., Plank, T.D., Su, F., Shi, X., Liu, C., Ji, Y., Li, S., Huynh, A., Shi, C., Zhu, B., Yang, G., Wu, Y., Wilkinson, M.F. & Lu, Y. The nonsense-mediated RNA decay pathway is disrupted in inflammatory myofibroblastic tumors. J Clin Invest. 126, 3058-3062 (2016).

204) Keeling, K.M., Wang, D., Dai, Y., Murugesan, S., Chenna, B., Clark, J., Belakhov, V., Kandasamy, J., Velu, S.E., Baasov, T. & Bedwell, D.M. Attenuation of nonsense-mediated mRNA decay enhances in vivo nonsense suppression. PLoS One. 8, e60478 (2013).

205) Du, M., Liu, X., Welch, E.M., Hirawat, S., Peltz, S.W. & Bedwell, D.M. PTC124 is an orally bioavailable compound that promotes suppression of the human CFTR-G542X nonsense allele in a CF mouse model. Proc Natl Acad Sci U S A. 105, 2064-2069 (2008).

206) Martin, L., Grigoryan, A., Wang, D., Wang, J., Breda, L., Rivella, S., Cardozo, T. & Gardner, L.B. Identification and characterization of small molecules that inhibit nonsense-mediated RNA decay and suppress nonsense p53 mutations. Cancer Res. 74, 3104-3113 (2014).

207) Pastor, F., Kolonias, D., Giangrande, P.H. & Gilboa, E. Induction of tumour immunity by targeted inhibition of nonsense-mediated mRNA decay. Nature. 465, 227-230 (2010).

208) Noensie, E.N. & Dietz, H.C. A strategy for disease gene identification through nonsense-mediated mRNA decay inhibition. Nat Biotechnol. 19, 434-439 (2001).

209) Shin, N., You, K.T., Lee, H., Kim, W.K., Song, M., Choi, H., Rhee, H., Nam, S.W. & Kim, H. Identification of frequently, mutates genes with relevance to nonsense mediated mRNA decay in the high microsatellite instability cancer. Int J Cancer. 128, 2872-2880 (2011).

210) Mattila, H., Schindler, M., Isotalo, J., Ikonen, T., Vihinen, M., Oja, H., Tammela, T.L., Wahlfors, T. & Schleutker, J. NMD and microRNA expression profiling of the HPCX1 locus reveal MAGEC1 as a candidate prostrate cancer predisposition gene. BMC Cancer. 11, 327 (2011).

211) Ivanov, I., Lo, K.C., Hawthorn, L., Cowell, J.K. & Ionov, Y. Identifying candidate colon cancer tumor suppressor genes using inhibition of nonsense-mediated mRNA decay in colon cancer cells. Oncogene. 26, 2873-2884 (2007).

212) Johnson, J.K., Waddell, N., kConFab Investigators, Chenevix-Trench, G. The application of nonsense-mediated mRNA decay inhibition to the identification of breast cancer susceptibility genes. BMC Cancer. 12, 246 (2012).

213) Paillusson, A., Hirschi, N., Vallan, C., Azzalin, C.M. & Mühlemann, O. A GFP-based reporter system to monitor nonsense-mediated mRNA decay. Nucleic Acids Res. 33, e54 (2005).

214) Boelz, S., Neu-Yilik, G., Gehring, N.H., Hentze, M.W. & Kulozik, A.E. A chemiluminescence-based reporter system to monitor nonsense-mediated mRNA decay. Biochem Biophys Res Commun. 349, 186-191 (2006).

215) Pereverzev, A.P., Gurskaya, N.G., Ermakova, G.V., Kudryavtseva, E., Markina, N.M., Kotlobay, A.A., Lukyanov, S.A., Zaraisky, A.G. & Lukyanov, K.A. Method for quantitative analysis of nonsense-mediated mRNA decay at the single cell level. Sci Rep. 5, 7729 (2015).

Chapter 2: Regulation of NMD by intracellular calcium

Preface

The following work was performed by me, Zhongsheng You, Erin Jackson, Jayne Marasa, Patrick Nugent, Robert W. Mercer, and David Piwnica-Worms. Z.Y. and D.P-W. conceived the project and supervised the studies. A.N. and Z.Y. designed and performed the experiments. E.J. contributed to the bioluminescence imaging and the analysis of screen and imaging data. J.M. assisted with the high-throughput chemical screen. P.N. assisted with the analysis of the screen results. R.W.M. provided expression constructs for rat Na+/K+-ATPase α subunits and technical advice. A.N., Z.Y., and D.P-W. wrote the manuscript.

This chapter is published in its entirety [Nickless, A., Jackson, E., Marasa, J., Nugent, P., Mercer, R.W., Piwnica-Worms, D. & You, Z. Intracellular calcium regulates nonsense-mediated mRNA decay. Nat Med 20, 961-966 (2014).] and is available online at http://www.nature.com/nm/journal/v20/n8/full/nm.3620.html. Reproduction of this article is permitted as part of our ownership of copyright and the author reuse guidelines of the Nature Publishing Group.

We thank Drs. Peng Wu and Xiaoqing Chen for their contributions in the early stage of this project. We are grateful to Dr. Oliver Mühlemann for providing the pβ510 reporter construct, which we used to obtain the TCRβ mini reporter sequence for our reporter construction, and Dr. Robert Mecham for providing primary mouse skin fibroblasts. This study was supported by a Molecular Imaging Center grant from the NIH to Washington University and The University of Texas M.D. Anderson Cancer Center (P50 CA94056, DP-W), by a Washington University Molecular Imaging Center Pilot Research Project Grant (ZY), and by an Interdisciplinary Research Initiative grant from the Children's Discovery Institute of Washington University (MC-

II-2012-215, ZY and DP-W). The HTS core is supported in part by the Siteman Cancer Center (NCI Cancer Center Support Grant P30 CA91842).

2.1 Abstract

The nonsense-mediated mRNA decay (NMD) pathway selectively eliminates aberrant transcripts containing premature translation termination codons (PTCs) and regulates the levels of a number of physiological mRNAs. NMD modulates the clinical outcome of a variety of human diseases, including cancer and many genetic disorders, and may represent an important target for therapeutic intervention. Here we have developed a novel multicolored, bioluminescence-based reporter system that can specifically and effectively assay NMD in live human cells. Using this reporter system, we conducted a high-throughput small-molecule screen in human cells and, unpredictably, identified a group of cardiac glycosides including ouabain and digoxin as potent inhibitors of NMD. Cardiac glycoside-mediated effects on NMD are dependent on binding and inhibiting the Na^+/K^+-ATPase on the plasma membrane and subsequent elevation of intracellular calcium levels. Induction of calcium release from the endoplasmic reticulum also leads to inhibition of NMD. Thus, this study reveals intracellular calcium as a key regulator of NMD and has important implications for exploiting NMD in the treatment of disease.

2.2 Introduction

The NMD pathway selectively degrades mRNAs harboring PTCs and, in so doing, guards cells against insults from potentially deleterious truncated proteins. In addition to eliminating faulty mRNA transcripts, NMD regulates the levels of many physiological mRNAs possessing features that are recognized by the NMD machinery[1,2]. By modulating the activity of NMD, cells can enact gene expression programs crucial for

normal development or for responding to environmental cues such as hypoxia and amino acid deprivation[3,4]. Furthermore, approximately one-third of human genetic diseases are the manifestation of PTC mutations[5], and whole genome sequencing has recently uncovered numerous somatic nonsense mutations in tumor samples[6]. Thus, NMD has become an attractive target for the treatment of many human diseases. For example, inhibiting NMD may alleviate the symptoms of certain genetic diseases caused by PTCs if the truncated protein products are functional or partially functional hypomorphs[7,8]. NMD inhibition also represents a promising cancer therapeutic strategy. Cancer cells likely have an elevated dependency on NMD for survival due to the production of many nonsense mRNAs as a result of their intrinsic genomic instability. Thus, inhibiting NMD may lead to preferential killing of cancer cells.

2.3 Results

To investigate the NMD pathway and to begin to develop NMD-targeting therapeutics, we constructed a multicolored, bioluminescence-based reporter for assaying NMD in mammalian cells, as illustrated in Fig. 1A and Supplementary Fig. 1. This reporter comprises a single expression vector containing two separate transcription units, each with a luciferase inserted into a TCRβ minigene at the same position within the second exon. The first transcription unit consists of a PTC-containing TCRβ minigene fused to click beetle red luciferase (CBR-TCR(PTC)). The second unit contains a wild-type TCRβ minigene fused to click beetle green 99 luciferase (CBG99, hereafter referred to as CBG for simplicity) (CBG-TCR(WT)). Expression of both fusion reporter genes are controlled by separate CMV promoters, splice sites, and polyadenylation signals of

identical sequences. A sequence encoding an HA-tag was included in the first exon of the fusion reporter genes, which provides an independent method to detect the translated fusion protein products through western blotting. PTCs in the well characterized TCRβ minigene are known to elicit robust NMD (but not 100% efficient as is the case for other reporter genes examined)[9,10]. The CBR-TCR(PTC) and CBG-TCR(WT) transcription units share > 99% sequence identity at the DNA, pre-mRNA, and mRNA levels (see the reporter sequence in Supplementary Fig. 2). Using this dual-colored reporter, NMD is quantified by the ratio of CBR activity to CBG activity, with an increase in the CBR/CBG (red/green) ratio representing inhibition of NMD. Here, the CBR luciferase activity serves as an indirect measure of the steady-state levels of the CBR-TCR(PTC) fusion mRNA, which is targeted for degradation by NMD, whereas the CBG luciferase activity reflects the steady-state levels of the CBG-TCR(WT) fusion mRNA, which is unresponsive to NMD. The use of CBG-TCR(WT) as an internal control in the same cell ensures that changes in the CBR/CBG ratio reflect effects specifically attributable to NMD and not indirect effects that result from variations in reporter DNA delivery or from effects on cell viability or various steps of gene expression such as transcription, splicing, polyadenylation, and translation. The use of the highly sensitive and closely related red-emitting CBR and green-emitting CBG luciferases, combined with a spectral deconvolution algorithm for unmixing CBR and CBG signals, allows for rapid and accurate measurement of their respective activities simultaneously in a single reaction with the same D-luciferin substrate[11].

To validate the NMD reporter system, we generated a human U2OS cell line

stably expressing the reporter. Western blot results indicate that while the CBG-TCR(WT) fusion protein was efficiently expressed, the basal level of the CBR-TCR(PTC) truncated protein was barely detectable (Fig. 1B). This result is consistent with the prediction that CBR-TCR(PTC) mRNA, but not CBG-TCR(WT) mRNA, is targeted for NMD. Treatment with caffeine, a potent (but not specific) inhibitor of the kinase activity of the NMD factor SMG1, restored the CBR-TCR(PTC) protein levels. Bioluminescence imaging reveals that the CBR/CBG ratio increased by ~ 3-fold following caffeine treatment (Fig. 1C). Importantly, quantitative RT-PCR (RT-qPCR) analysis performed with primers specific to CBR or CBG luciferases in the reporter revealed a similar increase in the ratio of CBR-TCR(PTC)/CBG-TCR(WT) reporter mRNAs (Fig. 1D and Supplementary Table 1). Furthermore, shRNA-mediated knockdown of NMD factors SMG1, Upf1 and Upf2 also inhibited NMD of the reporter, as measured by western blot, bioluminescence assay, and RT-qPCR (Fig. 1E-1H). Taken together, these data demonstrate that this mechanism-based NMD reporter system faithfully recapitulates the characteristics of NMD in human cells and is expected to be specific, rapid, and sensitive.

Using this reporter system, we next performed a high-throughput screen to identify drug candidates that can alter NMD activity in human cells. The Pharmakon library, which contains a diverse array of 1,600 clinically-evaluated compounds, was used as the source of small molecules in the hope of repurposing existing drug candidates to fast-track the drug development process. Human U2OS cells containing the dual-colored NMD reporter were seeded in 96-well plates, and individual drugs were added to each well at a concentration of 10 μM, along with appropriate controls. Twenty-four hours

after drug treatment, D-luciferin was added to the medium followed by bioluminescence imaging and spectral unmixing to obtain CBR and CBG signals (Fig. 2A). A *Z'* factor of 0.77 was calculated for the reporter assay, demonstrating the robustness of the strategy (see Methods). As shown in Fig. 2B and Supplementary Table 2, the majority of the compounds in the library exhibited little or no effect on NMD of the reporter. However, 8 candidate inhibitors and 14 candidate enhancers of NMD were identified by quartile analysis after employing stringent criteria for hit selection (Fig. 2B and Supplementary Table 3)[12]. Focusing on NMD inhibitors in this study, the effects of seven of the inhibitor hits were confirmed in follow-up analysis, and each validated compound inhibited NMD in a dose-dependent manner (data not shown). Strikingly, the top five verified hits, including digitoxin, digoxin, lanatoside C, proscillaridin and ouabain, are all cardiac glycosides (CGs), which inhibit Na^+/K^+-ATPase in cells (Fig. 2B)[13].

At the initial screening concentration (10 μM), all CGs increased CBR signal compared to DMSO treatment, but these drugs also decreased CBG signal, potentially due to non-specific toxic effects on cell viability (Supplementary Table 2). However, we identified a lower concentration for each drug at which the CBR activity was still dramatically increased while the CBG activity remained largely unaffected (Fig. 3A). At these modest concentrations, these drugs did not significantly impact general translation in cells and had only a mild inhibitory effect on cell viability (Supplementary Fig. 3A, 3B). Because CBR and CBG proteins are relatively stable, the inhibitory effects of CGs on the signal generated by the NMD reporter was time-dependent, increasing over the 24-hour treatment period; CG-mediated blockade of NMD was fully concentration-dependent,

showing reporter-generated EC_{50} values of ~70 nM and ~200 nM for ouabain and digoxin, respectively (Supplementary Fig. 4A, 4B). Importantly, our bioluminescence imaging results were corroborated by western blot and reporter-specific RT-qPCR analyses of the CBR-TCR(PTC) and CBG-TCR(WT) protein and mRNA levels, respectively (Fig. 3B, 3C).

To further validate the effects of CGs on NMD using an independent NMD model system, we used the human Calu-6 cell line, which expresses a PTC-containing nonsense mRNA of endogenous p53[14,15]. Calu-6 cells were first treated with CGs for 16 hrs. Subsequently, the transcription inhibitor actinomycin D was added to block new mRNA synthesis, and the levels of p53 mRNA were determined by RT-qPCR at 0 hr and 6 hr after actinomycin D treatment. All 5 CGs significantly increased the stability of the mutant p53 transcript, compared with DMSO (Fig. 3D). In further support of the idea that CGs inhibit NMD, we observed increased stability of wild-type endogenous mRNA targets of NMD, including UPP1, ATF4, Pim3, and Pisd, in Calu6 cells after treatment with ouabain. In comparison, the stability of endogenous ORCL transcripts, which are not targeted by NMD, was unaffected under the same condition (Fig. 3E)[16-19]. It has been previously shown that the mRNA levels of many of the NMD factors such as SMG1, Upf1, Upf2, Upf3B, SMG5, SMG6, and SMG7 are controlled by NMD via an autoregulatory loop, as they are themselves targets of NMD[20,21]. Consequently, these transcripts are upregulated upon ablation of NMD activity. If CGs inhibit NMD, one would expect an increase in these NMD factor transcript levels after CG treatment. Indeed, we found that ouabain treatment led to upregulation of all of these autoregulated NMD factors except SMG6 (whose upregulation

was also less obvious upon NMD inhibition after Upf1 knockdown in previous studies[20,21]) (Supplementary Fig. 5). Taken together, these data strongly suggest that CGs have a previously unrecognized ability to inhibit NMD in human cells.

Since the Na^+/K^+-ATPase (composed of a catalytic α subunit and a structural β subunit, each with various isoforms) is the only known pharmacological target of the identified CGs, our results suggest that CGs inhibit NMD via the sodium-potassium pump[22]. Consistent with this idea, our reporter assay indicates that mouse skin fibroblasts, which express a naturally CG- resistant α1 subunit of Na^+/K^+-ATPase, exhibited more than 100 times greater resistance to ouabain, compared to human cells in which all 4 isoforms of the α subunit have a much higher affinity for CGs (Fig. 4A)[23]. In contrast, NMD of the reporter exhibited a similar level of sensitivity to caffeine in both human and mouse cells (Fig. 4A). Moreover, overexpression in human cells of the rat α1 subunit of Na^+/K^+-ATPase, which also has a low affinity for CGs, abrogated the inhibitory effects of ouabain on NMD. In contrast, expression of a similar level of rat α3 subunit of Na^+/K^+-ATPase, which is sensitive to CGs[23,24], did not cause resistance of NMD to ouabain (Fig. 4B and Supplementary Fig. 6A). Furthermore, expression of a CG-resistant mutant version of the human α1 subunit also prevented the CG-mediated inhibition of NMD while the wild-type protein failed to do so (Fig. 4C and Supplementary Fig. 6B). To further demonstrate that CGs inhibit NMD through their binding and inhibition of Na^+/K^+-ATPase, we generated a catalytically inactive mutant of the rat α1 subunit (D376E) that

has diminished binding and hydrolysis of ATP[24]. Unlike the WT rat α1 subunit, expression of this mutant in human cells could not cause resistance of NMD to CGs, indicating that blockade of the sodium/potassium pump enzymatic activity is necessary for efficient CG-induced inhibition of NMD (Fig. 4D and Supplementary Fig. 6C). Taken together, these data strongly suggest that Na^+/K^+-ATPase is a robust regulator of NMD in mammalian cells and that CGs inhibit NMD through binding and inhibiting this sodium-potassium pump. Given the essential role of Na^+/K^+-ATPase for cell viability, the observation that CGs strongly inhibited NMD at concentrations where no obvious decrease in CBG activity or cell viability was observed suggests that partial inhibition of the sodium-potassium pump is sufficient to abolish NMD (Fig. 3 and Supplementary Fig. 3B).

Because a major effect of Na^+/K^+-ATPase inhibition is the elevation of intracellular calcium levels[13], we hypothesized that inhibition of NMD by the cardiac glycosides is due to increased intracellular calcium concentration. To test this, we co-treated U2OS reporter cells with ouabain and Bapta-AM, a cell-penetrating intracellular calcium chelator, to buffer cytosolic free calcium transients. Bapta-AM reversed the inhibitory effects of ouabain on NMD, although Bapta-AM treatment alone did not affect NMD (Fig. 4E). This suggests that calcium indeed mediates the inhibitory effects of cardiac glycosides on NMD. To further establish the regulation of NMD by calcium, we treated reporter cells with multiple drugs that raise intracellular calcium levels by independent mechanisms. We found that Thapsigargin, which induces the release of calcium stores from ER into the cytoplasm,

abrogated NMD in the reporter cells, and that this effect was also ablated by Bapta-AM (Fig. 4F). Furthermore, the calcium ionophore A23187, which also increases intracellular calcium concentration, exhibited similar inhibitory effects on NMD (data not shown). Taken together, these results strongly suggest that calcium is a crucial regulator of NMD in human cells.

2.4 Discussion

It is not clear at present how intracellular calcium regulates NMD in cells. Intracellular calcium may directly bind and regulate the activities and functions of NMD factors. Alternatively, it may indirectly regulate NMD through calcium-dependent signaling molecules such as kinases and phosphatases. Interestingly, Johansson and Jacobson have previously shown in yeast cells that elevated levels of another divalent cation, magnesium, inhibit NMD by promoting translation read-through at stop codons[25]. Unlike magnesium, intracellular calcium apparently does not promote translation read-through, as treatment with cardiac glycosides or Thasigargin resulted in the production of a truncated protein terminated at the PTC in the CBR-TCR(PTC) reporter (Fig. 3B and data not shown). Work is underway to dissect the precise mechanism of this calcium-mediated NMD regulation.

In summary, using a highly effective NMD bioluminescent reporter system, we identified CGs as potent inhibitors of NMD, leading to the discovery of a novel, calcium-mediated NMD regulatory pathway (Fig. 4G). These findings have important implications in both basic and translational research. First, our results suggest a novel therapeutic strategy for NMD inhibition by manipulating intracellular calcium levels. CGs or derivatives with low toxicity might also be effective in treating certain genetic diseases such as cystic fibrosis and Duchenne muscular dystrophy, wherein truncated protein

products encoded by the corresponding nonsense mRNAs are fully or partially functional[7,8]. Second, our results may, in part, explain the anticancer properties previously observed for CGs in both epidemiological and laboratory studies[13]. A recent study indicates that the same group of CGs we identified herein are potent inducers of an anticancer immune response[26]. Mechanistically, inhibition of NMD may result in the synthesis of novel, tumor-specific antigens that could induce antitumor immunity[27]. Given the antitumor immunity observed in mice after NMD disruption[27] and the inhibitory effects of CGs on NMD revealed by this study, it is possible the antitumor immunity induced by these drugs, in part, results from their chronic effects on NMD. Third, given the prominence of calcium signaling in many physiological processes, such as development, proliferation, synaptic transmission and immune activation, and the role of NMD in regulating the levels of many physiological mRNAs, our study suggests a novel mechanism for the calcium-mediated gene expression programs essential for these processes[3,28-34].

2.5 Methods

2.5.1 NMD reporter construction

The dual-color NMD reporter was generated by PCR cloning. The TCRβ mini gene sequence was derived from pβ510 (a gift from Dr. Oliver Mühlemann, University of Bern)[10]. The CBR and CBG99 ORF sequences were derived from pCBR-Basic and pCBG99-Basic vectors (Promega). The CMV promoter and SV40 polyadenylation signal sequences were derived from pmCherry-N1, a derivative of pEGFP-N1 vector (Promega) in which the EGFP ORF is replaced with mCherry ORF. These elements were first assembled in pmCherry-N1 deleted of the mCherry ORF to generate pN1-(CBR-TCR (PTC)) and pN1-(CBG-TCR(WT)). The CBR-TCR(PTC) transcription unit between the CMV promoter and SV40 polyadenylation signal in pN1-(CBR-TCR(PTC)) was then inserted into pBluescript SK(-) at Sac I (5') and Spe I (3') to generate the single-color reporter pBS-(CBR-TCR(PTC)). Similarly, the CBG-TCR(WT) transcription unit between the CMV promoter and SV40 polyadenylation signal in pN1-(CBG-TCR(WT)) was inserted into pBluescript SK(-) at Spe I (5') and Kpn I (3') to generate the single-color reporter pBS-(CBG-TCR(WT)). To generate the dual- color reporter pBS-(CBR-TCR(PTC)-CBG-TCR(WT)), the Spe I (5')-KpnI (3') fragment containing the CBG-TCR (WT) transcription unit from pBS-(CBG-TCR(WT)) was inserted into pBS-(CBR- TCR (PTC)) at Spe I (5') and Kpn I (3') sites. Detailed cloning strategy and PCR primer sequences are available upon request. An annotated, complete sequence of the dual-color NMD reporter is shown in Supplementary Fig. 1.

2.5.2 Cell culture, adenovirus and lentivirus production and infection, expression of α subunits of Na^+/K^+-ATPase, and chemical inhibitors

Primary fibroblasts from skin explants of newborn mice were kindly provided by Dr. Robert Mecham (Washington University School of Medicine). The cells were maintained in Dulbecco's modified Eagle's media (DMEM) supplemented with 100 units/ml penicillin, 100 μg/ml streptomycin, 0.1 mM nonessential amino acid, and 10% fetal bovine serum (FBS) in a 5% CO2 incubator at 37 °C. Human U2OS cells and HEK293T cells were cultured in DMEM with 10% FBS at 37 ºC with 5% CO_2.

To generate U2OS cells stably expressing the dual-colored or single-colored NMD reporters, pBS-(CBR-TCR(PTC))-(CBG-TCR(WT)), pBS-(CBR-TCR(PTC)) or pBS-(CBG- TCR(WT)) were co-transfected with a pMXs-puro vector that encodes a puromycin-resistance gene into U2OS cells using the TransIT-LT1 transfection reagent (Mirus). Single colonies were selected with puromycin (1.5 μg/ml) and expression of the reporters was verified by Western blot, bioluminescence imaging and RT-qPCR.

An adenovirus construct encoding our NMD reporter was generated by inserting the reporter into the pAdenoX-PRLS-ZsGreen1 vector using the In-Fusion HD cloning kit (Clontech), according to the manufacturer's protocol. Linearized adenoviral vector with exposed inverted terminal repeats was transfected into HEK293 cells for viral production, followed by viral amplification in the same cell line. Target cells were infected with adenoviruses for 48 hrs before bioluminescence imaging.

To knockdown NMD factors in NMD reporter cells, lentiviruses expressing a non-targeting control shRNA or shRNAs targeting SMG1, Upf1 or Upf2 were generated in

HEK293T cells as previously described[35]. Briefly, HEK293T cells were co-transfected with an shRNA-encoding lentiviral vector and packaging plasmids (pCMV-dR8.2 and pCMV-VSVG) using TransIT-LT1 transfection reagent (Mirus). Virus-containing supernatant was collected 48 and 72 hr after transfection. The U2OS cells stably expressing the dual-colored NMD reporter were then infected with the viruses. The lentiviral vectors expressing a control nontargeting shRNA (5'- CAACAA GAUGAAGAGCACCAA-3'), shSMG1-1 (5'-GCCGAGAUGUUGAUCCGAAUA-3'), shSMG1-2 (5'-GCACUGUAACUACGGCUACAA-3'), shUpf1 (5'-GCAUCUUAUUCUGGGUAAUAA-3'), shUpf2-1 (5'-GCGUUAUGUUUGGUGGAAGAA-3') and shUpf2-2 (5'-GCGAGAUACGUCACAAUGGUA-3') were purchased from Sigma.

The CG-resistant human α1 mutant containing two mutations (Q118R and N129D) and the catalytic inactive rat α1 subunit mutant containing the D376E mutation were generated by site-directed mutagenesis using the following primers: 5'-TATAGCATCCGAGCTGCTACAGAAGAGGAACCTCAAAACGATGATCTGTACCTG G-3'; 5'-CCAGGTACAGATCATCGTTTTGAGGTTCCTCTTCTGTAGCAGCTCGGATGCTATA-3', and 5'-CATCTGCTCCGAGAAGAC TGGAACTC-3'/5'-GAGTTCCAGTCTTCTCGGAGCAGATG-3', respectively. Because we observed inhibitory effects of a FLAG tag on the function of α subunits (data not shown), we used untagged forms for expression in human cells. All α subunits were expressed in U2OS cells by transfection using the TransIT-LT1 transfection reagent. Twenty fours hours

following transfection, cells were re-plated in 96-well plates before drug treatment and bioluminescence imaging (see below).

Cardiac glycosides, including ouabain, digoxin, digitoxin, proscillaridin and lanatoside C, were purchased from MicroSource. Ouabain (O3125) and digoxin (D6003) were also purchased from Sigma. Bapta-AM (A1076), thapsingargin (T9033), A23187 (C7522), actinomycin D (A1410) and caffeine (C0750) were purchased from Sigma. Caffeine was dissolved in H_2O, and all other inhibitors were dissolved in DMSO.

2.5.3 High-throughput screening

Human U2OS cells stably expressing our dual-colored NMD reporter were plated in black-walled 96-well dishes with 100 µl media using a Biomek FX liquid handler. Colorless DMEM with 10% FBS was used throughout the screening process. Eighteen hours following cell plating, original media were removed and replaced with media (130 µl) supplemented with individual drugs in the Pharmakon Library (PHARMAKON 1600, MicroSource) at a concentration of 10 µM. The liquid handling robot diluted the drugs from a stock concentration of 2 mM in dimethyl sulfoxide (DMSO) to the final 10 µM concentration. The final concentration of DMSO was 0.5%. Three wells treated with DMSO (0.5%, negative vehicle control for drugs in the Library) or caffeine (10 mM in H_2O, positive control) were also included on each plate. For the purpose of spectral unmixing of the CBR and CBG signals in the dual-colored reporter, control U2OS reporter cells stably expressing either the CBG-TCR(WT) alone or the CBR- TCR(PTC) alone (treated with 10 mM caffeine to increase signal) were included on the same plate to provide pure CBR and CBG reference signals. Cells were incubated in the presence of

compound for 24 hours followed by bioluminescence imaging (see below).

2.5.4 Bioluminescence imaging and spectral deconvolution

Cells were incubated with 150 µg/ml D-luciferin for 10 minutes at 37 °C and bioluminescence signals were measured sequentially using a charge-coupled device (CCD) camera-based bioluminescence imaging system (IVIS 100; Caliper) with appropriate open, red, or green filters and exposure settings (exposure time: 10 s; binning: 8; field of view: 15; f/stop: 1). Regions-of-interest (ROIs) were drawn over images of wells and bioluminescence signals were quantified using Living Image (Caliper) and Igor (Wavemetrics) analysis software packages as described previously[36]. Spectral unmixing was performed using an ImageJ plugin with an algorithm we developed previously[11]. The CBR/CBG ratio was calculated for each well and normalized by the CBR/CBG ratio in DMSO-treated wells. Data were presented as the $\log_2$ of the fold-change in the CBR/CBG ratio. To document the quality of our NMD reporter assay, we calculated the *Z'* factor for a 96-well screening plate based on the CBR/CBG ratios in caffeine-treated (control positive sample) and H_2O-treated (control negative sample) cells:

Z' factor = 1 - (3x (standard deviation$_{caffeine}$ + standard deviation$_{H_2O}$) / (average$_{caffeine}$ - average$_{H_2O}$)) = 1 - (3x (0.1123 + 0.0508) / (3.2356 – 1.0850)) = **0.77**

2.5.5 Screen hit selection and statistic analysis

A battery of statistical tests was employed to identify statistically significant screen hits. First, all compounds whose CBR/CBG ratio was less than 2 standard deviations above or below the CBR/CBG ratio for DMSO control wells on the same plate were excluded from further analysis. Compounds passing this initial criterion were then

subjected to quartile analysis. The first (Q1), third (Q3), and median (Q2) quartile values were calculated using the $\log_2$ of the ratio fold-change for compounds in the data set. Potential NMD inhibitors were selected using an upper boundary for hit selection calculated as Q3 + c(ICQ), where ICQ = Q3 - Q1, and c = 1.7239. This c value corresponds to a high stringency targeted error rate of $\alpha = 0.0027$[12]. Where multiple independent experiments are presented, *p*-values were calculated using a paired Student's *t*-test. Where biological replicates are presented (including the screen data), *p*-values were calculated using a unpaired Student's *t*-test. $*p \leq 0.05$, $**p \leq 0.01$, $***p \leq 0.001$, $****p \leq 0.0001$.

2.5.6 RT-qPCR and Western blotting

To measure levels of NMD reporter mRNAs in U2OS cells, or p53 and other endogenous mRNAs in Calu-6 cells, total RNA was isolated using a NucleoSpin RNA II kit (Clonetch) and cDNA was synthesized using a poly-dT primer and the SuperScript II cDNA synthesis kit (Invitrogen), according to the instructions of the manufacturers. All reactions were performed in at least duplicate using a three step PCR protocol (melting temperature: 95 °C; annealing temperature: 55 °C; extension temperature: 72 °C; cycle number: 40) on an ABI VII7 real-time PCR system with Maxima SYBR Green/ROX qPCR Master Mix (Thermo Scientific). The mRNA levels of the housekeeping gene GAPDH were used for normalization. Primers for qPCR are listed in Supplementary Table 4. Western blot to detect CBR-TCR(PTC) and CBG-TCR(WT) protein products in reporter cells using an HA-antibody (Convance, MMS-101R) was performed as described previously using a Li-Cor Odyssey system[35]. Anti-SMG1 antibody raised in rabbits

against *Xenopus* protein cross-reacts with human SMG1, as described previously[37]. Anti-Upf1 (NBP1-05967) and anti-Upf2 (NB2-20813) antibodies were purchased from Novus Biologicals. Anti-PCNA antibodies were home-made against full-length *Xenopus* PCNA protein, which also recognize human PCNA[38]. A pan-Na^+/K^+-ATPase antibody that recognizes all isoforms of the α subunit of Na^+/K^+-ATPase in human and rat cells (Cell Signaling Technology, 3010) was used in Supplementary Fig. 6.

2.5.7 Cell viability analysis

The AlamarBlue assay was used to measure the overall cytotoxicity of cardiac glycoside treatment[39]. Human U2OS NMD reporter cells were treated with DMSO, ouabain or digoxin in 96-well plates. Two hours prior to the each time point shown in Supplementary Fig. 3B, Alamar Blue was added to each well at a final concentration of 40 μM. Cells were incubated at 37 °C in the presence of AlamarBlue for 2 hours and then fluorescence measured (excitation 544 nm; emission 590 nm).

2.5.8 Analysis of general translation

Human U2OS NMD reporter cells were treated with DMSO or ouabain in methionine-free media (CellGro, 17-204-CI) supplemented with 2 mM L-glutamine, 10% dialyzed FBS (Sigma, F0392), and ^{35}S-labeled methionine (10 μCi/ml) for 24 hours prior to protein collection. Protein samples from the same number of cells were run on two separate SDS-PAGE gels, with one for ^{35}S autoradiography analysis (newly synthesized proteins) and one for Coomassie blue staining (total protein levels). Images were quantified using ImageJ and autoradiography intensity was normalized to the total protein level (Coomassie blue

intensity).

2.6 Figures

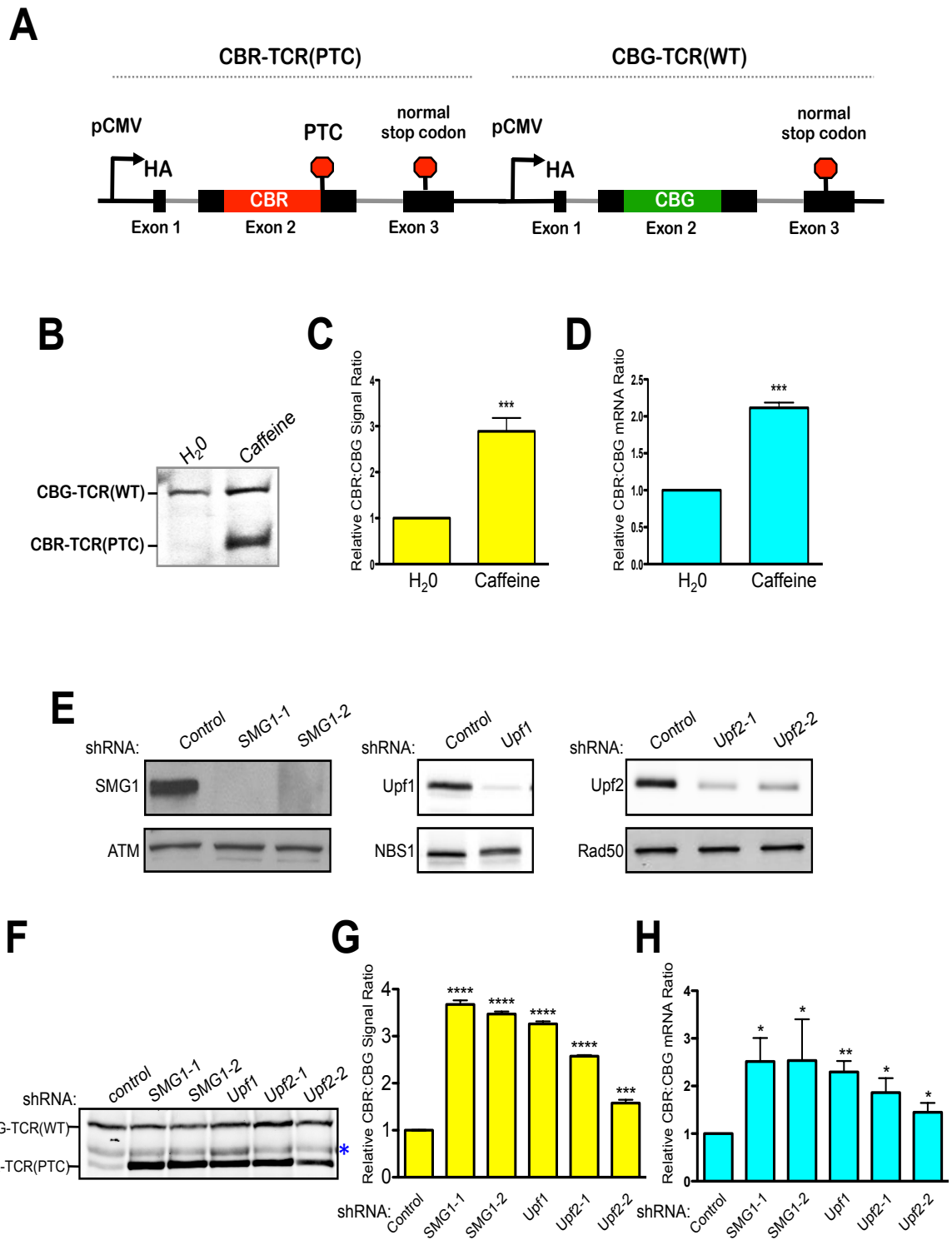
A
CBR-TCR(PTC)
CBG-TCR(WT)
pCMV
HA
PTC
normal stop codon
CBR
CBG
Exon 1
Exon 2
Exon 3
B
H20
Caffeine
CBG-TCR(WT)
CBR-TCR(PTC)
C
Relative CBR:CBG Signal Ratio
***
D
Relative CBR:CBG mRNA Ratio
***
E
shRNA:
Control
SMG1-1
SMG1-2
SMG1
ATM
Upf1
NBS1
Upf2-1
Upf2-2
Upf2
Rad50
F
control
Upf1
G
****
H
*
**

Figure 1. A dual-color bioluminescence-based NMD reporter system

A). Schematic diagram of the reporter construct containing two tandem, highly homologous transcription units, CBR-TCR(PTC) and CBG-TCR(WT). See Fig. S1 and text for details. **B-H**). Validation of the NMD reporter depicted in **A**. **B**). Western blot analysis of the CBR-TCR(PTC) and CBG-TCR(WT) protein levels in U2OS reporter cells treated with vehicle (H_2O) or caffeine. **C**). Ratios of CBR/CBG bioluminescence signals in reporter cells treated with vehicle (H_2O) or caffeine. The ratio in H_2O-treated reporter cells was normalized to 1. Data represent the mean ± SD of four independent experiments. **D**). Ratios of CBR-TCR(PTC)/CBG-TCR(WT) mRNA levels in reporter cells treated with vehicle (H_2O) or caffeine. The ratio in H_2O-treated reporter cells was normalized to 1. Data represent the mean ± SD of three independent experiments. **E**). shRNA-mediated knockdown of the NMD factors SMG1 (2 shRNAs), Upf1 (1 shRNA) or Upf2 (2 shRNAs) in the dual-colored U2OS reporter cells. **F**). Western blot analysis of CBR- TCR(PTC) and CBG-TCR(WT) protein levels in reporter cells after control-knockdown or SMG1-, Upf1-, or Upf2-knockdown. *, nonspecific band. **G**). Ratios of CBR and CBG bioluminescence signals in reporter cells after control-knockdown or SMG1-, Upf1- or Upf2-knockdown. The ratio in control- knockdown reporter cells was normalized to 1. Data represent the mean ± SD of three biological replicates. **H**). Ratios of CBR-TCR(PTC) and CBG-TCR(WT) mRNA levels in reporter cells after control-knockdown or SMG1-, Upf1- or Upf2-knockdown. The ratio in control-knockdown reporter cells was normalized to 1. Data represent the mean ± SD of three independent experiments.

A

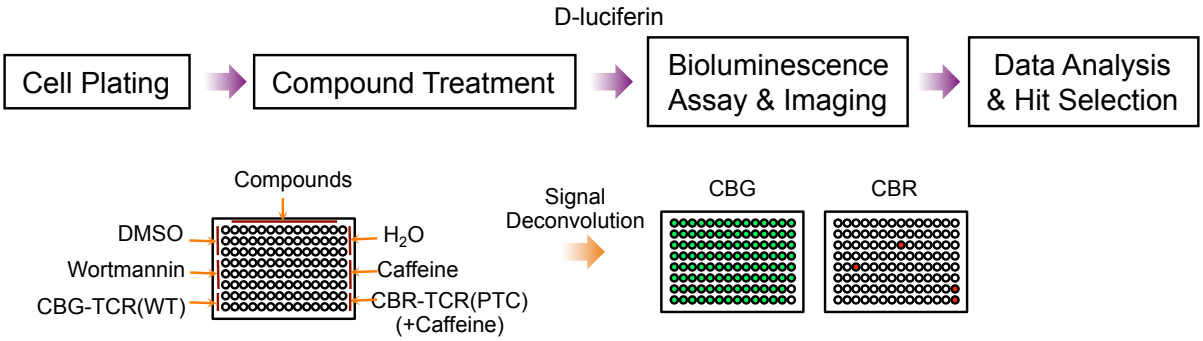

B

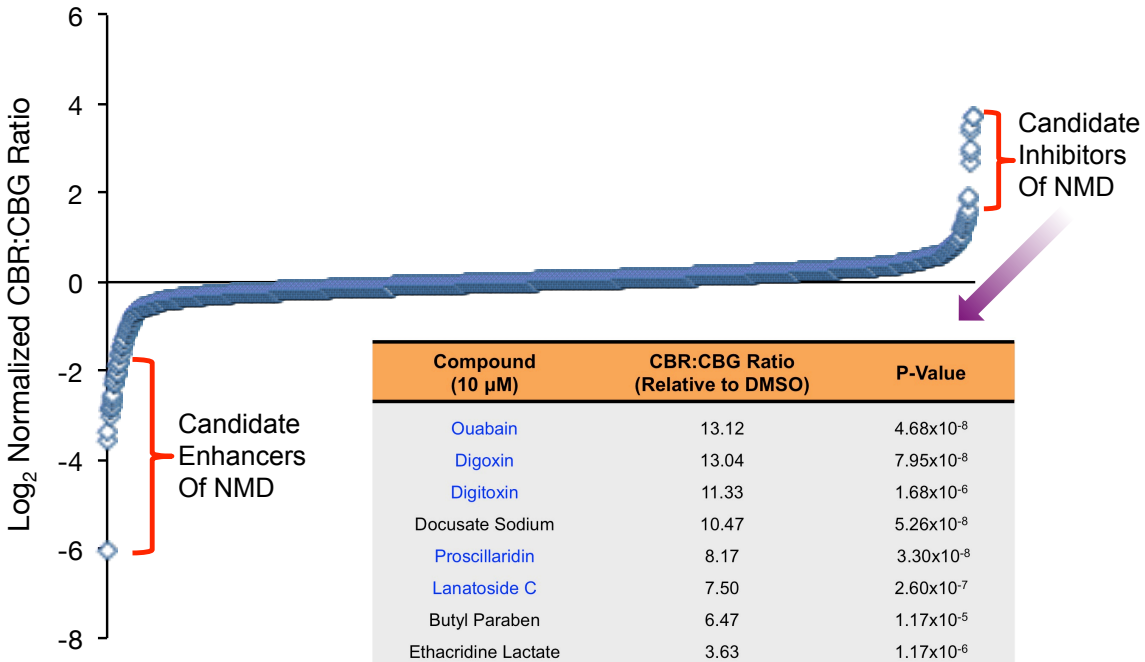

Compound (10 μM)	CBR:CBG Ratio (Relative to DMSO)	P-Value
Ouabain	13.12	4.68×10^{-8}
Digoxin	13.04	7.95×10^{-8}
Digitoxin	11.33	1.68×10^{-6}
Docusate Sodium	10.47	5.26×10^{-8}
Proscillaridin	8.17	3.30×10^{-8}
Lanatoside C	7.50	2.60×10^{-7}
Butyl Paraben	6.47	1.17×10^{-5}
Ethacridine Lactate	3.63	1.17×10^{-6}

Figure 2. A high-throughput screen using the NMD reporter identified existing drugs that modulate NMD

A). Procedure for a high-throughput screen of the Pharmakon 1600 drug library.

B). Primary screening data. Reporter cells were treated with individual compounds in the library for 24 hours followed by bioluminescence imaging in the presence of D-luciferin. Data are shown as the $\log_2$ of the normalized CBR/CBG ratio for each compound. Each ratio was normalized to the DMSO controls on the same plate. Data represent the average of three biological replicates. Compounds were ordered from left to right with increasing relative CBR/CBG ratios. Eight candidate NMD inhibitors of stringent statistical significance are shown in the table. See Table S2 for primary screen data of all compounds in the library.

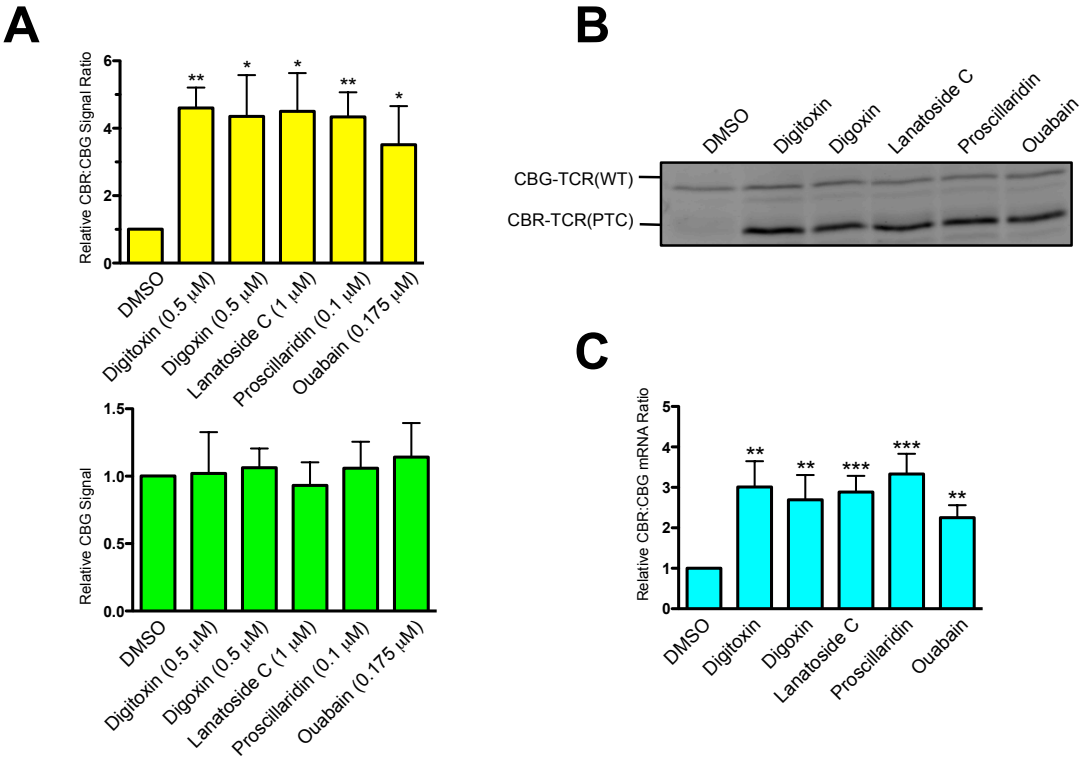
A
Relative CBR:CBG Signal Ratio
Relative CBG Signal
DMSO
Digitoxin (0.5 μM)
Digoxin (0.5 μM)
Lanatoside C (1 μM)
Proscillaridin (0.1 μM)
Ouabain (0.175 μM)
B
DMSO
Digitoxin
Digoxin
Lanatoside C
Proscillaridin
Ouabain
CBG-TCR(WT)
CBR-TCR(PTC)
C
Relative CBR:CBG mRNA Ratio
DMSO
Digitoxin
Digoxin
Lanatoside C
Proscillaridin
Ouabain
D
Percent p53 mRNA Remaining
DMSO
Digitoxin
Digoxin
Lanatoside C
Proscillaridin
Ouabain
E
DMSO
Ouabain
Percent mRNA Remaining
UPP1
ATF-4
Pim3
Pisd
ORCL

Figure 3. Cardiac glycosides are potent inhibitors of NMD

A). CBG bioluminescence signal (lower panel) and ratios of CBR/CBG bioluminescence signals (upper panel) in U2OS reporter cells treated with DMSO or cardiac glycosides for 24 hours at the indicated concentrations. The CBG signal and the CBR/CBG ratio in DMSO-treated reporter cells were normalized to 1. Data represent the mean ± SD of three independent experiments.

B). Western blot analysis of CBR-TCR(PTC) and CBG-TCR(WT) protein levels in U2OS reporter cells treated with DMSO or cardiac glycosides for 24 hours at the concentrations indicated in **A**.

C). Ratios of CBR-TCR(PTC)/CBG-TCR(WT) mRNA levels in U2OS reporter cells treated with DMSO or cardiac glycosides for 24 hours at the concentrations indicated in **A**. The ratio in DMSO- treated reporter cells was normalized to 1. Data represent the mean ± SD of four independent experiments.

D). Effects of cardiac glycosides on the stability of the PTC-containing p53 mRNA in Calu-6 cells. Cells were treated with DMSO or cardiac glycosides at the concentrations indicated in **A** for 16 hours before the addition of the transcriptional inhibitor actinomycin D (5 μg/ml) to block new RNA synthesis. Total RNA was collected immediately before or 6 hours after the addition of actinomycin D, and p53 mRNA levels were analyzed by RT-qPCR and normalized to GAPDH mRNA levels. Data represent the percent mRNA remaining six hours after transcriptional ablation (mean ± SD) from at least three independent experiments.

E). Effects of ouabain on the stability of wild-type endogenous NMD target transcripts (UPP1,

ATF-4, Pim3 and Pisd) in Calu-6 cells. ORCL mRNA, which is not a NMD target, was used as a control. Cells were treated with DMSO or ouabain, and then actinomycin D; samples were collected and analyzed as described in **D**. Data represent the percentage mRNA remaining six hours after transcriptional ablation (mean ± SD) from four independent experiments.

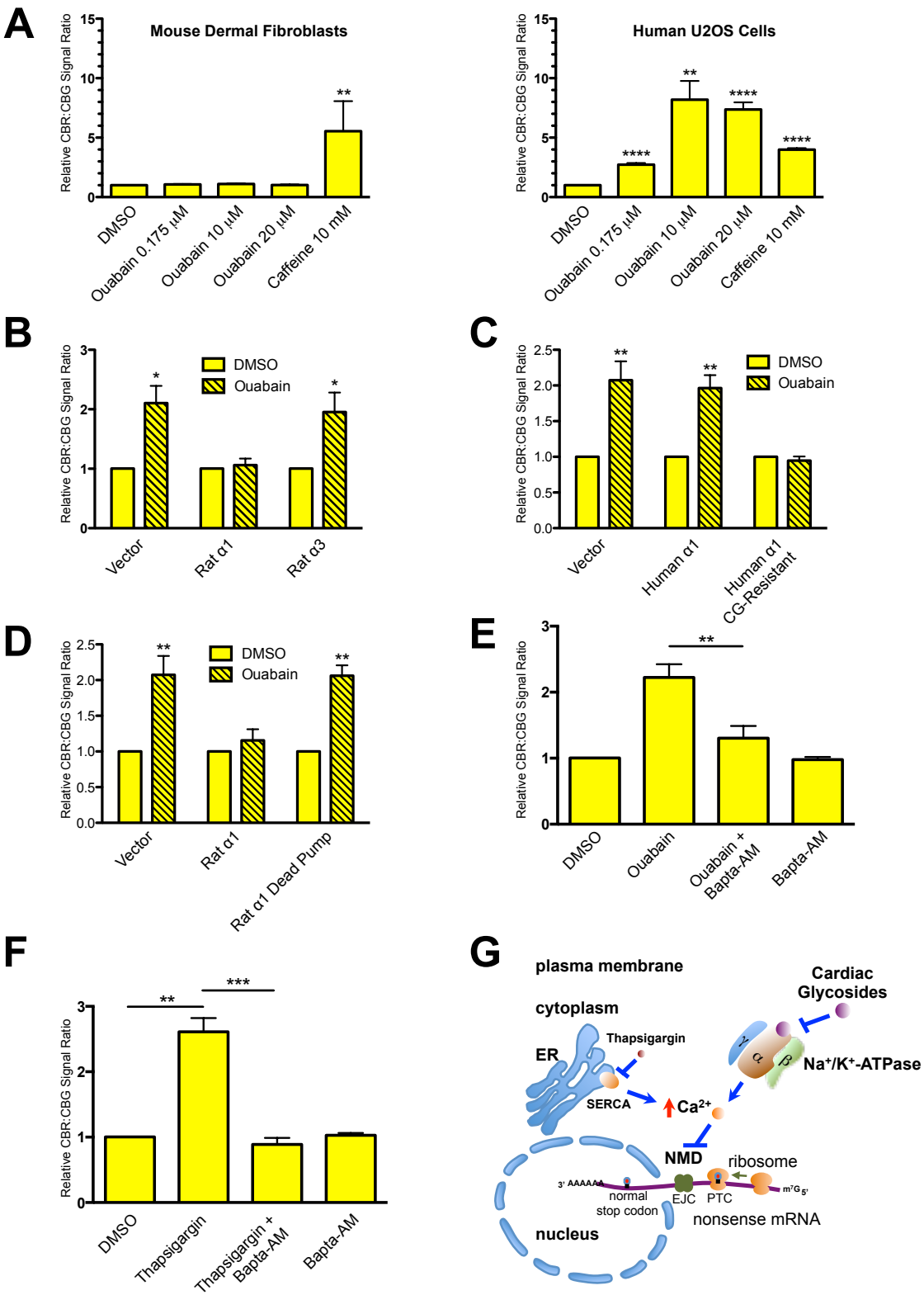
A
Mouse Dermal Fibroblasts
Relative CBR:CBG Signal Ratio
DMSO
Ouabain 0.175 µM
Ouabain 10 µM
Ouabain 20 µM
Caffeine 10 mM
Human U2OS Cells
B
DMSO
Ouabain
Vector
Rat α1
Rat α3
C
Human α1
Human α1 CG-Resistant
D
Rat α1 Dead Pump
E
Ouabain + Bapta-AM
Bapta-AM
F
Thapsigargin
Thapsigargin + Bapta-AM
G
plasma membrane
cytoplasm
ER
Cardiac Glycosides
Thapsigargin
SERCA
Ca2+
Na+/K+-ATPase
NMD
ribosome
normal stop codon
EJC
PTC
nonsense mRNA
nucleus

Figure 4. Cardiac glycosides block NMD through inhibition of Na^+/K^+-ATPase and elevation of intracellular calcium

A). Ratios of CBR/CBG bioluminescence signals in mouse dermal fibroblasts (left panel) or human U2OS cells (right panel) expressing the NMD reporter after 24 hours treatment with DMSO, caffeine, or various concentrations of ouabain. Data represent the mean ± SD of three biological replicates.

B). Ratios of CBR/CBG bioluminescence signals in human U2OS reporter cells expressing either empty vector, rat α1 subunit or rat α3 subunit of Na^+/K^+-ATPase after 24 hours treatment with DMSO or ouabain. Data represent the mean ± SD of three independent experiments.

C). Ratios of CBR/CBG bioluminescence signals in human U2OS reporter cells expressing either empty vector, human α1 subunit, or CG-resistant mutant human α1 subunit of Na^+/K^+-ATPase after 24 hours treatment with DMSO or ouabain. Data represent the mean ± SD of three independent experiments.

D). Ratios of CBR/CBG bioluminescence signals in human U2OS reporter cells expressing either empty vector, rat α1 subunit, or catalytically-inactive rat α1 subunit of Na^+/K^+-ATPase after 24 hours treatment with DMSO or ouabain. Data represent the mean ± SD of three independent experiments.

E). Ratios of CBR/CBG bioluminescence signals in human U2OS reporter cells following 24 hours treatment with DMSO, ouabain, ouabain and Bapta-AM, or Bapta-AM. Ouabain, 0.175 μM; Bapta-AM, 25 μM. Data represent the mean ± SD of three independent experiments.

F). Ratios of CBR/CBG bioluminescence signals in human U2OS reporter cells following 4 hours treatment with DMSO, Thapsigargin, Thapsigargin and Bapta-AM, or Bapta-AM. Cells were pre-treated with either DMSO or Bapta-AM for 1 hr before addition of Thapsigargin. Thasipgargin, 0.2 μM; Bapta-AM, 50 μM. Data represent the mean ± SD of three independent experiments.

G). A model for the regulation of NMD by cardiac glycosides, Na^+/K^+-ATPase and intracellular calcium.

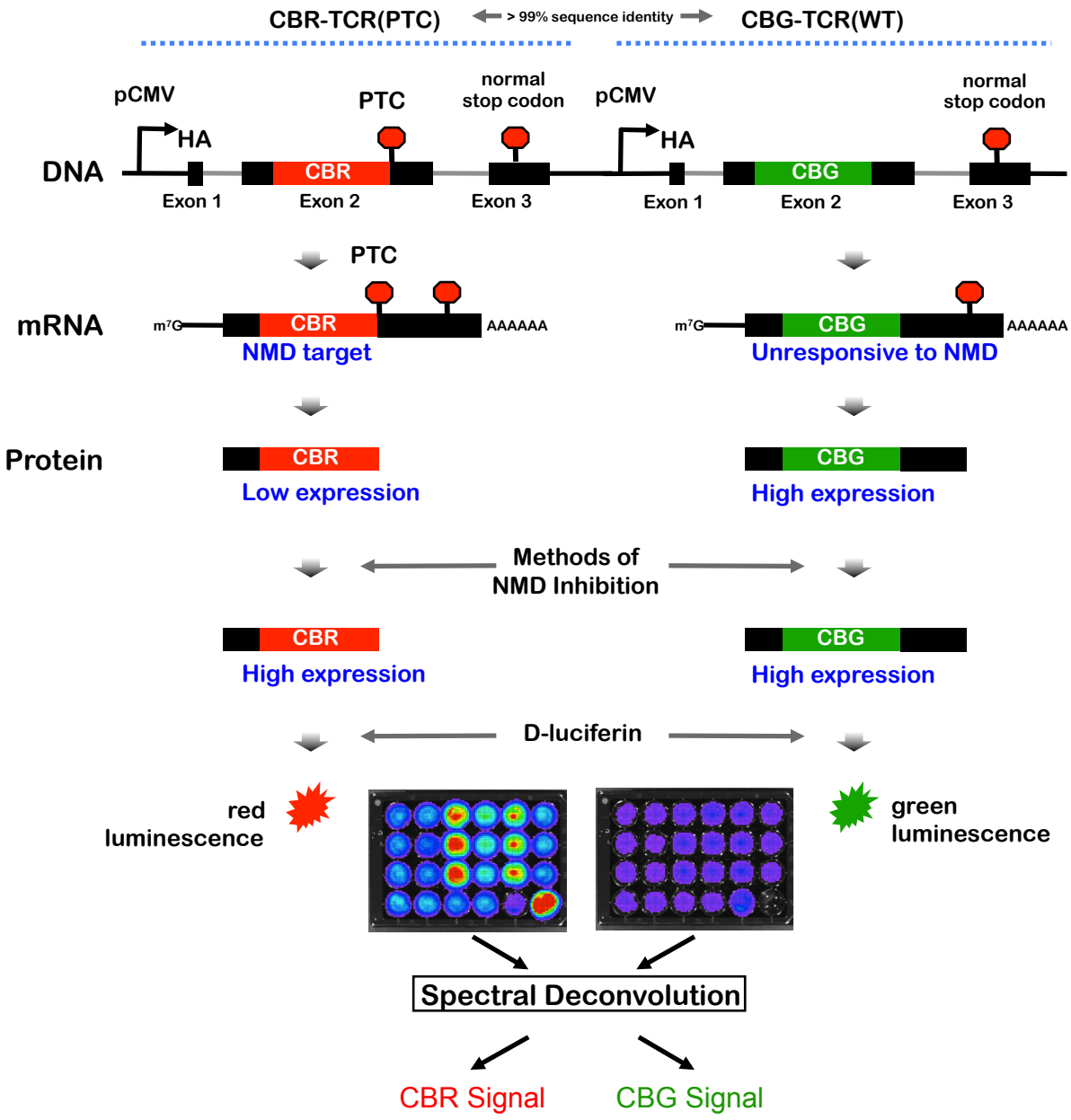
CBR-TCR(PTC)
> 99% sequence identity
CBG-TCR(WT)
pCMV
HA
PTC
normal stop codon
pCMV
HA
normal stop codon
DNA
CBR
CBG
Exon 1
Exon 2
Exon 3
Exon 1
Exon 2
Exon 3
PTC
mRNA
m7G
CBR
AAAAAA
NMD target
m7G
CBG
AAAAAA
Unresponsive to NMD
Protein
CBR
Low expression
CBG
High expression
Methods of NMD Inhibition
CBR
High expression
CBG
High expression
D-luciferin
red luminescence
green luminescence
Spectral Deconvolution
CBR Signal
CBG Signal

Supplementary Figure 1. Design of the NMD reporter system.

Two highly homologous transcription units were inserted in tandem into the pBluescript SK(-) vector. In the first unit, the CBR ORF is inserted into the second exon of a TCRβ mingene. The stop codon of CBR is used as a PTC in the fusion reporter gene. In the second unit, the CBG99 ORF without a stop codon is inserted into the same position of the TCRβ minigene. Expression of both fusion reporter genes are controlled by separate CMV promoter and polyadenylation signals of identical sequences. The protein products of these two fusion reporter units in each cell are measured by rapid sequential bioluminescence imaging using proper red/green filters. After spectral deconvolution, the pure CBR and CBG bioluminescence signals are obtained, which reflect the steady-state mRNAs levels of the two fusion reporter genes. Inhibition of NMD (e.g., by addition of caffeine) would increase the CBR/CBG ratio. An HA-tag-encoding sequence inserted into the first exons of both reporter genes provides an independent strategy to measure the translation products of these two fusion reporter genes through Western blotting.

Supplementary Figure 2. Sequence annotation of the dual-color NMD reporter.

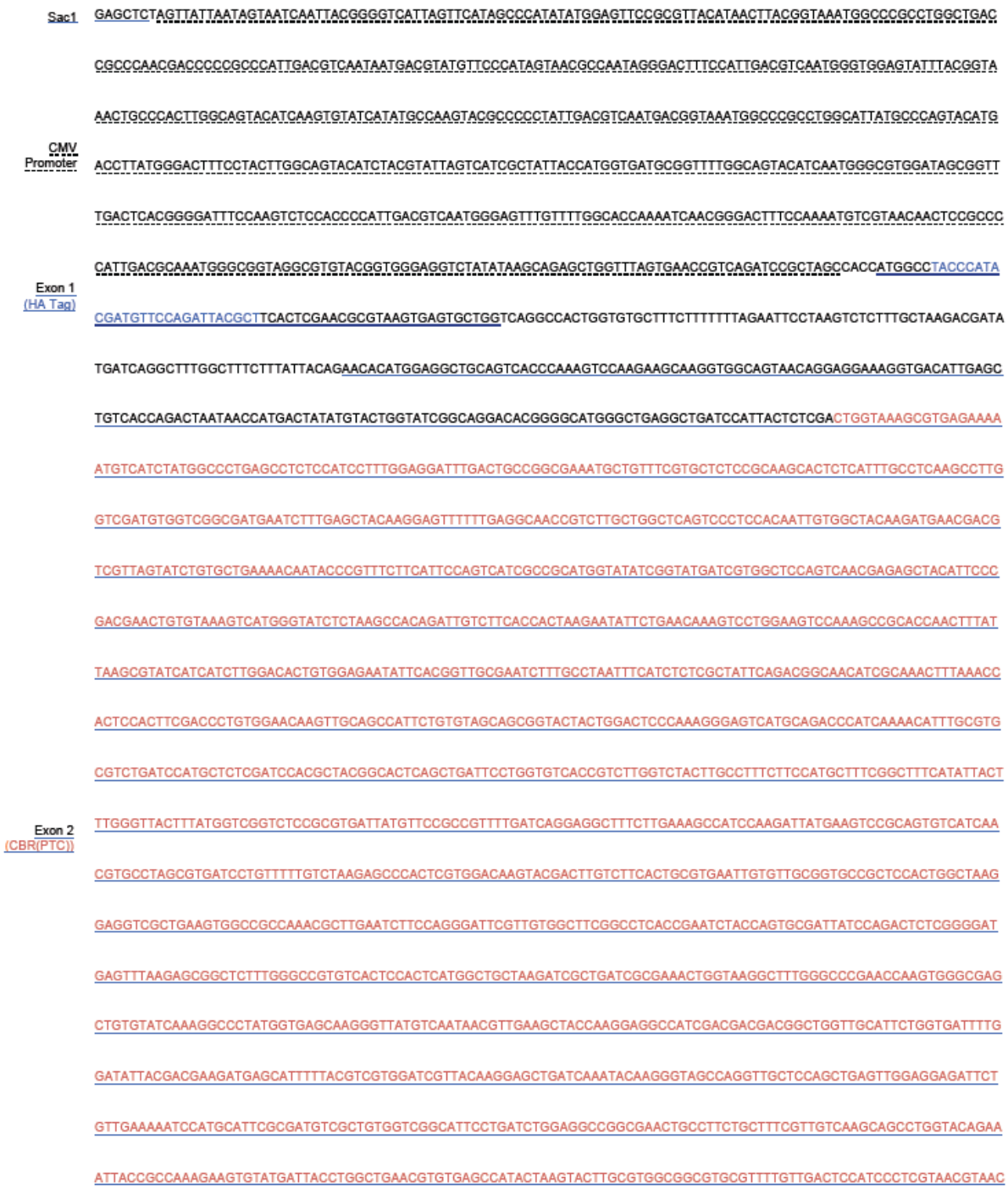

PTC AGGCAAAATTACCCGCAAGGAGCTGTTGAAACAATTGTTGGTGAAGGCCGGCGGTTGATCTCGAGCATATGTCGCTGACAGCACGGAGAAAGGAGATATCCC

TGATGGGTACAAGGCCTCCAGACCAAGCCAAGAGAATTTCTCTCTCATTCTGGAGTTGGCTTCCCTTTCTCAGACAGCTGTATATTTCTGTGCCAGCAGTCGGG

ACTGGGGGGGCGGTGCAGAAACGCTGTATTTTGGCTCAGGAACCAGACTGACTGTTCTCGGTAAGTTGGGAGCTAGTAATGAAGGGGAGGGAGCATTTCCCA

GGCTAAGGATAGCCAGAGCCAGTTTTTGTCCTGTACCAAGAGGCTGTGAGTCAAAACACCTTGTACTTTGGTGCGGGCACCCGACTATCGGTGCTAGGTAAGC

TGGGGTATAGTTTTTGTGTTGGGTTCTGGGGCTGTGAACCAAGACACCCAGTACTTTGGGCCAGGCACTCGGCTCCTCGTGTTAGGTGAGCTGGGGCCTGCT

TGCTTTTTCAGAAACTCTCTCAGCCCTGAACCTTTCCAAATACAAATGATTTGTACCTGATCCAGACAGTTATCAGCAAAATACTAATTCCACCTCTCTTTACTTT

Exon 3 CCAGAGGATCTGAGAAATGTGACTCCACCCAAGGTCTCCTTGTTTGAGCCATCAAAAGCAGAGATTGCAAACAAACAAAAGGCTACCCTCGTGTGCTTGGCCA

GGGGCTTCTTCCCTGACCACCTTCCTCGTTGACACCTTGACTCTGAAACAGACTAAATCAATAAAAACATGGAGTTCTGAAGCTTGCATGCCTGCAGCCCGGG

SV40 polyadenylation Signal GGATCCAGACATGATAAGATACATTGATGAGTGCGGCCGCGACTCTAGATCATAATCAGCCATACCACATTTGTAGAGGTTTTACTTGCTTTAAAAAACCTCCC

ACACCTCCCCCTGAACCTGAAACATAAAATGAATGCAATTGTTGTTGTTAACTTGTTTATTGCAGCTTATAATGGTTACAAATAAAGCAATAGCATCACAAATTTC

Spe1 ACAAATAAAGCATTTTTTTCACTGCATTCTAGTTGTGGTTTGTCCAAACTCATCAATGTATCTTAAGGCGTAAATTGACTAGTTATTAATAGTAATCAATTACGGG

GTCATTAGTTCATAGCCCATATATGGAGTTCCGCGTTACATAACTTACGGTAAATGGCCCGCCTGGCTGACCGCCCAACGACCCCCGCCCATTGACGTCAATA

ATGACGTATGTTCCCATAGTAACGCCAATAGGGACTTTCCATTGACGTCAATGGGTGGAGTATTTACGGTAAACTGCCCACTTGGCAGTACATCAAGTGTATCA

CMV Promoter TATGCCAAGTACGCCCCCTATTGACGTCAATGACGGTAAATGGCCCGCCTGGCATTATGCCCAGTACATGACCTTATGGGACTTTCCTACTTGGCAGTACATCT

ACGTATTAGTCATCGCTATTACCATGGTGATGCGGTTTTGGCAGTACATCAATGGGCGTGGATAGCGGTTTGACTCACGGGGATTTCCAAGTCTCCACCCCATT

GACGTCAATGGGAGTTTGTTTTGGCACCAAAATCAACGGGACTTTCCAAAATGTCGTAACAACTCCGCCCCATTGACGCAAATGGGCGGTAGGCGTGTACGGT

GGGAGGTCTATATAAGCAGAGCTGGTTTAGTGAACCGTCAGATCCGCTAGCCACCATGGCCTACCCATACGATGTTCCAGATTACGCTTCACTCGAACGCGTA

Exon 1 (HA Tag) AGTGAGTGCTGGTCAGGCCACTGGTGTGCTTTCTTTTTTTAGAATTCCTAAGTCTCTTTGCTAAGACGATATGATCAGGCTTTGGCTTTCTTTATTACAGAACAC

ATGGAGGCTGCAGTCACCCAAAGTCCAAGAAGCAAGGTGGCAGTAACAGGAGGAAAGGTGACATTGAGCTGTCACCAGACTAATAACCATGACTATATGTACT

GGTATCGGCAGGACACGGGGCATGGGCTGAGGCTGATCCATTACTCTCGACCTCGACTGGTAAAGCGTGAGAAAAATGTCATCTATGGCCCTGAGCCTCTCC

Exon 2 (CBG(WT)) ATCCTTTGGAGGATTTGACTGCCGGCGAAATGCTGTTTCGTGCTCTCCGCAAGCACTCTCATTTGCCTCAAGCCTTGGTCGATGTGGTCGGCGATGAATCTTT

GAGCTACAAGGAGTTTTTTGAGGCAACCGTCTTGCTGGCTCAGTCCCTCCACAATTGTGGCTACAAGATGAACGACGTCGTTAGTATCTGTGCTGAAAACAATA

CCCGTTTCTTCATTCCAGTCATCGCCGCATGGTATATCGGTATGATCGTGGCTCCAGTCAACGAGAGCTACATTCCCGACGAACTGTGTAAAGTCATGGGTATC

TCTAAGCCACAGATTGTCTTCACCACTAAGAATATTCTGAACAAAGTCCTGGAAGTCCAAAGCCGCACCAACTTTATTAAGCGTATCATCATCTTGGACACTGTG

GAGAATATTCACGGTTGCGAATCTTTGCCTAATTTCATCTCTCGCTATTCAGACGGCAACATCGCAAACTTTAAACCACTCCACTTCGACCCTGTGGAACAAGTT

GCAGCCATTCTGTGTAGCAGCGGTACTACTGGACTCCCAAAGGGAGTCATGCAGACCCATCAAAACATTTGCGTGCGTCTGATCCATGCTCTCGATCCACGCG

TGGGCACTCAGCTGATTFCCTGGTGTCACCGTCTTGGTCTACTTGCCTTTCTTCCATGCTTTCGGCTTTAGCATTACTTTGGGTTACTTTATGGTCGGTCTCCGC

GTGATTATGTTCCGCCGTTTTGATCAGGAGGCTTTCTTGAAAGCCATCCAAGATTATGAAGTCCGCAGTGTCATCAACGTGCCTAGCGTGATCCTGTTTTTGTC

TAAGAGCCCACTCGTGGACAAGTACGACTTGTCTTCACTGCGTGAATTGTGTTGCGGTGCCGCTCCACTGGCTAAGGAGGTCGCTGAAGTGGCCGCCAAACG

CTTGAATCTTCCAGGGATTCGTTGTGGCTTCGGCCTCACCGAATCTACCAGCGCTAACATTCACTCTCTCGGGGATGAGTTTAAGAGCGGCTCTTTGGGCCGT

GTCACTCCACTCATGGCTGCTAAGATCGCTGATCGCGAAACTGGTAAGGCTTTGGGCCCGAACCAAGTGGGCGAGCTGTGTATCAAAGGCCCTATGGTGAGC

AAGGGTTATGTCAATAACGTTGAAGCTACCAAGGAGGCCATCGACGACGACGGCTGGTTGCATTCTGGTGATTTTGGATATTACGACGAAGATGAGCATTTTTA

CGTCGTGGATCGTTACAAGGAGCTGATCAAATACAAGGGTAGCCAGGTTGCTCCAGCTGAGTTGGAGGAGATTCTGTTGAAAAATCCATGCATTCGCGATGTC

GCTGTGGTCGGCATTCCTGATCTGGAGGCCGGCGAACTGCCTTCTGCTTTCGTTGTCAAGCAGCCTGGTAAAGAAATTACCGCCAAAGAAGTGTATGATTACC

TGGCTGAACGTGTGAGCCATACTAAGTACTTGCGTGGCGGCGTGCGTTTTGTTGACTCCATCCCTCGTAACGTAACAGGCAAAATTACCCGCAAGGAGCTGTT

GAAACAATTGTTGGAGAAGGCCGGCGGTTCTCGAGCATATGTCGCTGACAGCACGGAGAAAGGAGATATCCCTGATGGGTACAAGGCCTCCAGACCAAGCCA

AGAGAATTTCTCTCTCATTCTGGAGTTGGCTTCCCTTTCTCAGACAGCTGTATATTTCTGTGCCAGCAGTCGGGACTGGGGGGGCGGTGCAGAAACGCTGTAT

TTTGGCTCAGGAACCAGACTGACTGTTCTCGGTAAGTTGGGAGCTAGTAATGAAGGGGAGGGAGCATTTCCCAGGCTAAGGATAGCCAGAGCCAGTTTTTGTC

CTGTACCAAGAGGCTGTGAGTCAAAACACCTTGTACTTTGGTGCGGGCACCCGACTATCGGTGCTAGGTAAGCTGGGGTATAGTTTTTGTGTTGGGTTCTGGG

GCTGTGAACCAAGACACCCAGTACTTTGGGCCAGGCACTCGGCTCCTCGTGTTAGGTGAGCTGGGGCCTGCTTGCTTTTTCAGAAACTCTCTCAGCCCTGAAC

CTTTCCAAATACAAATGATTTGTACCTGATCCAGACAGTTATCAGCAAAATACTAATTCCACCTCTCTTTACTTTCCAGAGGATCTGAGAAATGTGACTCCACCCA

Exon 3

AGGTCTCCTTGTTTGAGCCATCAAAAGCAGAGATTGCAAACAAACAAAAGGCTACCCTCGTGTGCTTGGCCAGGGGCTTCTTCCCTGACCACCTTCCTCGTTG

ACACCTTGACTCTGAAACAGACTAAATCAATAAAAACATGGAGTTCTGAAGCTTGCATGCCTGCAGCCCGGGGGATCCAGACATGATAAGATACATTGATGAGT

GCGGCCGCGACTCTAGATCATAATCAGCCATACCACATTTGTAGAGGTTTTACTTGCTTTAAAAAACCTCCCACACCTCCCCCTGAACCTGAAACATAAAATGA

SV40 polyadenylation Signal

ATGCAATTGTTGTTGTTAACTTGTTTATTGCAGCTTATAATGGTTACAAATAAAGCAATAGCATCACAAATTTCACAAATAAAGCATTTTTTTCACTGCATTCTAGT

Kpn1 TGTGGTTTGTCCAAACTCATCAATGTATCTTAAGGCGTAAATTGGGTACC

A

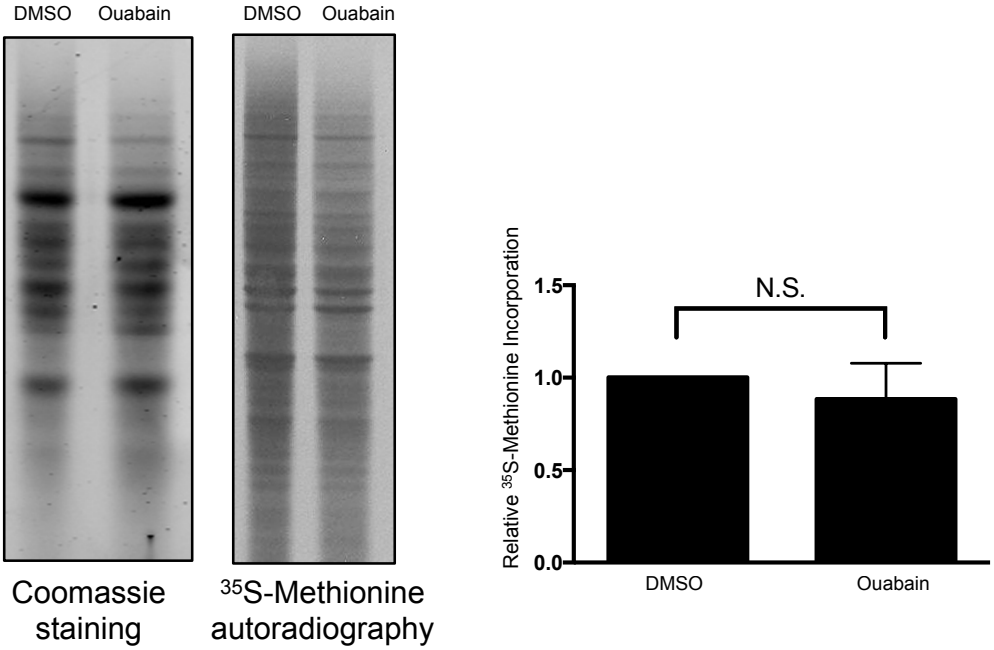
DMSO
Ouabain
DMSO
Ouabain
Coomassie staining
35S-Methionine autoradiography
Relative 35S-Methionine Incorporation
1.5
1.0
0.5
0.0
N.S.
DMSO
Ouabain

B

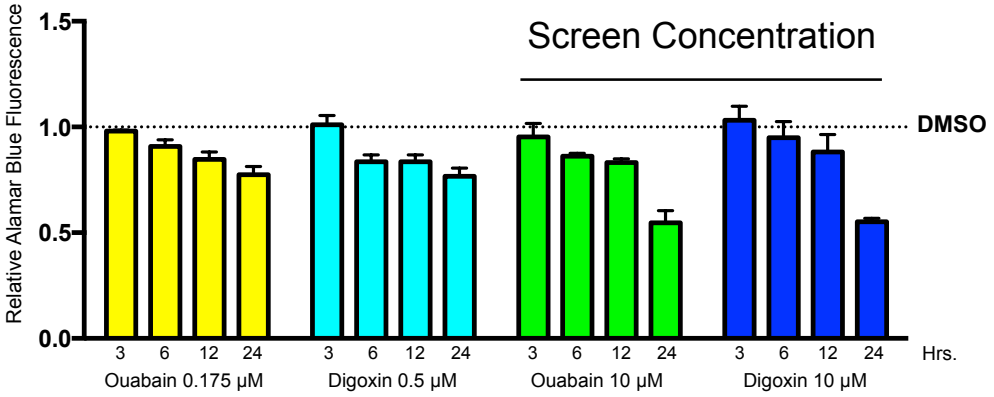
Relative Alamar Blue Fluorescence
1.5
1.0
0.5
0.0
Screen Concentration
DMSO
3
6
12
24
Hrs.
Ouabain 0.175 µM
Digoxin 0.5 µM
Ouabain 10 µM
Digoxin 10 µM

Supplementary Figure 3. Effects of the cardiac glycosides on general translation and cell viability.

A). Effects of ouabain on general translation. Left panel: representative images of Comassie blue staining of total proteins and ^{35}S-methionine incorporation in newly synthesized proteins in the NMD reporter cells treated with DMSO or ouabain. Right panel: quantified results for ^{35}S-methionine incorporation in cells treated with DMSO or ouabain. Data represent the mean ± SD of three independent experiments. The signal in DMSO-treated cells was normalized to 1.

B). Effects of ouabain on cell viability. AlamarBlue fluorescence levels in NMD U2OS reporter cells treated with DMSO, ouabain or digoxin for 3, 6, 12, or 24 hours. Data represent the mean ± SD of three independent experiments. The fluorescence in DMSO-treated cells was normalized to 1.

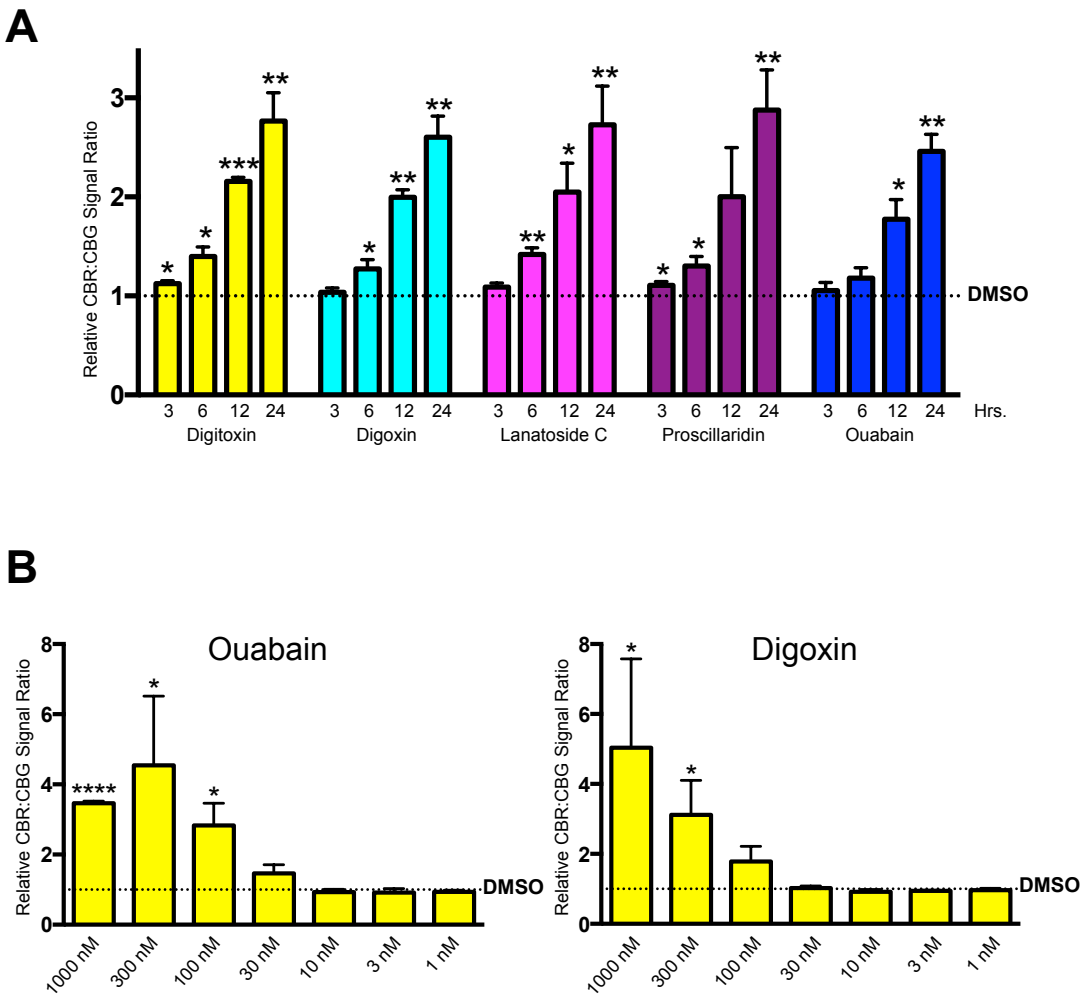

Supplementary Figure 4. Effects of the cardiac glycosides on NMD.

A). Ratios of CBR/CBG bioluminescence signals in NMD reporter cells treated with DMSO or cardiac glycosides for 3, 6, 12, or 24 hours at the indicated concentrations. Data represent the mean ± SD of three independent experiments. The ratio in DMSO-treated cells was normalized to 1.

B). Ratios of CBR/CBG bioluminescence signals in NMD reporter cells treated with various concentration of ouabain and digoxin for 24 hours. Data represent the mean ± SD of three independent experiments. The ratio in DMSO-treated cells was normalized to 1.

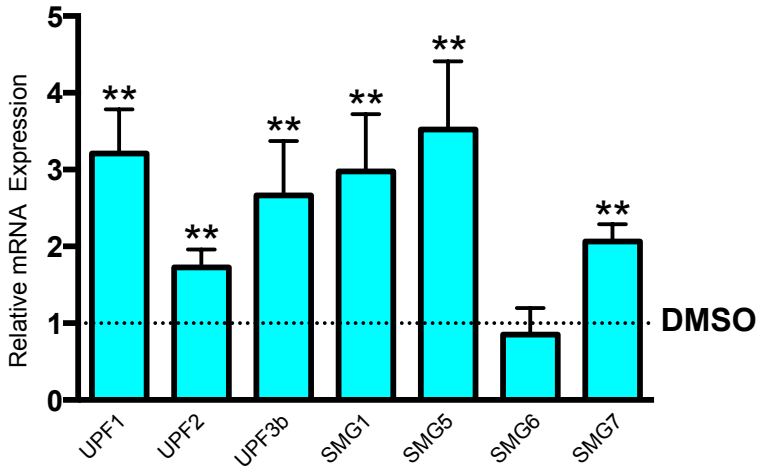

Supplementary Figure 5. Effects of ouabain on the levels of endogenous NMD factor transcripts.

Results of qPCR analysis of NMD factor mRNAs in NMD reporter cells treated with DMSO or ouabain for 24 hours. Data represent the mean ± SD of four independent experiments. The mRNA expression in DMSO-treated cells was normalized to 1.

A

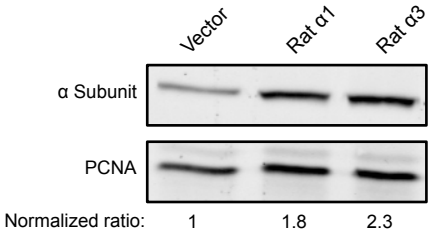
Vector
Rat α1
Rat α3
α Subunit
PCNA
Normalized ratio:
1
1.8
2.3

B

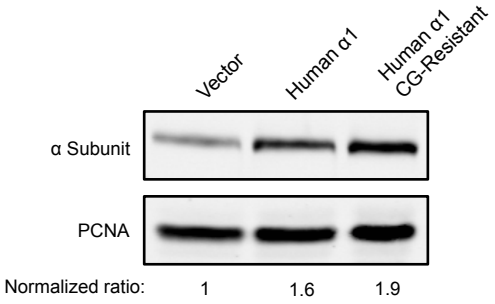
Vector
Human α1
Human α1
CG-Resistant
α Subunit
PCNA
Normalized ratio:
1
1.6
1.9

C

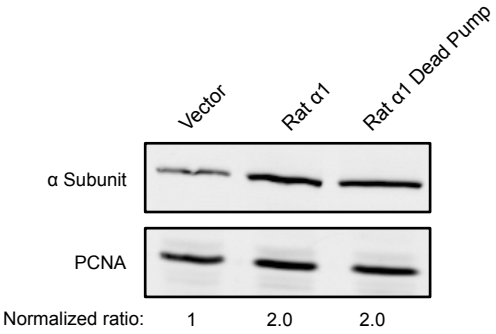
Vector
Rat α1
Rat α1 Dead Pump
α Subunit
PCNA
Normalized ratio:
1
2.0
2.0

Supplementary Figure 6. Expression levels of Na^+/K^+-ATPase α subunit isoforms and mutants.

A). Related to Fig. 4B. Levels of all α subunits of Na^+/K^+-ATPase in human U2OS reporter cells transfected with empty vector, rat α1 subunit or rat α3 subunit of Na^+/K^+-ATPase.

B). Related to Fig. 4C**.** Levels of all α subunits of Na^+/K^+-ATPase in human U2OS reporter cells transfected with empty vector, human α1 subunit, or CG-resistant mutant human α1 subunit of Na^+/K^+-ATPase.

C). Related to Fig. 4D**.** Levels of all α subunits of Na^+/K^+-ATPase in human U2OS reporter cells transfected with empty vector, rat α1 subunit, or catalytically-inactive rat α1 subunit of Na^+/K^+-ATPase.

Protein levels of α subunits of Na^+/K^+-ATPase were determined by a pan-Na^+/K^+-ATPase antibody that recognizes all α isoforms from both human and rat. Normalized expression levels relative to a house-keeping protein PCNA were quantified using Odyssey (Li-Cor) software.

2.7 Tables

Supplementary Table 1. Specificity of qPCR analysis for the CBR-TCR(PTC) and CBG-TCR(WT) reporter mRNAs. Two regions with clustered sequence variations in the open reading frames of CBR and CBG were chosen to design qPCR primer sets for CBR-TCR(PTC) and CBG-TCR(WT) mRNAs, respectively. Results of qPCR analysis of the two reporter DNA templates show that CBR-specific primer set could not anneal to and amplify CBG-TCR(WT) and that CBG-specific primer sets could not anneal to and amplify CBR-TCR(PTC), demonstrating the specificity of these primers.

DNA Sample	Primer Set	Relative Signal (Arbitrary Units)
CBG-TCR(WT)	CBR	0.004
	CBG	2420.133
CBR-TCR(PTC)	CBR	1044.636
	CBG	0.053

Supplementary Table 2. Primary data of the Pharmakon drug library screen.

Compound	CBR:CBG Ratio (Relative to DMSO)	STDEV for Relative CBR:CBG Ratio	P-Value	CBG (Relative to DM
OUABAIN	13.11573875	2.770982402	4.67787E-08	0.284422046
DIGOXIN	13.04031444	2.909425255	7.95344E-08	0.195833991
DIGITOXIN	11.32623422	3.462787645	1.67383E-06	0.187529381
DOCUSATE SODIUM	10.47335893	2.135605626	5.25643E-08	0.349535902
PROSCILLARIDIN	8.170570565	1.460230803	3.29538E-08	0.31273244
LANATOSIDE C	7.50198789	1.744622647	2.60071E-07	0.723547258
BUTYL PARABEN	6.47305491	2.261641368	1.16848E-05	0.251007595
GENTIAN VIOLET	3.818000549	1.4374894	7.48864E-05	1.322600348
ETHACRIDINE LACTATE	3.636277473	0.601180089	1.17182E-06	0.147268365
PERHEXILINE MALEATE	3.108779281	0.868736631	1.3514E-05	0.382982542
THIMEROSAL	2.938604024	1.952301931	0.007944026	1.319435208
DANTROLENE SODIUM	2.915480009	0.748318486	9.35144E-06	1.42198679
PHENYL AMINOSALICYLATE	2.747733135	0.581989524	5.74853E-06	0.182877577
ACRISORCIN	2.723372554	0.174804788	4.27791E-10	0.362588036
TRIMIPRAMINE MALEATE	2.558155916	0.136640538	2.5411E-09	0.581061265
ACRIFLAVINIUM HYDROCHLORIDE	2.524211505	0.194478913	1.59518E-06	0.240401917
FELBINAC	2.521500047	0.041909154	9.5857E-08	0.536563669
TENIPOSIDE	2.383709621	0.14818139	1.72925E-09	1.407257225
PROFLAVINE HEMISULFATE	2.340827716	0.236444348	7.64423E-06	0.755432613
ERYTHROSINE SODIUM	2.328350506	0.337079434	6.89295E-07	0.648857707
SECURININE	2.306075764	0.802547325	0.000862207	2.631667288
DAUNORUBICIN	2.073758224	0.255009526	1.26961E-05	0.139350195
AMCINONIDE	2.048417138	0.617856442	0.000547235	1.899372051
DACTINOMYCIN	2.000874906	0.372078481	2.64758E-05	0.111039469
VARDENAFIL HYDROCHLORIDE	1.967234609	0.180228885	1.4929E-05	1.667127224
BENZETHONIUM CHLORIDE	1.935684809	0.556506455	0.000493805	2.09820458
OXYBENZONE	1.926824891	0.15422391	1.67086E-06	0.404646597
METHSCOPOLAMINE BROMIDE	1.918513351	0.624344624	0.003136994	1.50545159
RALOXIFENE HYDROCHLORIDE	1.913821816	0.318718962	6.52806E-05	1.429752677
EQUILIN	1.911484702	0.320538864	0.000102739	0.768798802
TRIFLUPROMAZINE HYDROCHLORIDE	1.855890417	0.433360574	0.00015898	1.516465067
MONOBENZONE	1.849949218	0.4847508	0.003422507	0.29201115
CETRIMONIUM BROMIDE	1.795356397	0.516813317	0.007471041	1.046789269
DIPYRIDAMOLE	1.787258169	0.192933597	9.4806E-05	1.420048493
CETYLPYRIDINIUM CHLORIDE	1.766292929	0.20097289	1.93883E-05	0.288983268
PODOFILOX	1.762268783	0.578443002	0.001725158	3.020968491
AMINACRINE	1.748318648	0.066712164	3.26572E-05	0.473973468
EMETINE DIHYDROCHLORIDE	1.747823619	0.242140605	0.000224045	0.11289672
PRAZOSIN HYDROCHLORIDE	1.732579761	0.203857567	0.000227345	2.202421447
TACRINE HYDROCHLORIDE	1.722661435	0.523477326	0.002470128	2.104874993
DOXORUBICIN	1.715761543	0.361335598	0.00070555	0.11384062
DROFENINE HYDROCHLORIDE	1.703219226	0.780262031	0.027181833	1.079376301
THIORIDAZINE HYDROCHLORIDE	1.699483065	1.242874666	0.101766209	0.079065192
CHLORPROTHIXENE HYDROCHLORIDE	1.694710439	0.46933045	0.001205858	1.440021766
DICHLORVOS	1.691396932	0.363740579	0.001949291	1.591769841
ALFUZOSIN HYDROCHLORIDE	1.665774396	0.170273984	0.000620715	1.416119004
ANAGRELIDE HYDROCHLORIDE	1.664705477	0.138808332	0.000128461	1.272319782
BENZALKONIUM CHLORIDE	1.649714327	0.085678984	9.86255E-05	2.251442355
VINBLASTINE SULFATE	1.640718958	0.293205574	0.00031248	2.825357924
IMIPRAMINE HYDROCHLORIDE	1.596345274	0.394067849	0.002397232	0.913505301
NITROFURANTOIN	1.581256702	0.466088819	0.00729223	1.418205975
ALTRENOGEST	1.575948832	0.165755294	0.000486545	1.371162138
MEGESTROL ACETATE	1.565364115	0.232532906	0.000347222	1.64202152
FLUROXENE	1.559890523	0.155819031	0.00058749	1.435558873
FINASTERIDE	1.558397784	0.197557708	0.005632739	1.651301546
MOGUISTEINE	1.556547552	1.289557417	0.203998567	1.245302393
PHENYLBUTAZONE	1.553361645	0.519968093	0.010103202	1.114196252
LOPERAMIDE HYDROCHLORIDE	1.542080142	0.312142938	0.000462682	1.273140198
FENOFIBRIC ACID	1.541917699	0.328075596	0.006792115	1.222448791
OCTOPAMINE HYDROCHLORIDE	1.536005223	0.121106963	0.004232354	1.14689652
PIMOZIDE	1.525290106	0.391760381	0.004143808	1.470402881
GEMIFLOXACIN MESYLATE	1.522708567	0.319369904	0.000688077	1.290706282
FAMPROFAZONE	1.51939058	0.087909861	0.000503427	1.54683724
INDOMETHACIN	1.519324098	0.462202837	0.010227528	1.348391513
TRICHLORFON	1.519061025	0.372831357	0.002893694	1.282300788
DIFLOXACIN HYDROCHLORIDE	1.511913604	0.052164651	2.40722E-06	1.292318213
PAZUFLOXACIN MESYLATE	1.510434826	0.810288414	0.098016345	1.124427475
TETRAMIZOLE HYDROCHLORIDE	1.508466162	0.370946791	0.003223168	3.400941425

DOXAZOSIN MESYLATE	1.503355836	0.186842635	0.000475097	1.446986217
ETHYL PARABEN	1.500356253	0.166003975	0.029087273	0.476471883
FLUNARIZINE HYDROCHLORIDE	1.500153597	0.133347471	0.001116463	1.470422903
DANTHRON	1.497589328	0.046250558	2.8678E-06	0.810533484
AZELASTINE HYDROCHLORIDE	1.495416951	0.077997624	0.002014742	1.149468946
OLMESARTAN	1.489936555	0.64013501	0.039759763	1.272551328
BERBERINE CHLORIDE	1.488014402	0.386044393	0.023055472	1.068738761
PROPANTHELINE BROMIDE	1.471496058	0.096367882	0.002724065	1.063635939
COLCHICINE	1.468732911	0.220802959	0.004786654	3.238146193
DERACOXIB	1.463778266	0.208067274	0.005798464	1.579204567
BUDESONIDE	1.462741165	0.290911992	0.006449903	1.292035918
MELENGESTROL ACETATE	1.458971498	0.374065141	0.012938561	1.732538565
NONOXYNOL-9	1.456648839	0.393348853	0.005113855	1.655448382
QUINETHAZONE	1.452113848	0.677451484	0.073257916	1.958304905
CYCLOBENZAPRINE HYDROCHLORIDE	1.446792877	0.054829825	0.000299956	1.202994255
MEBEVERINE HYDROCHLORIDE	1.446186064	0.423563964	0.0210532	1.583634201
CYANOCOBALAMIN	1.444993092	0.216093738	0.004441087	1.260521796
KETOROLAC TROMETHAMINE	1.443440741	0.12232434	0.002076046	1.6322347
BETAHISTINE HYDROCHLORIDE	1.44281054	0.224667114	0.004892295	1.658017213
HYDROXYPROGESTERONE CAPROATE	1.440645781	0.306016438	0.01775295	1.747806615
FLUTAMIDE	1.440520677	0.355532219	0.013924845	1.646295733
VANCOMYCIN HYDROCHLORIDE	1.439249426	0.542391942	0.045127054	1.154776942
SITAGLIPTIN MONOPHOSPHATE MONOHY	1.433562267	0.337221072	0.022690196	1.070542014
BEKANAMYCIN SULFATE	1.430414066	0.241277703	0.006577342	1.437136731
NADIFLOXACIN	1.423976235	0.19221331	0.004174262	1.111661452
ROFECOXIB	1.419500469	0.183262825	0.008879429	1.126493381
RIBAVIRIN	1.416845982	0.416838274	0.096466716	1.207595529
DANAZOL	1.416761327	0.131371808	0.005612204	1.474117481
PROMAZINE HYDROCHLORIDE	1.413649958	0.300507844	0.018004649	1.619404775
ISOETHARINE MESYLATE	1.411038682	0.363956648	0.020281024	1.03522298
THONZONIUM BROMIDE	1.410845676	0.401622363	0.026121215	1.139395727
PENFLURIDOL	1.407633286	0.473313331	0.094663058	1.607649885
ISOLEUCINE (L)	1.405453658	0.162821029	0.005017138	1.105541724
DROSPIRENONE	1.40240464	0.189614372	0.070073645	1.566274469
PENTAGASTRIN	1.395816011	0.41456456	0.032695484	1.338749562
MANIDIPINE HYDROCHLORIDE	1.395353881	0.282846958	0.086627871	1.122527772
ISOXSUPRINE HYDROCHLORIDE	1.393731178	0.283348646	0.009636213	1.491950873
CHLORCYCLIZINE HYDROCHLORIDE	1.390656481	0.422550072	0.026478764	1.211330951
HYMECHROME	1.385007975	0.251180461	0.006017513	1.148671138
CLOFAZIMINE	1.382945786	0.449071703	0.130744941	1.614098474
TANNIC ACID	1.380020196	0.049734735	3.21386E-05	1.465578606
KETOTIFEN FUMARATE	1.379465067	0.271277417	0.016084747	1.314422734
HEXYLRESORCINOL	1.376539276	0.358315617	0.022448466	0.894822802
DEXCHLORPHENIRAMINE MALEATE	1.375217542	0.120740215	0.006138704	1.201138094
PERPHENAZINE	1.372276021	0.033902775	0.004400549	1.722547701
FLORFENICOL	1.371669435	0.176904303	0.009050938	1.16421294
LETROZOLE	1.371382829	0.837624309	0.183645132	0.124574221
RISEDRONATE SODIUM	1.370078096	0.159536437	0.088453492	1.364123165
ZIPRASIDONE MESYLATE	1.367449521	0.121170763	0.006937946	1.322384843
VINPOCETINE	1.364455699	0.222460292	0.100557816	1.253539593
ALVERINE CITRATE	1.363643101	0.302488463	0.013671978	1.347875956
VIGABATRIN	1.362429593	0.451967898	0.057852536	0.929194389
ETHAVERINE HYDROCHLORIDE	1.361164288	0.166020594	0.036280126	1.580939726
CLIOQUINOL	1.35692365	0.149802043	0.010001512	1.464201682
TESTOSTERONE PROPIONATE	1.347702776	0.345077013	0.012788055	1.738338126
NILUTAMIDE	1.345777338	0.222968412	0.002080505	1.517464228
SODIUM PHENYLACETATE	1.34570668	0.123430115	0.024966459	1.028715903
RISPERIDONE	1.345474071	0.393720336	0.050839588	0.937757513
BENZYL BENZOATE	1.344881825	0.207866339	0.003792247	0.791813663
BEPRIDIL HYDROCHLORIDE	1.343305302	0.330200497	0.016688023	1.73176085
ERGOTAMINE TARTRATE	1.341086976	0.352526066	0.064282896	1.574021822
OFLOXACIN	1.339628103	0.209944145	0.060418355	1.422540124
TORSEMIDE	1.335625779	0.128386674	0.028887503	1.02007574
PROGESTERONE	1.332647067	0.453900744	0.06781627	1.771443487
LINAGLIPTIN	1.330015249	0.600311344	0.123944357	1.188980471
LOXAPINE SUCCINATE	1.329356768	0.213456198	0.021826209	1.255900586
MEDROXYPROGESTERONE ACETATE	1.327402448	0.237485352	0.016942781	1.507434341
NIFEDIPINE	1.326970285	0.151451361	0.015882997	1.372093887
CHLOROTHIAZIDE	1.325183159	0.292871015	0.021671131	1.281258821
TELMISARTAN	1.324261676	0.312116222	0.156724296	0.863931263
ALBUTEROL	1.322311667	0.270857467	0.149913203	1.540932595
YOHIMBINE HYDROCHLORIDE	1.321976257	0.297213233	0.039642445	1.503849808

CEPHRADINE	1.318028285	0.0777598	0.003857359	1.149246779
VINCRISTINE SULFATE	1.317760451	0.164072192	0.102419561	3.202049464
VALGANCICLOVIR HYDROCHLORIDE	1.317042887	0.355658843	0.056939639	1.193587171
TRAZODONE HYDROCHLORIDE	1.316583587	0.350831474	0.029483904	1.096852827
THIOPENTAL SODIUM	1.315115757	0.114624453	0.036400871	0.892302382
CHLORQUINALDOL	1.314180406	0.662432785	0.185891153	1.023198923
ASTEMIZOLE	1.311471608	0.291355317	0.018051941	1.401223973
TANDUTINIB	1.311288183	0.164834085	0.066779048	1.140003944
FLURBIPROFEN	1.309870778	0.355368645	0.049861926	1.889264048
OXELAIDIN CITRATE	1.309801837	0.085092506	0.055913386	1.09048287
BISACODYL	1.304239092	0.257230159	0.021844614	1.316316296
IMIQUIMOD	1.30358209	0.426447022	0.051168859	1.74712915
TRIMETHADIONE	1.302482239	0.363286539	0.069822799	1.110052746
BUTACAINE	1.302166917	0.109248499	0.017523026	1.283081037
ENTACAPONE	1.300602024	0.211986948	0.058713431	1.087135854
NISOLDIPINE	1.299812073	0.214596659	0.048819894	1.057426837
EVANS BLUE	1.29975287	0.142666447	0.11768176	1.256046358
THIOTHIXENE	1.298620598	0.287607883	0.065033783	1.457203749
TICLOPIDINE HYDROCHLORIDE	1.296373656	0.431115376	0.101420441	0.894788486
IRSOGLADINE MALEATE	1.29472008	0.117524604	0.070018069	0.927714732
OXYPHENBUTAZONE	1.294685724	0.110431843	0.007141165	0.969734388
ACONITINE	1.293443263	0.599000081	0.17295489	1.24374549
DICLAZURIL	1.291998951	0.275200421	0.023500173	1.038625769
TEPOXALIN	1.291895563	0.096680537	0.081273476	1.356799639
NORTRIPTYLINE HYDROCHLORIDE	1.291551212	0.220057949	0.018929039	1.036867728
MITOXANTRONE HYDROCHLORIDE	1.291462357	0.211516676	0.034649021	0.126967234
ESTRADIOL CYPIONATE	1.286777169	0.267099094	0.063489332	1.394119403
CASANTHRANOL [cascaroside A shown]	1.285289458	0.254094537	0.050197153	1.254622499
FULVESTRANT	1.285274589	0.385671779	0.158614269	1.43009598
MECHLORETHAMINE	1.284906188	0.201518873	0.068464002	1.185589842
ATOVAQUONE	1.28351952	0.265396461	0.198823647	1.362643108
MEXILETINE HYDROCHLORIDE	1.282652692	0.247961547	0.047811037	1.222266849
MEBHYDROLIN NAPHTHALENESULFONAT	1.280778654	0.064108441	0.076768312	1.307400859
TYROTHRICIN	1.280691355	0.367280779	0.091933964	3.225728185
TRAVOPROST	1.280326386	0.034245197	0.17191574	1.293173793
PRANOPROFEN	1.279574202	0.348026404	0.141395284	1.231429267
ALTHIAZIDE	1.277593958	0.406879485	0.112192173	1.350915014
ESTRONE	1.275666458	0.369183667	0.081152341	1.776736273
ACETOPHENAZINE MALEATE	1.275179891	0.172906417	0.192874694	1.366297086
SULISOBENZONE	1.27414811	0.242739533	0.030234401	1.046596754
FOLIC ACID	1.273954552	0.248736919	0.128553878	1.572845149
TRIMEBUTINE MALEATE	1.271847976	0.400692641	0.172083826	1.168150969
CLOBETASOL PROPIONATE	1.27155321	0.075937891	0.02571932	1.880294077
N-METHYL (-)EPHEDRINE [1R,2S]	1.27083999	0.269151292	0.126036497	1.094028613
ALRESTATIN	1.269593238	0.393778731	0.074981792	1.071242778
ALLANTOIN	1.267953239	0.231169636	0.0564449	1.454825815
CAPOBENIC ACID	1.267627239	0.219602322	0.052198207	1.127734339
TERBINAFINE HYDROCHLORIDE	1.26654097	0.341913602	0.041625487	1.279972102
GRAMICIDIN (gramicidin A shown)	1.26634516	0.10990881	0.019358725	1.214496961
CINNARAZINE	1.26624768	0.262030173	0.027856585	1.311480988
CEPHARANTHINE	1.266227876	0.223668729	0.050564981	1.188429667
NIFENAZONE	1.265866292	0.150778113	0.10685304	0.914592249
DILAZEP DIHYDROCHLORIDE	1.26546968	0.344532185	0.070841061	1.286553279
TERBUTALINE HEMISULFATE	1.265122519	0.408888204	0.145939327	1.893243061
THEOBROMINE	1.263302108	0.134801734	0.002353464	1.286808739
CYCLOHEXIMIDE	1.262451991	0.18199735	0.015755943	0.802633468
DEHYDROACETIC ACID	1.262197073	0.355628455	0.180007894	1.400767472
CHLOROQUINE DIPHOSPHATE	1.261870497	0.191627495	0.025447766	1.41681527
AMODIAQUINE DIHYDROCHLORIDE	1.260382528	0.300750411	0.057578783	1.311123099
PIROMIDIC ACID	1.259300506	0.47291842	0.22267568	1.185915072
TEMOZOLAMIDE	1.258626398	0.165282743	0.127875159	1.588419123
MEGLUTOL	1.258429403	0.137375996	0.122864224	1.691200711
LISINOPRIL	1.257204119	0.368918354	0.192892025	1.447815513
EUCALYPTOL	1.257054385	0.27034768	0.241800608	1.112432419
TIOXOLONE	1.25669268	0.725349355	0.343549781	1.285319183
LOMEFLOXACIN HYDROCHLORIDE	1.256519388	0.072228288	0.164939026	1.199807305
LIPOAMIDE	1.256031103	0.446269219	0.216078856	1.309908824
CYPROHEPTADINE HYDROCHLORIDE	1.255316752	0.184796446	0.006855797	1.647508698
OXEDRINE	1.254441093	0.351628963	0.17824269	1.550423465
ACETYLCYSTEINE	1.252382292	0.262726922	0.050039473	1.155178357
MOMETASONE FUROATE	1.251582568	0.298586904	0.258600534	1.673205571
ACYCLOVIR	1.251480164	0.231410925	0.06723133	1.307900082

CEFTRIAXONE SODIUM TRIHYDRATE	1.251155474	0.175320013	0.015082246	1.382615597
MIFEPRISTONE	1.250884004	0.206193782	0.195003356	1.686897408
OLSALAZINE SODIUM	1.250846052	0.137191155	0.02940862	1.440655395
EFLOXATE	1.25029175	0.310992192	0.168893816	1.327680169
CLEMIZOLE HYDROCHLORIDE	1.250101839	0.228407949	0.225858853	1.900892663
PROTRYPTYLINE HYDROCHLORIDE	1.248804155	0.171306749	0.052985022	1.004358178
ARECOLINE HYDROBROMIDE	1.24780373	0.331012724	0.049989902	1.397221239
PAROXETINE HYDROCHLORIDE	1.247783575	0.198586481	0.060787864	1.537919397
ETOMIDATE	1.247160042	0.262813875	0.084156916	1.25428433
METICRANE	1.246987717	0.27100235	0.159568775	1.177401378
FLUOXETINE	1.246857179	0.350879511	0.120825634	1.310169737
SELEGILINE HYDROCHLORIDE	1.246000294	0.422936212	0.197575905	1.101820431
BETAINE HYDROCHLORIDE	1.2451383	0.205149268	0.023079338	1.31252034
CHOLESTEROL	1.244399107	0.389514594	0.147060297	1.413301719
BEMOTRIZINOL	1.243953819	0.284772593	0.26872212	1.124389804
LEVOSIMENDAN	1.243147534	0.171490622	0.020641894	1.171513816
IDOXURIDINE	1.242186936	0.053839085	0.186139539	1.320060261
PEFLOXACINE MESYLATE	1.240939853	0.128800911	0.079691469	0.998420018
FIUMAZENIL	1.2408886	0.39278702	0.152459916	1.02240516
SELAMECTIN	1.24050481	0.228959123	0.077212075	1.664238417
NATAMYCIN	1.239712259	0.206948842	0.11822497	1.044408943
TETROQUINONE	1.23868248	0.119338363	0.050357954	1.474981622
EXEMESTANE	1.238049873	0.214638986	0.105386512	1.917251969
BENZYL ALCOHOL	1.23792663	0.347295405	0.203722112	1.168375846
CAMYLOFINE DIHYDROCHLORIDE	1.237825841	0.329041202	0.196349184	1.20311886
METERGOLINE	1.237781629	0.120036607	0.048404745	1.099090006
QUININE ETHYL CARBONATE	1.237257159	0.221940784	0.158722303	1.146028276
CANDESARTAN	1.236299295	0.508070234	0.290285976	1.126176321
TRIACETIN	1.234621337	0.215877653	0.107016244	1.120184975
LOSARTAN	1.234608866	0.385011568	0.091579929	1.336166093
LOBELINE HYDROCHLORIDE	1.23429656	0.329557187	0.20273691	1.295041247
DILTIAZEM HYDROCHLORIDE	1.233038347	0.126780905	0.060331964	1.524375407
CARBADOX	1.232751726	0.293809865	0.292421968	1.193738765
CHLORMADINONE ACETATE	1.232746829	0.17823668	0.101065751	1.665996538
CLOPIDOGREL SULFATE	1.232039091	0.371377501	0.153019794	1.248438716
ALLYLISOTHIOCYANATE	1.230422239	0.243782381	0.098254129	2.430771883
GUANADREL SULFATE	1.227322865	0.165145563	0.037509146	1.168805776
ACECLOFENAC	1.223522566	0.400186263	0.258032639	1.174769175
SPARFLOXACIN	1.221789704	0.118397531	0.229946049	1.13487664
SULOCTIDIL	1.221512547	0.295216953	0.226827867	1.240364056
BENOXINATE HYDROCHLORIDE	1.221120789	0.097328155	0.228330504	1.374696875
BENZOYLPAS	1.220831266	0.325231046	0.148340075	0.991276621
MEFENAMIC ACID	1.22034483	0.088281282	0.027155757	1.076549798
METHICILLIN SODIUM	1.219708582	0.254857994	0.091580182	1.401864677
KETOPROFEN	1.219537383	0.258699766	0.217241928	1.276523844
NIMODIPINE	1.218703923	0.183189738	0.086478297	1.365770383
ESTRADIOL	1.217851617	0.095561695	0.088815003	1.412584376
MERBROMIN	1.217344809	0.303858738	0.090265415	1.04075939
AZITHROMYCIN	1.217224015	0.113718299	0.06930497	1.799539433
SULFAGUANIDINE	1.214363187	0.45405828	0.230936131	0.95629956
alpha-TOCHOPHERYL ACETATE	1.213744783	0.152411186	0.045544969	1.166843824
PIPERIDOLATE HYDROCHLORIDE	1.213458436	0.33866772	0.110054644	1.156629821
PERMETHRIN	1.211626726	0.297562307	0.094205467	1.364236661
ESTRIOL	1.210287397	0.200225736	0.079984528	1.315791531
PANTOPRAZOLE	1.210250434	0.338696342	0.093039063	1.124245337
MEPENZOLATE BROMIDE	1.209877529	0.289645356	0.123212056	1.38560806
AMSACRINE	1.209849467	0.269584466	0.135600952	1.482039778
DOBUTAMINE HYDROCHLORIDE	1.208577587	0.268429609	0.1924359	1.236354104
OXYPHENCYCLIMINE HYDROCHLORIDE	1.208382248	0.236774848	0.038054774	1.43603975
DIBENZOTHIOPHENE	1.206842373	0.045716444	0.096694043	0.969082093
ALLOPURINOL	1.205795529	0.05921357	0.033810089	1.196635799
MEPIVACAINE HYDROCHLORIDE	1.205354599	0.355184274	0.111499277	1.402127095
AZASERINE	1.204572613	0.2803247	0.063502939	1.289773262
RABEPRAZOLE SODIUM	1.204267755	0.43495616	0.395785607	1.22477588
METHOPRENE (S)	1.203955723	0.031241774	0.287771928	1.596375065
ARIPIPRAZOLE	1.202371428	0.100689335	0.318075587	1.342633461
CLEMASTINE FUMARATE	1.20146114	0.329953062	0.206355087	1.055436515
CARVEDILOL PHOSPHATE	1.200936347	0.31897043	0.123509072	1.427891628
BENZYDAMINE HYDROCHLORIDE	1.200929616	0.082024183	0.319476211	1.369703612
SERTRALINE HYDROCHLORIDE	1.200561132	0.378634301	0.246358751	1.423439771
FOMEPIZOLE HYDROCHLORIDE	1.200357731	0.334032973	0.190886876	1.107938611
BENZBROMARONE	1.199863311	0.021333942	0.31841154	1.216463175

ALGESTONE ACETOPHENIDE	1.199762294	0.232818341	0.24920442	1.241856838
ZOMEPIRAC SODIUM	1.199650564	0.174868622	0.335312298	1.195678301
PACLITAXEL	1.199581379	0.123771414	0.093749518	1.869297472
QUINAPRIL HYDROCHLORIDE	1.199118353	0.159623222	0.037371936	1.57073445
PRIDINOL METHANESULFONATE	1.198787145	0.147519748	0.208127707	1.317567869
COLISTIN SULFATE	1.198570686	0.331855318	0.37621823	1.12350619
ALEXIDINE HYDROCHLORIDE	1.198339513	0.32667909	0.184906404	1.288426578
CEFPIRAMIDE	1.198188505	0.287605441	0.364605082	1.114703699
CLINAFOXACIN HYDROCHLORIDE	1.197536651	0.210767119	0.34738905	1.14920001
PRAVASTATIN SODIUM	1.196522744	0.045299308	0.00406134	1.205252168
SULFAMERAZINE	1.19585335	0.02141329	0.122192173	1.523259945
TILMICOSIN	1.195449734	0.09819863	0.204624079	1.175881753
FENBUFEN	1.195219544	0.339919445	0.207266343	0.690449447
SPECTINOMYCIN HYDROCHLORIDE	1.195199334	0.213345634	0.170377049	1.307549947
SULFAMETHAZINE	1.194978674	0.249914997	0.18720282	1.420568315
NOSCAPINE HYDROCHLORIDE	1.194711522	0.18169204	0.12624041	1.779745499
ERYTHROMYCIN ETHYLSUCCINATE	1.194611657	0.270241914	0.188757051	1.081288067
EDETATE DISODIUM	1.194573986	0.259373003	0.088126271	1.413222339
DESOXYCORTICOSTERONE ACETATE	1.19384138	0.188229358	0.028852688	1.992364574
ROSUVASTATIN CALCIUM	1.192919021	0.217854536	0.181047207	1.1167956
THIOCTIC ACID	1.192559703	0.095839286	0.092694499	1.225629547
SULFINPYRAZONE	1.190748213	0.456997753	0.311182044	1.030785225
METOCLOPRAMIDE HYDROCHLORIDE	1.190468013	0.355603217	0.274199056	1.000167183
OXICONAZOLE NITRATE	1.190031187	0.235603564	0.195010608	1.280904019
ISOPROTERENOL HYDROCHLORIDE	1.189006106	0.298647076	0.166166573	1.663790362
MEPRYLCAINE HYDROCHLORIDE	1.188005574	0.102985989	0.05525631	1.134915299
LINEZOLID	1.187610378	0.233371866	0.221514797	1.179428382
TYLOXAPOL	1.186952971	0.201059732	0.066117899	1.310535636
CORTISONE ACETATE	1.186793694	0.191743603	0.168284742	1.225254509
CEFACLOR	1.186310892	0.152103639	0.129900167	1.35375583
CHLORALOSE	1.186130576	0.259764389	0.367613529	1.394857321
BIPERIDEN	1.185537166	0.10319307	0.113198807	1.15572641
BUPROPION	1.185245501	0.341447397	0.326269336	1.337668825
AZATHIOPRINE	1.184400273	0.064632252	0.053077784	2.784240026
IOVERSOL	1.184126973	0.187802366	0.211215962	1.100053739
CIPROFLOXACIN	1.183763204	0.226338032	0.161924884	1.663870104
CLINDAMYCIN PALMITATE HYDROCHLORI	1.182931138	0.31180343	0.215269214	1.084622927
RIFAXIMIN	1.181767955	0.264659945	0.082202337	1.198412914
BENZONATATE	1.181684862	0.158235555	0.083381785	1.250240568
SIMVASTATIN	1.181432839	0.106348297	0.166600117	1.294516974
MEXENEONE	1.180925622	0.240754272	0.28497591	1.228233089
KAINIC ACID	1.180914735	0.494367341	0.333085436	1.067289832
CEFTIOFUR HYDROCHLORIDE	1.17657997	0.109217938	0.381760978	1.151840572
OCTODRINE	1.176483457	0.273462304	0.320358279	1.032045499
RIFAMPIN	1.176006609	0.243446799	0.226834583	1.212983723
ISOPROPAMIDE IODIDE	1.175657333	0.484005361	0.325897809	1.579208722
DORAMECTIN	1.175330666	0.167148208	0.345275002	1.313843876
CREATININE	1.174380752	0.409753531	0.375985678	0.92083968
CEPHALEXIN	1.173952131	0.383768123	0.373927066	1.619138794
OXOLINIC ACID	1.173815208	0.373432188	0.369672828	1.062463224
HYDROQUINONE	1.173694495	0.137306442	0.063111392	1.589985943
RIZATRIPTAN BENZOATE	1.173342984	0.252031127	0.242039754	1.152620955
EPRINOMECTIN	1.17060344	0.219476402	0.19048702	1.038714825
MERCAPTOPURINE	1.17017257	0.187794763	0.245210131	2.591957456
PANCURONIUM BROMIDE	1.169872763	0.2861058	0.231133514	1.305306729
AMILORIDE HYDROCHLORIDE	1.169778025	0.202049362	0.125766225	1.257947028
AMOROLFINE HYDROCHLORIDE	1.169202033	0.043080567	0.131967179	1.100568914
MEPARTRICIN	1.169000557	0.156732533	0.035066597	1.41993737
PEMPIDINE TARTRATE	1.168726482	0.559251328	0.509051027	1.20521289
TRANYLCYPROMINE SULFATE	1.168582197	0.257955645	0.253143713	1.082849801
BITHIONATE SODIUM	1.167933211	0.155855722	0.104712259	1.24512064
ERYTHROMYCIN ESTOLATE	1.167203616	0.215215276	0.103991631	1.119255352
STAVUDINE	1.167167646	0.217667049	0.265379904	1.084800808
ACEXAMIC ACID	1.166714448	0.092735751	0.137766635	0.987554527
TERAZOSIN HYDROCHLORIDE	1.16641251	0.124140781	0.157245538	1.239068904
DOCONEXENT	1.166135196	0.255909768	0.214848617	1.063001406
METHACHOLINE CHLORIDE	1.16534583	0.248496758	0.284245052	0.977626461
VERAPAMIL HYDROCHLORIDE	1.163714392	0.148809879	0.082486258	1.418128622
DISOPYRAMIDE PHOSPHATE	1.163289858	0.128629937	0.197907172	1.00905833
PIPERACILLIN SODIUM	1.162056097	0.404892791	0.355524812	1.256073001
NIKETHAMIDE	1.16203597	0.664257872	0.526796587	1.32026143
CEFORANIDE	1.160366555	0.236939897	0.447701396	1.043810391

PROTOPORPHYRIN IX	1.160153733	0.141685271	0.302171411	1.402572513
TRIOXSALEN	1.159773963	0.540997103	0.423778984	1.435342494
CICLOPIROX OLAMINE	1.159223336	0.162414689	0.097260378	1.07411388
CARBENICILLIN DISODIUM	1.158277314	0.122192595	0.107745434	1.061863994
DIETHYLTOLUAMIDE	1.156528575	0.101704282	0.207138178	0.986142505
SUCRALFATE	1.156316845	0.10827582	0.076659383	1.253880777
CYCLAMIC ACID	1.156273493	0.303728449	0.227466318	1.091817311
AMMONIUM LACTATE	1.155600027	0.149519129	0.444308111	1.238980892
RETINOL	1.154405709	0.255126417	0.161123468	1.35659228
ZALEPLON	1.154003899	0.121961713	0.086255683	0.980794197
ACETANILIDE	1.153615688	0.482961206	0.440651855	0.976365359
beta-CAROTENE	1.153308219	0.185934419	0.151998525	1.194521348
ACEPROMAZINE MALEATE	1.153166692	0.084683307	0.176875772	1.31322976
FUSIDIC ACID	1.153002417	0.155836444	0.161583423	1.305770889
ANTHRALIN	1.152519618	0.053406425	0.097327837	1.220074919
CANRENONE	1.151477833	0.302302118	0.488247368	1.789788131
FLUMETHASONE	1.15146814	0.226481562	0.373188514	1.307992022
CEFMENOXIME HYDROCHLORIDE	1.151275914	0.458220837	0.363387907	1.093485546
LOMERIZINE HYDROCHLORIDE	1.150822471	0.173577185	0.339051666	1.265345673
PHENTOLAMINE HYDROCHLORIDE	1.150408532	0.310434066	0.303842858	1.793761668
PENICILLIN G POTASSIUM	1.149969149	0.378150104	0.375328861	1.184893977
GLAFENINE	1.149428564	0.09512169	0.179525319	1.195432188
PHENOLPHTHALEIN	1.149135994	0.198221173	0.141384933	1.267054194
CELECOXIB	1.148951839	0.254620834	0.266451074	1.84780068
ERDOSTEINE	1.148894395	0.35997069	0.333111208	0.991011385
LEVOCARNITINE	1.148620845	0.117271191	0.199406626	1.119908853
DIAZOXIDE	1.147585988	0.111046758	0.203858489	1.657211391
FLUPHENAZINE HYDROCHLORIDE	1.146741373	0.232831517	0.265935606	1.319244896
PHENYLPROPANOLAMINE HYDROCHLOR	1.146566812	0.219954197	0.326325256	1.077102223
NITROGLYCERIN	1.145823832	0.123382084	0.292434042	1.028529313
ACEMETACIN	1.14572793	0.064111859	0.181183807	1.286242072
SEVOFLURANE	1.145508657	0.227144118	0.332901193	1.047172201
PAPAVERINE HYDROCHLORIDE	1.14525258	0.263295541	0.455542185	1.625453518
DESOXYMETASONE	1.145190076	0.143826209	0.220007833	1.207596564
FLUCYTOSINE	1.144496853	0.110920257	0.208819493	1.213079397
ESTRAMUSTINE	1.143853475	0.08226299	0.288465773	1.344387228
AMITRIPTYLINE HYDROCHLORIDE	1.143844111	0.34358013	0.2983451	1.422085201
LEVOBUNOLOL HYDROCHLORIDE	1.143708995	0.317399971	0.32684128	0.959418097
CANDESARTAN CILEXTIL	1.143516908	0.125466598	0.300325451	1.263161018
DECAMETHONIUM BROMIDE	1.141214114	0.400357019	0.543578358	1.23045179
OXYBUTYNIN CHLORIDE	1.139983415	0.154915895	0.164377081	1.20712011
NONIVAMIDE	1.139754502	0.261195715	0.411244504	0.908019641
PHTHALYLSULFATHIAZOLE	1.139392347	0.064962794	0.371721332	1.407242538
PIPERACETAZINE	1.138822767	0.187784795	0.400331034	1.406116421
ENROFLOXACIN	1.138202216	0.168813015	0.083296906	1.390852235
SULFADIAZINE	1.13792448	0.188703539	0.309244546	1.248319672
BISOPROLOL FUMARATE	1.137111458	0.294541116	0.333255449	1.051442208
SULFATHIAZOLE	1.136822687	0.081952083	0.274565803	1.049432011
SARAFLOXACIN HYDROCHLORIDE	1.136489755	0.148054195	0.30206558	1.13030795
TOLPERISONE HYDROCHLORIDE	1.13585344	0.183361844	0.390192276	1.237953294
SULBACTAM	1.13579336	0.156856156	0.503970006	1.205984832
SULFASALAZINE	1.13538818	0.157453259	0.304058328	1.169581556
IDAZOXAN HYDROCHLORIDE	1.134655744	0.078545168	0.478558515	1.141977454
DEHYDROCHOLATE SODIUM	1.134548067	0.105207004	0.274292003	1.067846904
BENURESTAT	1.134121389	0.195331694	0.330259635	1.02888044
SURAMIN HEXASODIUM	1.13383522	0.362981648	0.521369978	1.268440603
NORETHYNODREL	1.133405482	0.33301908	0.322460414	1.508503058
RETINYL PALMITATE	1.133375637	0.236362277	0.305010185	1.689637872
CEFDINIR	1.132278702	0.059504531	0.291345483	1.3342213
NORFLOXACIN	1.13213686	0.205188412	0.222368367	1.091373793
PROCYCLIDINE HYDROCHLORIDE	1.132015	0.207405661	0.338346564	1.545428256
DEFEROXAMINE MESYLATE	1.131260109	0.201337396	0.326005722	1.209667877
DARIFENACIN HYDROBROMIDE	1.131104881	0.202658673	0.370104793	1.23820103
DENATONIUM BENZOATE	1.130996254	0.165240117	0.271701178	1.360705091
ETHOTOIN	1.130510473	0.180747441	0.524110055	1.057570852
BUPIVACAINE HYDROCHLORIDE	1.130427414	0.237523188	0.316001776	1.914026427
OXETHAZAINE	1.130099278	0.447223471	0.455112703	1.633662754
GLIPIZIDE	1.129720496	0.389909482	0.42185455	1.018007225
PENICILLAMINE	1.128554744	0.335310498	0.420393892	1.195874497
DAPSONE	1.128431654	0.17235662	0.321890342	1.271524813
IOTHALAMIC ACID	1.127841323	0.172113252	0.286381534	1.231823528
MONENSIN SODIUM (monensin A is shown	1.126933442	0.222437155	0.211032627	1.791632552

CARBETAPENTANE CITRATE	1.12613711	0.20808065	0.364567521	1.114112747
ESCITALOPRAM OXALATE	1.125781554	0.125758083	0.153597581	1.441193496
MAFENIDE HYDROCHLORIDE	1.124911936	0.22050403	0.258954035	0.996850879
OXALIPLATIN	1.124619997	0.090092578	0.137298721	1.269411429
MEGLUMINE	1.124390181	0.013858832	0.528029094	1.255412658
PENTOXIFYLLINE	1.124263789	0.394637322	0.355763921	1.224664581
HYDROXYAMPHETAMINE HYDROBROMIDI	1.12415414	0.209866139	0.25319043	1.074362997
PIRACETAM	1.123298378	0.131198903	0.08491147	1.053626999
CINCHONIDINE	1.123133659	0.196597886	0.39625371	0.913770389
MICONAZOLE NITRATE	1.122857938	0.487199216	0.488517023	1.860709528
NAPHAZOLINE HYDROCHLORIDE	1.122291301	0.189814818	0.316568423	1.019925451
ADENOSINE PHOSPHATE	1.121856601	0.264621348	0.370845803	1.59435942
BETAMETHASONE ACETATE	1.121641794	0.030113583	0.263801468	1.256519278
NITARSONE	1.121638154	0.217498211	0.410658251	1.026078915
BENZYL ISOTHIOCYANATE	1.12150457	0.280134243	0.480352835	0.428536843
RESERPINE	1.120975674	0.15455188	0.354648069	1.329518897
MORANTEL CITRATE	1.120966216	0.072890831	0.269874272	1.572113613
NALIDIXIC ACID	1.120527816	0.212986464	0.521279589	1.585288388
ONDANSETRON	1.120463914	0.058592526	0.542447115	1.256968965
TAMSULOSIN HYDRCHLORIDE	1.120339685	0.153208463	0.390202348	0.945468525
RESORCINOL	1.120142932	0.075725648	0.143861607	1.029260937
PROADIFEN HYDROCHLORIDE	1.119550681	0.31397756	0.325812599	1.230815582
SIBUTRAMINE HYDROCHLORIDE	1.119219485	0.146921889	0.363854892	1.245177971
BENZOYL PEROXIDE	1.118284371	0.084461779	0.133881997	1.300554513
UNDECYLENIC ACID	1.117166042	0.313600093	0.417759562	1.164683656
OXANTEL PAMOATE	1.116969819	0.484091201	0.543645563	1.266086907
SALICYL ALCOHOL	1.116680961	0.362395102	0.478241651	1.356768758
IODIPAMIDE	1.116646707	0.076555726	0.296399474	1.654255028
GALLIC ACID	1.116285151	0.358812523	0.444700204	0.976042809
TETRACYCLINE HYDROCHLORIDE	1.116248895	0.390905299	0.495397028	1.297726581
ESTRADIOL BENZOATE	1.116045641	0.042433861	0.12430719	1.272493185
DIMPYLATE	1.115669791	0.246366534	0.567644331	1.404675121
CARBINOXAMINE MALEATE	1.115476927	0.107173934	0.218126535	1.174583755
ACEBUTOLOL HYDROCHLORIDE	1.115236474	0.258552113	0.550502787	1.345954832
VILAZODONE HYDROCHLORIDE	1.114814567	0.228846791	0.496695373	1.508972506
IODOQUINOL	1.114803513	0.368660016	0.437672162	1.526535506
RIMANTADINE HYDROCHLORIDE	1.114566831	0.308683862	0.516112578	1.241805315
AZAPERONE	1.11362413	0.140450787	0.383474698	1.155816952
CITIOLONE	1.112848909	0.082652829	0.448827512	1.006323958
CILOSTAZOL	1.112395937	0.137619908	0.387410169	1.097992435
TENOFOVIR	1.112027715	0.245247481	0.459550438	1.057958605
MECLOFENOXATE HYDROCHLORIDE	1.111926007	0.249881701	0.498838394	1.172774079
ISOSORBIDE DINITRATE	1.111040953	0.135699485	0.472629014	1.178630204
AMINOTHIAZOLE	1.110915859	0.110023079	0.314953208	1.003372847
ATRACURIUM BESYLATE	1.110537634	0.142470918	0.34203293	1.109447949
NATEGLINIDE	1.110473883	0.352487147	0.496059463	1.174265994
IMATINIB	1.110286989	0.090248834	0.466470113	1.374258344
CHLORPROMAZINE	1.110121114	0.114261582	0.369096049	1.321689955
METHYSERGIDE MALEATE	1.108099985	0.128894364	0.346079473	1.083330931
IODIXANOL	1.107919594	0.319283892	0.488084107	1.333678921
IBUPROFEN	1.107899198	0.32340155	0.432219512	1.464266615
PANTHENOL (dl)	1.106882778	0.10568437	0.250958459	1.166798003
ACECAINIDE HYDROCHLORIDE	1.106677936	0.386886151	0.444121114	1.389104765
DIHYDROSTREPTOMYCIN SULFATE	1.106584204	0.088375964	0.376135269	1.49366521
FLOXURIDINE	1.105928479	0.210303212	0.278769336	1.812771058
VENLAFAXINE HYDROCHLORIDE	1.105773169	0.169418041	0.371931314	1.589306189
ANTAZOLINE PHOSPHATE	1.105663043	0.191003303	0.314221207	1.212972459
DESVENLAFAXINE SUCCINATE	1.105480259	0.235540262	0.348534323	0.905042441
ADIPHENINE HYDROCHLORIDE	1.105354108	0.155459598	0.229351976	1.257019531
CYPERMETHRIN	1.104525499	0.170162481	0.591174185	1.059063327
LEUCOVORIN CALCIUM	1.104429102	0.481380361	0.551285882	1.428729211
FIROCOXIB	1.104409807	0.211604839	0.286608767	1.640133767
FLUCONAZOLE	1.104292221	0.141975569	0.14778099	1.48298524
NYSTATIN	1.10412072	0.628667391	0.637155129	1.428452989
TAZOBACTAM	1.102917466	0.280445622	0.397565241	1.378014307
BENFOTIAMINE	1.101485011	0.139326433	0.369062551	1.062459438
TICARCILLIN DISODIUM	1.101278684	0.191663363	0.40782655	0.968558041
ACECLIDINE	1.101129601	0.33223637	0.419619354	1.16209182
ZAPRINAST	1.100935431	0.154969569	0.379475202	1.046983788
LAMOTRIGINE	1.100290371	0.09010484	0.365572687	1.034501065
ACETOHYDROXAMIC ACID	1.099655316	0.112089453	0.28599303	1.346638677
SCOPOLAMINE HYDROBROMIDE	1.098821485	0.302908739	0.618604844	1.122898195

LONIDAMINE	1.098806429	0.167668368	0.396006356	1.012637343
SECNIDAZOLE	1.098207952	0.224531359	0.543382704	1.231072657
NAPROXOL	1.097995746	0.231064939	0.442205505	1.680043032
ARSENIC TRIOXIDE	1.09780928	0.230952508	0.35043205	1.425945975
BORNYL ACETATE	1.09737161	0.122940726	0.519098665	1.07702996
FAMCICLOVIR	1.0969539	0.321498949	0.536766125	1.067081664
REPAGLINIDE	1.096873502	0.248231756	0.522247805	0.955449678
PROPAFENONE HYDROCHLORIDE	1.096524655	0.150596596	0.18704147	1.684111221
OLTIPRAZ	1.096487791	0.086823651	0.516231504	1.246110942
TRIMETHOPRIM	1.096324327	0.4986384	0.606383688	1.414994576
AMINOSALICYLATE SODIUM	1.096061849	0.22414114	0.384687604	1.182876255
PYRITINOL	1.095711184	0.040385761	0.514235887	1.117342087
PIMETHIXENE MALEATE	1.095273487	0.45800331	0.683657211	1.339843805
MOXISYLYTE HYDROCHORIDE	1.095000561	0.264682474	0.569659515	1.243297178
IPRATROPIUM BROMIDE	1.094795368	0.128871603	0.635763429	1.221784016
ORNIDAZOLE	1.094578347	0.046389792	0.442301363	1.161769736
CAPREOMYCIN SULFATE	1.093804121	0.318532915	0.471576465	1.255158532
SPIRONOLACTONE	1.093746423	0.116017731	0.45592997	1.745849219
NIZATIDINE	1.093656074	0.125174956	0.414125449	1.453558589
BENZOIC ACID	1.093643341	0.037893191	0.20414422	1.429872342
CHINIOFON	1.093627676	0.169458173	0.629815871	1.346178103
ITRACONAZOLE	1.093577314	0.250763188	0.656865323	1.397908397
HYDROQUINIDINE	1.093484741	0.033482283	0.372226176	1.506576855
HYDROXYCHLOROQUINE SULFATE	1.093453386	0.229053152	0.299433055	1.659989963
ROXITHROMYCIN	1.09337876	0.410637345	0.569734468	1.419049016
ROLIPRAM	1.093353744	0.397544711	0.564334614	1.038013313
ENOXACIN	1.093315477	0.35609445	0.476222802	1.321933505
ADIPIC ACID	1.093305904	0.178854745	0.485913966	1.024017722
CIPROFIBRATE	1.093149668	0.332822494	0.554971126	1.446630189
CYCLOPHOSPHAMIDE	1.092815142	0.092240217	0.439705999	1.263883234
DOXOFYLLINE	1.092187701	0.153167665	0.611589408	1.081382463
HETACILLIN POTASSIUM	1.091950199	0.330777136	0.506524929	1.451634902
GUANFACINE HYDROCHLORIDE	1.091925867	0.229355974	0.472362323	1.149777251
BENSERAZIDE HYDROCHLORIDE	1.091776572	0.104272953	0.319229347	1.456495384
FLUTICASONE PROPIONATE	1.091503883	0.223085938	0.626771324	1.902599849
ADENINE	1.091121144	0.145386589	0.435256225	1.607133984
LEVOMENTHOL	1.090754644	0.161098651	0.555995834	1.145562696
GEFITINIB	1.090450566	0.458825862	0.662899626	1.190762396
CAMPHOR (1R)	1.090182324	0.09264137	0.321099066	1.353154541
GLUTAMINE (L)	1.09015796	0.244207386	0.549308072	1.18554592
PYRAZINAMIDE	1.090003285	0.20282497	0.506560151	1.244577827
CLOFOCTOL	1.089969555	0.189664991	0.450263092	1.192293003
FLUMEQUINE	1.089223676	0.196498185	0.470054495	1.387426562
NYLIDRIN HYDROCHLORIDE	1.088904997	0.323152331	0.496233632	1.504925814
MOXALACTAM DISODIUM	1.088883952	0.301972882	0.561377645	1.101779557
HEPTAMINOL HYDROCHLORIDE	1.087780873	0.483658852	0.672651493	1.078198135
TOREMIPHENE CITRATE	1.087699676	0.168821294	0.532470965	1.157048516
METHSUXIMIDE	1.087489788	0.146771065	0.364596109	1.176583177
CHLORAMPHENICOL SODIUM SUCCINATE	1.085916148	0.160983117	0.386519546	1.161775265
TODRALAZINE HYDROCHLORIDE	1.085792095	0.10859982	0.566402102	1.117287888
CHLORAMPHENICOL	1.08572063	0.15546938	0.383589834	1.082134917
BENZTHIAZIDE	1.08566643	0.086926181	0.341923064	1.317214273
FLUOCINOLONE ACETONIDE	1.085580663	0.30021116	0.515280933	1.488722956
STRYCHNINE	1.085216302	0.070644889	0.284310413	1.328399211
NITRENDIPINE	1.084868799	0.174427727	0.473082067	1.898124443
DIPHENHYDRAMINE HYDROCHLORIDE	1.084857695	0.045156058	0.469298685	1.353229727
ELTANOLONE	1.084018182	0.195582357	0.59402087	1.373359627
PRULIFLOXACIN	1.083126898	0.152396453	0.587116735	1.166462752
CLOPIDOL	1.083038826	0.097481444	0.31173203	1.152347469
CLOFIBRIC ACID	1.082600036	0.202166049	0.49413606	1.037329973
BETAMETHASONE 17,21-DIPROPIONATE	1.081756126	0.077721329	0.281617623	1.380674985
PENTAMIDINE ISETHIONATE	1.081653925	0.173386334	0.67430274	1.459784542
AZATADINE MALEATE	1.081621709	0.060608923	0.678326713	1.304836134
SUCCINYLSULFATHIAZOLE	1.08158509	0.393487872	0.674644555	1.427553457
TRANDOLAPRIL	1.08121902	0.186209741	0.659156997	1.33251217
HALAZONE	1.081008811	0.267881652	0.515871228	1.294081805
CLOXACILLIN SODIUM	1.080799402	0.083407943	0.497389603	1.241653532
DIMERCAPROL	1.080263435	0.280383259	0.508281653	1.569882536
AMIODARONE HYDROCHLORIDE	1.080058949	0.070485738	0.286908428	1.695069532
HYDRASTINE (1R, 9S)	1.079804194	0.132653028	0.487460334	1.558489739
STREPTOMYCIN SULFATE	1.079403032	0.145271845	0.53520228	1.237897223
CEFOXITIN SODIUM	1.079085463	0.157989344	0.663218465	1.276692238

CHOLINE CHLORIDE	1.078736379	0.126403668	0.244178682	1.288061742
PROCHLORPERAZINE EDISYLATE	1.078642053	0.185192214	0.55359353	1.368310726
HALOPERIDOL	1.078446159	0.509763312	0.666345044	1.686434899
ISOTRETINON	1.078396363	0.303662878	0.504453206	1.312627813
TERCONAZOLE	1.077913554	0.222049414	0.539910452	1.967826316
HOMOSALATE	1.077910678	0.111471092	0.231053728	1.419377002
AMINOCAPROIC ACID	1.077436513	0.146480225	0.423395088	1.244456621
HALOTHANE	1.077403305	0.217390736	0.443932272	1.160854953
BICALUTAMIDE	1.077384414	0.148227778	0.382693264	1.020642017
COLISTIMETHATE SODIUM	1.077370737	0.235341803	0.571277539	1.294981701
CEFSULODIN SODIUM	1.077329493	0.290723631	0.498728998	1.409603153
BISMUTH SUBSALICYLATE	1.076869701	0.331181312	0.600664191	1.012683178
CAPTOPRIL	1.076651299	0.398257029	0.63685489	1.580566962
ANTIPYRINE	1.076556025	0.18680396	0.457256685	1.190968912
LINCOMYCIN HYDROCHLORIDE	1.07629857	0.133760835	0.455938985	1.357590532
MEDRYSONE	1.076080582	0.182214578	0.453624551	1.458526613
THIAMPHENICOL	1.075868884	0.108300768	0.337265385	1.297326354
PIROCTONE OLAMINE	1.075726139	0.264654245	0.568340041	1.516235206
COLESEVALAM HYDROCHLORIDE (high m	1.075433697	0.288674184	0.51740325	1.154405822
FLUVOXAMINE MALEATE	1.074903628	0.018982108	0.66875995	0.973897654
DEHYDROCHOLIC ACID	1.074677423	0.08743344	0.499661669	1.453263437
CHLORAMBUCIL	1.073577206	0.049707982	0.397189174	1.064322811
FENOFIBRATE	1.073360062	0.132946121	0.435114718	1.185794067
DICYCLOMINE HYDROCHLORIDE	1.073187721	0.136025651	0.552704668	1.363969963
MYCOPHENOLATE MOFETIL	1.07309484	0.334141794	0.740605144	0.858747611
PIRENPERONE	1.072942523	0.160908199	0.536574094	1.893681509
DICHLOROPHEN	1.072762075	0.29832147	0.675117619	1.134203833
PYRIDOXINE	1.072478025	0.15752807	0.534298357	1.134485784
ROSIGLITAZONE MALEATE	1.072472473	0.286642334	0.483769185	1.278813274
AMOXICILLIN	1.071628519	0.099363518	0.429778089	1.375367979
BROMPERIDOL	1.071079447	0.304452789	0.742918885	1.868525593
PROCARBAZINE HYDROCHLORIDE	1.070745977	0.09576583	0.689907683	1.56195654
MECLOFENAMATE SODIUM	1.070381335	0.342135225	0.600882503	1.03880456
THIAMINE	1.069895101	0.069550436	0.518443132	1.060954315
METHYCLOTHIAZIDE	1.069529579	0.293365418	0.64505934	1.054989491
SUMATRIPTAN SUCCINATE	1.069462296	0.397531775	0.762986662	1.141536595
CROMOLYN SODIUM	1.069158623	0.217842126	0.604930053	1.236518527
AZELAIC ACID	1.067320383	0.04518742	0.533022501	1.356287786
RACEPHEDRINE HYDROCHLORIDE	1.066472184	0.158645198	0.631935737	1.334421109
KETOCONAZOLE	1.066419687	0.442787206	0.686326993	1.660661627
CLORSULON	1.066314555	0.137137014	0.74029418	1.217475426
PROTIRELIN	1.06608699	0.072774845	0.262592714	1.364169541
PHENACEMIDE	1.065559314	0.424213514	0.671802617	1.059331585
AMIFOSTINE	1.065319585	0.044005841	0.367793252	1.337454602
SULFABENZAMIDE	1.065227344	0.117760628	0.601686068	1.167613514
XYLOMETAZOLINE HYDROCHLORIDE	1.064723475	0.209528249	0.603803346	1.670596895
GUANIDINE HYDROCHLORIDE	1.064611508	0.240796547	0.747356687	1.076123353
POTASSIUM p-AMINOBENZOATE	1.064113174	0.032834659	0.714156949	1.369108368
PYRIMETHAMINE	1.063702854	0.265935471	0.659609413	1.357791785
CHLORAMPHENICOL PALMITATE	1.063586545	0.084453781	0.474864678	1.09109147
TADALAFIL	1.063380299	0.110786462	0.636933376	1.067907248
SULFANILAMIDE	1.063248217	0.327328267	0.72268793	1.002838226
CYTISINE	1.062745312	0.281393692	0.713242655	1.316249712
TRIENTINE HYDROCHLORIDE	1.062679337	0.232728037	0.623208419	0.925300963
TAMOXIFEN CITRATE	1.062373842	0.049024778	0.604784404	1.72220548
TOLAZOLINE HYDROCHLORIDE	1.060666985	0.214760628	0.656439583	1.305491423
CITALOPRAM HYDROBROMIDE	1.060660426	0.050335906	0.430619173	1.353141054
SULINDAC	1.060492439	0.121656418	0.628943433	1.385750516
SILDENAFIL CITRATE	1.060486271	0.335186148	0.765188003	1.934604994
ORNITHINE HYDROCHLORIDE	1.060199128	0.287416388	0.656574212	1.036947948
BETAMETHASONE VALERATE	1.060197017	0.262702583	0.534643918	1.296498198
EZETIMIBE	1.060129158	0.104569726	0.631314703	1.056943974
ETHACRYNIC ACID	1.059641922	0.425596931	0.709383686	1.654379759
TRILOSTANE	1.058815082	0.13443225	0.493132082	1.428864012
BIFONAZOLE	1.05876815	0.276644536	0.690754248	1.142908879
QUINACRINE HYDROCHLORIDE	1.058544009	0.198142706	0.662094862	1.556831221
CYCLOSPORINE	1.058321443	0.053136366	0.423037098	1.027956108
LEVAMISOLE HYDROCHLORIDE	1.058238925	0.065808284	0.455022338	1.331883969
CAFFEINE	1.057951449	0.095474452	0.518818218	1.135700288
PYRILAMINE MALEATE	1.057910208	0.056421618	0.63140408	1.245261615
BAMBUTEROL HYDROCHLORIDE	1.057879855	0.15198444	0.763268501	1.494224726
GLUTATHIONE	1.05574621	0.082978115	0.705182413	1.152984916

FLUDARABINE PHOSPHATE	1.055528886	0.180404375	0.64136641	0.759229781
AZLOCILLIN SODIUM	1.055372163	0.165763224	0.454798515	1.063046627
OXIDOPAMINE HYDROCHLORIDE	1.055363831	0.187674658	0.612552594	1.485003912
VIDARABINE	1.054814362	0.126334447	0.629152157	1.1846823
CHLORHEXIDINE DIHYDROCHLORIDE	1.054768048	0.279388933	0.6491485	1.339179658
THIOGUANINE	1.054401996	0.037621192	0.650126866	1.285021332
METHYLDOPA	1.054160342	0.16281655	0.64555141	1.532548116
MOLSIDOMINE	1.053823968	0.261315452	0.798765675	0.922710874
ACETAMINOPHEN	1.053159445	0.055336574	0.489980144	1.301333531
DIBUCAINE HYDROCHLORIDE	1.053113145	0.252272957	0.702099904	1.442005142
CHLOROPHYLLIDE Cu COMPLEX Na SALT	1.053061987	0.206922173	0.588978546	1.281169356
NETILMICIN SULFATE	1.052337772	0.155716257	0.651405466	1.111544231
NORGESTIMATE	1.052333737	0.260083954	0.692177872	1.548126645
ACETYL-L-LEUCINE	1.052085764	0.127569089	0.635625696	0.987388358
HYDROCHLOROTHIAZIDE	1.051739302	0.334015647	0.707870253	1.568055057
CARBACHOL	1.051709453	0.085619377	0.559879731	0.950601751
PYRANTEL PAMOATE	1.051144123	0.232967783	0.712811609	1.386096863
ADRENOLONE HYDROCHLORIDE	1.050748024	0.044196076	0.36028788	1.820721202
ACEDAPSONE	1.050712958	0.02969123	0.352645189	1.215284285
PRALIDOXIME CHLORIDE	1.050638947	0.072561669	0.638754783	1.018316748
DIMETHYL FUMARATE	1.050599041	0.113699406	0.429534507	1.669799052
OXFENDAZOLE	1.050550161	0.224011541	0.687875201	1.338227347
TIGECYCLINE	1.050415565	0.152076345	0.714331466	0.969331245
PRAMOXINE HYDROCHLORIDE	1.05026865	0.157957345	0.71633775	1.060015316
GLIMEPIRIDE	1.050089889	0.078134183	0.799120743	1.159759966
CEFEPIME HYDROCHLORIDE	1.049907631	0.111277579	0.544546658	1.195147177
SULFANILATE ZINC	1.049713117	0.108305998	0.544271427	1.40645279
CARBARSONE	1.048993395	0.346565301	0.76977797	1.033401697
MEVASTATIN	1.047848407	0.134927033	0.665415698	1.144853336
NIACIN	1.046856037	0.509057811	0.790912889	1.105521484
CEPHAPIRIN SODIUM	1.046821523	0.080629589	0.595157614	1.179433201
SACCHARIN	1.046433433	0.23865445	0.78288281	1.6378778
DIETHYLSTILBESTROL	1.04639035	0.131574093	0.704092317	1.558349504
TOLTRAZURIL	1.046302666	0.40465538	0.7757589	1.106771752
SISOMICIN SULFATE	1.045820889	0.045814538	0.702622438	1.543065171
EPINEPHRINE BITARTRATE	1.045610429	0.19298479	0.724743861	1.900865051
QUINIDINE GLUCONATE	1.045517561	0.123858869	0.71588589	1.766366869
RITONAVIR	1.044713686	0.452287555	0.782055239	1.362377961
LAMIVUDINE	1.04441546	0.276333568	0.818735986	1.436042562
CHLORPYRIFOS	1.044413282	0.325640896	0.756028292	1.157397102
AKLOMIDE	1.044408209	0.15824227	0.603287286	1.269275303
ZILEUTON	1.044325211	0.047571418	0.820943633	1.14531896
SULFAMETHOXAZOLE	1.044277472	0.112386636	0.721080237	1.17614609
ETHOPABATE	1.044088202	0.122411529	0.804803924	1.109854311
PHENACETIN	1.043800161	0.088673455	0.690139954	1.522382736
LOMUSTINE	1.04372297	0.122715228	0.779837366	1.428297973
SULCONAZOLE NITRATE	1.043385187	0.175549525	0.756965781	1.272788837
CLARITHROMYCIN	1.043350732	0.147263831	0.535146215	1.269551749
THIODIGLYCOL	1.043312271	0.282730911	0.746750003	1.01976098
AMINOPYRINE	1.043267679	0.246069772	0.73372163	1.005041601
BUTYLATED HYDROXYTOLUENE	1.04287718	0.253769545	0.738801405	1.037645267
HYDROCORTISONE HEMISUCCINATE	1.042398362	0.122361987	0.671475987	1.267302335
LEVOFLOXACIN	1.042169721	0.21580649	0.759258703	1.220405827
STREPTOZOSIN	1.041918999	0.169851734	0.747009027	1.11382634
HEXESTROL	1.041138217	0.113887349	0.703974543	1.186266049
OROTIC ACID	1.040222002	0.39098242	0.798368029	1.062483283
SALICYLAMIDE	1.040069786	0.088496777	0.742831627	1.394778641
MEFLOQUINE	1.039873896	0.392132616	0.774159592	1.54707525
AVOBENZONE	1.039608661	0.189095685	0.767279398	1.364767466
CEFADROXIL	1.03913514	0.125031739	0.672719352	1.303085517
PENTETIC ACID	1.038908016	0.215970527	0.814156177	1.148697443
FAMPRIDINE	1.03878571	0.130591109	0.631294541	1.104468897
ESTRADIOL DIPROPIONATE	1.038700882	0.161499655	0.763986933	1.314977291
CHLOROCRESOL	1.038204181	0.179631741	0.680161316	1.070877274
AMINOLEVULINIC ACID HYDROCHLORIDE	1.037780053	0.129670797	0.569314925	1.386074215
ORPHENADRINE CITRATE	1.037732646	0.190840901	0.775941043	1.162954463
PANTOTHENIC ACID(d) Na salt	1.037731748	0.117227725	0.680585217	1.102650464
ELETRIPTAN HYDROBROMIDE	1.037708555	0.132523276	0.849997306	1.125588519
FOMEPIZOLE	1.037394704	0.179992752	0.790308363	0.921956334
CARMUSTINE	1.03738508	0.041682309	0.600451629	1.530607094
BETAXALOL HYDROCHLORIDE	1.03737462	0.309938903	0.863254176	0.974652533
CARBAMAZEPINE	1.037094445	0.062345493	0.667943351	1.25826589

CLOSANTEL	1.036533896	0.28397331	0.749594652	1.372983279
AZILSARTAN KAMEDOXOMIL	1.036157204	0.117907702	0.646810823	1.513488729
DEMECLOCYCLINE HYDROCHLORIDE	1.036142735	0.227212981	0.788095245	0.973657737
DYCLONINE HYDROCHLORIDE	1.035680422	0.092067829	0.763383615	1.382870892
SULFAMETHIZOLE	1.035622613	0.073349691	0.768857015	1.258093394
BENDROFLUMETHIAZIDE	1.035573956	0.02177607	0.613840279	1.355990364
CEFAMANDOLE SODIUM	1.035332771	0.067691773	0.84048743	1.372127379
QUINAPRILAT	1.03529629	0.250982739	0.852977269	1.293178546
CEPHALOSPORIN C SODIUM	1.035127661	0.160559326	0.818294508	1.019146053
ECAMSULE TRIETHANOLAMINE	1.035028139	0.153794952	0.846169657	1.43390753
PARAMETHADIONE	1.034367538	0.125904974	0.862855562	1.050613991
HOMATROPINE METHYLBROMIDE	1.034302022	0.246874374	0.773898334	1.408029902
TAPENTADOL HYDROCHLORIDE	1.034272746	0.286397983	0.826338429	1.02870531
TIMOLOL MALEATE	1.034073281	0.321279025	0.825213741	1.15710743
NORETHINDRONE	1.034042339	0.613489735	0.868278676	1.439579135
BUFEXAMAC	1.033924788	0.353646919	0.81976229	1.402763188
FENDILINE HYDROCHLORIDE	1.033650769	0.121023137	0.821845111	1.139323435
BRUCINE	1.033631652	0.092953661	0.673322057	1.611840449
METITEPINE MALEATE	1.03345937	0.086175991	0.858751697	1.173924672
BUTOCONAZOLE	1.033401815	0.332290537	0.879343238	1.526124932
ANETHOLE	1.032781264	0.243435356	0.797789853	1.726293203
SULFAPYRIDINE	1.032574335	0.183059471	0.804318937	1.451664161
LACITOL	1.032360622	0.361897353	0.860358501	1.095032812
ETIDRONATE DISODIUM	1.032278301	0.119053506	0.771824766	1.259990627
TIOCONAZOLE	1.032265447	0.162157854	0.781420351	1.390243035
BUTAMBEN	1.032014177	0.232310729	0.80219671	0.889199454
DACARBAZINE	1.031953132	0.035325317	0.805539437	1.031166311
METHYLBENZETHONIUM CHLORIDE	1.031753589	0.105386116	0.770683164	2.450990636
SENNOSIDE A	1.031741483	0.24494761	0.847395739	1.293146106
FENOTEROL HYDROBROMIDE	1.031689601	0.157074006	0.785778708	1.664110688
CHLORMEZANONE	1.031656597	0.246393383	0.832490958	1.038385855
ACADESINE	1.031503509	0.226892149	0.844411439	1.28789069
DIATRIZOIC ACID	1.031335245	0.202329873	0.764272879	1.288811182
HOMATROPINE HYDROBROMIDE	1.031229868	0.41253262	0.841707498	1.669059124
PRASTERONE ACETATE	1.030850297	0.068646744	0.869181256	1.969863494
ERGOCALCIFEROL	1.030766929	0.099032994	0.795945454	1.22117945
KETANSERIN TARTRATE	1.030621038	0.15167423	0.812635102	1.121325566
AMPHOTERICIN B	1.029801012	0.073162383	0.732287951	1.257107088
NICOTINYL ALCOHOL TARTRATE	1.028773402	0.233048997	0.773308942	1.58461863
DILOXANIDE FUROATE	1.028439806	0.035110058	0.787843794	1.07206496
ZIDOVUDINE [AZT]	1.028381727	0.131117546	0.724986261	1.98604037
IFOSFAMIDE	1.027910322	0.133556164	0.888664782	1.058464189
EPIESTRIOL	1.0279052	0.147037827	0.884119647	1.048996757
PIPAMPERONE	1.027902025	0.207976763	0.820334716	1.016812897
NITROMIDE	1.027719517	0.230202151	0.811387344	1.445299448
OXACILLIN SODIUM	1.026906615	0.132686596	0.773311957	1.265548056
SPARTEINE SULFATE	1.026618525	0.341578812	0.820109044	1.643978087
ARTEMETHER	1.026516915	0.336470424	0.841224124	1.044844958
IVERMECTIN	1.026409588	0.209567594	0.897682285	1.010886925
CEFOTAXIME SODIUM	1.026244975	0.072044819	0.762826079	1.21633969
CEFPROZIL	1.025740007	0.2046743	0.889420561	1.394634204
CIANIDANOL	1.025677256	0.18120703	0.825255148	1.091896899
DOXIFLURIDINE	1.02541333	0.316412867	0.885113906	1.138877998
TROCLOSENE POTASSIUM	1.025394213	0.425081042	0.898807952	1.610129225
CLAVULANATE LITHIUM	1.024767283	0.057177432	0.899394275	1.025671071
ACETYLCHOLINE CHLORIDE	1.024466722	0.172252118	0.805242912	1.167523909
CISPLATIN	1.023763502	0.084339195	0.762651302	1.123183285
MINAPRINE HYDROCHLORIDE	1.023454111	0.100039564	0.894513163	0.992865474
CEFPODOXIME PROXETIL	1.02318228	0.137958852	0.837755741	1.109780805
BROMHEXINE HYDROCHLORIDE	1.022659806	0.281536764	0.838061793	1.606175076
CLIMBAZOLE	1.022326506	0.1277043	0.881562026	1.369363462
NICOPHOLINE	1.022218246	0.073810962	0.881143923	1.05183725
ATOMOXETINE HYDROCHLORIDE	1.022135839	0.088753489	0.709235666	1.264038879
CHLOROBUTANOL	1.021811445	0.28694257	0.89854418	1.138295085
MODAFINIL	1.0214163	0.12953562	0.87410145	1.13528754
HYDROFLUMETHIAZIDE	1.020941396	0.254788709	0.862357809	1.497966994
PRILOCAINE HYDROCHLORIDE	1.020887321	0.114399005	0.848923647	1.410952563
METHOCARBAMOL	1.020653224	0.280922138	0.862889483	1.034056283
2-THIOURACIL	1.020582949	0.40977204	0.898685418	1.048909651
CINOXACIN	1.020300701	0.065150222	0.861843448	1.454655776
ETHISTERONE	1.019010744	0.074450735	0.740667693	1.347680588
BUSULFAN	1.018669532	0.103866169	0.835356743	1.239122326

TYLOSIN TARTRATE	1.018634784	0.085978107	0.879858287	1.224406569
GLYCOPYRROLATE	1.018576591	0.202902107	0.927693615	1.062192591
SULFISOXAZOLE ACETYL	1.018172455	0.103401182	0.868390875	1.084936267
MILRINONE	1.0179223	0.039032006	0.811653098	1.542121397
CORTISONE	1.017801015	0.146871792	0.873269076	1.166223725
DUTASTERIDE	1.017410116	0.142404247	0.922750098	1.130067519
CAPSAICIN	1.017368992	0.113235822	0.823642836	1.230404157
FLUOCINONIDE	1.017024543	0.394154452	0.910682962	1.636520779
CYCLOPENTOLATE HYDROCHLORIDE	1.016735572	0.31193628	0.910760523	1.127008176
PALIPERIDONE	1.016206826	0.305238631	0.927447091	1.38856913
MEFEXAMIDE HYDROCHLORIDE	1.01599587	0.162697667	0.868906504	1.412769217
TRAMADOL HYDROCHLORIDE	1.015817627	0.182730035	0.836786607	1.437549314
LEVOCARNITINE PROPIONATE HYDROCH	1.01579192	0.217724097	0.899637937	1.297863256
NEOSTIGMINE BROMIDE	1.015754203	0.174554017	0.857700962	1.318771849
AMOXAPINE	1.015744265	0.070023224	0.892844461	1.118356633
METHYLTHIOURACIL	1.01558361	0.295301263	0.903906725	1.644010668
PANTETHINE	1.015436286	0.275149004	0.926490032	1.098309148
MUPIROCIN	1.014905013	0.056195304	0.93213165	1.414763994
DIHYDROERGOTAMINE MESYLATE	1.014860274	0.178482936	0.906991784	1.992330776
PENBUTOLOL SULFATE	1.014772636	0.266202004	0.944278678	1.300862751
DIMETHADIONE	1.014725231	0.09286638	0.900981934	1.267431139
AMINOHIPPURIC ACID	1.01468076	0.088717	0.844563455	1.339071502
CYPROTERONE ACETATE	1.014278603	0.113267089	0.942544523	1.586249923
HYDROXYPROGESTERONE	1.014275703	0.06331844	0.890778438	1.441908077
TESTOSTERONE	1.014063234	0.222904701	0.89653654	1.322195227
LEVONORGESTREL	1.013839863	0.160192017	0.886792275	1.498282352
ARSANILIC ACID	1.013489328	0.120718907	0.870706452	1.3093563
SULFAQUINOXALINE SODIUM	1.0129816	0.07201905	0.941051584	1.338424582
PROCAINAMIDE HYDROCHLORIDE	1.012870463	0.19749809	0.923046051	1.333417304
HYDROCORTISONE VALERATE	1.012760714	0.496789187	0.952570732	2.132905395
CEPHALOTHIN SODIUM	1.012598642	0.120209218	0.890674169	1.17399994
FLURANDRENOLIDE	1.012366092	0.260545821	0.942418155	1.199969183
RANOLAZINE	1.012181982	0.094062944	0.839044128	1.106571346
SODIUM OXYBATE	1.011965492	0.060303959	0.926930985	0.929706877
ACETRIAZOIC ACID	1.011923899	0.124816657	0.914174138	1.239325216
FTAXILIDE	1.011907724	0.37299895	0.956475669	1.180741379
DIMENHYDRINATE	1.011730943	0.127786146	0.92297971	1.167727164
ACETAMINOSALOL	1.011420237	0.153804097	0.919089971	0.945086134
PROBUCOL	1.011375905	0.174167496	0.908267349	1.180687538
RAMOPLANIN [A2 shown; 2mM]	1.011352542	0.157803462	0.94990968	1.488949074
URETHANE	1.01070902	0.110636004	0.89549914	1.069546135
MYCOPHENOLIC ACID	1.01055124	0.134312141	0.926063596	1.50140794
SPIRAMYCIN	1.010392057	0.076209722	0.887627873	1.180014015
TERPENE HYDRATE	1.010362146	0.192589529	0.949179052	1.522167576
DONEPEZIL HYDROCHLORIDE	1.010319861	0.160539555	0.936736461	1.495174411
RIBOFLAVIN	1.009174212	0.198331162	0.955174953	1.330999242
FENOLDIPAM MESYLATE	1.009123693	0.072850411	0.952499867	1.437710049
TAURINE	1.008594714	0.219994691	0.945027923	1.069253126
SODIUM SALICYLATE	1.007712958	0.206748239	0.954277625	1.459696722
INDAPAMIDE	1.007259225	0.20941164	0.948439329	1.367465651
PILOCARPINE NITRATE	1.006366259	0.234137352	0.963376937	1.333280924
BETHANECHOL CHLORIDE	1.005584014	0.048552624	0.947764662	1.430141908
CHROMOCARB	1.005104237	0.176276127	0.964733748	0.969146916
URACIL	1.004794894	0.04584488	0.955062838	1.186582117
MECLOCYCLINE SULFOSALICYLATE	1.004789661	0.207795293	0.979385668	1.116831731
POLYMYXIN B SULFATE	1.004620731	0.194072665	0.972230648	1.343964983
MODALINE SULFATE	1.004194119	0.167444755	0.954415279	1.312649529
TOLAZAMIDE	1.0039695	0.313400569	0.982334184	1.612079849
SULFACETAMIDE	1.003964167	0.054503771	0.973626318	1.181602449
RITODRINE HYDROCHLORIDE	1.003782286	0.225798023	0.97939272	1.421171319
ISONIAZID	1.003708979	0.291648706	0.976929514	1.411110703
ANASTROZOLE	1.003638284	0.052903917	0.961764551	1.26242017
FLUROTHYL	1.003194933	0.136489992	0.987219673	1.04666342
MESORIDAZINE BESYLATE	1.002916087	0.173680264	0.976409944	1.413791364
DESLORATIDINE	1.002665578	0.100884711	0.987974269	1.198882167
ACEGLUTAMIDE	1.001510542	0.188508057	0.992256816	1.195442336
TULOBUTEROL HYDROCHLORIDE	1.001499966	0.237761318	0.992604613	1.606621533
AMIKACIN SULFATE	1.001498664	0.132550204	0.987169352	1.280654584
CEFUROXIME SODIUM	1.00148841	0.397451871	0.994407007	1.587060114
TOPIRAMATE	1.001128625	0.187065587	0.988406111	1.165363793
PROPIOLACTONE	1.000482231	0.162029578	0.99568491	1.148964541
ATORVASTATIN CALCIUM	1.000247129	0.170799659	0.997338425	1.362565658

MOXIFLOXACIN HYDROCHLORIDE	0.999945992	0.187563231	0.999676815	1.05267266
PINDOLOL	0.999866024	0.282371354	0.999271799	1.495332222
SULBENTINE	0.99986279	0.230712449	0.999117687	1.075438465
METARAMINOL BITARTRATE	0.999851725	0.081735466	0.99889204	1.730980907
PIOGLITAZONE HYDROCHLORIDE	0.999824018	0.238587355	0.999002375	1.488070156
SUCRALOSE	0.999301428	0.22586298	0.996193694	1.043110906
THONZYLAMINE HYDROCHLORIDE	0.99908494	0.123542261	0.9907917	1.198632937
PREGNENOLONE SUCCINATE	0.998862897	0.120034439	0.990403122	1.215178987
PIPEMIDIC ACID	0.998637634	0.062976366	0.992547976	1.202922087
TOLBUTAMIDE	0.998557215	0.172656482	0.991140963	1.202004835
IOXILAN	0.998053754	0.013407692	0.987108163	1.18875656
PALMIDROL	0.998011145	0.328783311	0.988923398	1.075937563
MEROPENEM	0.997968864	0.242929588	0.991439601	1.050131803
OXINIACIC ACID	0.997532108	0.200718098	0.987464085	1.132745483
TROPISETRON HYDROCHLORIDE	0.997447106	0.132248914	0.986433487	1.155899179
METHAPYRILENE HYDROCHLORIDE	0.997208814	0.229347003	0.977478281	1.431350922
ETHOSUXIMIDE	0.997162188	0.424315103	0.98462445	1.367251306
METACETAMOL	0.995976738	0.355540656	0.98225459	1.131950405
RIVASTIGMINE TARTRATE	0.995959125	0.141399457	0.983862056	0.999828922
CARZENIDE	0.995686078	0.082375728	0.98166385	1.525695214
SALSALATE	0.995061585	0.050760924	0.928213066	1.382111057
DOXEPIN HYDROCHLORIDE	0.994455407	0.133222427	0.963708668	1.2574466
CRYOFLURANE	0.994156805	0.126002488	0.965416088	1.093288338
ETHENZAMIDE	0.993921847	0.182773813	0.95835029	0.940333624
NICARDIPINE HYDROCHLORIDE	0.993850098	0.166254479	0.964655349	1.278250674
CEFMETAZOLE SODIUM	0.993826662	0.068417205	0.936142296	1.192311883
MINOCYCLINE HYDROCHLORIDE	0.993800275	0.230680479	0.964556239	1.0396419
PRIMIDONE	0.99366668	0.119181636	0.95933487	1.473088291
DIETHYLCARBAMAZINE CITRATE	0.992964836	0.133152186	0.953960847	1.363590795
METHOTREXATE(+/-)	0.992633372	0.445386743	0.963165151	0.969672831
CLOTRIMAZOLE	0.992158921	0.157651642	0.94980605	1.436665436
ANIRACETAM	0.992127892	0.174078209	0.916200671	1.142360506
NIMUSTINE	0.99209268	0.08175185	0.940038112	1.041685551
TIBOLONE	0.991781929	0.12107322	0.928034988	1.262369615
MIDODRINE HYDROCHLORIDE	0.991229977	0.032001513	0.932984968	1.252108098
GADOTERIDOL	0.991119529	0.207845361	0.947987115	1.06879148
MAPROTILINE HYDROCHLORIDE	0.990943882	0.047316429	0.944446035	1.270484813
BRONOPOL	0.990756319	0.229651624	0.954142343	1.293749906
ADENOSINE	0.990229363	0.080191632	0.911046063	1.234096598
METHYLPHENIDATE HYDROCHLORIDE	0.990195936	0.190242324	0.934346242	1.812944436
IOHEXOL	0.989942295	0.097586574	0.89452889	1.261869086
FURALTADONE	0.989589187	0.187473353	0.957344299	1.299485294
METOPROLOL TARTRATE	0.989196189	0.105807405	0.935330173	0.948415257
NIALAMIDE	0.989039622	0.088477771	0.917367336	0.98439262
AFALANINE	0.988958727	0.045808277	0.940319278	1.074230746
BETAMETHASONE	0.988923039	0.119619515	0.903724041	1.390620527
INAMRINONE	0.988279078	0.084815763	0.881448236	1.286482548
MITOMYCIN	0.988096045	0.078176483	0.891539477	1.085344484
TUBOCURARINE CHLORIDE	0.987520764	0.014539594	0.866676315	1.239062814
OLMESARTAN MEDOXOMIL	0.987342187	0.252304559	0.929463772	1.129149507
HOMIDIUM BROMIDE	0.986753237	0.057225842	0.943480179	1.103341672
MOROXYDINE HYDROCHLORIDE	0.985325698	0.151745417	0.923032291	1.057232841
CYCLOSERINE (D)	0.984762012	0.169501851	0.903772379	1.490834262
EPHEDRINE (1R,2S) HYDROCHLORIDE	0.984404111	0.200559744	0.913150576	1.113544944
PREDNISONE	0.98413275	0.163560201	0.902020326	1.953309647
EFAROXAN HYDROCHLORIDE	0.98373426	0.015054498	0.930349295	1.722858504
TRIMEPRAZINE TARTRATE	0.983733221	0.350987536	0.914137347	1.338076753
FURAZOLIDONE	0.983657243	0.470211793	0.923773862	1.715416665
DICLOXACILLIN SODIUM	0.983564486	0.124045373	0.891956733	1.236646159
TOBRAMYCIN	0.982803155	0.042839406	0.885597125	1.192351849
ZALCITABINE	0.982001653	0.154967084	0.920577432	1.560877142
BROMOPRIDE	0.981703829	0.167693326	0.90509999	1.020047163
KHELLIN	0.981376676	0.09204948	0.860512862	1.189218644
HEXACHLOROPHENE	0.981357628	0.540889598	0.921573838	1.793681027
CINTRIAMIDE	0.98095021	0.078398898	0.92279094	1.009161766
MECLIZINE HYDROCHLORIDE	0.980445288	0.051194873	0.880577708	1.107625288
TELITHROMYCIN	0.980116743	0.205540512	0.883647926	1.070078547
CLIDINIUM BROMIDE	0.979886833	0.218464628	0.879733348	1.079385572
AMINOGLUTETHIMIDE	0.979835165	0.074649003	0.816896098	1.270316009
PASINIAZID	0.979398244	0.261549583	0.918969685	1.505526565
RIBOFLAVIN 5-PHOSPHATE SODIUM	0.979376045	0.105530429	0.916934725	1.079826864
PUROMYCIN DIHYDROCHLORIDE	0.979170969	0.494991409	0.9280722	1.447105153

VALPROATE SODIUM	0.978955483	0.10360847	0.849276031	1.592353674
PROMETHAZINE HYDROCHLORIDE	0.978940563	0.077587987	0.904654483	0.897462482
NORGESTREL	0.978185386	0.087618863	0.842014066	2.390899679
OXYMETAZOLINE HYDROCHLORIDE	0.977270036	0.118793575	0.898366631	1.20137991
AMPYZINE SULFATE	0.977079825	0.245409961	0.903821767	1.493702479
TOPOTECAN HYDROCHLORIDE	0.976808709	0.187297336	0.765927903	1.479114928
D-LACTITOL MONOHYDRATE	0.976565672	0.12029483	0.833264823	1.071824128
COTININE	0.976083982	0.118370818	0.842719564	1.26125439
ERYTHROMYCIN STEARATE	0.975719972	0.246261738	0.883052466	1.247946405
VALACYCLOVIR HYDROCHLORIDE	0.975576344	0.140900464	0.848643215	1.087820811
DICHLORISONE ACETATE	0.975396895	0.226020273	0.901357677	1.840967857
PHENINDIONE	0.975102372	0.304223601	0.841928132	1.096320587
ANISODAMINE HYDROBROMIDE	0.974783957	0.107062028	0.86693983	0.973895308
TIOPRONIN	0.974454329	0.138880336	0.817527728	1.012117168
ASCORBIC ACID	0.973473024	0.196875119	0.773796142	1.396586484
ASPARTIC ACID (L)	0.973160764	0.220025885	0.788999804	1.018070151
SOTALOL HYDROCHLORIDE	0.97229129	0.153126477	0.890180258	1.056398243
AMLEXANOX	0.97185024	0.453882514	0.889214025	1.081303985
DIMINAZENE ACETURATE	0.971328066	0.266841386	0.862983179	1.241640938
MEQUINOL	0.970994016	0.203924294	0.765134839	1.067713644
GLICLAZIDE	0.970797814	0.100294674	0.78452802	1.099617471
CRESOPIRINE	0.970650614	0.121062884	0.87708817	1.048761801
ISOXICAM	0.970191617	0.311024879	0.832493344	1.350496259
SULFADOXINE	0.970157158	0.184555447	0.853690863	1.781951534
OMEGA-3-ACID ESTERS (EPA shown)	0.969477508	0.155336474	0.750439743	1.229372178
ALTRETAMINE	0.96936008	0.170192813	0.725509292	1.427716226
NEFOPAM	0.969357705	0.117574001	0.844163062	1.1452656
CYCLIZINE	0.969327333	0.044660715	0.791221063	1.336375886
CLOXYQUIN	0.969227321	0.163297249	0.806182088	1.185768376
TOLMETIN SODIUM	0.968994028	0.191963628	0.796829617	0.897252733
METHACYCLINE HYDROCHLORIDE	0.968987806	0.322679801	0.876931039	1.154352777
DEXTROMETHORPHAN HYDROBROMIDE	0.968815313	0.3146173	0.859069875	1.179246142
TRIPELENNAMINE CITRATE	0.968448664	0.062063217	0.770025538	1.236489661
CHOLECALCIFEROL	0.968217102	0.138740574	0.781150073	1.591106242
DOXAPRAM HYDROCHLORIDE	0.968000266	0.06725675	0.855320256	1.484456392
SODIUM TETRADECYL SULFATE	0.967951293	0.158789965	0.867684994	1.148189221
SULFACHLORPYRIDAZINE	0.967871893	0.216818389	0.846118467	1.476034884
PENICILLIN V POTASSIUM	0.967243734	0.164784982	0.799855055	1.327912202
PROXYPHYLLINE	0.967197843	0.355540411	0.826097718	1.021522796
OXYPHENONIUM BROMIDE	0.967177357	0.151856913	0.864158756	1.206406558
DIBUTYL PHTHALATE	0.966911362	0.266266453	0.80026399	1.018473511
METHENAMINE	0.966704106	0.122468143	0.689745519	1.299535092
CANDICIDIN	0.966668942	0.114789497	0.86652819	1.023664314
DOXYLAMINE SUCCINATE	0.96533333	0.026292458	0.763864839	1.230278315
PROPOXUR	0.96527602	0.116726449	0.748796169	1.047926482
QUININE SULFATE	0.963677841	0.154097141	0.776606045	1.548431997
NICOTINE BITARTRATE	0.9635062	0.165441464	0.685565667	1.258757448
DOMPERIDONE	0.963309753	0.272780626	0.802475072	1.455469432
RUTIN	0.96330627	0.426274191	0.841630601	1.185873168
DESIPRAMINE HYDROCHLORIDE	0.963291177	0.069226294	0.753871106	1.148902819
CYCLANDELATE	0.962890088	0.400129605	0.846148813	1.116537177
BETAMIPRON	0.96283386	0.106367188	0.729490127	1.177071854
NEOMYCIN SULFATE	0.962491599	0.317372243	0.779722332	1.54548016
PENTYLENETETRAZOL	0.962312773	0.035258497	0.75255219	1.445807508
DOPAMINE HYDROCHLORIDE	0.962059556	0.445815328	0.831607393	2.051089034
PHYSOSTIGMINE SALICYLATE	0.961949462	0.20355187	0.776984629	1.427223117
ACETAZOLAMIDE	0.961694023	0.075502792	0.661450609	1.258115552
EPROBEMIDE	0.961465967	0.252385162	0.848384096	1.499264682
ISOSORBIDE MONONITRATE	0.961451597	0.061408123	0.616574153	1.281287817
BUTYLATED HYDROXYANISOLE	0.961182318	0.105554964	0.753019297	1.785756878
DIPYRONE	0.961080458	0.237032084	0.759093075	2.057570193
RESORCINOL MONOACETATE	0.960708774	0.070067852	0.711864747	1.810282064
TERFENADINE	0.960461345	0.167012981	0.733302124	1.111152068
ACAMPROSATE CALCIUM	0.960215976	0.181906493	0.73835414	1.027449487
ETHAMBUTOL HYDROCHLORIDE	0.959909246	0.299530129	0.758254622	1.370242947
CEFOTETAN	0.959442484	0.373832334	0.774550089	1.324029608
PIZOTYLINE MALATE	0.959240594	0.205583215	0.764593644	1.454035734
MITOTANE	0.958814704	0.228122479	0.706865509	1.280549566
TACROLIMUS	0.958692698	0.194797608	0.730780907	1.329102171
AMPIROXICAM	0.958480431	0.031480823	0.686811191	1.079293319
BISOCTRIZOLE	0.9582619	0.169425084	0.818539999	1.422291605
PRIMAQUINE PHOSPHATE	0.958019398	0.15425902	0.743160231	1.486359252

TYROSINE	0.957909031	0.144901043	0.71269238	0.925080888
PHENOTHIAZINE	0.957788326	0.289507216	0.715590656	0.131536355
RAMIPRIL	0.957683009	0.016016875	0.744012839	1.046851108
PROBENECID	0.956762231	0.064905863	0.720372121	1.087062943
BIOTIN	0.956653656	0.113763146	0.580965052	1.216433589
NOREPINEPHRINE	0.95631645	0.528905611	0.810371566	2.06066018
SODIUM PHENYLBUTYRATE	0.956206927	0.195330807	0.830202373	1.123040565
DIRITHROMYCIN	0.955844553	0.141349851	0.825284687	1.229783669
LUFENURON	0.955489141	0.173446434	0.775951942	1.348458687
PHENSUCCIMIDE	0.954310209	0.131798638	0.771226898	1.498478766
ASPIRIN	0.953833842	0.059142241	0.548993687	1.12786746
ENILCONAZOLE	0.953799048	0.008316456	0.389193007	1.228736662
THIOSTREPTON	0.952753308	0.17855388	0.81580016	2.51869295
PERGOLIDE MESYLATE	0.952298242	0.156667724	0.677876259	2.410418005
PHENYLEPHRINE HYDROCHLORIDE	0.95148963	0.320972687	0.753422244	2.027753671
AMPROLIUM	0.951203107	0.183626137	0.630934304	1.451355147
GLUCONOLACTONE	0.951173124	0.082926651	0.411044619	1.376330173
VORICONAZOLE	0.950868495	0.10120728	0.781600304	1.503585496
CEFONICID SODIUM	0.95073313	0.162612214	0.672778839	1.18624259
ACENOCOUMAROL	0.950718355	0.133348173	0.783307742	1.04376931
GLUCOSAMINE HYDROCHLORIDE	0.950557468	0.423736232	0.756410782	1.60904365
OXAPROZIN	0.949833605	0.106466016	0.68870356	1.111577831
GABOXADOL HYDROCHLORIDE	0.949641722	0.05796057	0.629055836	1.03243519
SULPIRIDE	0.94959654	0.307570851	0.777890205	1.288236045
AMINOPENTAMIDE SULFATE	0.949594834	0.125838998	0.65368951	1.077054897
ETHYNODIOL DIACETATE	0.949459084	0.116638783	0.688508933	1.152141391
CEFALONIUM	0.94939891	0.039160693	0.786417187	1.427289306
BROMPHENIRAMINE MALEATE	0.948517897	0.039717939	0.624503461	1.52770508
MIANSERIN HYDROCHLORIDE	0.948488425	0.182108878	0.505990799	1.242514215
BRINZOLAMIDE	0.948476783	0.096388323	0.79429137	1.067630726
CARISOPRODOL	0.948339521	0.04196671	0.546668485	1.316053207
PROPARACAINE HYDROCHLORIDE	0.94759958	0.170020021	0.595631559	1.168135415
FENCLONINE	0.947488033	0.132820131	0.731045662	1.100858182
OXYQUINOLINE SULFATE	0.947104721	0.064075755	0.577767492	1.049303688
MOXIDECTIN	0.947066788	0.414412303	0.789071078	1.258844275
QUIPAZINE MALEATE	0.946890235	0.055424811	0.615949525	1.84466085
PAROMOMYCIN SULFATE	0.946662713	0.429634896	0.720695715	1.422708766
FLUVASTATIN	0.946581824	0.30020325	0.725011836	1.513009921
FOSFOSAL	0.946486886	0.261497869	0.749485335	1.104090879
SALICIN	0.946302758	0.071717316	0.468613998	1.363263757
OCTISALATE	0.94624456	0.233150384	0.796081443	1.257035147
NALOXONE HYDROCHLORIDE	0.945997624	0.151148573	0.636583862	1.873101586
INOSITOL	0.945855537	0.248095212	0.651893516	1.380682048
AJMALINE	0.945675059	0.326226276	0.760070344	0.945890534
HEXAMETHONIUM BROMIDE	0.945298471	0.099557923	0.712202316	1.121688375
ROXARSONE	0.945113529	0.171791353	0.549530842	1.103480848
TEICOPLANIN [A(2-1) shown]	0.944922446	0.025830602	0.671771894	1.168244673
MEMANTINE HYDROCHLORIDE	0.944814832	0.130745466	0.684392705	1.151111549
HYDROCORTISONE	0.944738859	0.118302016	0.395362693	1.317223534
ISAXONINE	0.94450147	0.103890656	0.769169681	1.103350188
TIMONACIC	0.944118194	0.079420112	0.766294494	1.320735083
CLOMIPHENE CITRATE	0.944067412	0.035126163	0.629822585	1.586360606
AMANTADINE HYDROCHLORIDE	0.943765457	0.032403367	0.51055581	1.274635501
BLEOMYCIN (bleomycin B2 shown)	0.943540744	0.228491598	0.522797286	1.302121854
CYROMAZINE	0.943468186	0.097217008	0.702813658	1.227827146
BECLOMETHASONE DIPROPIONATE	0.943459766	0.019032884	0.506435689	1.467809797
DEXIBUPROFEN	0.943319353	0.073119019	0.599913989	1.239320815
MEPIROXOL	0.942797463	0.131329073	0.764244218	1.09954649
APOMORPHINE HYDROCHLORIDE	0.942170957	0.310647192	0.649915877	1.77633485
alpha-TOCHOPEROL	0.941969438	0.140045675	0.541854628	1.277190321
MANNITOL	0.941891075	0.161250601	0.748800578	1.279053786
METAXALONE	0.941700568	0.047092212	0.298425087	1.1632457
CLOZAPINE	0.941459005	0.309268722	0.787481134	1.110688887
ALENDRONATE SODIUM	0.940269747	0.170366082	0.650572694	1.395407307
ESTROPIPATE	0.939922788	0.126925211	0.63674854	1.190107291
TEGASEROD MALEATE	0.939886213	0.189904509	0.743985576	1.631155926
ALOIN	0.93984935	0.147824027	0.696468263	1.08390756
FLUROFAMIDE	0.939737309	0.39613295	0.68286948	1.153203208
ROPINIROLE HYDROCHLORIDE	0.939687554	0.119435848	0.633630745	1.339427917
LOVASTATIN	0.938853886	0.095257819	0.32135548	1.45999508
LEVOCETIRIZINE DIHYDROCHLORIDE	0.938750954	0.241468279	0.584540739	1.029644952
PITAVASTATIN CALCIUM	0.938616385	0.229580902	0.575656476	1.145006624

ACTARIT	0.937997242	0.029176407	0.739883688	1.169311871
CHLOROGUANIDE HYDROCHLORIDE	0.937761135	0.107554573	0.327595195	1.274874861
METOLAZONE	0.937690463	0.131849489	0.611105866	1.088878707
ISRADIPINE	0.93764052	0.229822307	0.656244018	1.218296552
SERATRODAST	0.937001994	0.12667574	0.724834988	1.384717148
GANCICLOVIR	0.936967095	0.294775281	0.748497515	1.41932291
BACAMPICILLIN HYDROCHLORIDE	0.936822469	0.113995823	0.425321373	1.446842816
LOBENDAZOLE	0.936693066	0.229211366	0.618135245	1.097951614
TROPICAMIDE	0.936364182	0.081901829	0.562483682	1.6637447
ACESULFAME POTASSIUM	0.936293862	0.11740534	0.328946482	1.221639463
SODIUM GLUCONATE	0.935752396	0.070165666	0.597088716	1.093567248
LEVALBUTEROL HYDROCHLORIDE	0.935175988	0.04098053	0.246832994	1.035828206
SULFANITRAN	0.93503307	0.148915835	0.637126347	0.981035642
ESTRADIOL VALERATE	0.934903754	0.240451893	0.583855044	1.219142021
LABETALOL HYDROCHLORIDE	0.934739119	0.198196196	0.589998482	1.61679539
GRANISETRON HYDROCHLORIDE	0.934497039	0.093234341	0.711462354	1.146554289
PYRETHRINS	0.933518267	0.237925095	0.750077471	1.199445118
TRIPROLIDINE HYDROCHLORIDE	0.932981601	0.114462011	0.551941663	1.726329257
BROMOCRIPTINE MESYLATE	0.932855543	0.077399522	0.448119775	1.728796294
DOXYCYCLINE HYDROCHLORIDE	0.932156658	0.020842423	0.558827625	1.165202112
MESNA	0.932066838	0.021439295	0.343351275	1.108273803
THIAMYLAL SODIUM	0.932045236	0.16249564	0.625482231	1.106627209
PHYTONADIONE	0.932002665	0.040241927	0.430272848	1.166632256
PROGLUMIDE	0.931861808	0.141574255	0.473068079	1.149236671
PINACIDIL	0.931800528	0.168161021	0.45626432	1.322947522
METHIMAZOLE	0.931758011	0.08468279	0.440184065	1.167404679
TINIDAZOLE	0.931167823	0.141593335	0.409921703	1.240695665
GABAPENTIN	0.93116193	0.111213402	0.72888086	1.15427526
PROPOFOL	0.931038839	0.037233842	0.217954486	1.148757233
NEVIRAPINE	0.931005373	0.201902934	0.571053659	1.763489473
DESONIDE	0.930992505	0.165517967	0.732773923	1.865993543
LACTULOSE	0.930139848	0.331707891	0.61261137	1.514248794
GRISEOFULVIN	0.928603348	0.098998726	0.382196589	1.693456298
AMPICILLIN SODIUM	0.928088647	0.158907503	0.464590372	1.364037888
PREDNICARBATE	0.92787468	0.247733663	0.614400468	1.534616616
METFORMIN HYDROCHLORIDE	0.92772676	0.098794839	0.24958659	1.056310851
SYMCLOSENE	0.927486401	0.121768961	0.369008319	1.292215089
PEMETREXED	0.92744025	0.106621739	0.588747164	1.059047247
LACTOSE MONOHYDRATE	0.927137267	0.240876627	0.658893792	1.140175441
MENADIONE	0.927132068	0.214203308	0.452819465	1.492230329
FENOPROFEN	0.926850059	0.021470087	0.389444449	1.132509937
DIBEKACIN	0.926659981	0.231635529	0.713464365	1.307393795
CHLORTHALIDONE	0.926445767	0.104432877	0.541151188	1.276019855
ARGININE HYDROCHLORIDE	0.926233825	0.113943631	0.679218758	1.348122852
FIPRONIL	0.925655048	0.144884204	0.398186749	1.456545367
CARTEOLOL HYDROCHLORIDE	0.924721552	0.236617884	0.49955414	1.319419749
FLUOROMETHOLONE	0.924409882	0.363887968	0.603395868	1.457172831
DYDROGESTERONE	0.924340426	0.207314314	0.713144954	1.554844861
TRISODIUM ETHYLENEDIAMINE TETRACE	0.923956454	0.109909756	0.529373071	1.145232633
DYCLONINE HYDROCHLORIDE	0.923317486	0.201312056	0.46737677	1.410543729
TELENZEPINE HYDROCHLORIDE	0.923104072	0.143243551	0.688616344	1.254331711
NAFRONYL OXALATE	0.92285744	0.282290974	0.502766904	1.179557691
CLENBUTEROL HYDROCHLORIDE	0.92272269	0.118876064	0.684736728	1.664696843
CEFUROXIME AXETIL	0.922408889	0.352952659	0.633257916	1.171748106
PIRENZEPINE HYDROCHLORIDE	0.922284797	0.042089831	0.552945481	1.085059408
METHYLERGONOVINE MALEATE	0.922236993	0.602668699	0.706851718	1.985402161
ETHANOLAMINE OLEATE	0.921941004	0.197384703	0.422030209	1.067300237
MILNACIPRAN HYDROCHLORIDE	0.921728933	0.359480713	0.704908521	1.747928963
IDEBENONE	0.921550323	0.123009299	0.680644708	1.482441103
AMISULPRIDE	0.921549217	0.12725607	0.602885056	1.172213502
SORBITOL	0.921314308	0.070773206	0.598541951	1.050612966
BACLOFEN	0.920965405	0.145046724	0.413232558	1.226276371
CITICOLINE	0.92080783	0.197197611	0.559872429	1.172906269
THALIDOMIDE	0.920633188	0.164350561	0.496571014	1.816973037
ATROPINE OXIDE	0.919760879	0.165416213	0.486770363	0.945313726
APRAMYCIN SULFATE	0.919080777	0.153908782	0.535366827	1.343357292
THEOPHYLLINE	0.91861002	0.089397016	0.189268919	1.417067449
DIENESTROL	0.918278569	0.114128314	0.501047997	1.687672688
IMIPENEM	0.918252926	0.182352255	0.65647296	1.457907296
PRASUGREL	0.917023156	0.067672061	0.638036238	1.256997367
HISTAMINE DIHYDROCHLORIDE	0.916731704	0.74747196	0.736148362	2.134637693
ERYTHRITOL	0.916120027	0.188742628	0.597516294	1.281716541

ACARBOSE	0.915815887	0.205426642	0.539241411	1.539593586
SAXAGLIPTIN	0.915442821	0.041121274	0.275807826	1.137744596
CLOFIBRATE	0.915144651	0.144870799	0.458631396	1.662148278
ADAPALENE	0.915120866	0.045195513	0.517991134	0.99061375
SULFISOXAZOLE	0.914913646	0.096879798	0.492235715	1.192396279
RIBOSTAMYCIN SULFATE	0.914544661	0.154018715	0.657685026	1.765172455
DIMETRIDAZOLE	0.914164615	0.123747268	0.574379168	1.051232969
SPAGLUMIC ACID	0.91401589	0.201425191	0.591863791	1.101511434
PENCICLOVIR	0.913926877	0.212067533	0.604032162	1.469314469
RASAGILINE	0.913228274	0.085778484	0.624373172	1.377924617
OSELTAMIVIR PHOSPHATE	0.912738548	0.07113442	0.621247713	1.414048438
CYPROTERONE	0.912401315	0.099493077	0.643937247	1.901847917
ENALAPRIL MALEATE	0.912398343	0.273536898	0.65192643	1.452514148
OLEANDOMYCIN PHOSPHATE	0.912000456	0.120820115	0.190456924	1.209557057
AMITRAZ	0.91180833	0.210963962	0.379149891	1.351263708
GUAIACOL	0.911627323	0.061552405	0.55403713	1.000018856
CHLORPHENIRAMINE MALEATE	0.910837502	0.148580319	0.476193894	1.185051726
CEFAZOLIN SODIUM	0.910778356	0.107759783	0.508071925	1.127606464
PREDNISOLONE	0.91069093	0.114523833	0.476503756	1.851336241
CEFOPERAZONE	0.910675084	0.096443861	0.277780944	1.220909821
DIPYROCETYL	0.910673451	0.284740235	0.665119	1.297837943
DEBRISOQUIN SULFATE	0.91004094	0.088050897	0.500370574	1.060768839
HYDROCORTISONE ACETATE	0.909780589	0.347379386	0.525546094	1.57526814
GUANABENZ ACETATE	0.909737192	0.422908506	0.572917861	1.515813436
PHENFORMIN HYDROCHLORIDE	0.909678892	0.244440232	0.635598103	1.678931015
LIDOCAINE HYDROCHLORIDE	0.909447991	0.118005437	0.426369956	1.578780154
FAMOTIDINE	0.909382553	0.204606645	0.467732293	1.333572152
DIACETAMATE	0.909093573	0.240518974	0.651194483	1.158037922
CETIRIZINE HYDROCHLORIDE	0.908638804	0.14256219	0.613160973	1.146627126
FIPEXIDE HYDROCHLORIDE	0.90832555	0.177043125	0.637984522	1.287593225
MANGAFODIPIR TRISODIUM	0.907231462	0.180653476	0.327813494	1.143001608
ARTEMISININ	0.907118696	0.215603957	0.567099203	1.314797693
URAPIDIL HYDROCHLORIDE	0.906697621	0.250964324	0.571876119	1.325860465
LITHIUM CITRATE	0.90667586	0.197279737	0.493534486	1.085042783
EBSELEN	0.906643054	0.186093662	0.633271522	1.329287599
BACITRACIN	0.906467208	0.067498045	0.293123297	1.335616673
PYRITHYLDIONE	0.906451949	0.215858234	0.564442735	1.080745897
CALCIUM GLUCEPTATE	0.905736587	0.086793753	0.480341017	1.091899111
NITROFURAZONE	0.905401865	0.288534179	0.464713825	1.37178641
INOSINE	0.905399647	0.240855469	0.563284453	1.126719223
LORNOXICAM	0.905288633	0.04991156	0.630370752	1.088299121
BARBITAL	0.905123941	0.134882316	0.532220815	1.188571498
EDARAVONE	0.904621593	0.166824858	0.411558494	0.950615591
DASATINIB	0.904464074	0.478441825	0.651805659	1.179929143
CEFTIBUTEN	0.904291946	0.063475942	0.439669694	1.305185611
CARBOPLATIN	0.90425889	0.18403311	0.316383644	1.147839153
PYRIDOSTIGMINE BROMIDE	0.903995367	0.168211017	0.210312531	1.340545168
RONIDAZOLE	0.903763191	0.05680415	0.466371343	1.578506595
CHLORINDANOL	0.903569796	0.062924034	0.225851361	1.274182995
CHLORTETRACYCLINE HYDROCHLORIDE	0.903282827	0.108914512	0.426293647	1.373659622
RUFLOXACIN HYDROCHLORIDE	0.903244809	0.213111029	0.54563464	1.316615293
PIDOLIC ACID	0.903112635	0.066958176	0.517877374	1.043563607
EDOXUDINE	0.903051378	0.234473485	0.343608521	1.202050871
HYCANTHONE	0.902527942	0.119341811	0.385139117	1.025751152
EUCATROPINE HYDROCHLORIDE	0.901725682	0.320421369	0.471082525	1.399945149
CLOPERASTINE HYDROCHLORIDE	0.90140846	0.03902362	0.599461239	1.87885266
ETHYLNOREPINEPHRINE HYDROCHLORIE	0.901192826	0.07850022	0.511270152	1.924378783
ATROPINE SULFATE	0.901161305	0.057409178	0.264570342	1.08703143
ENALAPRILAT	0.901126535	0.103860907	0.619091889	1.417607222
ISOVALERAMIDE	0.901047625	0.064304771	0.191579121	1.180589564
BUCLADESINE	0.901028513	0.306472086	0.480772035	1.443151483
DEXPANTHENOL	0.900100496	0.13858388	0.297913206	1.162777606
CINOCTRAMIDE	0.899299409	0.190235935	0.527911595	1.297948298
BETAMETHASONE SODIUM PHOSPHATE	0.898479772	0.090247969	0.110061917	1.384962206
LEVCYCLOSERINE	0.898284912	0.181535582	0.475181006	0.99669618
CEFTAZIDIME	0.898183734	0.129102504	0.611297738	1.190782907
FENSPIRIDE HYDROCHLORIDE	0.897643278	0.071426512	0.24996204	1.21787958
DIOXYBENZONE	0.897590259	0.230514396	0.453868488	0.835427449
PIPERONYL BUTOXIDE	0.89733503	0.239605931	0.535531424	1.129842682
VIOMYCIN SULFATE	0.897170335	0.013577622	0.162076384	1.235776416
OLANZAPINE	0.897148423	0.270864433	0.389831069	1.228536085
NAFTIFINE HYDROCHLORIDE	0.89689896	0.310616673	0.421744403	1.081866983

NICERGOLINE	0.896802914	0.109993683	0.201567414	1.167091791
DEXFOSFOSERINE	0.896326517	0.338246429	0.566985924	1.124306279
DISULFIRAM	0.893992497	0.088405321	0.483195574	1.071644761
FLUORESCEIN	0.893659791	0.107245886	0.250299722	1.251163075
DECOQUINATE	0.89355649	0.168557874	0.424050502	1.097783031
ETHAMIVAN	0.893554212	0.025906268	0.319212779	1.436610125
PREGABALIN	0.893438935	0.149813569	0.148131824	1.171937688
ROXATIDINE ACETATE HYDROCHLORIDE	0.893059124	0.037694582	0.543915125	1.309006215
RACTOPAMINE HYDROCHLORIDE	0.892805516	0.176841871	0.560093071	1.807152056
FENBENDAZOLE	0.892683433	0.194484629	0.306847349	2.930515002
SULFAPHENAZOLE	0.892429885	0.127773544	0.336771938	1.075593763
FLOPROPIONE	0.892210216	0.03268173	0.30662013	1.159884011
VINCAMINE	0.891970089	0.284926976	0.531004789	1.067690809
PAROXYPROPIONE	0.891812973	0.232508444	0.511860565	0.959564559
CHLORPROPAMIDE	0.891722389	0.249252171	0.439267381	1.212616275
NORETHINDRONE ACETATE	0.891528146	0.514282411	0.555322348	1.575341164
TIAPRIDE HYDROCHLORIDE	0.891394149	0.027359185	0.14385659	1.186417543
HEXYLENE GLYCOL	0.890690131	0.140182356	0.429323272	1.102081458
PIPERAZINE	0.890419063	0.066547411	0.174640918	1.327401059
TUAMINOHEPTANE SULFATE	0.889409276	0.074926403	0.320391921	1.570267065
BITOSCANATE	0.88926602	0.150547178	0.5667621	1.625160694
ALPRENOLOL	0.88844663	0.073400338	0.149425799	1.337023683
PYRITHIONE ZINC	0.888314048	0.261754004	0.318554557	0.091564018
ETODOLAC	0.888233909	0.144972839	0.34210326	1.419336289
SODIUM MONOFLUOROPHOSPHATE	0.887459309	0.251100058	0.512354623	1.359845536
IRBESARTAN	0.886181431	0.061578112	0.360765166	1.236930369
METHYLATROPINE NITRATE	0.88543169	0.011590945	0.144635511	1.278555489
ACETOHEXAMIDE	0.885396207	0.209360481	0.361615701	1.079058796
PREDNISOLONE HEMISUCCINATE	0.885284539	0.255417291	0.389663427	1.465432665
DEFLAZACORT	0.885064817	0.217077915	0.395173822	1.560511307
PHTHALYLSULFACETAMIDE	0.884961709	0.040165324	0.541104612	1.419310423
DEQUALINIUM CHLORIDE	0.884796251	0.146822028	0.550828477	1.18661876
LORATADINE	0.884576841	0.186688847	0.341379548	1.500045064
MALATHION	0.883910199	0.055722386	0.148763627	1.435249402
CARSALAM	0.882143381	0.090084665	0.534912207	1.431106469
FELODIPINE	0.881707764	0.084235881	0.327074174	2.325322493
IDRAMANTONE	0.881492105	0.022880274	0.262521172	1.066673055
BENFLUOREX HYDROCHLORIDE	0.880540682	0.051006926	0.526518265	1.118239815
DIOSMIN	0.880110072	0.05436995	0.424786127	1.096390947
NELARABIN	0.879823657	0.086510131	0.441714758	1.608777032
CIMETIDINE	0.87976237	0.085584327	0.147977987	1.28141846
CANRENOIC ACID, POTASSIUM SALT	0.879703476	0.102371124	0.290551341	1.424726279
VALSARTAN	0.879193889	0.08007392	0.058404675	1.199740128
AMYLENE HYDRATE	0.878871941	0.092674458	0.425521213	1.22498695
EDROPHONIUM CHLORIDE	0.878440016	0.237810139	0.475384976	1.473257402
IOPANIC ACID	0.878208445	0.208485533	0.32948409	1.509134503
PERINDOPRIL ERBUMINE	0.877592864	0.145590514	0.351205072	1.286420576
gamma-AMINOBUTYRIC ACID	0.87758982	0.08600982	0.261344407	1.038121931
AMLODIPINE BESYLATE	0.877038241	0.066205192	0.326037538	1.270915255
NOVOBIOCIN SODIUM	0.876276862	0.047577528	0.163601241	1.115073376
RILUZOLE	0.874848326	0.098454076	0.18064259	1.287714767
BERGAPTEN	0.874800639	0.127250875	0.267230548	1.099043511
NADIDE	0.874437011	0.044288436	0.24697328	1.894976928
ZOLPIDEM	0.873871776	0.263738108	0.468556536	1.382341458
AMINOPTERIN	0.873462448	0.123931276	0.261001807	1.110275007
DEXPROPRANOLOL HYDROCHLORIDE	0.873170531	0.32963603	0.423219919	1.089316836
CEFDITORIN PIVOXIL	0.872617375	0.235115386	0.373519873	0.915876875
HYOSCYAMINE	0.872498312	0.444974511	0.444778085	1.516383195
GALANTAMINE	0.872144372	0.159377266	0.429368959	1.632624965
PRAZIQUANTEL	0.871837601	0.111040459	0.31233973	1.746941548
TRIMETAZIDINE DIHYDROCHLORIDE	0.871194031	0.201410347	0.515565763	1.069296403
PHENIRAMINE MALEATE	0.871022215	0.149876832	0.479577869	1.27179995
CINCHONINE	0.869916693	0.162368671	0.35776425	0.949134033
PIDOTIMOD	0.869748632	0.110398821	0.389568562	1.294071999
ETHOPROPAZINE HYDROCHLORIDE	0.869299893	0.097118344	0.196633408	0.705754682
PREDNISOLONE ACETATE	0.869091746	0.147789396	0.315610239	1.799437767
ROLITETRACYCLINE	0.869089853	0.076202021	0.240220975	0.941238091
NITROXOLINE	0.868628852	0.290978617	0.528304425	0.843772317
CEFAMANDOLE NAFATE	0.868619422	0.106968435	0.054607131	1.61404643
CHLOROPYRAMINE HYDROCHLORIDE	0.868393465	0.106144172	0.491173202	1.445998024
PRONETALOL HYDROCHLORIDE	0.868025616	0.105750483	0.489945821	1.383920275
DIACERIN	0.867789618	0.161128684	0.395695262	0.728203863

GUANETHIDINE MONOSULFATE	0.867687428	0.296225067	0.318547195	1.398576774
PHENYLETHYL ALCOHOL	0.867643945	0.065628007	0.456754766	1.791938722
METHYLPREDNISOLONE	0.867486234	0.607159626	0.519179739	1.452608156
KANAMYCIN A SULFATE	0.866971003	0.286920878	0.308989384	1.254682714
BETAZOLE HYDROCHLORIDE	0.866342252	0.140800313	0.462543629	1.573811763
TETRAHYDROZOLINE HYDROCHLORIDE	0.866200265	0.139946707	0.302575125	1.453847928
FLUDROCORTISONE ACETATE	0.865996431	0.105459626	0.18984936	1.196933581
TRYPTOPHAN	0.86577844	0.223802467	0.30095329	1.543956539
IMEXON	0.865648652	0.085288212	0.22712031	1.559364913
GUAIFENESIN	0.86534254	0.294106406	0.30886803	1.354455473
RITANSERIN	0.865299916	0.240286307	0.431239619	1.201214517
ORLISTAT	0.864241545	0.12532052	0.296352328	1.117122712
CLOMIPRAMINE HYDROCHLORIDE	0.863426688	0.133808802	0.393257747	1.212288513
SELENOMETHIONINE	0.863181573	0.198191464	0.397779813	0.998119668
FOSFOMYCIN CALCIUM	0.862986478	0.117957474	0.103763124	1.285370006
FLUNIXIN MEGLUMINE	0.862871513	0.449465549	0.507474374	0.374798285
DABIGATRAN ETEXILATE MESYLATE	0.862272058	0.537484844	0.541688631	0.117790771
beta-ESCIN	0.862025695	0.21647267	0.400251359	1.204877637
ABAMECTIN (avermectin B1a shown)	0.861300206	0.176436072	0.151946952	0.953745059
HYDROXYUREA	0.861294644	0.568085459	0.486062067	1.723598443
CARPROFEN	0.861097998	0.041128746	0.024939995	1.407993731
FENIPENTOL	0.861051102	0.095483098	0.209370404	1.264780558
BECLAMIDE	0.860857706	0.019911961	0.461052379	1.298158972
DIPHENYLPYRALINE HYDROCHLORIDE	0.860714838	0.069056578	0.249381667	1.068658871
QUETIAPINE	0.859602662	0.142255824	0.287009147	1.298710406
PARGYLINE HYDROCHLORIDE	0.857159563	0.119059849	0.42958189	1.03499757
LINDANE	0.857077566	0.089926955	0.09357561	0.887700355
CHENODIOL	0.857071242	0.108112963	0.216321136	1.412070306
TILETAMINE HYDROCHLORIDE	0.856350223	0.065522092	0.25525043	1.123926525
QUINESTROL	0.855944327	0.134016609	0.42827926	1.261014132
ALCLOMETAZONE DIPROPIONATE	0.855742007	0.212702198	0.305056607	1.70131261
PROCODAZOLE	0.855330063	0.234980551	0.385417992	0.988272055
SUXIBUZONE	0.855255258	0.078778094	0.187497727	1.070243978
MINOXIDIL	0.854892034	0.243682322	0.21206959	1.241630802
TOLFENAMIC ACID	0.854852044	0.060431682	0.18198181	1.456837219
AMINOHYDROXYBUTYRIC ACID	0.854631407	0.168249222	0.221512744	1.045115837
CARBENOXOLONE SODIUM	0.854408955	0.117219695	0.420749922	1.698668879
TROXERUTIN	0.853991908	0.02387806	0.174283941	1.036445214
CLONIDINE HYDROCHLORIDE	0.853921496	0.023355264	0.222243869	1.437775384
PROPYLTHIOURACIL	0.853863988	0.127880136	0.104144234	1.272968242
HYDROCORTISONE PHOSPHATE TRIETHY	0.853843829	0.437317982	0.377853284	1.445812245
MESTRANOL	0.853788406	0.113970171	0.288583429	1.487443991
NIACINAMIDE	0.853729513	0.281069846	0.40942971	1.417624388
DROPROPIZINE	0.852877287	0.220790805	0.372477735	1.23740186
ZINC UNDECYLENATE	0.852816921	0.049096584	0.074030899	1.259538334
ISOFLUPREDONE ACETATE	0.852709728	0.29082131	0.497178679	1.336913327
DEFERIPRONE	0.852036511	0.059350324	0.435832048	1.082131905
PICOLAMINE	0.851774315	0.057559364	0.328191031	0.957169407
THIOTEPA	0.851695166	0.206578673	0.239287375	1.759814046
BUCETIN	0.851408673	0.049316727	0.319321069	1.184686232
SIROLIMUS	0.851198667	0.150593153	0.208827199	1.331914983
CRESOL	0.8511274	0.050752416	0.071581708	1.676057358
PYRONARIDINE TETRAPHOSPHATE	0.850662143	0.13268429	0.331956206	1.363640278
BEZAFIBRATE	0.850251977	0.276991115	0.397177804	1.657763133
DIXANTHOGEN	0.849847298	0.155407843	0.341896269	1.053955748
SULFAMETER	0.84891241	0.169746913	0.356258564	1.713078208
BENAZEPRIL HYDROCHLORIDE	0.848421314	0.262298744	0.330686686	1.500876967
DIFLORASONE DIACETATE	0.848121581	0.166945732	0.353063112	1.235768933
BALSALAZIDE DISODIUM	0.847806853	0.196366288	0.158950399	1.212752183
ACIPIMOX	0.847762526	0.110283876	0.324445043	1.227754993
DAPTOMYCIN (5 millimolar/DMSO)	0.847388772	0.083818273	0.262106052	1.345472808
ETHIONAMIDE	0.847084271	0.323163678	0.272899407	1.354198359
PRASTERONE	0.84618505	0.147914105	0.429228489	1.463912468
PIPOBROMAN	0.845877955	0.067409373	0.166303124	1.408578866
OXCARBAZEPINE	0.845550606	0.059145252	0.222480588	1.324926961
HYDROXYTOLUIC ACID	0.844837465	0.161417197	0.322264151	1.015056163
TRIHEXYPHENIDYL HYDROCHLORIDE	0.844507649	0.198781396	0.221191742	1.481372462
PICONOL	0.844436809	0.175545008	0.331537194	0.949835258
HYDROXYZINE PAMOATE	0.844391253	0.422271075	0.338243378	1.588739024
BUSPIRONE HYDROCHLORIDE	0.84381711	0.128472789	0.073236164	1.33904321
MEPHENESIN	0.841603839	0.132867536	0.324944756	1.304586328
NITHIAMIDE	0.840053006	0.076742755	0.158205955	1.345804404

METHOXAMINE HYDROCHLORIDE	0.839992692	0.102715751	0.094561764	1.168624095
NEFIRACETAM	0.839618662	0.076991655	0.294584041	1.079223996
PIMAGEDINE HYDROCHLORIDE	0.839108274	0.102769494	0.166547655	1.528391258
OXTRIPHYLLINE	0.838204921	0.155561175	0.407806051	0.970764487
PARACHLOROPHENOL	0.838124275	0.165243272	0.094058848	1.083461362
LUMIRACOXIB	0.837612477	0.117555101	0.209256237	1.310450965
ALMOTRIPTAN	0.836937954	0.091771381	0.365554573	1.528722993
GLYBURIDE	0.836785739	0.175176025	0.216063894	1.005639113
LEVONORDEFRIN	0.836371867	0.724532295	0.500300586	2.046825044
CLORGILINE HYDROCHLORIDE	0.836330125	0.100711967	0.394338116	1.39742367
CLINDAMYCIN HYDROCHLORIDE	0.836173183	0.055518122	0.178552499	1.328293037
IPRONIAZID SULFATE	0.835504043	0.243032525	0.41944132	1.520604582
ETHINYL ESTRADIOL	0.834644267	0.587143049	0.420419784	1.859702697
meta-CRESYL ACETATE	0.832651306	0.212883528	0.404331953	1.15196618
ECONAZOLE NITRATE	0.832235715	0.093815385	0.222677787	1.39094915
NALBUPHINE HYDROCHLORIDE	0.831459503	0.031760015	0.345163764	1.356496982
GENTAMICIN SULFATE	0.831101084	0.475744989	0.338284587	1.593783706
COUMARIN	0.830750159	0.237323303	0.314160594	1.150944071
DICLOFENAC SODIUM	0.830609873	0.087476017	0.171564338	1.269292925
TRIMETOZINE	0.82970242	0.253770871	0.250738774	1.263567859
TRIAMCINOLONE	0.82794017	0.031901052	0.128473129	1.268524699
ESZOPICLONE	0.827808488	0.088502022	0.39101431	1.03489734
CARBIMAZOLE	0.827142957	0.126096413	0.269987077	0.954231038
BUFLOMEDIL HYDROCHLORIDE	0.826900669	0.102743204	0.368959893	1.361337949
DIPERODON HYDROCHLORIDE	0.826787985	0.191671793	0.403640503	1.291336645
ETHOXZOLAMIDE	0.825212664	0.11361868	0.136020944	1.448549527
GALLAMINE TRIETHIODIDE	0.824295568	0.388861906	0.258723845	1.451140266
PHENETHICILLIN POTASSIUM	0.824257558	0.188061637	0.074116166	1.278748515
DEXAMETHASONE	0.824101472	0.085047068	0.156631687	1.396272021
LOXOPROFEN	0.823989911	0.2791946	0.204871292	1.094008315
ARMODAFINIL	0.823118859	0.199864521	0.292966883	1.478407236
HYDRASTININE HYDROCHLORIDE	0.82279916	0.187212842	0.372516371	1.211118729
CHLOROXINE	0.822719885	0.155220044	0.056550596	1.035475527
NADOLOL	0.821685834	0.262397856	0.193648047	1.479938564
XYLAZINE	0.820973183	0.122290748	0.266788926	1.740034421
METHYLPREDNISOLONE SODIUM SUCCIN	0.820822403	0.048257001	0.234907691	1.260970227
CINCHOPHEN	0.820570082	0.080214589	0.34993398	1.149772182
ETHYL VANILLIN	0.819864438	0.214435825	0.111592598	1.16016212
PHENOXYBENZAMINE HYDROCHLORIDE	0.816686498	0.099802852	0.01139297	1.51209587
RANITIDINE HYDROCHLORIDE	0.816525261	0.080670388	0.1829794	1.317693218
TROSPIUM CHLORIDE	0.816440019	0.195060176	0.076125603	1.359667729
ZOXAZOLAMINE	0.815063035	0.10358398	0.184318657	1.067481735
LORGLUMIDE SODIUM	0.814859098	0.147369731	0.238573508	1.153237327
CARVEDILOL	0.814751076	0.171735851	0.178714433	1.589846402
FLUOROURACIL	0.813281378	0.727043691	0.444715738	2.00419055
PROPRANOLOL HYDROCHLORIDE (+/-)	0.812911852	0.062348271	0.237657963	1.232942834
ASPARTAME	0.812563274	0.248362797	0.283282185	1.535247031
PHENOTHRIN	0.812563082	0.287076275	0.287388879	1.237506224
AMBROXOL HYDROCHLORIDE	0.810937597	0.029773407	0.322433798	1.307409992
ERYTHROMYCIN	0.810716132	0.582899911	0.320772299	0.068954203
DEXAMETHASONE ACETATE	0.810710753	0.087107142	0.13074706	1.451543949
ARTENIMOL	0.810424329	0.038989413	0.321579053	1.303271806
ELLAGIC ACID	0.810231446	0.133466895	0.107199917	0.984069453
ALLYLTHIOUREA	0.808393303	0.045125179	0.212276729	1.149973978
NIMESULIDE	0.808086577	0.119699701	0.323731591	1.276723396
PIROXICAM	0.807737403	0.065936252	0.132734985	1.45556743
THIRAM	0.807333934	0.056911144	0.026778887	2.064039559
RAMIFENAZONE	0.806379462	0.110005902	0.094526166	1.173938287
LANSOPRAZOLE	0.805781615	0.236396363	0.146499157	1.855221468
RAMELTEON	0.805734369	0.126234199	0.231532417	1.568592822
DROPERIDOL	0.805155295	0.152554387	0.115233713	1.390609728
FLUNISOLIDE	0.804106352	0.043437834	0.216109319	1.264433101
NAFTOPIDIL	0.804048922	0.073099291	0.308735245	1.329862283
AZACITIDINE	0.803374015	0.031982722	0.326243961	1.382045221
EUGENOL	0.802917315	0.359347637	0.189169854	1.441397298
VORINOSTAT	0.800765815	0.188728436	0.236320394	1.413152862
ARTESUNATE	0.799091433	0.264135043	0.257892563	1.501400111
METRONIDAZOLE	0.798996974	0.14572417	0.053729082	1.216916809
TILORONE	0.798938964	0.047627045	0.205471028	1.139779034
OXYTETRACYCLINE	0.798454046	0.078833067	0.267047361	1.268490368
TRICHLORMETHINE HYDROCHLORIDE	0.798189966	0.139533729	0.199890818	1.194648652
TENOXICAM	0.794879253	0.168975514	0.035825256	1.474167311

CHLORZOXAZONE	0.793857777	0.092334633	0.104212416	1.25808357
PREGNENOLONE	0.792926145	0.050741438	0.180886028	1.685751145
TRIAMCINOLONE DIACETATE	0.792121657	0.291132533	0.154604614	1.446839659
CYSTEAMINE HYDROCHLORIDE	0.792090135	0.198768868	0.144997854	1.30794725
FOSCARNET SODIUM	0.791814792	0.028328606	0.012497892	1.379700043
CARBIDOPA	0.79143457	0.268553404	0.232343229	1.03067122
GEMFIBROZIL	0.791144306	0.431043214	0.212563947	1.526800951
ACETARSOL	0.790921179	0.252306102	0.225156536	1.283816437
TOLNAFTATE	0.790620563	0.081676857	0.004182235	1.655897092
PREDNISOLONE SODIUM PHOSPHATE	0.789401459	0.225506146	0.116208598	1.216380119
BENZOCLIDINE	0.788831849	0.388827031	0.278361675	1.021066437
EPRODISATE DISODIUM	0.787952972	0.221263223	0.109851542	1.428437809
DIAVERIDINE	0.787377439	0.065940927	0.184292205	1.597089846
CROTAMITON	0.786046569	0.110224152	0.187962688	1.213142612
TRIAMCINOLONE ACETONIDE	0.786004882	0.161872756	0.090183708	1.449982734
ASCORBYL PALMITATE	0.785730031	0.185237604	0.204276647	1.408497205
d-LIMONENE	0.785439554	0.111626885	0.175053768	1.073998081
PROCAINE HYDROCHLORIDE	0.783839233	0.131820198	0.107593299	1.522707232
LEVODOPA	0.782898666	0.301012825	0.062020168	1.532663596
MECYSTEINE HYDROCHLORIDE	0.782817892	0.215955266	0.285575194	1.678830616
MONTELUKAST SODIUM	0.781706813	0.125216949	0.1068387	0.96498856
CYTARABINE	0.780578036	0.19621788	0.113153888	0.81595583
TRICHLORMETHIAZIDE	0.779338103	0.246344212	0.112493754	1.398751572
PROTIONAMIDE	0.778956953	0.048952372	0.052759481	1.202076623
METHAZOLAMIDE	0.777321902	0.05865823	0.055442002	1.547168454
TIRATRICOL	0.776735699	0.101342995	0.158035993	1.183235813
IRINOTECAN HYDROCHLORIDE	0.774319866	0.341918617	0.228068513	0.906087508
UREA	0.773013389	0.13086742	0.067050537	1.703103858
PHENYLMERCURIC ACETATE	0.772308611	0.186292805	0.031608249	0.084018667
ORBIFLOXACIN	0.771821179	0.059881314	0.239160481	1.153278583
ALISKIREN HEMIFUMARATE	0.770540411	0.138231039	0.064230202	0.987424023
BENZOCAINE	0.770062623	0.014317383	0.018623553	0.958695526
ITOPRIDE HYDROCHLORIDE	0.768356262	0.205254184	0.254147364	1.521713889
TRANEXAMIC ACID	0.767441639	0.145560927	0.162015046	2.05552886
FENACLON	0.767266123	0.170615987	0.156579743	1.042224817
GATIFLOXACIN	0.767009928	0.133964983	0.089720418	1.125774893
WARFARIN	0.766724786	0.018357478	0.009230035	1.256479586
ATENOLOL	0.766320068	0.30712267	0.08507776	0.9894169
CHLOROXYLENOL	0.765618789	0.148846719	0.080371067	1.223075009
NABUMETONE	0.764282985	0.138403791	0.056508248	1.406258545
NAPROXEN(+)	0.763267024	0.126667917	0.024421622	1.375954131
FUROSEMIDE	0.762084321	0.539893452	0.225970286	1.687219069
DEXAMETHASONE SODIUM PHOSPHATE	0.762062628	0.028230112	0.060207322	1.379128116
FORMESTANE	0.759260093	0.152023074	0.139996575	1.55656524
NALTREXONE HYDROCHLORIDE	0.757786237	0.179700744	0.060595051	1.657787159
CHLORAMINE-T	0.757675378	0.018627578	0.211436396	1.072803388
MILTEFOSINE	0.757042378	0.302345121	0.258043898	1.312474801
TRIFLURIDINE	0.755402228	0.257218269	0.111728595	1.099953455
THYMOPENTIN	0.755391936	0.213186868	0.065211683	0.994093426
MELPHALAN	0.753685176	0.390073786	0.112923775	1.270180436
CARMOFUR	0.753375973	0.04505991	0.033991679	1.27769623
CARGLUMIC ACID	0.753217277	0.112341915	0.124196589	1.05829178
METAPROTERENOL	0.753162114	0.038173771	0.012989674	1.450781164
METHOXSALEN	0.751636811	0.38739635	0.120606953	1.443187889
ALAPROCLATE	0.7480137	0.25188193	0.073525815	1.366615838
NICORANDIL	0.745126004	0.078536417	0.104934207	0.978715802
FLUMETHAZONE PIVALATE	0.744386625	0.36308158	0.099371014	1.26618459
RACECADOTRIL	0.740548882	0.080120748	0.104151358	1.000314037
PHENYTOIN SODIUM	0.740323295	0.02727998	0.157714469	1.315017826
MIGLITOL	0.739208693	0.168376172	0.068380119	1.003397801
TRIMETHOBENZAMIDE HYDROCHLORIDE	0.73884198	0.077549343	0.000916597	1.923166355
HYDROCORTISONE BUTYRATE	0.738149115	0.198772967	0.04968396	1.723705592
FASUDIL HYDROCHLORIDE	0.73648055	0.082331693	0.095455135	0.913591094
CLOFARABINE	0.728508615	0.328948682	0.058643745	1.237582213
ENOXOLONE	0.728226972	0.21519678	0.044683102	1.037766
MEPARFYLON	0.726402383	0.057603472	0.086993691	1.003802034
OXOLAMINE CITRATE	0.723168968	0.088891329	0.161996897	1.467353827
OMEPRAZOLE	0.721479709	0.131066262	0.141107195	1.709955607
SODIUM NITROPRUSSIDE	0.721287204	0.075942606	0.041987909	1.208586346
CARNITINE (dl) HYDROCHLORIDE	0.720351589	0.053353943	0.077084312	1.08926939
DINITOLMIDE	0.712694219	0.103202949	0.078181634	1.063414044
DYPHYLLINE	0.712273528	0.046850846	0.028918464	1.148288775

REBAMIPIDE	0.712004419	0.258225898	0.103314467	0.958736391
LOFEXIDINE HYDROCHLORIDE	0.711327218	0.077175124	0.082429258	1.221104463
URSODIOL	0.710275025	0.097622813	0.02241185	1.617892899
PROPOXYCAINE HYDROCHLORIDE	0.705139321	0.146751069	0.009472484	1.309529174
BUMETANIDE	0.702114558	0.418670938	0.093530164	1.676241802
VECURONIUM BROMIDE	0.701296798	0.149889949	0.023304478	0.952574918
SOLIFENACIN SUCCINATE	0.696992714	0.138493137	0.007605051	1.411974451
D-PHENYLALANINE	0.696348228	0.10697016	0.015720439	1.233842419
BENZOXIQUINE	0.695837373	0.068104006	0.028731522	0.861428252
NOMIFENSINE MALEATE	0.695105408	0.067256981	0.142037516	1.172769059
ACEDOBEN	0.693566725	0.178407889	0.069445281	1.283909956
BROXYQUINOLINE	0.693560601	0.176822598	0.07234842	0.826244102
SULFACARBAMIDE	0.691967748	0.068254028	0.059009652	0.990043438
DULOXETINE HYDROCHLORIDE	0.688669351	0.085693938	0.026904258	1.21120575
SALINOMYCIN, SODIUM	0.688120168	0.157880473	0.127079903	1.65168618
ACENEURAMIC ACID	0.685837149	0.024571687	0.114257669	1.381196773
FEXOFENADINE HYDROCHLORIDE	0.679929238	0.199503671	0.03534053	1.190401777
SULFAMETHOXYPYRIDAZINE	0.678320221	0.104550796	0.059043918	1.456825405
CHLORMIDAZOLE	0.677200632	0.083241173	0.108391757	1.604676924
PYRVINIUM PAMOATE	0.672698684	0.072142283	0.019497124	1.939314524
OCTOCRYLENE	0.672142872	0.229398278	0.062939052	1.294284966
CHLORINDIONE	0.670629801	0.177188985	0.053596125	1.234058765
NEFAZODONE HYDROCHLORIDE	0.670455262	0.133748482	0.056790058	1.114696998
SULFADIMETHOXINE	0.66705183	0.204829934	0.063969865	1.193830278
DEXLANSOPRAZOLE	0.661462278	0.172561912	0.005480651	1.441651758
ISOBUTAMBEN	0.660027267	0.19154272	0.006451359	0.352038776
ERGONOVINE MALEATE	0.659779678	0.471708888	0.062500401	1.746312543
SULFAMONOMETHOXINE	0.656107552	0.046260352	0.043001919	1.234977592
BEPHENIUM HYDROXYNAPTHOATE	0.655623433	0.061580658	0.101732238	1.145613769
COUMOPHOS	0.652143804	0.26257175	0.058841475	1.754030752
RETINYL ACETATE	0.645236639	0.166508464	0.009678447	1.31155368
CAPECITABINE	0.636477298	0.025188871	0.033873729	1.513330556
TRIFLUOPERAZINE HYDROCHLORIDE	0.635247597	0.297632796	0.023207105	1.715323123
DOCETAXEL	0.63094696	0.049806212	0.032283737	1.567842204
METYRAPONE	0.625769518	0.080304493	0.027505679	1.065839148
LEVOTHYROXINE	0.621420434	0.172700299	0.013643713	1.514259411
COLFORSIN	0.61128351	0.159753035	0.005982498	2.360281253
IBANDRONATE SODIUM	0.601897526	0.074631211	0.000796546	1.138459051
MESALAMINE	0.58992983	0.073967875	0.002699096	1.555896935
ZOLMITRIPTAN	0.576456934	0.083963054	0.017986088	1.451961846
BROXALDINE	0.575683393	0.124767207	0.044918954	0.917280453
SPIPERONE	0.566409261	0.050398007	9.80149E-05	0.95172571
ANCITABINE HYDROCHLORIDE	0.543970225	0.01733977	0.008998047	0.866920358
BURAMATE	0.539563671	0.054007375	0.004642774	1.01416341
TRICLOSAN	0.516770857	0.146135334	0.001456693	1.003406882
TRETINOIN	0.516012049	0.079280292	0.030139014	1.229501748
LIOTHYRONINE (L- isomer) SODIUM	0.511877182	0.144803425	0.000121932	1.287246541
OXIBENDAZOLE	0.499023992	0.146291147	0.001068079	3.974572354
TRIAMTERENE	0.489763545	0.246554611	0.00243009	1.848366525
TETRACAINE HYDROCHLORIDE	0.486654776	0.025880773	0.001288614	1.535695975
ESOMEPRAZOLE POTASSIUM	0.465027851	0.051306948	0.010563125	1.328084433
DOCOSANOL	0.448609489	0.05960253	0.004079645	2.749552856
CINROMIDE	0.444429597	0.050439909	0.000849926	1.25856418
NIFUROXAZIDE	0.442503838	0.064617066	0.012130346	1.77583017
CHLORAZANIL HYDROCHLORIDE	0.416876135	0.097563891	0.009924319	1.049481206
SALICYLANILIDE	0.416378103	0.048814897	6.86769E-07	0.515732301
beta-NAPHTHOL	0.414653766	0.169300991	0.011089776	1.043760508
INDOPROFEN	0.389718994	0.741739767	0.028550397	1.680445955
ABACAVIR SULFATE	0.376905954	0.225632148	0.000147952	1.124916899
EPIRUBICIN HYDROCHLORIDE	0.376371119	0.354020104	0.001711687	0.071879464
LIOTHYRONINE	0.371394723	0.092289234	7.78983E-07	1.394216971
ALBENDAZOLE	0.360938647	0.075955602	0.000125593	3.649616415
HEXETIDINE	0.331255576	0.20285006	0.00018766	0.05505182
SEMUSTINE	0.325258744	0.222711117	0.000236576	1.594468399
SANGUINARINE SULFATE	0.317377073	0.263423562	0.000123897	1.625130308
DIFLUNISAL	0.284796616	0.116471704	0.000115913	1.153925612
NIFURSOL	0.279129461	0.128613218	5.02812E-06	1.087063566
THIABENDAZOLE	0.278334151	0.013700933	1.64423E-06	0.649239346
MEBENDAZOLE	0.274401842	0.175616745	2.01709E-05	2.980830602
LEFLUNOMIDE	0.243229498	0.054202967	0.001263113	1.096543994
MELOXICAM SODIUM	0.242457506	0.091955777	9.1064E-05	1.397485554
PHENAZOPYRIDINE HYDROCHLORIDE	0.234299155	0.103053254	0.001261914	0.321139386

TOLONIUM CHLORIDE	0.227776552	0.036125539	1.62411E-05	0.571313178
PHENELZINE SULFATE	0.212324693	0.094927603	0.00101919	1.624715936
MEPHENTERMINE SULFATE	0.209005935	0.097092465	2.037E-05	1.726746216
ANISINDIONE	0.205557894	0.010025995	8.84425E-05	0.891600635
PIPERINE	0.172792954	0.180410706	3.30393E-05	1.187851515
NIFLUMIC ACID	0.165075091	0.068518639	9.33816E-06	0.939680038
BROMINDIONE	0.159500399	0.120101966	1.55062E-05	1.163377248
IPRIFLAVONE	0.153528274	0.173412252	1.96009E-05	0.934820563
NITAZOXANIDE	0.145469691	0.115092872	3.77956E-05	0.399063421
EXALAMIDE	0.141933212	0.049918983	6.73557E-06	1.54032908
HYDRALAZINE HYDROCHLORIDE	0.138763231	0.781757707	0.006253376	1.521085027
TRANILAST	0.138060212	0.082439945	3.10791E-07	1.404364371
DICUMAROL	0.121070953	0.029185856	1.4317E-05	1.15622099
NAFCILLIN SODIUM	0.096472104	0.044070947	4.81641E-06	1.981133344
FEBUXOSTAT	0.083987719	0.023669527	2.72254E-05	1.193105491
METHYLENE BLUE	0.015467107	0.012883039	2.28006E-06	0.81696441
FLUFENAMIC ACID	-0.028087744	0.169182945	8.02884E-07	1.18307401
TENATOPRAZOLE	-0.048159476	0.110107952	2.79489E-05	1.347244967
NICLOSAMIDE	-0.060898972	0.047859798	1.13322E-06	0.471417873
TENYLIDONE	-0.062036818	0.129179601	3.05585E-05	1.152349514

Supplementary Table 3. List of 14 candidate NMD enhancers identified in the high-throughput compound screen that passed quartile analysis.

Compound (10μM)	CBR:CBG Ratio (Relative to DMSO)	P-value
Methylene Blue	0.02	2.28×10^{-6}
Febuxostat	0.08	2.75×10^{-5}
Nafcillin Sodium	0.10	4.82×10^{-6}
Dicumarol	0.12	1.43×10^{-5}
Tranilast	0.14	3.11×10^{-7}
Exalamide	0.14	6.74×10^{-6}
Nitazoxanide	0.15	3.78×10^{-5}
Ipriflavone	0.15	1.96×10^{-5}
Bromindione	0.16	1.55×10^{-5}
Niflumic Acid	0.17	9.34×10^{-6}
Piperine	0.17	3.30×10^{-5}
Anisindione	0.21	8.84×10^{-5}
Mephentermine Sulfate	0.21	2.04×10^{-5}
Phenelzine Sulfate	0.21	1.02×10^{-3}

Supplementary Table 4. Sequences of qPCR Primers.

Name	Sequence
CBG99-F	ATGCTCTCGATCCACGCGTG
CBG99-R	CGAGAGAGTGAATGTTAGCG
CBR-F	TCCATGCTTTCGGCTTTCAT
CBR-R	CGAGAGTCTGGATAATCGCA
p53-F	GAGGTTGGCTCTGACTGTACC
p53-R	TCCGTCCCAGTAGATTACCAC
UPP1-F	CCAGCCTTGTTTGGAGATGT
UPP1-R	ACATGGCATAGCGGTCAGTT
ATF4-F	ATGTCCCCCTTCGACCA
ATF4-R	CCATTTTCTCCAACATCCAATC
Pim3-F	GCACCGCGACATTAAGGAC
Pim3-R	TCCCCACACACCATATCGTAG
Pisd-F	TCCCTGATGTCAGTGAACCCT
Pisd-R	TGGTGTGCGTCACGAAGC
ORCL-F	GGCAGCAGATGAAATCTGAA
ORCL-R	TCCAGAATGTGATTTTTGCAG
UPF1-F	CCCTCCAGAATGGTGTCACT
UPF1-R	CTTCAGCAACTTCGTGGTGA
UPF2-F	CAGGAAGAAGTTGGTACGGG
UPF2-R	ACATGCAGGGATGCAATGTA
UPF3b-F	TTTTGTTCAGGGATCGCTTT
UPF3b-R	GCTTTTTGAAAAGGTGCAAAT
SMG1-F	CTGGCAACCCAGAACTGATAG
SMG1-R	TGTAGCCACCCTTTTCGTCAT
SMG5-F	CAGTCTGAGCAGGAGAGCCT
SMG5-R	TGAAGTCGTAGCTGAGCCAT
SMG6-F	CTCTCCCATTGGAAGTACCCG
SMG6-R	CGGCGGACCAGTAGAGAAAAC
SMG7-F	CTCTGGAATCACGCCTTTAAGAA
SMG7-R	CTTCACACGGCATGGTAAATCT
GAPDH-F	CCTGTTCGACAGTCAGCCG
GAPDH-R	CGACCAAATCCGTTGACTCC

2.8 References

1) Kervestin, S. & Jacobson, A. NMD: a multifaceted response to premature translational termination. Nat Rev Mol Cell Biol 13, 700-712 (2012).

2) Schoenberg, D.R. & Maquat, L.E. Regulation of cytoplasmic mRNA decay. Nat Rev Genet 13, 246-259 (2012).

3) Bruno, I.G., Karam, R., Huang, L., Bhardwaj, A., Lou, C.H., Shum, E.Y., Song. H.W., Corbett, M.A., Gifford, W.D., Gecz, J., Pfaff, S.L. & Wilkinson, M.F. Identification of a microRNA that activates gene expression by repressing nonsense-mediated RNA decay. Mol Cell. 42, 500-510 (2011).

4) Gardner, L.B. Nonsense-mediated RNA decay regulation by cellular stress: implications for tumorigenesis. Mol Cancer Res 8, 295-308 (2010).

5) Frischmeyer, P.A. & Dietz, H.C. Nonsense-mediated mRNA decay in health and disease. Hum Mol Genet 8, 1893-1900 (1999).

6) Ellis, M.J., Ding, L., Shen, D., Luo, J., Suman, V.J., Wallis, J.W., Van Tine, B.A., Hoog, J., Goiffon, R.J., Golstein, T.C., Ng, S., Lin, L., Crowder, R., Snider, J., Ballman, K., Weber, J., Chen, K., Koboldt, D.C., Kandoth, C., Schierding, W.S., McMichael, J.F., Miller, C.A., Lu, C., Harris, C.C., McLellan, M.D., Wendl, M.C., DeSchryver, K., Allred, D.C., Esserman, L., Unzeitig, G., Margenthaler, J., Babiera, G.V., Marcom, P.K., Guenther, J.M., Leitch, M., Hunt, K., Olson, J., Tao, Y., Maher, C.A., Fulton, L.L., Fulton, R.S., Harrison, M., Oberkfell, B., Du, F., Demeter, R., Vickery, T.L., Elhammali, A., Piwnica-Worms, H., McDonald, S., Watson, M., Dooling, D.J., Ota, D., Chang, L.W., Bose, R., Ley, T.J., Piwnica-Worms, D., Stuart, J.M., Wilson, R.K. & Mardis, E.R. Whole-genome analysis informs breast cancer response to aromatase inhibition. Nature 486, 353-360 (2012).

7) Holbrook, J.A., Neu-Yilik, G., Hentze, M.W. & Kulozik, A.E. Nonsense-mediated decay approaches the clinic. Nat Genet 36, 801-808 (2004).

8) Kuzmiak, H.A. & Maquat, L.E. Applying nonsense-mediated mRNA decay research to the clinic: progress and challenges. Trends Mol Med 12, 306-316 (2006).

9) Gudikote, J.P. & Wilkinson, M.F. T-cell receptor sequences that elicit strong down-regulation of premature termination codon-bearing transcripts. EMBO J 21, 125-134 (2002).

10) Paillusson, A., Hirschi, N., Vallan, C., Azzalin, C.M. & Muhlemann, O. A GFP-based reporter system to monitor nonsense-mediated mRNA decay. Nucleic Acids Res 33, e54 (2005).

11) Gammon, S.T., Leevy, W.M., Gross, S., Gokel, G.W. & Piwnica-Worms, D. Spectral unmixing of multicolored bioluminescence emitted from heterogeneous biological sources. Anal Chem 78, 1520-1527 (2006).

12) Zhang, X.D., Yang, X.C., Chung, N., Gates, A., Stec, E., Kunapuli, P., Holder, D.J., Ferrer, M. & Espeseth, A.S. Robust statistical methods for hit selection in RNA interference high-throughput screening experiments. Pharmacogenomics 7, 299-309 (2006).

13) Prassas, I. & Diamandis, E.P. Novel therapeutic applications of cardiac glycosides. Nat Rev Drug Discov 7, 926-935 (2008).

14) Brumbaugh, K.M., Otterness, D.M., Geisen, C., Oliveira, V., Brognard, J., Li, X., Lejeune, F., Tibbetts, R.S., Maquat, L.E. & Abraham, R.T. The mRNA surveillance protein hSMG-1 functions in genotoxic stress response pathways in mammalian cells. Mol Cell 14, 585-598 (2004).

15) Yamashita, A., Ohnishi, T., Kashima, I., Taya, Y. & Ohno, S. Human SMG-1, a novel phosphatidylinositol 3-kinase-related protein kinase, associates with components of the mRNA surveillance complex and is involved in the regulation of nonsense-mediated mRNA decay. Genes Dev 15, 2215-2228 (2001).

16) Mendell, J.T., Sharifi, N.A., Meyers, J.L., Martinez-Murillo, F. & Dietz, H.C. Nonsense surveillance regulates expression of diverse classes of mammalian transcripts and mutes genomic noise. Nat Genet 36, 1073-1078 (2004).

17) Gardner, L.B. Hypoxic inhibition of nonsense-mediated RNA decay regulates gene expression and the integrated stress response. Mol Cell Biol 28, 3729-3741 (2008).

18) Wang, D., Wengrod, J. & Gardner, L.B. Overexpression of the c-myc oncogene inhibits nonsense-mediated RNA decay in B lymphocytes. J Biol Chem 286, 40038-40043 (2011).

19) Hu, J., Li, Y. & Li, P. MARVELD1 Inhibits Nonsense-Mediated RNA Decay by Repressing Serine Phosphorylation of UPF1. PLoS One 8, e68291 (2013).

20) Huang, L., Lou, C.H., Chan, W., Shum, E.Y., Shao, A., Stone, E., Karam, R., Song, H.W. & Wilkinson, M.F. RNA homeostasis governed by cell type-specific and branched feedback loops acting on NMD. Mol. Cell 43, 950–961 (2011).

21) Yepiskoposyan, H., Aeschimann, F., Nilsson, D., Okoniewski, M. & Muhlemann, O. Autoregulation of the nonsense-mediated mRNA decay pathway in human cells. RNA 17, 2108-2118 (2011).

22) Dostanic-Larson, I., Van Huysse, J.W., Lorenz, J.N. & Lingrel, J.B. The highly conserved

cardiac glycoside binding site of Na,K-ATPase plays a role in blood pressure regulation. Proc Natl Acad Sci USA 102, 15845-15850 (2005).

23) Lingrel, J.B. The physiological significance of the cardiotonic steroid/ouabain-binding site of the Na,K-ATPase. Annu Rev Physiol 72, 395-412 (2010).

24) Ye, J., Chen, S. & Maniatis, T. Cardiac glycosides are potent inhibitors of interferon-beta gene expression. Nat Chem Biol 7, 25-33 (2011).

25) Johansson, M.J. & Jacobson, A. Nonsense-mediated mRNA decay maintains translational fidelity by limiting magnesium uptake. Genes Dev 24, 1491-1495 (2010).

26) Menger, L., Vacchelli, E., Adjemian, S., Martins, I., Ma, Y., Shen, S., Yamazaki, T., Sukkurwala, A.Q., Michaud, M., Mignot, G., Schlemmer, F., Sulpice, E., Locher, C., Gidrol, X., Ghiringhelli, F., Modjtahedi, N., Galluzzi, L., André, F., Zitvogel, L., Kepp, O. & Kroemer, G. Cardiac glycosides exert anticancer effects by inducing immunogenic cell death. Sci Transl Med 4, 143ra199 (2012).

27) Pastor, F., Kolonias, D., Giangrande, P.H. & Gilboa, E. Induction of tumour immunity by targeted inhibition of nonsense-mediated mRNA decay. Nature 465, 227-230 (2010).

28) Colak, D., Ji, S.J., Porse, B.T. & Jaffrey, S.R. Regulation of axon guidance by compartmentalized nonsense-mediated mRNA decay. Cell 153, 1252-1265 (2013).

29) Giorgi, C., Yeo, G.W., Stone, M.E., Katz, D.B., Burge, C., Turrigiano, G. & Moore, M.J. The EJC factor eIF4AIII modulates synaptic strength and neuronal protein expression. Cell. 130, 179-191 (2007).

30) Long, A.A., Mahapatra, C.T., Woodruff, E.A., Rohrbough, J., Leung, H.T., Shino, S., An, L., Doerge, R.W., Metzstein, M.M., Pak, W.L. & Broadie, K. The nonsense-mediated decay pathway maintains synapse architecture and synaptic vesicle cycle efficacy. J Cell Sci. 123, 3303-3315 (2010).

31) Mcllwain, D.R., Pan, Q., Reilly, P.T., Elia, A.J., McCracken, S., Wakeham, A.C., Itie-Youten, A., Blencowe, B.J. & Mak, T.W. Smg1 is required for embryogenesis and regulates diverse genes via alternative splicing coupled to nonsense-mediated mRNA decay. Proc Natl Acad Sci U S A 107, 12186-12191 (2010).

32) Tarpey, P.S., Raymond, F.L., Nguyen, L.S., Rodriguez, J., Hackett, A., Vandeleur, L., Smith, R., Shoulbridge, C., Edkins, S., Stevens, C., O'Meara, S., Tofts, C., Barthorpe, S., Buck, G., Cole, J., Halliday, K., Hills, K., Jones, D., Mironenko, T., Perry, J., Varian, J., West, S., Widaa, S., Teague, J., Dicks, E., Butler, A., Menzies, A., Richardson, D., Jenkinson, A., Shepherd, R., Raine, K., Moon, J., Luo, Y., Parnau, J., Bhat, S., Gardner, A., Corbett, M., Brooks, D.,

Thomas, P., Parkinson-Lawrence, E., Porteous, M., Warner, J., Sanderson, T., Pearson, P., Simensen, R., Skinner, C., Hoganson, G., Superneau, D., Wooster, R., Bobrow, M., Turner, G., Stevenson, R., Schwartz, C., Futreal, P., Srivastava, A., Stratton, M. & Gecz, J. Mutations in UPF3B, a member of the nonsense-mediated mRNA decay complex, cause syndromic and nonsyndromic mental retardation. Nat Genet. 39, 1127-1133 (2007).

33) Wong, J.J., Ritchie, W., Ebner, O.A., Selbach, M., Wong, J.W., Huang, Y., Gao, D., Pinello, N., Gonzalez, M., Baidya, K., Thoeng, A., Khoo, T.L., Bailey, C.G., Holst, J. & Rasko, J.E. Orchestrated intron retention regulates normal granulocyte differentiation. Cell 154, 583-595 (2013).

34) Eom, T., Zhang, C., Wang, H., Lay, K., Fak, J., Noebels, J.L. & Darnell, R.B. NOVA-dependent regulation of cryptic NMD exons controls synaptic protein levels after seizure. Elife. 2, e00178 (2013).

35) You, Z., Shi, L.Z. Zhu, Q., Wu, P., Zhang, Y.W., Basilio, A., Tonnu, N., Verma, I.M., Berns, M.W. & Hunter, T. CtIP links DNA double-strand break sensing to resection. Mol Cell 36, 954-969 (2009).

36) Gross, S. & Piwnica-Worms, D. Real-time imaging of ligand-induced IKK activation in intact cells and in living mice. Nat Methods 2, 607-614 (2005).

37) You, Z., Bailis, J.M., Johnson, S.A., Dilworth, S.M. & Hunter, T. Rapid activation of ATM on DNA flanking double-strand breaks. Nat Cell Biol 9, 1311-1318 (2007).

38) Chen, X., Paudyal, S.C., Chin, R.I. & You, Z. PCNA promotes processive DNA end resection by Exo1. Nucleic Acids Res 41, 9325-9338 (2013).

39) Nociari, M.M., Shalev, A., Benias, P. & Russo, C. A novel one-step, highly sensitive fluorometric assay to evaluate cell-mediated cytotoxicity. J Immunol Methods 213, 157-167 (1998).

Chapter 3: Regulation of NMD by persistent DNA damage

Preface

The following work was performed by me, Zhongsheng You, Abigael Cheruiyot, Kevin Flanagan, Sheila Stewart, and David Piwnica-Worms. I designed and performed all experiments and wrote the manuscript. A.C. ran western blots and provided valuable feedback. K.F. and S.S. provided reagents, protocols, and critical feedback. D.P.W. provided critical feedback. Z.Y. conceived and supervised the study and wrote the manuscript.

This chapter is a reproduction of a pre-copyedited, author-produced PDF of an article submitted for publication in eLife in October 2016.

We thank Dr. Tatiana Efimova (George Washington University) for providing LacZ and MKK6-CA-expressing adenovirus and Shankar Parajuli for technical assistance. This study was supported by a NIH grant (R01GM098535 to Z.Y), an American Cancer Society Research Scholar Grant (RSG-13-212-01-DMC to Z.Y.) and an Interdisciplinary Research Initiative grant from the Children's Discovery Institute of Washington University (MC-II-2012-215 to Z.Y.).

3.1 Abstract

Persistent DNA damage in non-cycling cells can induce senescence and profound gene expression alterations, which in turn influence tissue homeostasis, tumorigenesis, and the efficacy of a broad range of cancer therapeutics. However, the molecular basis of the persistent DNA damage response and the mechanisms that control gene expression remain poorly understood. Here we report that persistent DNA damage inhibits nonsense-mediated RNA decay (NMD)—an RNA degradation pathway that controls gene expression in addition to its role in eliminating faulty transcripts. In contrast to persistent DNA damage, transient DNA damage does not affect NMD activity. We also find that NMD inhibition by persistent DNA damage appears to be independent of cellular senescence. Furthermore, we find that NMD suppression by persistent DNA damage requires the activity of p38 MAP kinase, although p38 activation alone is not sufficient to suppress NMD. Lastly, we find that ATF3, an NMD target and a key stress-inducible transcription factor, is stabilized in a p38- and NMD-dependent manner following persistent DNA damage. Our results reveal a novel p38-dependent pathway that regulates NMD activity in response to persistent DNA damage, which in turn contributes to gene expression reprogramming in inflicted cells.

3.2 Introduction

Nonsense-mediated RNA decay (NMD) was originally identified as an RNA quality control pathway that detects and degrades aberrant mRNAs with premature translation termination codons (PTCs) that are often caused by genetic mutations, inaccurate transcription, or mis-splicing[1,2]. By eliminating these abnormal mRNAs, NMD mitigates the effects of potentially deleterious truncated proteins and preserves cellular homeostasis. However, more

recent studies have revealed a second function of NMD as a regulator of normal transcripts that contain features recognizable to the NMD machinery such as upstream open reading frames (uORFs), 3' UTR introns, alternative splice variants that introduce a PTC, or exceedingly long 3' UTRs[2-4]. By regulating the stability of transcripts bearing such NMD-inducing features, NMD contributes to gene expression profiles important for development and other cellular processes[5-14]. For instance, in commissural neurons, NMD limits expression of Robo 3.2 to ensure proper axonal migration[6]. Additionally, expression of many synaptic proteins is controlled by alternative splicing (AS)-coupled NMD; neuronal activity influences the retention of cryptic PTC-containing exons in these transcripts that mark them for degradation via NMD[7]. Expression of the SR and hnRNP families of splicing regulators is controlled in a similar manner[15,16]. Alternative splicing of the transcripts encoding these factors—which in turn regulate the splicing of many transcripts, including their own—induces NMD and, consequently, maintains the proper levels of these RNA binding proteins[15,16].

In addition to "constitutively" degrading target mRNAs to control cellular function and homeostasis, NMD also contributes to gene expression changes in response to developmental and environmental cues that adjust NMD efficiency. Although a significant number of genes are regulated by NMD, the current understanding of how the cellular milieu influences NMD activity is limited to a few mechanisms and biological settings. For instance, differentiating neurons express miR-128, which targets NMD factor mRNAs and enhances the expression of neuron-specific NMD target transcripts[5]. During myogensis NMD activity diminishes as a competing RNA decay pathway, Staufen-mediated decay, becomes more dominant, resulting in elevated expression of NMD target transcripts such as myogenin[10]. These alterations of NMD

activity appear to be essential in vertebrates as many NMD deficient mutants exhibit abnormal brain, eye, and cardiovascular development and are lethal[17]. In addition to controlling gene expression during development, NMD helps coordinate the cellular response to several forms of stress—including amino acid deprivation, hypoxia, and ER stress—by governing the expression levels of many stress response genes via a mechanism involving eukaryotic initiation factor 2α (eIF2α) phosphorylation[8,11,13,14,18]. Finally, when proliferating cells are exposed to severe stresses that cause apoptosis, caspases cleave UPF1, a core NMD factor, leading to NMD attenuation and upregulation of several apoptosis genes[19]. Despite these major advances, our understanding of the physiological role of NMD is still limited, and the function and regulation of NMD remain to be explored in other contexts.

DNA damage is a common cellular stress with tens of thousands of DNA lesions occurring daily in each human cell[20]. Although in most cases these lesions can be efficiently repaired, DNA damage can sometimes persist in nonproliferating cells. Persistent DNA damage can arise from a variety of sources. For example, persistent DNA damage often occurs at telomeres where damage is particularly difficult to repair, and because progressive telomere erosion from repeated cell divisions elicits a protracted DNA damage response (DDR)[21-26]. Additionally, conditions that prevent efficient DNA repair, such as mutations in DNA repair genes, or that constantly induce damage, such as excessive mitogenic signals, are capable of eliciting a persistent DDR[27-32]. Finally, common cancer treatments such as radiation and chemotherapy induce persistent DNA damage[33-35]. The persistent DDR induced by these conditions influences tissue homeostasis, tumorigenesis, and cancer treatment outcome[36-39]. One prominent aspect of the persistent DNA damage response is cellular senescence, which is characterized by a permanent exit from the cell

cycle and profound changes in morphology, signaling, and gene expression[38,40-43]. In certain contexts where persistent DNA damage is present, including cells experiencing excessive mitogenic signals or telomere erosion, p38 can promote cellular senescence[44-49]. Additionally, p38 drives the expression of the senescence associated secretory phenotype (SASP)—a collection of secreted factors such as cytokines, chemokines, growth factors, and proteases produced in cells harboring persistent DNA damage[50-53]. Both senescence and the SASP influence the tumorigenic process and cancer treatment outcome by influencing tumor cell growth and by modifying the tumor microenvironment[36,37,51,52,54-59]. Another important player of the persistent DDR is the transcription factor ATF3, whose mRNAs are targeted by NMD due to alternative splicing[8,13]. Like p38, ATF3 can suppress tumorigenesis by promoting senescence in response to genotoxic stress but paradoxically can also establish a largely pro-tumorigenic microenvironment by altering the expression of secreted factors[60-63]. In addition to persistent DNA damage, p38 is also involved in the cellular responses to other forms of stress, such as osmotic shock, and induces dramatic gene expression changes[64-68]. Despite the recognition of the importance of the gene expression alterations following cellular stresses, the underlying molecular mechanisms remain poorly understood. In this paper we investigated the regulation and role of the NMD pathway in the cellular response to persistent DNA damage. Using a highly effective bioluminescent NMD reporter system, we found that NMD activity is attenuated by persistent DNA damage, leading to stabilization of ATF3 transcripts. This repression of NMD is mediated in part by p38, although p38 activation alone is not sufficient to inhibit NMD. Our results reveal a novel p38-dependent pathway that regulates NMD activity specifically in response to persistent DNA damage which contributes to gene expression alterations in non-

cycling cells.

3.3 Results

3.3.1 Persistent DNA damage, but not transient DNA damage, inhibits NMD in non-cycling cells

To determine whether DNA damage modulates NMD activity, we treated confluent nontransformed human RPE1 cells with the DNA damaging cancer drug bleomycin (63 μg/ml) for 24 hours. Immediately after treatment, we assessed NMD activity using a bioluminescent NMD reporter system that we developed previously[69]. Using this reporter, NMD is quantified by the ratio of red bioluminescence signal, produced by the CBR luciferase fused to the a PTC-containing TCRβ minigene (CBR-TCR(PTC)), to green bioluminescence signal, produced by the CBG luciferase fused to a wild type TCRβ minigene (CBG-TCR(WT)). As expected, bleomycin generated significant amounts of DNA damage and induced a robust DDR, as indicated by the phosphorylation of the histone variant H2AX (γH2AX), a widely used DDR marker (Fig. 1a; Fig. S1a). A similar level of NMD activity was detected in bleomycin-treated and H_2O-treated (control) cells, indicating that NMD activity is not altered immediately after DNA damage (Fig. 1a). However, when the damaged RPE1 cells were allowed to recover from the 24 hour bleomycin treatment for four days before NMD analysis, bleomycin-treated cells exhibited an approximately 2-fold reduction in NMD activity (Fig. 1b, left panel). The DNA damage was not yet resolved at the time of NMD activity analysis, as indicated by γH2AX western blot signal and by γH2AX foci detected by immunofluorescence staining (Fig. 1b, left panel; Fig. S1b). This bioluminescence imaging result was corroborated by qPCR analysis of the mRNA levels of the CBR-TCR(PTC) and CBG-TCR(WT) reporters (Fig. 1b, right panel). Similar results were

obtained in confluent human BJ fibroblasts (Fig. 1c), indicating that bleomycin-mediated NMD suppression is not specific to RPE1 cells. Together, these data suggest that persistent DNA damage represses NMD.

We next determined whether a low level of transient DNA damage, which can be readily repaired, exerts a delayed effect on NMD activity or whether DNA damage must persist in order to induce NMD repression. To this end, RPE1 cells were treated for 1 hour with the same dose of bleomycin and allowed to recover for 3 hours (to detect an immediate response) or 5 days (to detect a delayed response). These conditions generated a robust DNA damage response initially but little or no DNA damage persisted to day 5 (γH2AX signal in Fig. 1d). In this setting, no difference in NMD efficiency was observed at either time-point (Fig. 1d), indicating that transient DNA damage does not affect NMD activity.

To further demonstrate that persistent DNA damage attenuates NMD activity, we used other methods to induce persistent DNA damage and examined NMD efficiency using our bioluminescent reporter. Continuous treatment of RPE1 cells with a low concentration (60 nM) of the topoisomerase I inhibitor camptothecin (CPT) for five days also diminished NMD activity (Fig. 1e). Similarly, exposing cells to high doses (10 Gy) of ionizing radiation (IR) 6 days prior to NMD analysis also resulted in NMD repression (Fig. 1f). In contrast, a 0.5 Gy dose of IR, which does not generate enough damage to persist for days, did not affect NMD activity (Fig. 1f). Taken together, these data strongly suggest that NMD is inhibited in response to persistent DNA damage in non-cycling human cells.

3.3.2 NMD repression is not a common feature of cellular senescence

Persistent DNA damage induces cellular senescence, which is accompanied by substantial

changes in cellular morphology, metabolism, and gene expression[38,40-43]. It is possible that the NMD attenuation caused by persistent DNA damage stems from the establishment of a senescent state rather than directly from DNA damage signaling. To determine whether NMD inhibition is a facet of the senescence phenotype—even in the absence of DNA damage—we induced senescence by infecting RPE1 cells with lentiviruses expressing the cell cycle inhibitor p16 and then measured NMD activity using our bioluminescent reporter. Similar to bleomycin treatment, p16 over-expression efficiently induced senescence, as indicated by flattened cellular morphology and positive senescence-associated β-galactosidase (SA-β-Gal) staining signal[40,43] (Fig. 2a and Fig. S1c). However, no DDR was induced by p16 overexpression as indicated by the lack of γH2AX signal in cells under the condition (Fig. 2b). In contrast to cells with persistent DNA damage, no significant changes in NMD activity were detected in p16-expressing senescent cells compared to the nonsenescent control cells expressing the empty vector (Fig. 2b). These results suggest that NMD repression is not an obligate consequence of cellular senescence; rather, NMD activity is directly influenced by signals emanating from persistent DNA lesions.

3.3.3 Persistent DNA damage inhibits NMD in a p38α-dependent manner

p38 is a key player in the cellular response to persistent DNA damage. Consistent with previous findings, bleomycin-treated RPE1 cells exhibited robust p38 activation and signaling, as evidenced by the increase in p38 phosphorylation at T180/Y182 and the phosphorylation of HSP27 at S82, a downstream target of p38[51] (Fig. 3a). Given its central role in persistent DDRs, we speculated that p38 mediates NMD suppression in cells with persistent DNA damage. To test this possibility, we depleted p38α, a major isoform of p38 in RPE1 cells, using a previously validated shRNA[70] (Fig. 3b). Cells were grown to confluence and then treated with bleomycin

for 24 hours. Four days after treatment, NMD activity was analyzed through reporter imaging. p38α-knockdown indeed significantly restored NMD activity in the presence of persistent DNA damage, albeit partially (Fig. 3c). In further support of the role of p38α as a mediator of NMD suppression, CDD111, a p38α-specific kinase inhibitor that prevents downstream p38 signaling but not phosphorylation of p38 itself, also partially restored NMD activity in the presence of persistent DNA damage (Fig. 3d). These results indicate that p38 is a novel regulator of NMD in response to persistent DNA damage. In addition, the requirement of p38 for NMD suppression further demonstrates that the effects of persistent DNA damage on NMD are not caused simply by an increase in the production of mutant mRNAs in the damaged cells that may overwhelm the NMD machinery.

3.3.4 p38 activation is not sufficient to inhibit NMD

p38 activation is sufficient to induce certain aspects of the persistent DNA damage response such as expression and maintenance of several SASP factors[51,53]. To determine whether p38 activation is also sufficient to attenuate NMD, we expressed a constitutively active version of MKK6 (MKK6-CA), an upstream kinase that directly phosphorylates and activates p38, in RPE1 cells, and then assessed NMD activity via reporter imaging. Cells were infected with adenoviruses expressing either LacZ (control) or MKK6-CA and incubated for 7 days to induce an extended period of p38 activation that mimics the prolonged p38 activation in cells harboring persistent DNA damage. MKK6-CA expression induced a level of p38 activation similar to that induced by bleomycin treatment; however, it failed to alter NMD activity (Fig. 3e-f; Fig. S2). Importantly, MKK6-CA expression had no effect on γH2AX levels (data not shown). These data suggest that p38 activation alone is insufficient to inhibit NMD and that a second signal induced

by persistent DNA damage is needed for NMD suppression.

In addition to DNA damage, p38 plays a crucial role in the cellular response to other stresses such as osmotic shock[64,66-68]. Since p38 mediates NMD inhibition in response to persistent DNA damage, we investigated whether osmotic stress also suppresses NMD, and if so, whether p38 is required for the suppression. RPE1 cells were exposed to hyperosmotic conditions by supplementing their growth medium with either 80 mM KCl or 275 mM sorbitol for 5 hours before analyzing NMD via reporter imaging. Interestingly, NMD was efficiently inhibited in the presence of KCl or sorbitol (Fig. S3a&d, S3b&e), suggesting that osmotic stress indeed suppresses NMD activity. However, this inhibition is independent of p38α. shRNA-mediated knockdown of p38α or inhibition of its kinase activity with CDD111 failed to reverse the inhibitory effects of osmotic shock on NMD, although p38α signaling was clearly abrogated, as indicated by the inhibition of HSP27 phosphorylation (Fig. S3a-f). Taken together, the results described above demonstrate that although both persistent DNA damage and osmotic stress activate p38, they inhibit NMD via distinct mechanisms.

3.3.5 ATF3 mRNA is stabilized by persistent DNA damage in a p38α- and NMD-dependent manner

In addition to RNA quality control, NMD also controls gene expression by degrading many normal endogenous transcripts that possess NMD-inducing features (e.g. uORFs, 3' UTR introns, alternatively spliced variants, long 3' UTRs)[2-4]. The stress-induced transcription factor ATF3 is a known NMD target and is upregulated in cells harboring persistent DNA damage[8,13,71]. Notably, ATF3 promotes cellular senescence in response to genotoxic stress and oncogene activation, thereby preventing tumorigenesis[61-63]. However, ATF3 also fosters a pro-tumorigenic

microenvironment by altering expression of many secreted factors[60]. The observed inhibitory effects of persistent DNA damage on NMD activity lead us to predict that ATF3 and likely many other NMD targets will be stabilized under this condition. To test whether this is the case for ATF3 mRNAs, confluent RPE1 cells were treated with bleomycin or H_2O for 24 hours and allowed to recover for 4 days. Subsequently, cells were treated with actinomycin D for 6 hours to prevent new RNA synthesis. Cellular RNA was collected immediately before and after actinomycin D treatment and mRNA stability was assessed by RT-qPCR. Consistent with ATF3 mRNAs being targets of NMD, ATF3 transcripts exhibited much greater stability and steady-state expression in bleomycin-treated cells, which have low levels of NMD activity, than in H_2O-treated cells (Fig. 4a). Non-target mRNAs such as ORCL were not stabilized by bleomycin under the same condition (Fig. S4a). Furthermore, we found that the elevated expression and stabilization of ATF3 mRNA in response to persistent DNA damage is largely dependent on p38α, which mediates NMD inhibition. Knockdown of p38α using an shRNA or inhibition of p38α kinase activity using CDD111 largely reversed the stabilization and upregulation of ATF3 transcripts after bleomycin treatment (Fig. 4b-d). In contrast, ORCL mRNAs remained unaffected by these treatments (Fig. S4b-c). These data support the idea that NMD inhibition by persistent DNA damage prevents ATF3 mRNA degradation, thereby augmenting its expression.

To further demonstrate that NMD inhibition contributes to ATF3 mRNA stabilization in response to persistent DNA damage, we knocked down the essential NMD factor SMG1 and assessed the stability of ATF3 transcripts in these NMD-deficient cells after inducing persistent DNA damage. In the absence of DNA damage, ATF3 mRNAs exhibited much higher stability in SMG1-depleted RPE1 cells while ORCL transcripts do not, consistent with the previous finding

that ATF3 is a bona fide NMD target (Fig. 4e-f, Fig. S4d). If stabilization of ATF3 mRNAs by persistent DNA damage occurs independently of NMD inhibition, one would predict that control- and SMG1-knockdown cells will exhibit a similar level of increase in ATF3 stability after bleomycin treatment. However, if NMD inhibition contributes to ATF3 stabilization by persistent DNA damage, the extent of stabilization caused by bleomycin treatment will be reduced in SMG1-knockdown cells because NMD is already disrupted in these cells. Results shown in Fig. 4g indicate that knockdown of SMG1 reduced the increase in ATF3 stability after bleomycin treatment by nearly half, demonstrating a role for NMD attenuation in stabilizing ATF3 mRNAs in the presence of persistent DNA damage. These data likely underestimate the contribution of NMD inhibition to ATF3 mRNA stabilization after persistent DNA damage as NMD activity may not be fully inhibited in SMG1-knockdown cells, and therefore the observed partial stabilization of ATF3 mRNAs after bleomycin treatment still occurred because NMD was further inhibited by persistent DNA damage (Fig. S5). Taken together, these results strongly suggest that NMD attenuation contributes to ATF3 upregulation in response to persistent DNA damage.

3.4 Discussion

In this study, we found that persistent DNA damage—but not transient DNA damage—induces NMD repression and that this repression contributes to the upregulation of ATF3 and likely other NMD targets in response to persistent DNA damage (Fig. 1 and Fig. 4). The inhibition of NMD by persistent DNA damage requires the p38α MAP kinase but is independent of cellular senescence (Fig. 2 and Fig. 3). Osmotic stress also causes NMD inhibition; however, p38α is apparently not involved in this regulation, indicating that NMD activity is controlled by

distinct mechanisms in response to different cellular stresses (Fig. S3).

Our study has significantly added to our understanding of the physiological functions and regulation of the NMD pathway. In addition to serving as an RNA surveillance pathway to eliminate faulty nonsense mRNAs, NMD also acts as a gene regulatory mechanism to control the stability and levels of many normal transcripts. NMD has been implicated in many physiological processes including development, differentiation, and synaptic regulation[5-7,9,10,12]. Various cellular stresses, including amino acid deprivation, ER stress, hypoxia, or double stranded RNA invasion, suppress NMD activity, thereby facilitating gene expression alterations and the adaptive response to the environmental insults[8,11,13,14,18]. Our study indicates that persistent DNA damage also inhibits NMD activity, which contributes to changes in levels of ATF3 mRNA, a bona fide NMD target (Fig. 4). As a transcription factor, ATF3 regulates the cellular responses to multiple forms of stress, including DNA damage, by controlling expression of many genes[72]. Thus, the upregulation of ATF3 caused by NMD inhibition is expected to contribute to expression changes for many genes in response to persistent DNA damage, which may directly facilitate cellular survival and adaptation. This novel regulation of NMD and ATF3 by persistent DNA damage may also have important relevance to tumorigenesis and cancer treatment. The mainstays of cancer treatment are radiation and chemotherapy, both of which generate DNA damage. However, the efficacy of DNA-damaging therapies is hampered by frequent cancer relapse, which is in part caused by the remodeling of the tumor microenvironment following treatment[36,52,56,73-76]. The gene expression changes in non-cycling stromal cells caused by therapy-induced persistent DNA damage promote cellular senescence and the SASP, both of which play a crucial role in shaping the tumor microenvironment[37,73-76]. Stabilization of ATF3

transcripts due to NMD attenuation under this condition may promote expression of pro-tumorigenic SASP factors such as CXCL12 and RGS4 that are target genes of ATF3[60]. In addition to ATF3, a number of key SASP factors such as IL-6 and CXCL2 have been identified as putative direct NMD targets[13,14,37]. Because many of these SASP factors are pro-tumorigenic, restoring NMD activity in the stromal cells in the tumor microenvironment could be beneficial during cancer treatment[77].

Our study also identified a novel role for p38 in regulating NMD activity. As a key player in the persistent DNA damage response, p38 controls senescence induction and SASP expression in part by regulating gene expression. p38 induces gene expression changes by altering the activities of transcription factors and RNA binding proteins to regulate transcription, mRNA stability, and translation[53,78-85]. It has been shown previously that p38 influences the stability of mRNAs by altering the activity of RNA binding proteins such as AUF1, which binds to AU-rich elements (AREs) in the 3' UTR of certain transcripts[51,86]. The suppression of NMD by p38 is a new p38-mediated mechanism to regulate mRNA stability. Although p38 is required for NMD attenuation after persistent DNA damage, p38 activation alone is not sufficient. Presumably, p38 functions in concert with another signal generated by persistent DNA damage to control NMD activity. Although p38 is also involved in the cellular response to osmotic stress, which also inhibits NMD, p38 is not required for NMD regulation by osmotic stress, suggesting that a distinct mechanism is employed to control NMD activity in this context. In addition to p38, previous studies have revealed that NMD activity can be suppressed by other kinases such as PKR and PERK in the cellular responses to amino acid deprivation, reactive oxygen species, dsRNA viruses, hypoxia, and ER stress[8,14,87]. These kinases apparently inhibit NMD through a

common mechanism by phosphorylating the translation initiation factor eIF2α at S51, although how this phosphorylation attenuates NMD remains to be determined[8,14]. Future work is needed to determine whether p38 governs NMD activity through eIF2α or through a completely different mechanism. In proliferating cancer cells treated with lethal doses of chemotherapeutics, NMD activity is suppressed by caspase-mediated UPF1 cleavage[19]. The sub-lethal DNA damaging treatments used in this study do not induce widespread apoptosis in non-cycling cells and, consequently, no UPF1 cleavage products were observed (data not shown). Further dissection of the mechanism of NMD regulation by p38 and other factors will provide crucial insights into the persistent DNA damage response and the physiological functions of the NMD pathway.

3.5 Methods

3.5.1 Cell culture, adenovirus and lentivirus production and infection

Human nontransformed RPE1 cells were maintained in Dulbecco's modified Eagle's medium (DMEM) nutrient mixture F-12 HAM (Sigma D6421) supplemented with 100 units/ml penicillin, 100 μg/ml streptomycin, 2.5 mM L-glutamine, and 7.5% fetal bovine serum (FBS) and grown in a 5% CO2 incubator at 37 °C. Human foreskin BJ fibroblasts were maintained in 70% DMEM (Sigma D5796), 15% Medium 199 (Sigma M7528), and 15% FBS supplemented with 100 units/ml penicillin and 100 μg/ml streptomycin and grown in a 5% CO2 incubator at 37 °C. Human HEK293T and HEK293 cells were cultured in DMEM (Sigma D5796) with 10% FBS at 37 ºC with 5% CO2.

An adenoviral construct encoding the bioluminescent NMD reporter was generated by inserting the reporter into the pAdenoX-PRLS-ZsGreen1 vector using the In-Fusion HD cloning kit (Clontech) according to the manufacturer's protocol. Linearized adenoviral vector with

exposed inverted terminal repeats was transfected into HEK293 cells for viral production, followed by viral amplification in the same cell line. Target cells were infected with adenoviruses for 24 hours before bioluminescence imaging.

To knockdown p38α in RPE1 cells, lentiviruses expressing a non-targeting control shRNA (5'- CAACAAGAUGAAGAGCACCAA-3') or an shRNA targeting p38α (5'-GTTACGTGTGGCAGTGAAGAA-3') were generated in HEK293T cells as previously described (Nickless et al. 2014). Briefly, HEK293T cells were co-transfected with an shRNA-encoding lentiviral vector and packaging plasmids (pCMV-dR8.2 and pCMV-VSVG) using the TransIT-LT1 transfection reagent (Mirus). Virus-containing supernatant was collected 48 and 72 hours after transfection. Filtered viruses were used to infect RPE1 cells, and infected cells were selected for with puromycin.

To generate recombinant retroviruses expressing the CDK inhibitor p16, HEK293T cells were co-transfected with either pBabe-puro or pBabe-puro-p16 and packaging plasmids (pCMV-UMVC and pCMV-VSVG) using TransIT-LT1 transfection reagent (Mirus). Virus-containing supernatant was collected 48 and 72 hours after transfection. RPE1 cells were then infected with the viruses followed by puromycin selection.

For the MKK6 experiments, RPE1 cells were plated at a density of 150,000 cells/well in a 6-well plate and allowed to grow for 48 hours before addition of either LacZ or MKK6-CA adenovirus at a 1:1000 dilution. Virus was removed after 24 hours, and cells were then allowed to recover for 6 days before NMD analysis. Reporter adenovirus was introduced 24 hours prior to NMD analysis at a 1:2500 dilution.

3.5.2 Cell plating conditions, induction of persistent DNA damage and osmotic stress

Bleomycin treatment: For all 24 hour bleomycin treatments, RPE1 cells or BJ fibroblast cells were plated at a density of 150,000 cells/well in 6-well plates and allowed to grow to confluency for 72 hours before the addition of bleomycin. For 1 hour bleomycin treatments, cells were plated at a density of 100,000 cells/well in 6-well plates and allowed to grow for 48 hours before beginning treatment. Bleomycin (B8416, Sigma) was dissolved in water at 15 units/ml (9.4 mg/ml) and diluted in medium 1:149.25 to a final concentration of ~ 63 μg/ml for treatment. CDD111 (10 mM stock solutions of in DMSO) was diluted 1:1000 in medium to a final concentration of 10 μM for treatment. Medium containing DMSO or CDD111 was refreshed daily.

CPT treatment: RPE1 cells were plated at a density of 50,000 cells/well in 6-well plates and cultured for 72 hours before beginning treatment. CPT in DMSO (60 μM in DMSO) was diluted 1:1000 in medium to a final concentration of 60 nM for treatment. Medium containing DMSO or CPT was refreshed daily.

Irradiation: RPE1 cells were plated at a density of 150,000 cells/well in 6-well plates and allowed to grow to confluency for 72 hours before irradiation. Cells were X-ray irradiated with doses of either 0.5 Gy or 10 Gy at 0.625 Gy/min using a Gammacell 40 irradiator (Atomic Energy of Canada).

Osmotic shock treatments: RPE1 cells were plated at a density of 35,000 cells/well in 96-well plates. Medium was removed 24 hours after plating and replaced with medium containing either DMSO or CDD111 (10 μM). Nineteen hours later, medium was removed and replaced with fresh medium containing DMSO or CDD111 supplemented with either H_2O, 80 mM KCl, or 275 mM sorbitol. After 5 hours of treatment, NMD activity was analyzed by bioluminescence

imaging. Control- or p38α-knockdown RPE1 cells were also treated with 80 mM KCl or 275 mM sorbitol for 5 hours before NMD analysis.

Reporter adenoviral transduction: For NMD analysis, the NMD reporter was introduced into cells via adenoviral infection. Adenoviruses expressing the NMD reporter were added to cell growth medium 24 hours prior to bioluminescence imaging.

3.5.3 Bioluminescence imaging and spectral deconvolution for signal unmixing

Cells were incubated with 150 μg/ml D-luciferin for 10 min at 37 °C and bioluminescence signals were measured using a charge-coupled device (CCD) camera-based bioluminescence imaging system (IVIS 50; Caliper) with appropriate open, red, or green filters and exposure settings (exposure time: 30 s, 60 s, 60 s; binning: 8; field of view: 15; f/stop: 1). Regions-of-interest (ROIs) were drawn over images of wells and bioluminescence signals were quantified using Living Image (Caliper) and Igor (Wavemetrics) analysis software packages as described previously[69,88]. Spectral unmixing was performed using a previously developed ImageJ plugin, as previously described[69,88].

3.5.4 Reverse transcription, qPCR, and western blotting

Total RNA was isolated using the NucleoSpin RNA kit from Clonetech (740955) and cDNA was synthesized using the PrimeScript RT Reagent Kit from Clonetech (RR037A) according to the instructions of the manufacturer. qPCR reactions were performed in triplicate using a two step PCR protocol (melting temperature: 95°C; annealing and extension temperature: 60°C; cycle number: 40) on an ABI VII7 real-time PCR system with PowerUp SYBR Green Master Mix (Thermo Scientific). The mRNA levels of the housekeeping gene GAPDH were used for normalization. Primers for ATF3 (F: 5’-GCCATTGGAGAGCTGTCTTC-3’, R: 5’-

GGGCCATCTGGAACATAAGA-3'), ORCL (F: 5'-GGCAGCAGATGAAATCTGAA-3', R: 5'-TCCAGAATGTGATTTTTGCAG-3'), and GAPDH (F: 5'-AACAGCCTCAAGATCATCAGC-3', R: 5'-GATGATGTTCTGGAGAGCC-3') were purchased from Integrated DNA Technologies.

Western blotting was performed using a Li-Cor Odyssey system. Briefly, cells were lysed with SDS sample buffer (90 mM Tris, 20% glycerol, 2% SDS, 5% β-mercaptoethanol). Samples were run on SDS-page gel and transferred to a PDVF membrane. Membranes were blocked in casein buffer and subsequently probed with primary antibody diluted in casein buffer. γH2AX (9718; 1:1,000), p38α (9218; 1:1,000), phospho-p38 (4511;1:1000), HSP27 (2402; 1:1500), phospho-HSP27 (9709; 1:1000), and MKK6 (9264; 1:1000) antibodies were purchased from Cell Signaling Technology. β-Actin (MA5-15739; 1:5,000) antibody was purchased from Thermo Scientific. CBR-TCR(PTC) and CBG-TCR(WT) reporter proteins were detected with an HA-antibody (Convance, MMS-101R, 1:1,000).

3.6 Figures

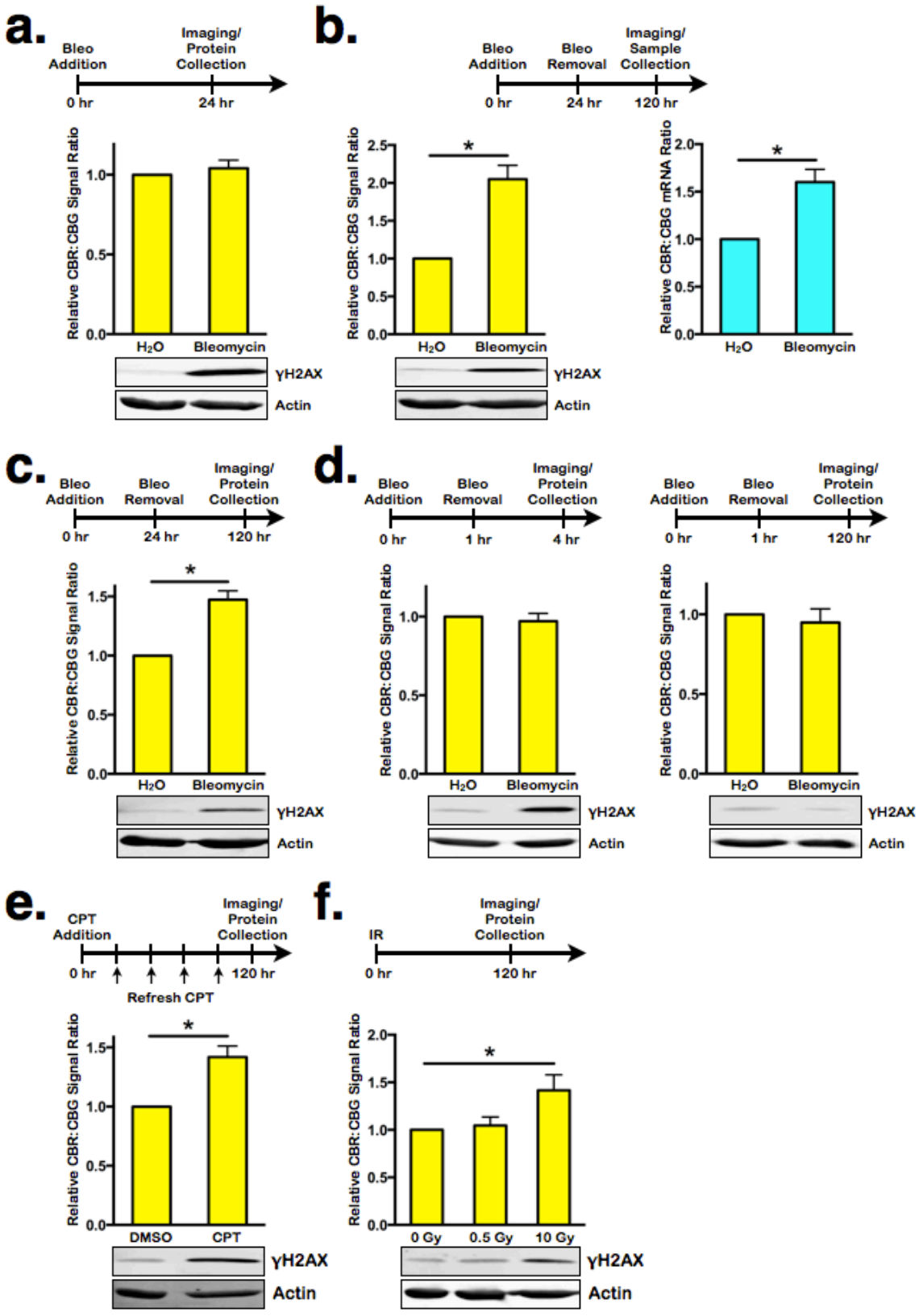
a.
Bleo Addition
Imaging/ Protein Collection
0 hr
24 hr
Relative CBR:CBG Signal Ratio
H2O
Bleomycin
γH2AX
Actin
b.
Bleo Addition
Bleo Removal
Imaging/ Sample Collection
0 hr
24 hr
120 hr
Relative CBR:CBG Signal Ratio
Relative CBR:CBG mRNA Ratio
c.
Bleo Addition
Bleo Removal
Imaging/ Protein Collection
0 hr
24 hr
120 hr
d.
0 hr
1 hr
4 hr
e.
CPT Addition
Refresh CPT
DMSO
CPT
f.
IR
0 Gy
0.5 Gy
10 Gy

Figure 1. Persistent DNA damage inhibits NMD

a). Ratios of CBR:CBG bioluminescence signals in RPE1 cells expressing the NMD reporter (hereafter referred to as RPE1 reporter cells for simplicity) after a 24 hr treatment with either H_2O or bleomycin. The ratio of H_2O-treated cells was normalized to 1. Data represent the mean ± SD of three independent experiments. Western blot showing γH2AX levels in lysates collected after a 24 hr treatment with either H_2O or bleomycin (bottom panel).

b). Left panels: Ratios of CBR:CBG bioluminescence signals (upper panel) and γH2AX levels (lower panel) in RPE1 reporter cells after a 24 hr treatment with either H_2O or bleomycin followed by a 96 hr recovery. The ratio of CBR:CBG signals in H_2O-treated cells was normalized to 1. Data represent the mean ± SD of four independent experiments. *$p < 0.05$ (paired t-test). Right Panel: Ratios of CBR-TCR(PTC): CBG-TCR(WT) mRNA expression in RPE1 reporter cells after a 24 hr treatment with either H_2O or bleomycin followed by a 96 hr recovery. The ratio of H_2O-treated cells was normalized to 1. Data represent the mean ± SD of four independent experiments.* $p < 0.05$ (paired t-test).

c). Ratios of CBR:CBG bioluminescence signals (upper panel) and γH2AX levels (lower panel) in primary BJ fibroblasts expressing the NMD reporter after a 24 hr treatment with either H_2O or bleomycin followed by a 96 hr recovery. The ratio of CBR:CBG signals in H_2O-treated cells was normalized to 1. Data represent the mean ± SD of three independent experiments. *$p < 0.05$ (paired t-test).

d). Left panels: Ratios of CBR:CBG bioluminescence signals (upper panel) and γH2AX levels (lower panel) in RPE1 reporter cells after a 1 hr treatment with either H_2O or bleomycin followed by a 3 hr recovery. The ratio of CBR:CBG signals in H_2O-treated cells was normalized

to 1. Data represent the mean ± SD of three independent experiments. $p > 0.05$ (paired t-test). Right panels: Ratios of CBR:CBG bioluminescence (upper panel) and γH2AX levels (lower panel) signals in RPE1 reporter cells after a 1 hr treatment with either H_2O or bleomycin followed by a 120 hr recovery. The ratio of CBR:CBG signals in H_2O-treated cells was normalized to 1. Data represent the mean ± SD of three independent experiments. *$p < 0.05$ (paired t-test).

e). Ratios of CBR:CBG bioluminescence signals (upper panel) and γH2AX levels (lower panel) in RPE1 reporter cells after a 120 hr treatment with either DMSO or 60 nM CPT. The ratio of CBR:CBG signals in DMSO-treated cells was normalized to 1. Data represent the mean ± SD of four independent experiments. *$p < 0.05$ (paired t-test).

f). Ratios of CBR:CBG bioluminescence signals (upper panel) and γH2AX levels (lower panel) in RPE1 reporter cells 144 hours after exposure to 0 Gy, 0.5 Gy, or 10 Gy of ionizing radiation. The ratio of CBR:CBG signals in cells receiving 0 Gy of ionizing radiation was normalized to 1. Data represent the mean ± SD of three independent experiments. *$p < 0.05$ (paired t-test).

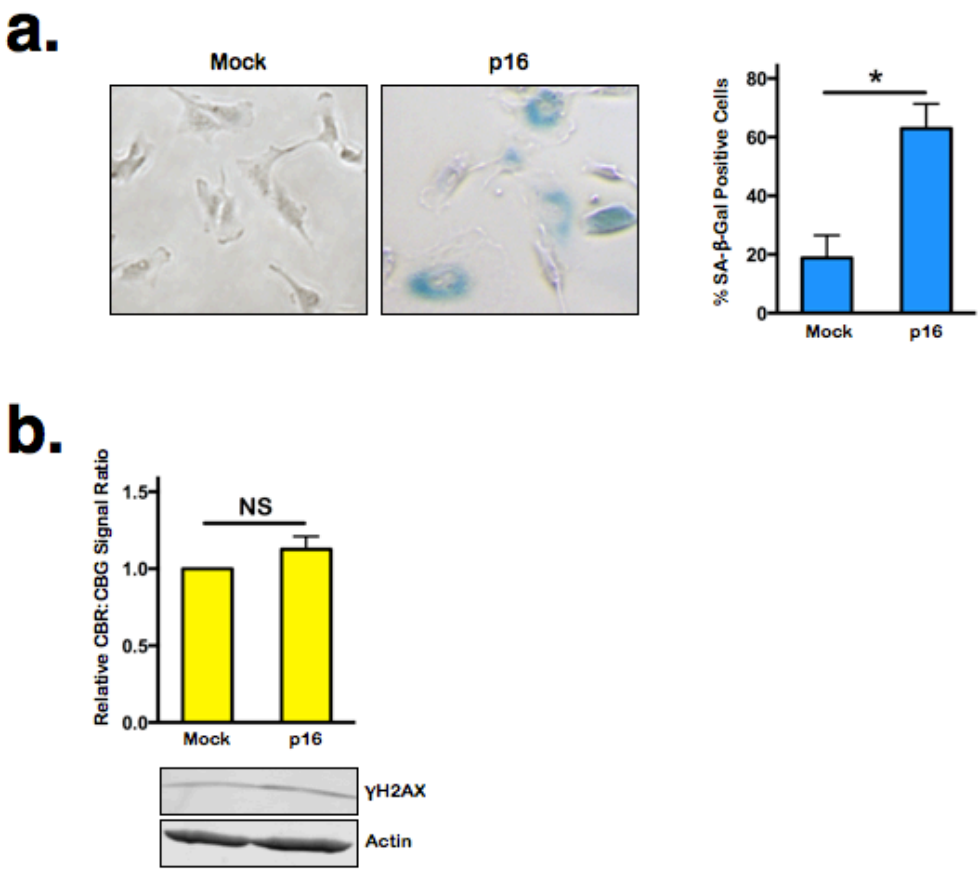

Figure 2. p16-induced cellular senescence does not alter NMD activity

a). Left panel: Representative images of RPE1 reporter cells expressing either empty vector or p16 after SA-β-Gal staining. Right panel: Percent of SA-β-Gal-positive RPE1 cells expressing either empty vector or p16. Data represent the mean ± SD of four independent experiments. *$p < 0.05$ (paired t-test).

b). Upper panel: Ratios of CBR:CBG bioluminescence signals in RPE1 reporter cells expressing either empty vector or p16. The ratio of CBR:CBG signals in the empty vector-expressing cells was normalized to 1. Data represent the mean ± SD of four independent experiments. $p > 0.05$ (paired t-test). Lower panel: Western blot showing γH2AX levels in cells over-expressing either empty vector or p16.

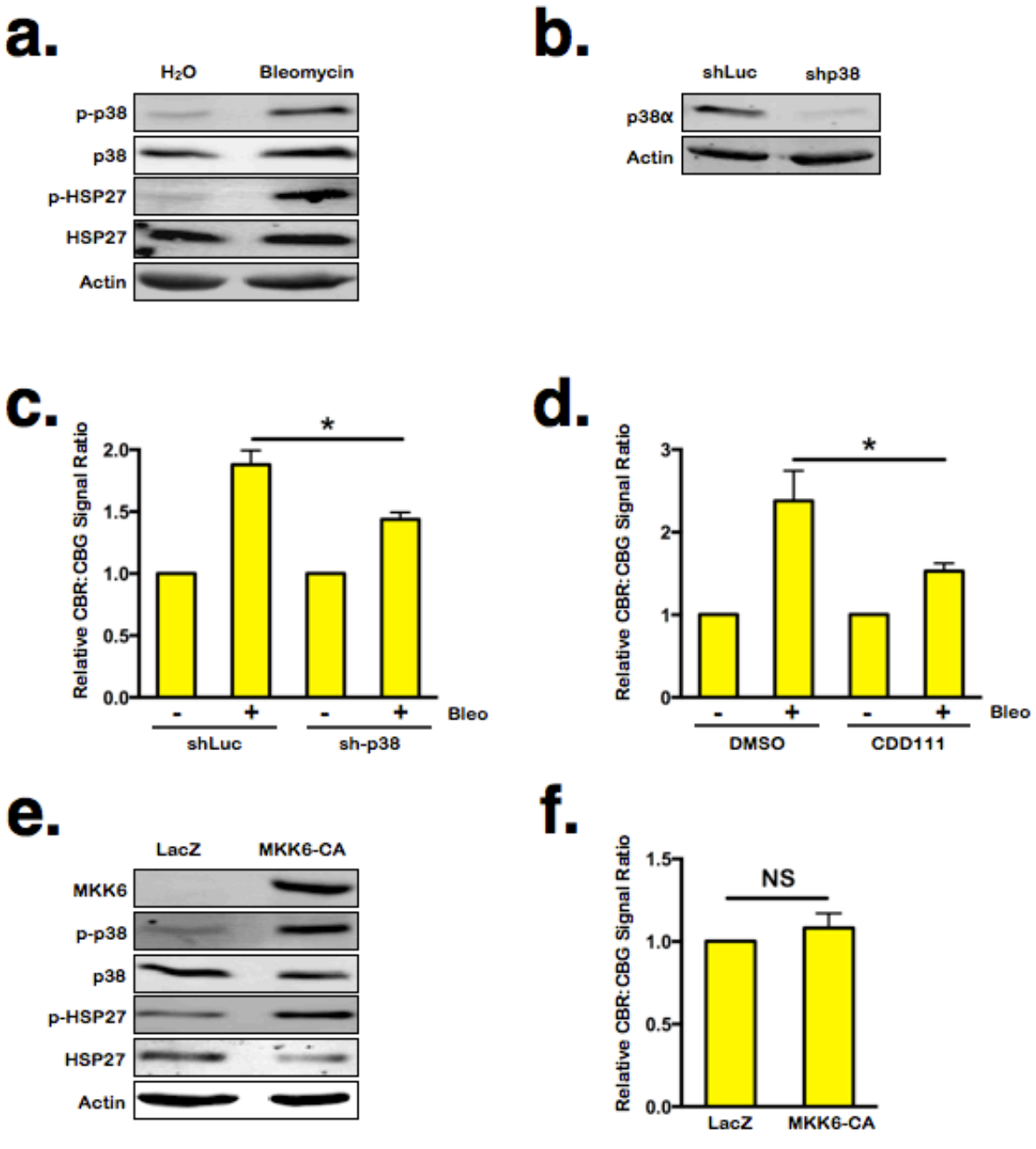
a.
H2O
Bleomycin
p-p38
p38
p-HSP27
HSP27
Actin
b.
shLuc
shp38
p38α
Actin
c.
Relative CBR:CBG Signal Ratio
2.0
1.5
1.0
0.5
0.0
*
- + - +
Bleo
shLuc
sh-p38
d.
Relative CBR:CBG Signal Ratio
3
2
1
0
*
- + - +
Bleo
DMSO
CDD111
e.
LacZ
MKK6-CA
MKK6
p-p38
p38
p-HSP27
HSP27
Actin
f.
Relative CBR:CBG Signal Ratio
1.5
1.0
0.5
0.0
NS
LacZ
MKK6-CA

Figure 3. NMD inhibition by persistent DNA damage is mediated in part by p38

a). Levels of total and phosphorylated p38 and HSP27 in RPE1 cells treated with either H_2O or bleomycin for 24 hrs followed by a 96 hr recovery.

b). shRNA-mediated knockdown of p38α in RPE1 cells.

c). Ratios of CBR:CBG bioluminescence signals in control- and p38-knockdown RPE1 reporter cells after a 24 hr treatment with either H_2O or bleomycin followed by a 96 hr recovery. The ratio of CBR:CBG signals in H_2O-treated cells was normalized to 1. Data represent the mean ± SD of four independent experiments. *$p < 0.05$ (paired t-test).

d). Ratios of CBR:CBG bioluminescence signals in DMSO- or CDD111-treated RPE1 reporter cells after a 24 hr treatment with either H_2O or bleomycin followed by a 96 hr recovery. The ratio of CBR:CBG signals in H_2O-treated cells was normalized to 1. Data represent the mean ± SD of three independent experiments. *$p < 0.05$ (paired t-test).

e). Levels of MKK6 and both total and phosphorylated p38 and HSP27 in RPE1 cells expressing LacZ or constitutively active MKK6-CA for 7 days.

f). Ratios of CBR:CBG bioluminescence signals in RPE1 reporter cells expressing either LacZ or MKK6-CA for 7 days. The ratio of CBR:CBG signals in LacZ-treated cells was normalized to 1. Data represent the mean ± SD of three independent experiments.

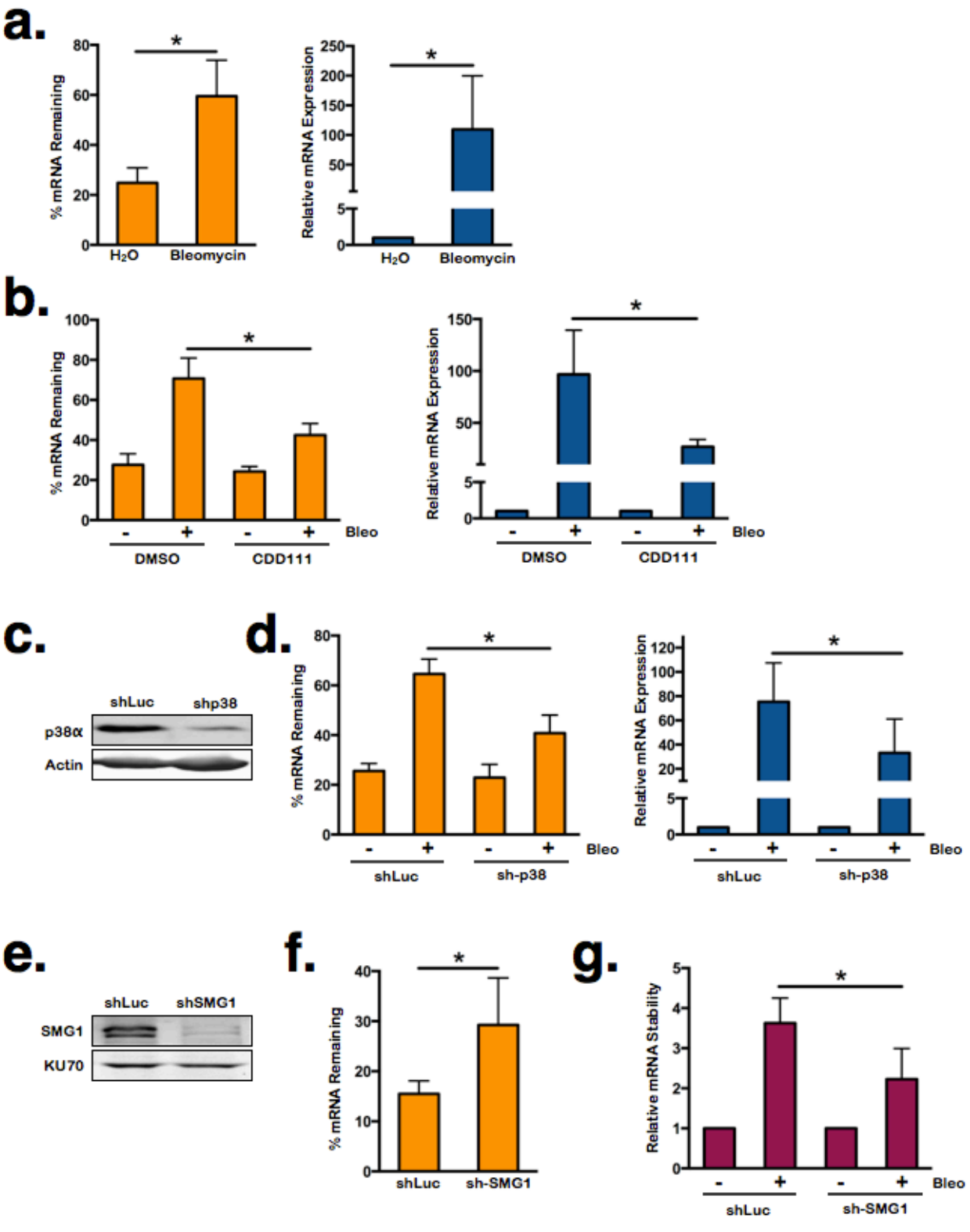
a.
% mRNA Remaining
80
60
40
20
0
*
H2O
Bleomycin
Relative mRNA Expression
250
200
150
100
50
5
0
*
H2O
Bleomycin
b.
% mRNA Remaining
100
80
60
40
20
0
*
-
+
-
+
Bleo
DMSO
CDD111
Relative mRNA Expression
150
100
50
5
0
*
-
+
-
+
Bleo
DMSO
CDD111
c.
shLuc
shp38
p38α
Actin
d.
% mRNA Remaining
80
60
40
20
0
*
-
+
-
+
Bleo
shLuc
sh-p38
Relative mRNA Expression
120
100
80
60
40
20
5
0
*
-
+
-
+
Bleo
shLuc
sh-p38
e.
shLuc
shSMG1
SMG1
KU70
f.
% mRNA Remaining
40
30
20
10
0
*
shLuc
sh-SMG1
g.
Relative mRNA Stability
5
4
3
2
1
0
*
-
+
-
+
Bleo
shLuc
sh-SMG1

Figure 4. ATF3 transcripts are stabilized by persistent DNA damage in a p38α-dependent manner

a). Left panel: Percent of ATF3 mRNAs remaining in RPE1 reporter cells after a 24 hr treatment with either H_2O or bleomycin followed by a 96 hr recovery. Following the recovery period, Actinomycin D was added to cells. Total RNA was collected immediately before or 6 hours after the addition of Actinomycin D followed by RT-qPCR analysis. Right panel: Steady-state levels of ATF3 transcripts in RPE1 reporter cells after a 24 hr treatment with either H_2O or bleomycin followed by a 96 hr recovery. Expression in the H_2O-treated cells was normalized to 1. Both panels: Data represent the mean ± SD of five independent experiments.

b). Left panel: Percent of ATF3 mRNAs remaining in DMSO- and CDD111-treated RPE1 reporter cells after a 24 hr treatment with either H_2O or bleomycin followed by a 96 hr recovery. Samples collected as in (a). Right panel: Steady-state levels of ATF3 transcripts in DMSO- and CDD111-treated RPE1 cells after a 24 hr treatment with either H_2O or bleomycin followed by a 96 hr recovery. Expression in the H_2O-treated cells was normalized to 1. Both panels: Data represent the mean ± SD of five independent experiments.

c). shRNA-mediated knockdown of p38α in RPE1 cells

d). Left panel: Percent of ATF3 mRNAs remaining in control- and p38α-knockdown RPE1 reporter cells after a 24 hr treatment with either H_2O or bleomycin followed by a 96 hr recovery. Samples collected as in (a). Right panel: Steady-state levels of ATF3 transcripts in control- and p38α-knockdown treated RPE1 reporter cells after a 24 hr treatment with either H_2O or bleomycin followed by a 96 hr recovery. Expression in the H_2O-treated cells was normalized to 1. Both panels: Data represent the mean ± SD of four independent experiments.

e). shRNA-mediated knockdown of SMG1 in RPE1 cells

f). Percent of ATF3 mRNAs remaining in control- and SMG1-knockdown RPE1 cells. Actinomycin D was added to cells to prevent transcription, and total RNA was collected immediately before or 6 hours after the addition of Actinomycin D followed by RT-qPCR analysis. Data represent the mean ± SD of four independent experiments.

g). ATF3 mRNA stability changes in control- and SMG1-knockdown RPE1 cells after a 24 hr treatment with either H_2O or bleomycin followed by a 96 hr recovery. Samples collected as in (a). Data represent the mean ± SD of four independent experiments.

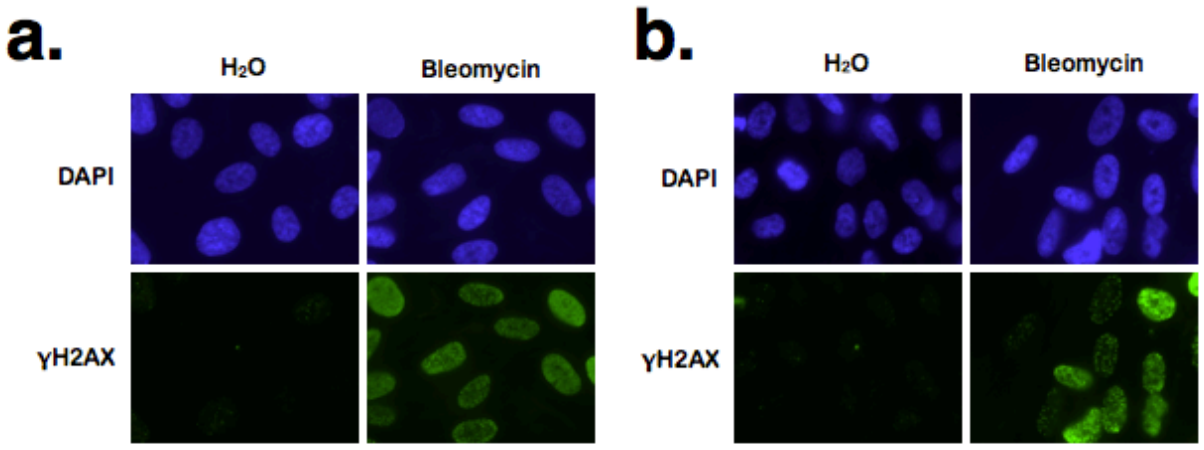
a.
H2O
Bleomycin
DAPI
γH2AX
b.
H2O
Bleomycin
DAPI
γH2AX

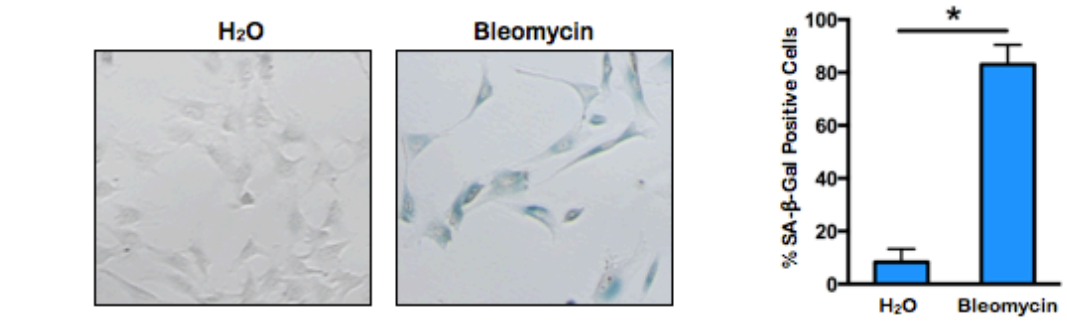
c.
H2O
Bleomycin
% SA-β-Gal Positive Cells
100
80
60
40
20
0
*
H2O
Bleomycin

Supplemental Figure 1. Bleomycin generates persistent γH2AX foci and induces senescence in human RPE1 cells

a). Representative images of immunofluorescence staining for DAPI or γH2AX in RPE1 cells after a 24 hr treatment with either H_2O or bleomycin.

b). Representative images of immunofluorescence staining for DAPI or γH2AX in RPE1 cells after a 24 hr treatment with either H_2O or bleomycin followed by a 96 hr recovery.

c). Left panel: Representative SA-β-Gal staining images of RPE1 reporter cells after a 24 hr treatment with either H_2O or bleomycin followed by a 96 hr recovery. Right panel: Percent of SA-β-Gal-positive RPE1 cells after a 24 hr treatment with either H_2O or bleomycin followed by a 96 hr recovery. Data represent the mean ± SD of three independent experiments. *$p < 0.05$ (paired t-test).

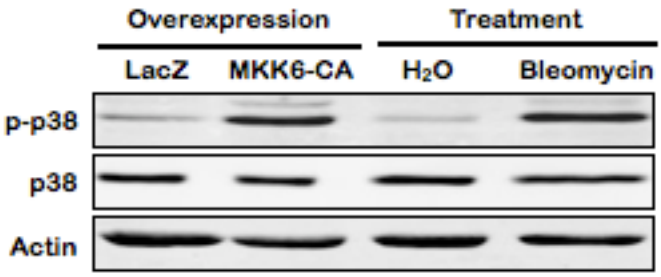

Supplemental Figure 2. MKK6 overexpression and bleomycin treatment similarly activate p38

Levels of total and phosphorylated p38 RPE1 cells overexpressing either empty vector or MKK6-CA for 6 days or treated with either H_2O or bleomycin for 24 hours followed by a 96 hr recovery.

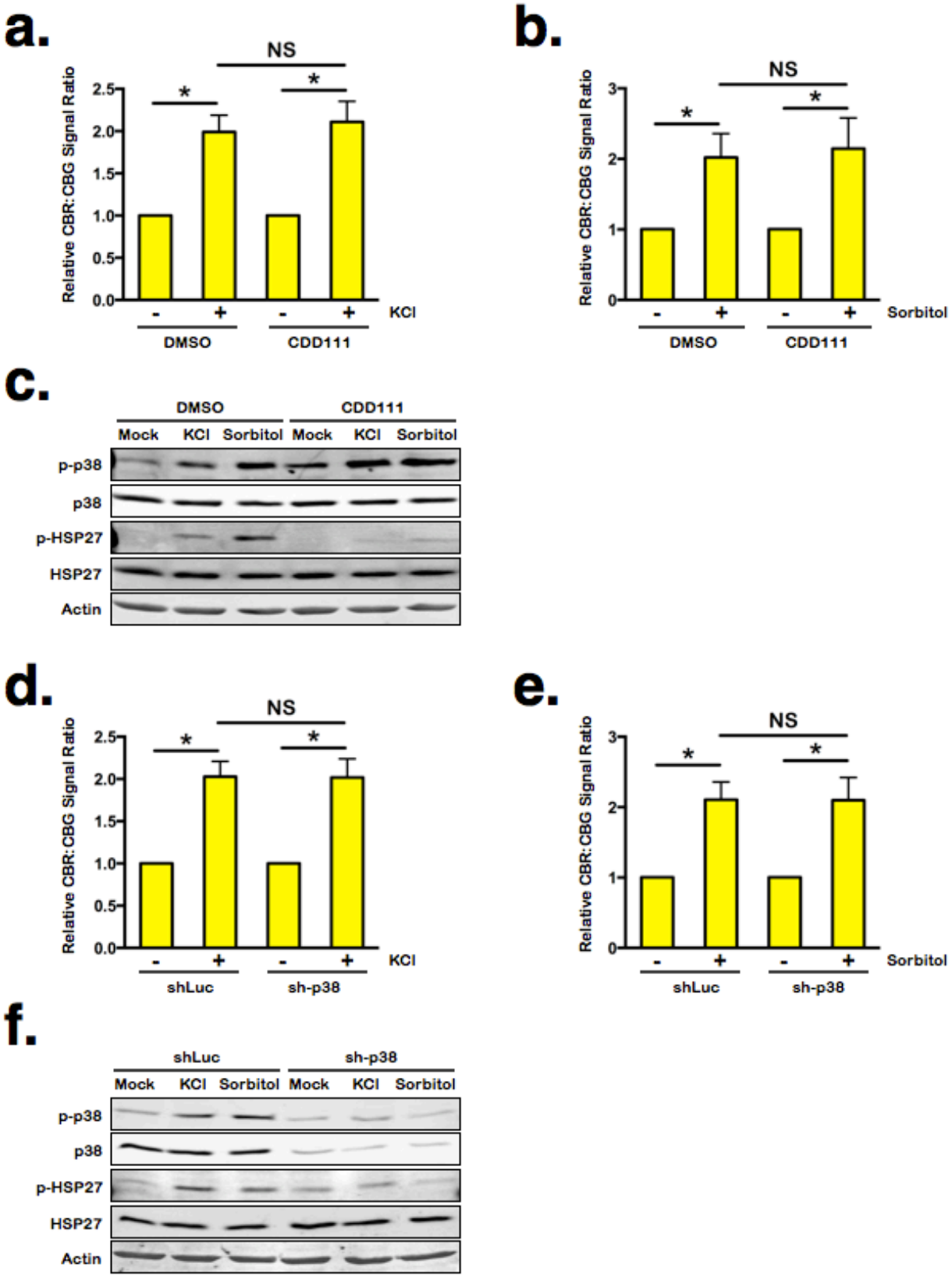
a.
NS
*
*
Relative CBR:CBG Signal Ratio
2.5
2.0
1.5
1.0
0.5
0.0
- + - +
KCl
DMSO
CDD111
b.
NS
*
*
Relative CBR:CBG Signal Ratio
3
2
1
0
- + - +
Sorbitol
DMSO
CDD111
c.
DMSO
CDD111
Mock KCl Sorbitol Mock KCl Sorbitol
p-p38
p38
p-HSP27
HSP27
Actin
d.
NS
*
*
Relative CBR:CBG Signal Ratio
2.5
2.0
1.5
1.0
0.5
0.0
- + - +
KCl
shLuc
sh-p38
e.
NS
*
*
Relative CBR:CBG Signal Ratio
3
2
1
0
- + - +
Sorbitol
shLuc
sh-p38
f.
shLuc
sh-p38
Mock KCl Sorbitol Mock KCl Sorbitol
p-p38
p38
p-HSP27
HSP27
Actin

Supplemental Figure 3. Hyperosmotic shock suppresses NMD in a p38α-independent manner

a). Ratios of CBR:CBG bioluminescence signals in DMSO- and CDD111-treated RPE1 reporter cells after a 5 hr treatment with normal medium or medium supplemented with 80 mM KCl. The ratio of CBR:CBG signals in the mock-treated cells was normalized to 1. Data represent the mean ± SD of four independent experiments. *$p < 0.05$ (paired t-test).

b). Ratios of CBR:CBG bioluminescence signals in DMSO- and CDD111-treated RPE1 reporter cells after a 5 hr treatment with normal medium or medium supplemented with 275 mM Sorbitol. The ratio of CBR:CBG signals in the of mock-treated cells was normalized to 1. Data represent the mean ± SD of four independent experiments. *$p < 0.05$ (paired t-test).

c). Levels of total and phosphorylated p38 and HSP27 in DMSO- and CDD111- RPE1 cells after a 5 hr treatment with osmotic stressors depicted in (a) and (b).

d). Ratios of CBR:CBG bioluminescence signals in control- and p38α-knockdown RPE1 reporter cells after a 5 hr treatment with normal medium or medium supplemented with 80 mM KCl. The ratio of CBR:CBG signals in the mock-treated cells was normalized to 1. Data represent the mean ± SD of three independent experiments. *$p < 0.05$ (paired t-test).

e). Ratios of CBR:CBG bioluminescence signals in control- and p38α-knockdown RPE1 reporter cells after a 5 hr treatment with normal medium or medium supplemented with 275mM Sorbitol. The ratio of CBR:CBG signals in the mock-treated cells was normalized to 1. Data represent the mean ± SD of three independent experiments. *$p < 0.05$ (paired t-test).

f). Levels of total and phosphorylated p38 and HSP27 in control- and p38α-knockdown RPE1 reporter cells after a 5 hr treatment with osmotic stressors depicted in (d) and (e).

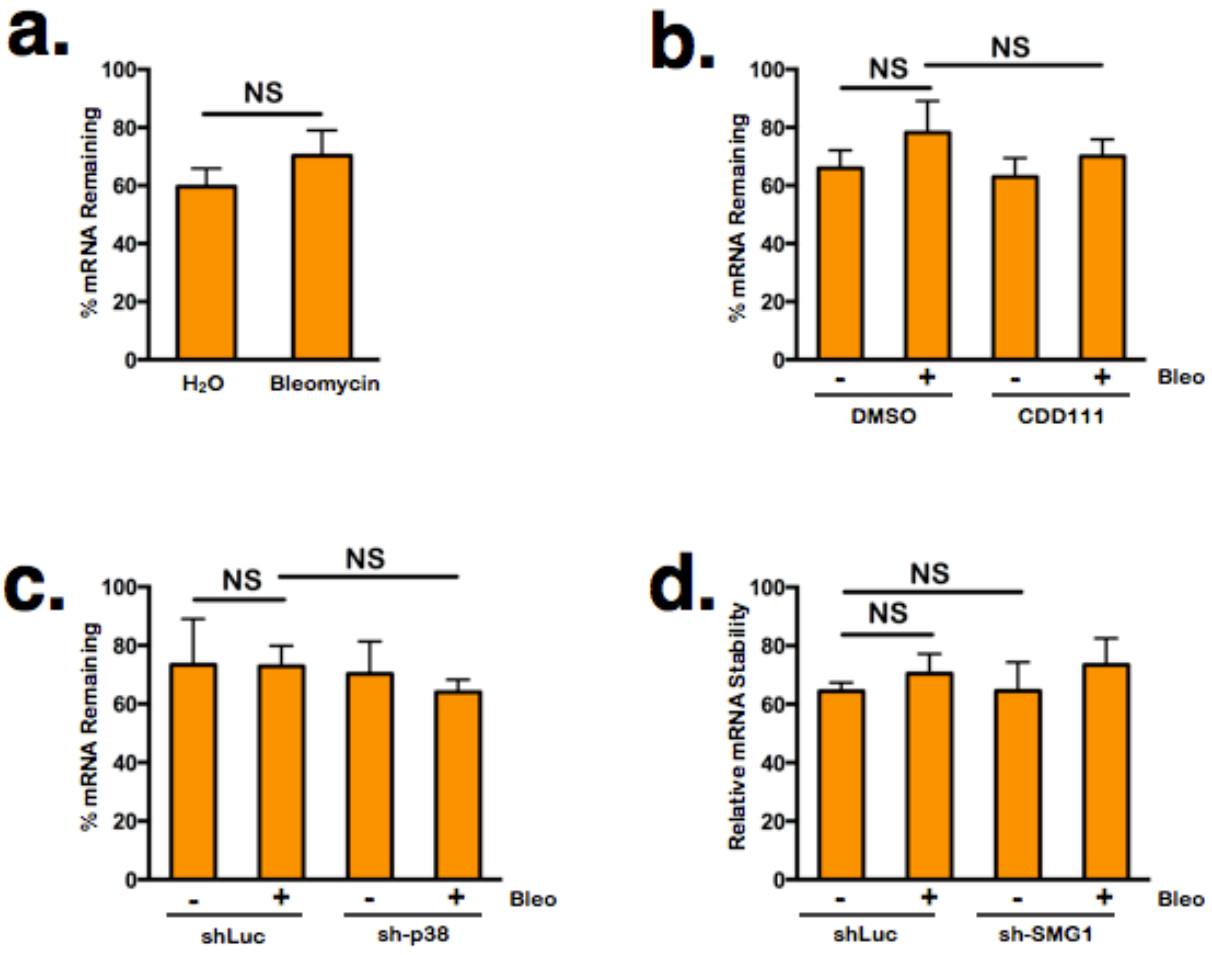
a.
% mRNA Remaining
100
80
60
40
20
0
NS
H2O
Bleomycin
b.
% mRNA Remaining
NS
NS
- + - +
Bleo
DMSO
CDD111
c.
% mRNA Remaining
NS
NS
- + - +
Bleo
shLuc
sh-p38
d.
Relative mRNA Stability
NS
NS
- + - +
Bleo
shLuc
sh-SMG1

Supplemental Figure 4. ORCL transcripts are not stabilized after bleomycin treatment or SMG1 knockdown.

a). Percent of ORCL mRNAs remaining in RPE1 reporter cells after a 24 hr treatment with either H_2O or bleomycin followed by a 96 hr recovery. Samples are the same as in Fig. 4a. Data represent the mean ± SD of five independent experiments.

b). Percent of ORCL mRNAs remaining in DMSO- and CDD111-treated RPE1 reporter cells after a 24 hr treatment with either H_2O or bleomycin followed by a 96 hr recovery. Samples are the same as in Fig. 4b. Data represent the mean ± SD of five independent experiments.

c). Percent of ORCL mRNAs remaining in control- and p38α-knockdown RPE1 reporter cells after a 24 hr treatment with either H_2O or bleomycin followed by a 96 hr recovery. Samples are the same as in Fig. 4d. Data represent the mean ± SD of four independent experiments.

d). Percent of ORCL mRNAs remaining in control- and SMG1-knockdown RPE1 reporter cells a 24 hr treatment with either H_2O or bleomycin followed by a 96 hr recovery. Samples are the same as in Fig. 4g. Data represent the mean ± SD of four independent experiments.

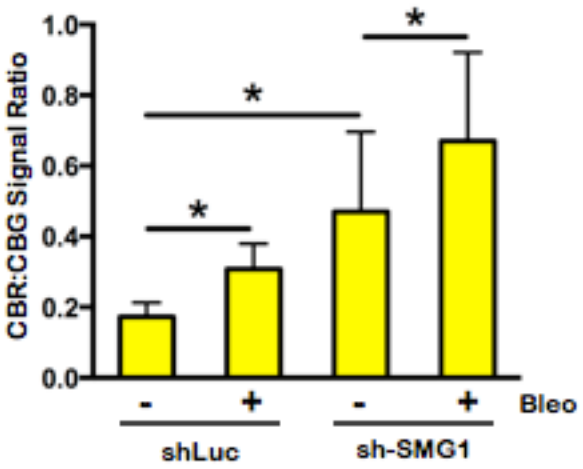

Supplemental Figure 5. SMG1 knockdown reduces NMD activity and bleomycin further inhibits NMD in SMG1 knockdown cells.

Ratios of CBR:CBG bioluminescence signals in control- and SMG1-knockdown RPE1 reporter cells after a 24 hr treatment with either H_2O or bleomycin followed by a 96 hr recovery. Data represent the mean ± SD of four independent experiments. *$p < 0.05$ (paired t-test).

3.7 References

1) Kervestin, S. & Jacobson, A. NMD: a multifaceted response to premature translational termination. Nat Rev Mol Cell Biol 13, 700-712 (2012).

2) Schweingruber, C., Rufener, S.C., Zund, D., Yamashita, A. & Muhlemann, O. Nonsense-mediated mRNA decay – mechanisms of substrate mRNA recognition and degradation in mammalian cells. Biochim Biophys Acta 1829, 612-623 (2013).

3) Hug, N,. Longman, D. & Cáceres, J.F. Mechanism and regulation of the nonsense-mediated decay pathway. Nucleic Acids Res 44, 1483-1495 (2016).

4) Lykke-Andersen, S. & Jensen, T.H. Nonsense-mediated mRNA decay: an intricate machinery that shapes transcriptomes. Nat Rev Mol Cell Biol 16, 665-677 (2015).

5) Bruno, I.G., Karam, R., Huang, L., Bhardwaj, A., Lou, C.H., Shum, E.Y., Song. H.W., Corbett, M.A., Gifford, W.D., Gecz, J., Pfaff, S.L. & Wilkinson, M.F. Identification of a microRNA that activates gene expression by repressing nonsense-mediated RNA decay. Mol Cell. 42, 500-510 (2011).

6) Colak, D., Ji, S.J., Porse, B.T. & Jaffrey, S.R. Regulation of axon guidance by compartmentalized nonsense-mediated mRNA decay. Cell 153, 1252-1265 (2013).

7) Eom, T., Zhang, C., Wang, H., Lay, K., Fak, J., Noebels, J.L. & Darnell, R.B. NOVA-dependent regulation of cryptic NMD exons controls synaptic protein levels after seizure. eLIFE 2:e00178, (2013).

8) Gardner, L.B. Hypoxic inhibition of nonsense-mediated RNA decay regulates gene expression and the integrated stress response. Mol Cell Biol 28, 3729-3741 (2008).

9) Giorgi, C., Yeo, G.W., Stone, M.E., Katz, D.B., Burge, C., Turrigiano, G. & Moore, M.J. The EJC factor eIF4AIII modulates synaptic strength and neuronal protein expression. Cell 130, 179-191 (2007).

10) Gong, C., Kim, Y.K., Woeller, C.F., Tang, Y. & Maquat, L.E. SMD and NMD are competitive pathways that contribute to myogenesis: effects on PAX3 and myogenin mRNAs. Genes Dev 23, 54-66 (2009).

11) Karam, R., Lou, C.H., Kroeger, H., Huang, L., Lin, J.H. & Wilkinson, M.F. The unfolded protein response is shaped by the NMD pathway. EMBO Rep 16, 599-609 (2015).

12) Long, A.A., Mahapatra, C.T., Woodruff, E.A., Rohrbough, J., Leung, H.T., Shino, S., An, L., Doerge, R.W., Metzstein, M.M., Pak, W.L. & Broadie, K. The nonsense-mediated decay

pathway maintains synapse architecture and synaptic vesicle cycle efficacy. J Cell Sci 123, 3303-3315 (2010).

13) Mendell, J.T., Sharifi, N.A., Meyers, J.L., Martinez-Murillo, F. & Dietz, H.C. Nonsense surveillance regulates expression of diverse classes of mammalian transcripts and mutes genomic noise. Nat Genet 36, 1073-1078 (2004).

14) Wang, D., Zavadil, J., Martin, L., Parisi, F., Friedman, E., Levy, D., Harding, H., Ron, D. & Gardner, L.B. Inhibition of Nonsense-mediated RNA decay by the tumor microenvironment promotes tumorigenesis. Mol Cell Biol 31, 3670-2680 (2011).

15) Lareau, L.F., Inada, M., Green, R.E., Wengrod, J.C. & Brenner, S.E. Unproductive splicing of SR genes associated with highly conserved and ultraconserved DNA elements. Nature 446, 926-929 (2007).

16) Ni, J.Z., Grate, L., Donohue, J.P., Preston, C., Nobida, N., O'Brien, G., Shiue, L., Clark, T.A., Blume, J.E. & Ares Jr., M. Ultraconserved elements are associated with homeostatic control of splicing regulators by alternative splicing and nonsense-mediated decay. Genes Dev 21, 708-718 (2007).

17) Hwang, J. & Maquat, L.E. Nonsense-mediated mRNA decay (NMD) in animal embryogenesis: to die or not to die, that is the question. Curr Opin Genet Dev. 21, 422-430 (2011).

18) Oren, Y.S., McClure, M.L., Rowe, S.M., Sorcher, E.J., Bester, A.C., Manor, M., Kerem, E., Rivlin, J., Zahdeh, F., Mann, M., Geiger, T. & Kerem, B. The unfolded protein response affects readthrough of premature termination codons. EMBO Mol Med 6, 685-701 (2014).

19) Popp, M.W. & Maquat, L.E. Attenuation of nonsense-mediated mRNA decay facilitates the response to chemotherapeutics. Nat Commun 6, 6632 (2015).

20) Hoeijmakers, J.H.J. DNA damage, aging, and cancer. N Engl J Med, 361, 1475-1485 (2009).

21) d'Adda di Fagagna, F., Reaper, P.M., Clay-Farrace, L., Fiegler, H., Carr, P., Von Zglinicki, T., Saretzki, G., Carter, N.P. & Jackson, S.P. A DNA damage checkpoint response in telomere-initiated senescence. Nature 426, 194-198 (2003).

22) Fumagalli, M., Rossiello, F., Clerici, M., Barozzi, S., Cittaro, D., Kaplunov, J.M., Bucci, G., Dobreva, M., Matti, V., Beausejour, C.M., Herbig, U., Longhese, M.P. & d'Adda di Fagagna, F. Telomeric DNA damage is irreparable and causes persistent DNA-damage-response activation. Nat Cell Biol 14, 355-365 (2012).

23) Herbig, U., Jobling, W.A., Chen, B.P., Chen, D.J. & Sedivy, J.M. Telomere shortening

triggers senescence of human cells through a pathway involving ATM, p53, and p21(CIP1), but not p16(INK4a). Mol Cell 14, 501–513 (2004).

24) Hewitt, G., Jurk, D., Marques, F.D., Correia-Melo, C., Hardy, T., Gackowska, A., Anderson, R., Taschuk, M., Mann, J. & Passos, J.F. Telomeres are favoured targets of a persistent DNA damage response in ageing and stress-induced senescence. Nat Commun 3, 708 (2012).

25) Takai, H., Smogorzewska, A. & de Lange, T. DNA damage foci at dysfunctional telomeres. Curr Biol 13, 1549–1556 (2003).

26) Talemi, S.R., Kollaravic, G., Lapytsko, A. & Schaber, J. Development of a robust DNA damage model including persistent telomere-associated damage with application to secondary cancer risk assessment. Sci Rep 5, 13540 (2015).

27) Bartkova, J., Rezaei N., Liontos M., Karakaidos P., Kletsas D., Issaeva N., Vassiliou L.V., Kolettas E., Niforou K., Zoumpourlis V.C., Takaoka, M., Nakagawa, H., Tort, F., Fugger, K., Johansson, F., Sehested, M,, Andersen, C.L., Dyrskjot, L., Orntoft, T., Lukas, J., Kittas, C., Helleday, T., Halazonetis, T.D., Bartek, J. & Gorgoulis, V.G. 2006. Oncogene-induced senescence is part of the tumorigenesis barrier imposed by DNA damage checkpoints. Nature 444, 633-637 (2006).

28) Chen, Y., Chen, P.L., Chen, C.F., Jiang, X. & Riley, D.J. Never-in-mitosis related kinase 1 functions in DNA damage response and checkpoint control. Cell Cycle 7, 3194-3201 (2008).

29) Di Micco R., Fumagalli M., Cicalese A., Piccinin S., Gasparini P., Luise C., Schurra C., Garre' M., Nuciforo P.G., Bensimon A., Maestro, R., Pelicci, P.G. & d'Adda di Fagagna, F. 2006. Oncogene-induced senescence is a DNA damage response triggered by DNA hyper-replication. Nature 444, 638-642 (2006).

30) Knobel, P.A., Kotov, I.N., Felley-Bosco, E., Stahel, R.A. & Marti, T.M. Inhibition of REV3 expression induces persistent DNA damage and growth arrest in cancer cells. Neoplasia 13, 961-970 (2011).

31) Martin, M., Terradas, M., Illiakis, G., Tusell, L. & Genesca, A. Breaks invisible to the DNA damage response machinery accumulate in ATM-deficient cells. Genes Chromosomes Cancer 48, 745-759 (2009).

32) Martin, N.T., Nakamura, K., Paila, U., Woo, J., Brown, C., Wright, J.A., Teraoka, S.N., Haghayegh, S., McCurdy, D., Schneider, M., Hu, H., Quinlan, A.R., Gatta, R.A. & Concannon, P. Homozygous mutation of MTPAP causes cellular radiosensitivity and persistent DNA double-strand breaks. Cell Death Dis 5, e1130 (2014).

33) Liu, M., Hales, B.F. & Robaire, B. Effects of four chemotherapeutic agents, bleomycin,

etoposide, cisplatin, and cyclophosphamide, on DNA damage and telomeres in a mouse spermatogonial cell line. Biol Reprod 90, 72 (2014).

34) Minieri, V., Saviozzi, S., Gambarotta, G., Lo lacono, M., Accomasso, L., Rocchietti, E.C., Gallina, C., Turinetto, V. & Giachino, C. Persistent DNA damage-induced premature senescence alters the functional features of human bone marrow mesenchymal stem cells. J Cell Mol Med 19, 734-743 (2015).

35) Soubeyrand, S., Pope, L. & Hache, R.J.G. Topoisomerase IIα-dependent induction of a persistent DNA damage response in response to transient etoposide exposure. Mol Onc 4, 38-51 (2010).

36) Canino C., Mori, F., Cambria, A., Diamantini, A., Germoni, S., Alessandrini, G., Borsellino, G., Galati, R., Battistini, L., Blandino, R., Facciolo, F., Citro, G., Strano, S., Muti, P., Blandino, G. & Cioce, M. SASP mediates chemoresistance and tumor-initiating-activity of mesothelioma cells. Oncogene 31, 3148-3163 (2012).

37) Davalos, A.R., Coppe, J.P., Campisi, J. & Desprez, P.Y. Senescent cells as a source of inflammatory factors for tumor progression. Cancer Metastasis Rev 29, 273-283 (2010).

38) Rodier, F. & Campisi, J. Four faces of cellular senescence. J Cell Biol 192, 547-556 (2011).

39) Rossiello, F., Herbig, U., Longhese, M.P., Fumagalli, M. & d'Adda di Fagagna, F. Irreparable telomeric DNA damage and persistent DDR signalling as a shared causative mechanism of cellular senescence and ageing. Curr Opin Genet Dev 26, 89-95 (2014).

40) Kuilman, T., Michaloglou, C., Mooi, W.J. & Peeper, D.S. The essence of senescence. Genes Dev 24, 2463-2479 (2010).

41) Muller, M. Cellular senescence: molecular mechanisms, in vivo significance, and redox considerations. Antioxid Redox Signal 11, 59-98 (2009).

42) Muñoz-Espín, D. & Serrano, M. Cellular senescence: from physiology to pathology. Nat Rev Mol Cell Biol 15, 482-496 (2014).

43) Salama, R., Sadaie, M., Hoare, M. & Narita, M. Cellular senescence and its effector programs. Genes Dev 28, 99-114 (2014).

44) Deng, Q., Liao, R., Wu, B.L. & Sun, P. High intensity ras signaling induces premature senescence by activating p38 pathway in primary human fibroblasts. J Biol Chem 279, 1050–1059 (2004).

45) Harada, G., Neng, Q., Fujiki, T. & Katakura, Y. Molecular mechanisms for the p38-induced

cellular senescence in normal human fibroblast. J Biochem 156, 283-290 (2014).

46) Iwasa, H., Han, J. & Ishikawa F. Mitogen-activated protein kinase p38 defines the common senescence-signalling pathway. Genes Cells 8, 131–144 (2004).

47) Kwong, J., Hong, L., Liao, R., Deng, Q., Han, J. & Sun, P. p38alpha and p38gamma mediate oncogenic ras-induced senescence through differential mechanisms. J Biol Chem. 284, 11237-11246 (2009).

48) Lanna, A., Henson, S.M., Escors, D. & Akbar, A.N. AMPK-TAB1 activated p38 drives human T cell senescence. Nat Immunol 15, 965-972 (2014).

49) Spallarossa, P., Altieri, P., Barisione, C., Passalacqua, M., Aloi, C., Fugazza, G., Frassoni, F., Podestà, M., Canepa, M., Ghigliotti, G. & Brunelli, C. p38 MAPK and JNK antagonistically control senescence and cytoplasmic p16INK4A expression in doxorubicin-treated endothelial progenitor cells. PLoS One 5, e15583 (2010).

50) Alimbetov, D., Davis, T., Brook, A.J., Cox, L.S., Faragher, R.G., Nurgozhin, T., Zhumadilov, Z. & Kipling, D. Suppression of the senescence-associated secretory phenotype (SASP) in human fibroblasts using small molecule inhibitors of p38 MAP kinase and MK2. Biogerontology 17, 305-315 (2016).

51) Alspach, E., Flanagan, K.C., Luo, X., Ruhland, M.K., Huang, H., Pazolli, E., Donlin, M.J., Marsh, T., Piwnica-Worms, D., Monahan, J., Novack, D.V., McAllister, S.S. & Stewart, S.A. p38MAPK plays a crucial role in stromal-mediated tumorigenesis. Cancer Discov 4, 716-729 (2014).

52) Bent, E.H., Gilbert, L.A. & Hemann, M.T. A senescence secratorty switch mediated by PI3K/AKT/mTOR activation controls chemoprotective endothelial secretory responses. Genes Dev 30, 1811-1821 (2016).

53) Freund, A., Patil, C.K. & Campisi, J. p38MAPK is a novel DNA damage response-independent regulator of the senescence-associated secretory phenotype. EMBO J 30, 1536-1548 (2011).

54) Alspach, E., Yujie, F. & Stewart, S.A. Senescence and the pro-tumorigenic stroma. Crit Rev Oncog 18, 549-558 (2013).

55) Coppe, J.P., Patil, C.K., Rodier, F., Sun, Y., Munoz, D.P., Goldstein, J., Nelson, P.S., Desprez, P.Y. & Campisi, J. Senescence-associated secretory phenotypes reveal cell-nonautonomous functions of oncogenic RAS and the p53 tumor suppressor. PLoS Biol 6, 2853-2868 (2008).

56) Gilbert, L.A. & Hemann, M.T. DNA damage-mediated induction of a chemoresistant niche.

Cell 143, 355-366 (2010).

57) Krtolica, A., Parrinello, S., Lockett, S., Desprez, P.Y. & Campisi, J. Senescent fibroblasts promote epithelial cell growth and tumorigenesis: A link between cancer and aging. Proc Natl Acad Sci USA 98, 12072-12077 (2001).

58) Liu, D. & Hornsby, P.J. Senescent human fibroblasts increase the early growth of xenograft tumors via matrix metalloproteinase. Cancer Res 67, 3117-3126 (2007).

59) Rodier, F., Coppe, J.P., Patil, C.K., Hoeijmakers, W.A., Munoz, D.P., Raza, S.R., Freund, A., Campeau, E., Davalos, A.R. & Campisi, J. Persistent DNA damage signaling triggers senescence-associated inflammatory cytokine secretion. Nat Cell Biol 11, 973-979 (2009).

60) Buganim, Y., Madar, S., Rais, Y., Pomeraniec, L., Harel, E., Solomon, H., Kalo, E., Goldstein, I., Brosh, R., Haimov, O., Avivi, C., Polak-Charcon, S., Goldfinger, N., Barshack, I. & Rotter, V. Transcriptional activity of ATF3 in the stromal compartment of tumors promotes cancer progression. Carcinogenesis 32, 1749-1757 (2011).

61) Kim, K.H., Park, B., Rhee, D.K. & Pyo, S. Acrylamide induces senescence in macrophages through a process involving ATF3, ROS, p38/JNK, and a telomerase-independent pathway. Chem Res Toxicol 28, 71-86 (2015).

62) Lu, D., Wolfgang, C.D. & Hai, T. Activating transcription factor 3, a stress-inducible gene, suppresses Ras-stimulated tumorigenesis. J Biol Chem 281, 10473-10481 (2006).

63) Yan, C., Lu, D., Hai, T. & Boyd, D.D. Activating transcription factor 3, a stress sensor, activates p53 by blocking its ubiquitination. EMBO J 24, 2425-2435 (2005).

64) Bulavin, D.V, Higashimoto, Y., Popoff, I.J., Gaarde, W.A., Basrur, V., Potapova, O., Appella, E. & Fornace, A.J. Jr. Initiation of a G2/M checkpoint after ultraviolet radiation requires p38 kinase. Nature 411, 102-107 (2011).

65) Cuadrado A. & Nebreda, A.R. Mechanisms and functions of p38 signalling. Biochem J 429, 403-417 (2010).

66) Han, J., Lee, J.D., Tobias, P.S. & Ulevitch, R.J. A MAP kinase targeted by endotoxin and hyperosmolarity in mammalian cells. Science 265, 808-811 (1994).

67) Rouse, J., Cohen, P., Trigon, S., Morange, M., Alonso-Llamazares, A., Zamanillo, D., Hunt, T. & Nebreda, A.R. A novel kinase cascade triggered by stress and heat shock that stimulates MAPKAP kinase-2 and phophorylation of the small heat shock proteins. Cell 78, 1027-1037 (1994).

68) Zarabun, T. & Han, J. Activation and signaling of the p38 MAP kinase pathway. Cell Res 15, 11-18 (2005).

69) Nickless, A., Jackson, E., Marasa, J., Nugent, P., Mercer, R.W., Piwnica-Worms, D. & You, Z. Intracellular calcium regulates nonsense-mediated mRNA decay. Nat Med 20, 961-966 (2014).

70) Yu, Y., Rajapakse, A.G., Montani, J.P., Yang, Z. & Ming, X.F. p38 mitogen-activated protein kinase is involved in arginase-II-mediated eNOS-uncoupling in obesity. Cardiovasc Diabetol 13:113. doi: 10.1186/s12933-014-0113-z (2014).

71) Chang, B.D., Swift, M.E., Shen, M., Fang, J., Broude, E.V. & Roninson, I.B. Molecular determinants of terminal growth arrest induced in tumor cells by a chemotherapeutic agent. Proc Natl Acad Sci USA 99, 389-394 (2002).

72) Hai, T., Wolfgang, C.D., Marsee, D.K., Allen, A.E. & Sivaprasad, U. ATF3 and stress responses. Gene Expr 7, 321-335 (1999).

73) Chen, F., Zhuang, X., Lin, L., Yu, P., Wang, Y., Shi, Y., Hu, G. & Sun, Y. New horizons in tumor microenvironment biology: challenges and opportunities. BMC Med 13, doi: 10.1186/s12916-015-0278-7 (2015).

74) Eckstein, N., Servan, K., Hildebrandt, B., Politz, A., von Jonquieres, G., Wolf-Kümmeth, S., Mapierski, I., Hamacher, A., Kassack, M.U., Budczies, J., Beier, M., Dietel, M., Royer-Pokora, B., Denkert, C. & Royer, H.D. Hyperactivation of the insulin-like growth factor receptor I signaling pathway is an essential event for cisplatin resistance of ovarian cancer cells. Cancer Res 69, 2996–3003 (2009).

75) Shree, T., Olson, O.C., Elie, B.T., Kester, J.C., Garfall, A.L., Simpson, K., Bell-McGuinn, K.M., Zabor, E.C., Brogi, E. & Joyce, J.A. Macrophages and cathepsin proteases blunt chemotherapeutic response in breast cancer. Genes Dev 25, 2465–79 (2011).

76) Williams, R.T., den Besten, W. & Sherr, C.J. Cytokine-dependent imatinib resistance in mouse BCR-ABL(+), Arf-null lymphoblastic leukemia. Genes Dev 21, 2283–7 (2007).

77) Tchkonia, T., Zhu, Y., van Deursen, J., Campisi, J. & Kirkland, J.L. Cellular senescence and the senescence secretory phenotype: therapeutic opportunities. J Clin Invest 123, 966-972 (2013).

78) Frevel, M.A., Bakheet, T., Silva, A.M., Hissong, J.G., Khabar, K.S. & Williams, B.R. p38 mitogen-activated protein kinase-dependent and -independent signaling of mRNA stability of AU-rich element-containing transcripts. Mol Cell Biol 23, 425-436 (2003).

79) Heidenreich, O., Neininger, A., Schratt, G., Zinck, R., Cahill, M.A., Engel, K., Kotlyarov, A., Kraft, R., Kostka, S., Gaestel, M. & Nordheim, A. MAPKAP kinase 2 phosphorylates serum response factor in vitro and in vivo. J Biol Chem 274, 14434-14443 (1999).

80) Tan, Y., Rouse, J., Zhang, A., Cariati, S., Cohen, P. & Comb, M.J. FGF and stress regulate CREB and ATF-1 via a pathway involving p38 MAP kinase and MAPKAP kinase-2. EMBO J 15, 4629-2642 (1996).

81) Vasudevan, S., Garneau, N., Tu Khounh, D. & Peltz, S.W. p38 mitogen-activated protein kinase/hog1p regulates translation of the AU-rich-element-bearing MFA2 transcript. Mol Cell Biol 25, 9753-9763 (2005).

82) Winzen, R., Gowrishankar, G., Bollig, F., Redich, N., Resch, K. & Holtmann, H. Distinct domains of AU-rich elements exert different functions in mRNA destabilization and stabilization by p38mitogen-activated protein kinase or HuR. Mol Cell Biol 23, 4835-4847 (2004).

83) Winzen, R., Kracht, M., Ritter, B., Wilhelm, A., Chen, C.Y., Shyu, A.B., Muller, M., Gaestel, M., Resch, K. & Holtmann, H. The p38 MAP kinase pathway signals for cytokine-induced mRNA stabilization via MAP kinase-activated proteinkinase 2 and an AU-rich region-targeted mechanism. EMBO J 18, 4969-4980 (1999).

84) Yamagiwa, Y., Marienfeld, C., Tadlock, L. & Patel, T. Translational regulation by p38 mitogen-activated protein kinase signaling during human cholangiocarcinoma growth. Hepatology 38, 158-166 (2003).

85) Zhao, W., Liu, M. & Kirkwood, K.L. p38α stabilizes interleukin-6 mRNA via multiple AU-rich elements. J Biol Chem 283, 1778-1785 (2008).

86) Knapinska, A.M., Gratacos, F.M., Krause, C.D., Hernandez, K., Jensen, A.G., Bradley, J.J., Wu, X., Pestka, S. & Brewer, G. Chaperone Hsp27 modulates AUF1 proteolysis and AU-rich element-mediated mRNA degradation. Mol Cell Biol 31,1419-1431 (2011).

87) Gardner, L.B. Nonsense-mediated RNA decay regulation by cellular stress: implications for tumorigenesis. Mol Cancer Res 8, 295-308 (2010).

88) Gammon, S.T., Leevy, W.M., Gross, S., Gokel, G.W. & Piwnica-Worms, D. Spectral unmixing of multicolored bioluminescence emitted from heterogeneous biological sources. Anal Chem 78, 1520-1527 (2006).

Chapter 4: Conclusion and future directions

4.1 Summary

The nonsense-mediated RNA decay (NMD) pathway is susceptible to regulation by a variety of developmental and environmental signals. We constructed a dual-color bioluminescent NMD reporter to elucidate the molecular signals that regulate NMD in mammalian cells and to identify drugs capable of manipulating NMD activity. We utilized this reporter to discover that the cardiac glycosides, calcium, persistent DNA damage, and osmotic stress repress NMD in human cells. We identified p38 as a negative regulator of NMD activity in response to persistent DNA damage. Regulation of NMD activity is a potent means of gene regulation, and we found that the repression of NMD by p38 after persistent DNA damage facilitates the upregulation of the stress responsive transcription factor ATF3, which is an NMD target.

4.2 Studying NMD using light-based reporters

Our bioluminescent NMD reporter is distinguished by its accuracy and simplicity; these advantages allowed me to perform a high-throughput chemical screen and make the discoveries described in chapters 2 and 3. The concept of dynamic NMD regulation is still relatively new and under-explored. Our reporter and others like it will prove invaluable to addressing unanswered questions in the field and advancing our understanding of this clinically relevant pathway, because it is ideally suited to identify novel NMD factors and regulators via genetic screens using RNAi or CRISPR/Cas-9 technology or NMD-modulating drugs through chemical screens..

Although our reporter has demonstrated an extraordinary ability to quickly assess NMD activity in populations of living cells, simple modifications can be made that will permit single-cell or even single-molecule analysis. For example, the insertion of GFP and mCherry (or other fluorophores) into the reporter will enable NMD assessment in single cells through fluorescence

microscopy or FACS analysis. It is important to consider the heterogeneity of cells within a population. Within a given population of genetically identical cells, morphological traits (e.g. size and shape) as well as gene expression, and signaling can vary widely from cell to cell[1,2]. Population-based measurements, like those made with our reporter—while expedient and generally informative—yield averages that sometimes obscure important patterns. A fluorescent NMD reporter would not only overcome this obstacle but would also be conducive to pooled genetic screens where numerous shRNAs or guide RNAs are introduced into cells, and those that elicit a response are isolated through cell sorting. Pooled libraries can vastly simplify the screening process and augment screening power by removing the need for hundreds of plates and individual experimental manipulations.

Studying NMD at an even finer level—that of single molecules—can address many outstanding questions in the field, such as where NMD occurs, and provide information regarding the kinetics of target identification and decay. Dual-color single molecule assays have been successfully used to interrogate multifarious aspects of gene expression including transcription and splicing[3]. These assays rely upon co-expressing fluorophore-tagged RNA binding proteins with reporter RNAs possessing binding sites for the tagged proteins. For example, addition of MS2 stem loops, which will associate with MS2-GFP, to the wild-type gene and PP7 stem loops, which will associate with PP7-mCherry, to the PTC-containing gene would facilitate examination of individual NMD target mRNAs whose abundance and behavior can be directly compared to controls within the same cell.

These variations on our current reporter design can further many aspects of NMD research, but perhaps the most significant modification is the simplest—replacing TCRβ with

other genes such as β-globin or triose phosphate isomerase. Many NMD researchers rely heavily on one or two reporter genes under the assumption that these reporters accurately reflect the fate of other NMD targets. Because of this, researchers corroborate reporter findings by assessing the stability and expression of endogenous NMD targets, but these results are complicated by the myriad mechanisms that regulate mRNA stability and gene expression. Employing multiple, defined luminescent reporters to rapidly assess NMD activity will vastly increase confidence in future findings.

4.3 Regulation of NMD by intracellular calcium

4.3.1 Targeting NMD with calcium-modulating drugs for therapeutic purposes

My work demonstrates that the cardiac glycosides (CGs) potently repress NMD activity by elevating cytoplasmic calcium levels and that other drugs that similarly increase calcium abundance also inhibit NMD. This discovery has profound clinical and physiological implications and raises many questions worthy of further research.

The therapeutic effects of many clinically prescribed drugs, including the cardiac glycosides themselves, stem from their ability to modulate intracellular calcium[4,5]. Many groups aspire to develop methods of treating genetic disorders by combinatorially inhibiting NMD and promoting translation stop codon read-through to restore expression of essential proteins whose genes harbor a nonsense mutation[6-8]. While a few chemicals are reported to specifically inhibit NMD with little or no observable toxicity, the safety and efficacy of these compounds has not been demonstrated in human clinical trials[8,9]. Repurposing existing, FDA-approved calcium-modifying drugs may expedite the development of NMD-based therapeutic strategies if these drugs alter NMD activity at their *in vivo* concentrations. To determine whether this is the case,

initial studies can be carried out in mice transgenically expressing the bioluminescent NMD reporter and, if efficacious, quickly extended to human studies.

In the same vein, the effects of calcium modifiers on NMD can be harnessed to target tumor cells. Genetic ablation of NMD activity in tumors can induce an antitumor immune response in certain mouse models[10]. Interestingly, the cardiac glycosides elicit a nearly identical response, and the administration of digoxin in combination with particular chemotherapeutics bolsters patient survival[11]. Whether the ability of the CGs to predispose tumor cells to immune-mediated death stems from effects on NMD is currently unclear, and determining whether this is the case may prove difficult. Observing similar effects when using other calcium modifiers would provide indirect evidence consistent with the hypothesis that NMD mediates the antitumor effects; however, any conclusions would be complicated by the many diverse functions of calcium in immune development and function[12]. To conclusively test the hypothesis that NMD mediates the antitumor effects of the CGs, a means of specifically restoring NMD activity in CG-treated tumor cells must be utilized. Identifying a highly specific means of restoring NMD activity will likely require a detailed mechanistic understanding of how calcium represses NMD. It is therefore critical to determine whether any calcium-dependent signaling proteins (e.g. Calmodulin, CAMKK) mediate the inhibition of NMD and, if so, to fully elucidate this pathway.

4.3.2 The molecular mechanism of NMD inhibition by calcium

Scores of proteins are sensitive to the presence of calcium, including many kinases, phosphatases, G-proteins, and other prominent signaling molecules with the potential to influence NMD either directly or indirectly[13]. Indeed, multiple NMD factors are phosphoproteins that may be particularly susceptible to regulation by calcium-dependent kinases or

phosphatases[14-16]. Computationally searching NMD factor proteins for sequences or motifs recognized by calcium-dependent molecules may reveal potential interactions essential for this regulation. Additionally, a suppressor screen can identify proteins that promote calcium-mediated NMD repression: abrogation of signaling proteins necessary for this regulation will render NMD insensitive to calcium. Of course, it is possible that calcium directly binds to and alters the activity of an NMD factor, although no known NMD factors contain classical calcium-binding motifs such as the EF-hand, EGF-like, and C2 domains[17-19].

It is also important to ascertain how these calcium-dependent signals negatively impact the process of NMD itself. Currently, six known mechanisms exist for repressing NMD: (1) increased efficiency of SMD (which competes with NMD), (2) UPF1 cleavage, (3) downregulation of NMD factors (4) UPF3a upregulation, (5) disruption of interactions between NMD factors, and (6) eIF2α phosphorylation[8,9,20-26]. The possibility that calcium increases SMD efficiency has not yet been explored, but I have addressed the remaining options to various degrees. To examine the possibility that UPF1 cleavage occurs in high-calcium environments, I immunoblotted for UPF1; no UPF1 cleavage products are evident in CG- or thapsigargin-treated cells, precluding this possibility (Fig. 1 and data not shown). Furthermore, UPF1 cleavage is only known to occur during apoptosis, and these treatments do not significantly affect cell viability (Chapter 2 Supplementary Fig. 3). To determine whether calcium disrupts expression of one or more NMD factors, I performed immunoblots and qPCRs for key factors and found that none of the factors assessed were significantly downregulated at the mRNA or protein level in response to CG-treatment (Fig. 2; Chapter 2 Supplementary Fig. 5). However, some factors were not included in these studies so it remains possible that calcium-mediated NMD inhibition may

result from downregulation of an essential NMD component. Notably, UPF3b expression remains robust in CG-treated samples; since UPF3b destabilizes UPF3a proteins, it is unlikely that high levels of UPF3a contribute to CG-mediated NMD inhibition (Fig. 2). Similarly, CG treatment does not ostensibly disturb any protein-protein interactions necessary for proper NMD, but I only examined a fraction of the critical interactions (Fig. 3). Finally, to determine whether eIF2α phosphorylation mediates the repression of NMD by calcium, I assayed its phosphorylation in both high and low calcium environments. Although the CGs and thapsigargin markedly induce eIF2α phosphorylation at serine 51, this site remains robustly phosphorylated even in the presence of Bapta-AM, which reverses the inhibitory phenotype (Fig. 4). This argues against the hypothesis that eIF2α phosphorylation inhibits NMD in high calcium environments; however, these results are preliminary and should be repeated before drawing firm conclusions. Additional experiments using mutant versions of eIF2α will conclusively demonstrate whether eIF2α is involved in the regulation of NMD by calcium. In summation, a myriad of ways exist for reducing NMD activity and, while I have excluded many obvious possibilities, more in-depth studies will be required to ascertain the mechanism by which calcium represses NMD.

Another possibility is that, although NMD is ostensibly regulated by calcium, the inhibitory effects of the CGs, thapsigargin, and calcium ionophores actually reflect the induction of ER stress, which induces eIF2α phosphorylation[27,28]. Indeed, depletion of calcium stores from the endoplasmic reticulum causes ER stress and Bapta-AM treatment may prevent this depletion from occurring[11,29-31]. If so, it is not the increase in cytoplasmic calcium that inhibits NMD but is in truth the relocalization of calcium from the ER to the cytoplasm. This possibility can be examined by monitoring ER stress markers in cells treated with our calcium-elevating drugs both

in the presence and absence of Bapta-AM. The drugs will likely increase detection of ER stress markers. If the presence of Bapta-AM abates detection of ER stress markers, NMD activity correlates with ER stress, and this connection should be further explored.

4.3.3 The physiological roles of calcium-mediated NMD regulation

In addition to characterizing the signaling pathway linking calcium to NMD and its effects on the NMD machinery, another important extension of my work will be to characterize the physiological relevance of this regulation. Many cell types, such as pancreatic β-cells and muscle cells, rely heavily upon calcium signaling for normal function[32,33]. It will be interesting to see whether calcium suppresses NMD activity in these cell types and, if so, whether this contributes to gene expression changes. I am most excited, however, by the possibility that calcium-mediated NMD regulation in the nervous system contributes to neuronal development and function. Indeed, NMD has many important roles in neurons, and defects in NMD cause errant synaptic behavior and a host of neurodevelopmental disorders[34-44].

The ability of calcium to control NMD activity potentially adds new dimensions to gene regulation by NMD in neurons. For example, action potential firing induces calcium release, and calcium levels can spike locally for many seconds[45-47]. It is conceivable that highly active neurons—or even localized neuronal regions—sustain increases in calcium abundance for long enough to repress NMD. Indeed, I have preliminary evidence suggesting that this may be the case. In a pilot experiment, I found that depolarization of embryonic mouse cortical neurons with KCl repressed NMD activity while NaCl, which served as a control for ionic strength, did not (Fig. 5). This result may actually underestimate the extent of activity-dependent NMD inhibition in neurons as many astrocytes were cultured alongside the neurons, and these cells are not

predicted to respond to KCl in the same manner (although they might be experiencing NMD inhibition as a result of osmotic shock). The inclusion of Ara C or similar compounds in the growth medium that restrict astrocyte proliferation may circumvent this issue. Additionally, longer treatment times, like those used in certain high-profile papers, may accentuate the inhibition of NMD[48]. If NMD is regulated in an activity-dependent manner, it may in turn alter the expression of NMD targets. Interestingly, one of the most prominent activity-regulated genes, Arc, has two 3' UTR introns and is actively degraded by NMD[49,50]. Arc is a critical promotor of synaptic plasticity, and reduced negative regulation of Arc by NMD may facilitate increases in expression and augment synaptic plasticity[49,50]. This is but one example of a physiological setting where NMD may be susceptible to repression by calcium.

4.4 Regulation of NMD by persistent DNA damage

In this dissertation, I demonstrated that p38 suppresses NMD activity in response to persistent, but not transient, DNA damage signals, and that this repression likely contributes to the upregulation of ATF3—a stress-response gene that mediates crucial functions in cells harboring persistent DNA damage with both pro- and anti-tumorigenic consequences[51-55]. Furthermore, I show that although p38 is activated by osmotic shock, it does not regulate NMD in this context, which suggests that persistent DNA damage generates another signal or induces expression of an alternative p38 target which cooperates with p38 to regulate NMD after damage. These findings illuminate new facets of gene regulation by both p38 and NMD. They also raise many questions to be addressed by future research. What is the cooperating signal that works with p38 to suppress NMD activity? How does it work with p38 to repress NMD? What other genes are regulated by NMD after persistent DNA damage? What effects does this

regulation have on the damaged cells and their neighbors? These questions and their physiological and clinical implications will be the subject of this section.

4.4.1 Identity of the signals that function alongside p38 to repress NMD in response to DNA damage

Regarding the identity of the cooperating signal, it must originate from the DNA damage response (DDR). This implicates ATM, ATR, and DNA-PK—three kinases paramount to the DDR—as the source of signal[56]. Entertaining this possibility, I chemically inhibited the activity of these kinases in cells harboring persistent DNA damage. Both ATM and ATR inhibition reduced the relative extent of bleomycin-mediated NMD inhibition, consistent with the notion that these proteins are necessary for NMD inhibition in response to persistent DNA damage (Fig. 6a-b). However, the reduced extent of bleo-mediated NMD inhibition in ATRi- and ATMi-treated cells is not caused by an inability to fully repress NMD; rather it is a byproduct of low basal levels of NMD in the inhibitor treated cells in the absence of DNA damage (Fig. 6a-b). The inhibitory effect of these inhibitors on NMD is intriguing but may result from non-specific inhibition of the SMG1 kinase, which belongs to the same molecular family[57]. Consequently, these results are difficult to interpret and further studies are required to conclusively elucidate the role of ATM and ATR in regulating NMD after persistent DNA damage. As such, genetic studies will be paramount to future research in this area. The DNA-PK inhibitor results are far less equivocal and strongly suggest that DNA-PK is not involved in the regulation of NMD in RPE1 cells with a protracted DDR (Fig. 6c).

ATM is the most promising cooperating signal candidate as it augments p38 function in other contexts and is highly active in non-proliferating cells with persistent DNA damage[58-60]. In

contrast, ATR functions primarily in S-phase[56]. Of course the cooperating signal may not depend on either of these kinases. Intriguingly, the cooperating signal may reside in the eIF2α pathway. Conditions brought about by persistent damage signaling may promote p38-dependent eIF2α phosphorylation; this possibility also provides a mechanistic explanation for how p38 regulates NMD.

4.4.2 The molecular mechanism of NMD inhibition by persistent DNA damage

The molecular mechanism underlying the regulation of NMD by protracted DNA damage signals also remains mysterious, but eIF2α phosphorylation may contribute. Indeed, I occasionally observed robust eIF2α phosphorylation in bleomycin-treated cells, although no increase was observed in the majority of experiments (data not shown). Notably, p38 activity is known to promote eIF2α phosphorylation in certain contexts[61,62]. Whether eIF2α phosphorylation regulates NMD when DNA damage signals linger can be confirmed by expressing the eIF2α S51A mutant which cannot be phosphorylated; expression of this mutant will prevent NMD inhibition by persistent DNA damage signals if eIF2α phosphorylation is essential for this regulation. If confirmed, eIF2α will be further cemented as the master regulator of NMD during cellular stress.

Of course, persistent DNA damage may inhibit NMD through any of the other mechanisms enumerated in section 4.3.2 (downregulation of NMD factor expression, disruption of NMD complex formation, UPF1 cleavage, upregulation of UPF3a, or activation of a competing degradation pathway) or through a completely novel mechanism. However, preliminary assessments of NMD factor mRNA and protein levels argue against many of these possibilities. I did not find that any key NMD factor mRNAs or proteins are signficantly

downregulated in bleomycin-treated cells (Table 1). Notably, UPF3b, which destabilizes UPF3a proteins, maintains robust expression in damaged cells (Table 1). Furthermore, UPF1 western blots give no indication of UPF1 cleavage after bleomycin treatment, and our sub-lethal concentrations of bleomycin are not predicted to activate the caspases responsible for cleaving UPF1 (Fig. 7). All of these results are preliminary however, so firm conclusions should no be drawn at this time. Indeed, much work remains to be done to determine how persistent DNA damage impinges upon the process of NMD.

4.4.3 The physiological roles of persistent DNA damage-mediated NMD regulation

Even without a complete understanding of the molecular underpinnings of NMD repression in response to DNA damage, the significance of this regulation can be further explored. As a proof-of-concept, I demonstrated that NMD facilitates the stabilization of ATF3 mRNAs, which—in conjunction with transcriptional upregulation—presumably accounts for the substantial increases in ATF3 mRNA and protein expression observed by myself and others (Chapter 3 Fig. 4)[63]. ATF3 promotes senescence in cells undergoing excessive mitogenic or genotoxic stress, thereby stifling tumor formation and growth[64-66]. Moreover, ATF3 reprograms the cellular secretome, making it far more pro-tumorigenic[52]. Indeed, ATF3 significantly influences diverse aspects of tumor biology, and its regulation by NMD may be exploited for therapeutic gain. Furthermore, many other genes frequently implicated in oncogenic transformation—including many pro-tumorigenic components of the Senescence Associated Secretory Phenotype (SASP) such as IL6 and CXCL2—are also putative NMD targets[25,67,68]. My approach to demonstrating the regulation of ATF3 by NMD can be expanded with RNA-sequencing to reveal the full repertoire of NMD targets upregulated following persistent DNA

damage. This information will prove useful when functionally examining the effects of NMD-dependent gene regulation on tumorigenesis.

DNA damage is a hallmark of many tumor cells—due to their genomic instability—and their neighboring cells, as senescent cells with prolonged DDRs encourage tumor growth[67,69]. It therefore seems likely that NMD activity is reduced in these cells and may impact tumor growth. To test this hypothesis, NMD activity will need to be selectively restored in both the tumor microenvironment and/or the tumor itself to discern how NMD influences the kinetics and extent of tumor growth. While I demonstrated that p38 inhibition restores NMD activity in cells harboring persistent DNA damage, p38 inhibitors are incapable of specifically probing the role of NMD in these cells as p38 affects multifarious cellular processes[70]. If eIF2α phosphorylation underlies NMD inhibition in these settings, expression of the eIF2α S51A mutant may serve this purpose; however, it too impacts multiple cellular processes[71]. Perhaps the most specific method of reversing NMD will be to overexpress UPF1, which increases NMD activity significantly[24,25,72]. If indeed NMD inhibition in the tumor microenvironment promotes tumor formation and development, UPF1 overexpression in these cells will impede tumor growth in xenograft models. Similarly, the cell autonomous influence of NMD on cancer growth can be interrogated by overexpressing UPF1 in the tumor cells themselves. It seems likely that the effects will depend upon the tumor type and specific transforming mutations, and a thorough study of how NMD influences oncogenesis in both cell autonomous and non-autonomous manners will clarify the currently ambiguous effects of NMD on cancer biology. Such knowledge will also facilitate development of therapeutic strategies that target tumor growth by modulating NMD activity in tumor cells and the tumor microenvironment.

4.4.4 Targeting NMD for cancer treatment

The ability of p38 to regulate NMD and drive SASP expression in cells harboring persistent DNA damage makes it a promising therapeutic target. Encouragingly, p38 inhibition reduces tumor volume in murine xenograft breast cancer models, presumably due to attenuated SASP expression[73]. Indeed, p38 drives SASP expression by augmenting NF-κB transcription activity and stabilizing SASP factor mRNAs[73-75]. Canonically, p38 influences mRNA stability by altering the activity of RNA binding proteins such as AUF1[73,76]. My studies reveal a novel means by which p38 can stabilize mRNAs and enhance gene expression—NMD repression. In addition to expanding the gene-regulatory repertoire of p38, my studies also allude to a negative feedback loop that diminishes p38 activity in cells exposed to hyperosmotic conditions. The chemical ablation of p38 activity causes p38 hyperphosphorylation in cells experiencing hyperosmotic shock, an effect likely caused by an inability of downstream p38 dependent signals to negatively regulate p38 activation (Fig. 8 and data not shown). While this is completely speculatory, it is possible that NMD promotes this feedback mechanism, because GADD45, an upstream activator of p38 kinase activity, is a well-characterized NMD target[21,77,78]. The new relationship between p38 and NMD raises many questions that will require further investigation and provides a new avenue for cancer treatment.

4.5 Final Thoughts

Nonsense-mediated RNA decay has been assiduously studied for more than thirty years. During this period a wealth of structural and functional data has provided insight into the nature of NMD, its mechanism, and its relevance. Indeed, the current state of NMD research has been described as, “approaching the end of its beginning,” meaning that most principle enzymatic

components have been identified and their functions somewhat elucidated[79]. Future work will largely focus on the complex regulatory networks that govern the activity of NMD in a developmental stage- and tissue-specific manner. The contribution of NMD to disease states, particularly mental disorders and cancer, will constitute a second major direction of NMD research. Progress in these areas will facilitate the development of therapeutic regimens for the treatment of simple genetic disorders and cancers by modulating NMD activity.

Such ponderous tasks, along with elucidating the remaining mechanistic unknowns, present novel challenges to NMD researchers. As the questions of the field become increasingly complex, progress becomes increasingly difficult. The cumbersome RNA-based methods of NMD analysis such as RT-PCR and northern blot, which rely upon RNA isolation and quantification, are not suitable for efficiently elucidating components of vast regulatory networks or identifying compounds capable of saving and improving lives. To effectively address these challenges, new tools—such as the reporter we developed and its future iterations—will be imperative to advance the field and translate discoveries to the clinic.

These tools will facilitate the complete characterization of the NMD pathway and, when complemented by genetic studies in model organisms, the physiological functions of NMD will be elucidated. The vast majority of NMD studies are currently performed in tissue culture models, which provide only a narrow glimpse of insight into NMD regulation during development or in tissue-specific manners. Future studies will rely heavily upon tissue-specific NMD mutant animals to tease out the contribution of NMD to proper development and tissue homeostasis. Genetic manipulation of NMD *in vivo*—combined with state-of-the-art reporter assays, high-throughput sequencing, and improved experimental and computational tools for

identifying NMD targets—will undoubtedly initiate a new era of NMD research heavily focused on its dynamic gene regulatory functions.

With our NMD reporter, we have laid a foundation upon which future NMD researchers can build. Our reporter can be introduced into model organisms and used to characterize the roles of NMD *in vivo*. Furthermore, discoveries made with our NMD reporter—the regulation of NMD by clinically relevant drugs (CGs), physiologically essential molecules (calcium and p38), and common cellular stresses (persistent DNA damage and osmotic shock)—have numerous clinical and physiological implications. Additional studies will continue to define the mechanism and significance of NMD regulation in mammalian cells.

4.6 Figures

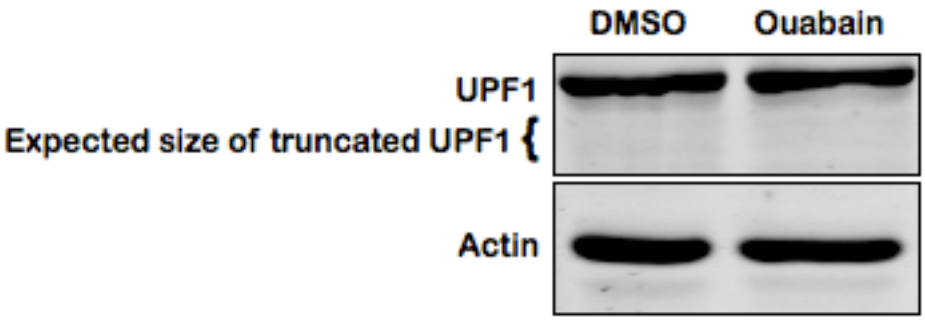

Figure 1. Effects of ouabain on UPF1 cleavage product generation.

Western blot analysis of UPF1 protein levels in U2OS reporter cells treated with DMSO or Ouabain for 24 hours at 0.175μM. Results shown are representative of multiple independent experiments.

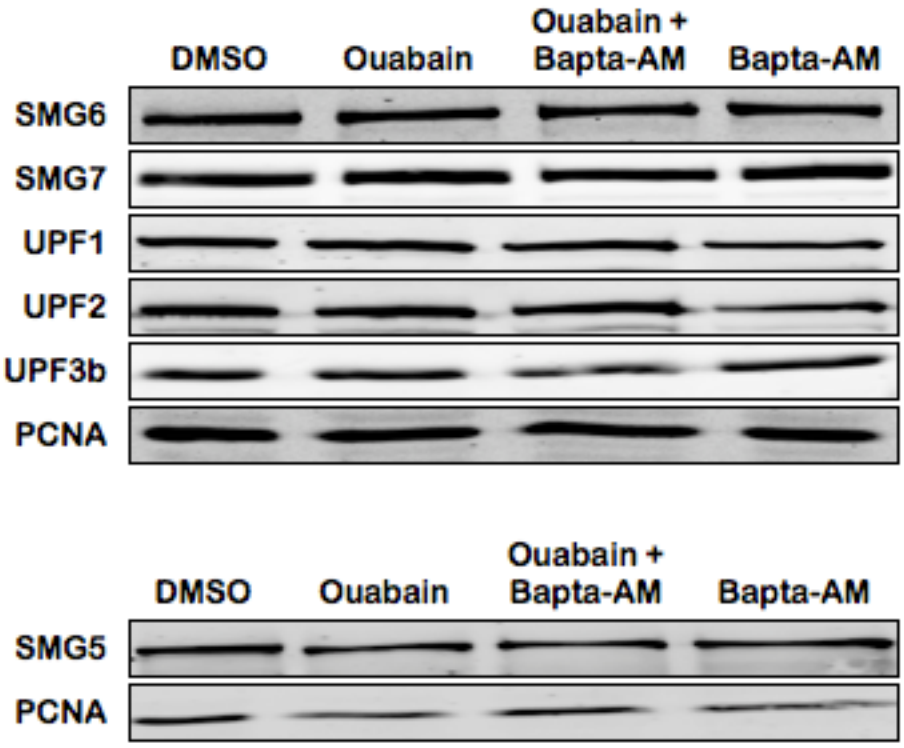

Figure 2. Effects of ouabain and Bapta-AM on the protein levels of key NMD factors.

Western blot analysis of NMD factor levels in U2OS reporter cells following 24 hours treatment with DMSO, ouabain, ouabain and Bapta-AM, or Bapta-AM. Ouabain, 0.175 μM; Bapta-AM, 25 μM. Results shown are representative of multiple independent experiments.

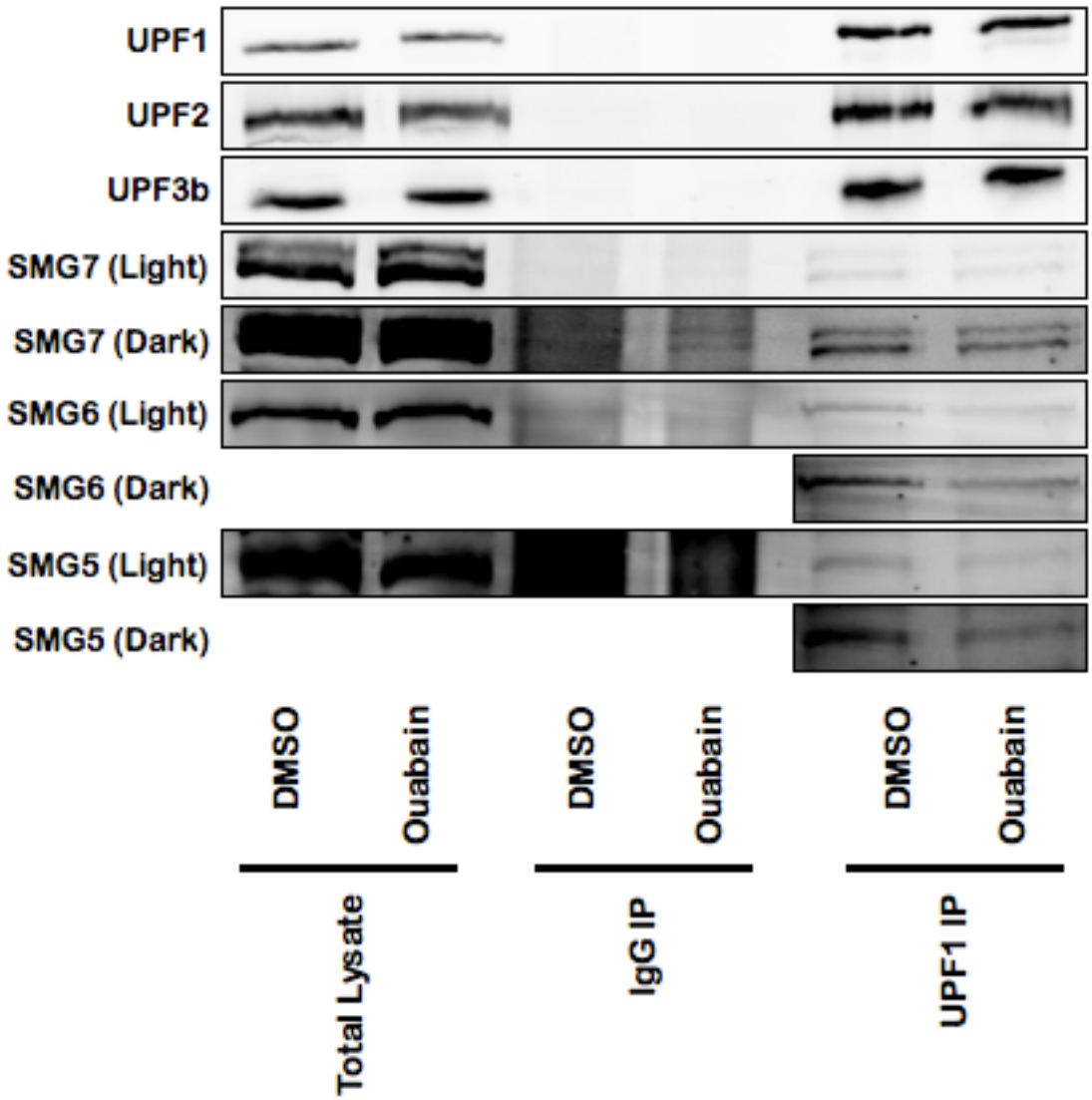

Figure 3. Effects of ouabain on NMD complex formation.

Interactions between components of the NMD machinery in U2OS cells treated with either DMSO or ouabain for 24 hours. U2OS cell lysates were immunoprecipitated with a UPF1 antibody. Immunoprecipitates were analyzed by western blotting with the indicated antibodies. Results shown are representative of multiple independent experiments.

a)

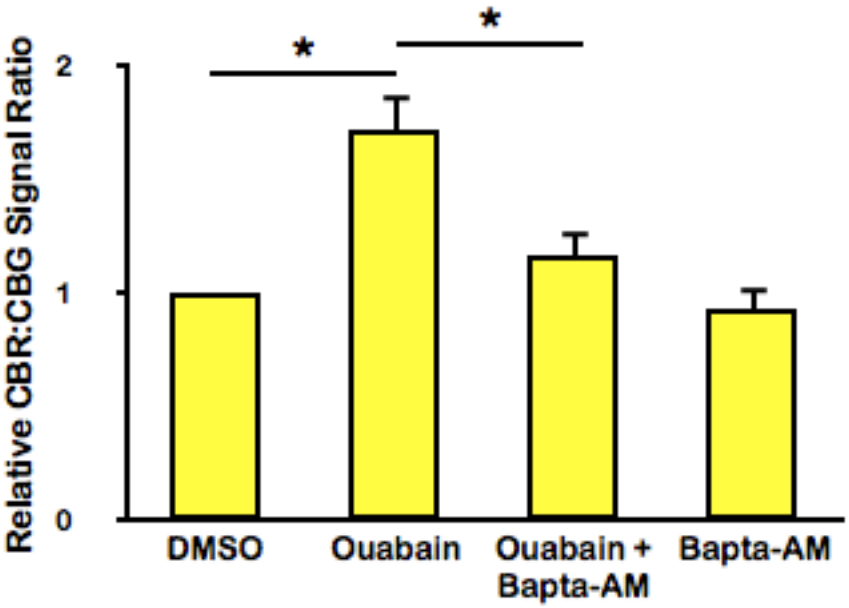
Relative CBR:CBG Signal Ratio
2
1
0
*
*
DMSO
Ouabain
Ouabain + Bapta-AM
Bapta-AM

b)

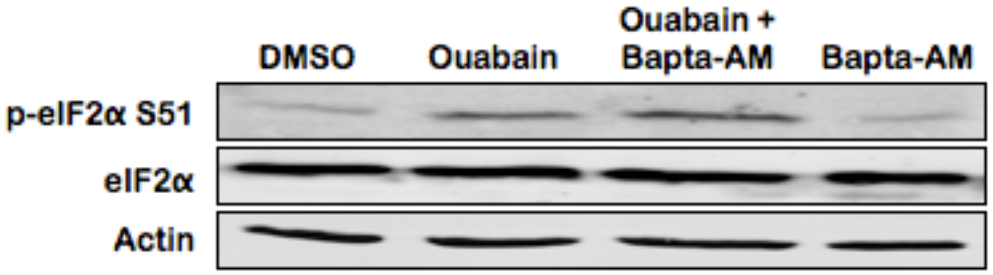
DMSO
Ouabain
Ouabain + Bapta-AM
Bapta-AM
p-eIF2α S51
eIF2α
Actin

Figure 4. Effects of ouabain and Bapta-AM on NMD activity and eIF2α phosphorylation.

a). Ratios of CBR/CBG bioluminescence signals in human U2OS reporter cells following 24 hours treatment with DMSO, ouabain, ouabain and Bapta-AM, or Bapta-AM. Ouabain, 0.175 μM; Bapta-AM, 25 μM and subsequently lysed for protein collection. Data represent the mean ± SD of three independent experiments. The ratio in DMSO-treated cells was normalized to 1.

b). Western blot analysis of eIF2α phosphorylation in human U2OS reporter cells following 24 hours treatment with DMSO, ouabain, ouabain and Bapta-AM, or Bapta-AM. Ouabain, 0.175 μM; Bapta-AM, 25 μM. Results shown are representative of three independent experiments.

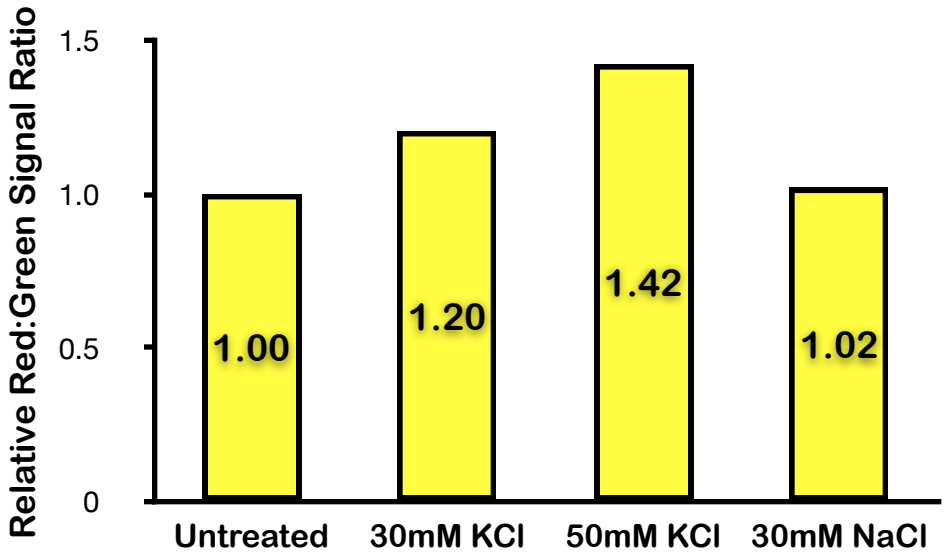

Figure 5. Effects of KCl-mediated depolarization on NMD in mouse embryonic cortical neurons.

Ratios of CBR/CBG bioluminescence signals in murine embryonic cortical neurons following an 8 hour treatment with control medium or medium supplemented with the indicated concentrations of KCl or NaCl. Data from a single experiment.

a)

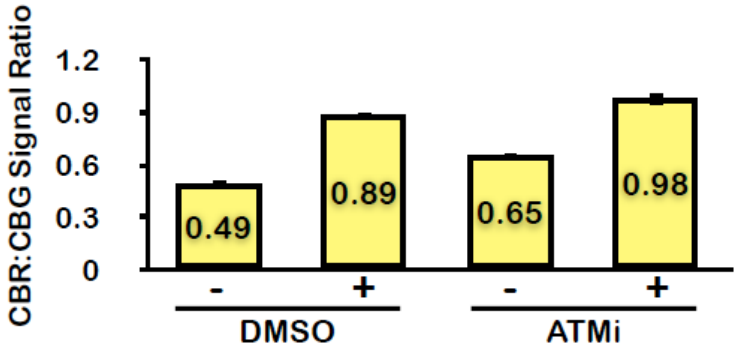
CBR:CBG Signal Ratio
1.2
0.9
0.6
0.3
0
0.49
0.89
0.65
0.98
-
+
-
+
DMSO
ATMi

b)

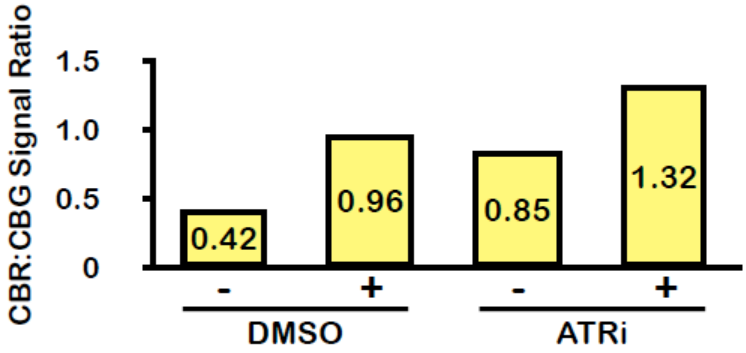
CBR:CBG Signal Ratio
1.5
1.0
0.5
0
0.42
0.96
0.85
1.32
-
+
-
+
DMSO
ATRi

c)

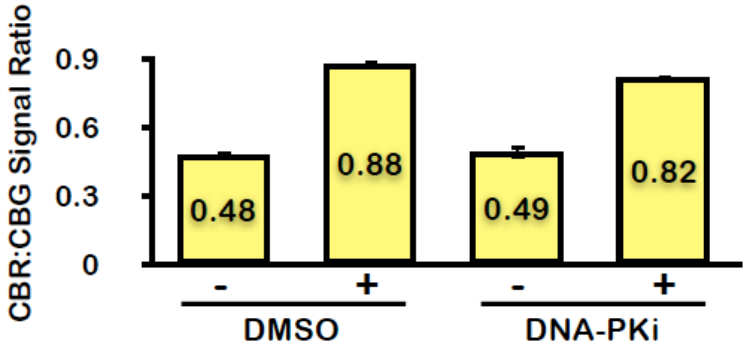
CBR:CBG Signal Ratio
0.9
0.6
0.3
0
0.48
0.88
0.49
0.82
-
+
-
+
DMSO
DNA-PKi

Figure 6. Effects of DNA damage response kinase inhibitors on NMD in bleomycin-treated cells.

a). Ratios of CBR/CBG bioluminescence signals in DMSO- or ATMi-treated RPE1 reporter cells after a 24 hr treatment with either H_2O or bleomycin followed by a 96 hr recovery. The ratio of CBR/CBG signals in H_2O-treated cells was normalized to 1. Data represent the mean ± SD of three independent experiments.

b). Ratios of CBR/CBG bioluminescence signals in DMSO- or ATRi-treated RPE1 reporter cells after a 24 hr treatment with either H_2O or bleomycin followed by a 96 hr recovery. The ratio of CBR/CBG signals in H_2O-treated cells was normalized to 1. Data represent the results of a single experiment.

c). Ratios of CBR/CBG bioluminescence signals in DMSO- or DNA-PK-treated RPE1 reporter cells after a 24 hr treatment with either H_2O or bleomycin followed by a 96 hr recovery. The ratio of CBR/CBG signals in H_2O-treated cells was normalized to 1. Data represent the mean ± SD of three independent experiments.

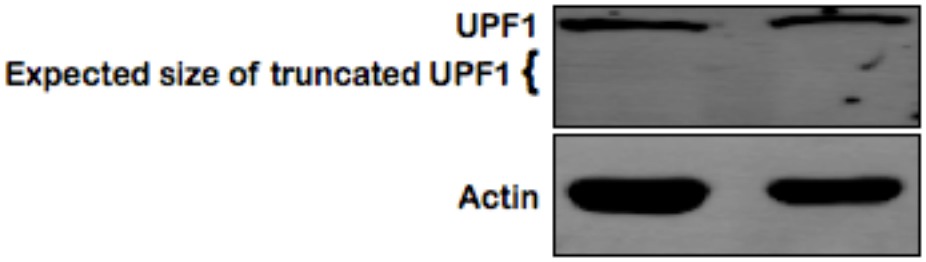

Figure 7. Effects of bleomycin on UPF1 cleavage product generation.

Western blot analysis of UPF1 protein levels in RPE1 cells after a 24 hr treatment with either H_2O or bleomycin followed by a 96 hr recovery. Data represent the results of a single experiment.

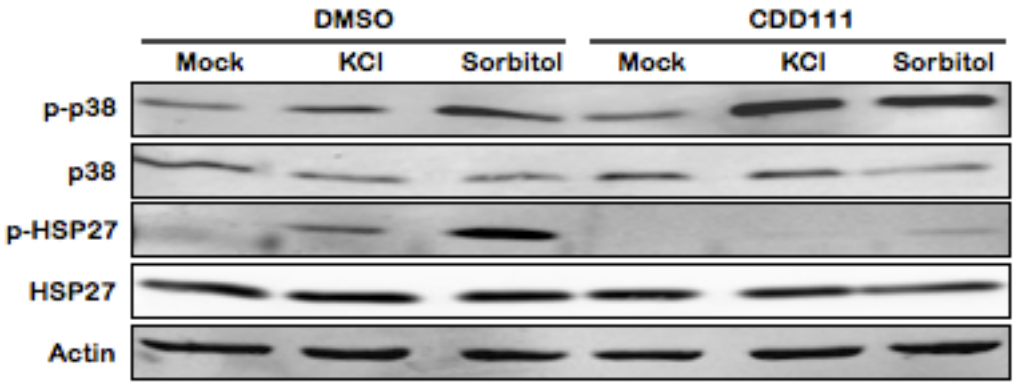

Figure 8. Effects of p38 inhibition on p38 phosphorylation in cells experiencing hyperosmotic shock.

Levels of total and phosphorylated p38 and HSP27 in DMSO- and CDD111- RPE1 cells after a 5 hr treatment with 80mM KCl or 275mM Sorbitol. Results shown are representative of three independent experiments.

4.7 Tables

Table 1: Relative NMD factor expression in bleomycin-treated RPE1 cells relative to H_2O-treated control cells. Steady-state mRNA and protein levels of key NMD factors in RPE1 reporter cells after a 24 hr treatment with either H_2O or bleomycin followed by a 96 hr recovery. Values represent the fold-change in expression relative to H_2O-treated cells. Results shown are representative of a single experiment.

Gene	mRNA	Protein
Upf1	1.78	1.59
Upf2	1.49	Not Assessed
Upf3b	1.42	1.67
SMG1	2.27	1.21
SMG5	1.88	Not Assessed
SMG6	1.37	1.22
SMG7	2.21	Not Assessed

4.8 References

1) Wang, D. & Bodovitz, S. Single cell analysis: the new frontier in 'omics.' Trends Biotechnol 28, 281-290 (2010).

2) Altschuler, S.J. Cellular heterogeneity: do differences make a difference? Cell 141, 559-563 (2010).

3) Coulon, A., Ferguson, M.L., de Turris, V., Palangat, M., Chow, C.C. & Larson, D.R. Kinetic competition during the transcription cycle results in stochastic RNA processing. eLife 3, e03939 (2014).

4) Gheorghiade, M., Adams., K.F. & Colucci, W.S. Digoxin in the management of cardiovascular disorders. Ciruculation 109, 2959-2964 (2004).

5) Katz, A.M., Hager, W.D., Messineo, F.C. & Pappano, A.J. Cellular actions and pharmacology of the calcium channel blocking drugs. Am J Med 7, 2-10 (1984).

6) Keeling, K.M., Wang, D., Dai, Y., Murugesan, S., Chenna, B., Clark, J., Belakhov, V., Kandasamy, J., Velu, S.E., Baasov, T. & Bedwell, D.M. Attenuation of nonsense-mediated mRNA decay enhances in vivo nonsense suppression. PLoS One. 8, e60478 (2013).

7) Du, M., Liu, X., Welch, E.M., Hirawat, S., Peltz, S.W. & Bedwell, D.M. PTC124 is an orally bioavailable compound that promotes suppression of the human CFTR-G542X nonsense allele in a CF mouse model. Proc Natl Acad Sci U S A. 105, 2064-2069 (2008).

8) Martin, L., Grigoryan, A., Wang, D., Wang, J., Breda, L., Rivella, S., Cardozo, T. & Gardner, L.B. Identification and characterization of small molecules that inhibit nonsense-mediated RNA decay and suppress nonsense p53 mutations. Cancer Res. 74, 3104-3113 (2014).

9) Durand, S., Cougot, N., Mahuteau-Betzer, F., Nguyen, C.H., Grierson, D.S., Bertrand, E., Tazi, J. & Lejeune, F. Inhibition of nonsense-mediated mRNA decay (NMD) by a new chemical molecule reveals the dynamic of NMD factors in P-bodies. J Cell Biol. 178, 1145-1160 (2007).

10) Pastor, F., Kolonias, D., Giangrande, P.H. & Gilboa, E. Induction of tumour immunity by targeted inhibition of nonsense-mediated mRNA decay. Nature. 465, 227-230 (2010).

11) Menger, L., Vacchelli, E., Adjemian, S., Martins, I., Ma, Y., Shen, S., Yamazaki, T., Sukkurwala, A.Q., Michaud, M., Mignot, G., Schlemmer, F., Sulpice, E., Locher, C., Gidrol, X., Ghiringhelli, F., Modjtahedi, N., Galluzzi, L., André, F., Zitvogel, L., Kepp, O. & Kroemer, G. Cardiac glycosides exert anticancer effects by inducing immunogenic cell death. Sci Transl Med 4, 143ra199 (2012).

12) Schwarz, E.C.,. Qu, B. & Hoth, M. Calcium, cancer and killing: the role of calcium in killing cancer cells by cytotoxic T lymphocytes and natural killer cells. Biochim Biophys Acta 1833, 1603-1611 (2013).

13) Berridge, M.J., Bootman, M.D. & Roderick, H.L. Calcium signalling: dynamics, homeostasis and remodelling. Nat Rev Mol Cell Biol 4, 517-529 (2003).

14) Chiu, S.Y., Serin, G., Ohara, O. & Maquat, L.E. Characterization of human SMG5/7a: a protein with similarities to Caenorhabditis elegans SMG5 and SMG7 that functions in the dephosphorylation of UPF1. RNA 9, 77-87 (2003).

15) Yamashita, A., Ohnishi, T., Kashima, I., Taya, Y. & Ohno, S. Human SMG-1, a novel phosphatidylinositol 3-kinase-related protein kinase, associates with components of the mRNA surveillance complex and is involved in the regulation of nonsense-mediated mRNA decay. Genes Dev 15, 2215–2228 (2001).

16) Pal, M., Ishigaki, Y., Nagy, E. & Maquat, L.E. Evidence that phosphorylation of human Upfl protein varies with intracellular location and is mediated by a wortmannin-sensitive and rapamycin-sensitive PI 3-kinase-related kinase signaling pathway. RNA 7, 5–15 (2001).

17) Nalefski, E.A. & Falke, J.J. The C2 domain calcium-binding motif: structural and functional diversity. Protein Sci 5, 2375-2390 (1996).

18) Lewit-Benley, A. & Rety, S. EF-hand calcium-binding proteins. Curr Opin Struct Biol 10, 637-643 (2000).

19) Rao, Z., Handford, P., Mayhew, M., Knott, V., Brownlee, G.G. & Stuart, D. The structure of a Ca^{2+}-binding epidermal growth factor-like domain: Its role in protein-protein interactions. Cell 82, 131-141 (1995).

20) Gong, C., Kim, Y.K., Woeller, C.F., Tang, Y. & Maquat, L.E. SMD and NMD are competitive pathways that contribute to myogenesis: effects on PAX3 and myogenin mRNAs. Genes Dev. 23, 54-66 (2009).

21) Popp, M.W. & Maquat, L.E. Attenuation of nonsense-mediated mRNA decay facilitates the response to chemotherapeutics. Nat Commun. 6, 6632 (2015).

22) Bruno, I.G., Karam, R., Huang, L., Bhardwaj, A., Lou, C.H., Shum, E.Y., Song. H.W., Corbett, M.A., Gifford, W.D., Gecz, J., Pfaff, S.L. & Wilkinson, M.F. Identification of a microRNA that activates gene expression by repressing nonsense-mediated RNA decay. Mol Cell. 42, 500-510 (2011).

23) Shum, E.Y., Jones, S.H., Shao, A., Dumdie, J., Krause, M.D., Chan, W.K., Lou, C.H., Espinoza, J.L., Song, H.W., Phan, M.H., Ramaiah, M., Huang, L., McCarrey, J.R., Peterson, K.J., De Rooij, D.G., Cook-Andersen, H. & Wilkinson, M.F. The antagonistic gene paralogs Upf3a and Upf3b govern nonsense-mediated RNA decay. Cell. 165, 382-395 (2016).

24) Gardner, L.B. Hypoxic inhibition of nonsense-mediated RNA decay regulates gene expression and the integrated stress response. Mol Cell Biol. 28, 3729-3741 (2008).

25) Wang, D., Zavadil, J., Martin, L., Parisi, F., Friedman, E., Levy, D., Harding, H., Ron, D. & Gardner, L.B. Inhibition of nonsense-mediated RNA decay by the tumor microenvironment promotes tumorigenesis. Mol Cell Biol. 31, 3670-3680 (2011).

26) Gardner, L.B. Nonsense-mediated RNA decay regulation by cellular stress: implications for tumorigenesis. Mol Cancer Res. 8, 295-308 (2010).

27) Ron, D. Translational control in the endoplasmic reticulum stress response. J Clin Invest 110, 1383-1388 (2002).

28) Karam, R., Lou, C.H., Kroeger, H., Huang, L., Lin, J.H. & Wilkinson, M.F. The unfolded protein response is shaped by the NMD pathway. EMBO Rep 16, 599-609 (2015).

29) Werno, C., Zhou, J. & Brüne, B. A23187, ionomycin and thapsigargin upregulate mRNA of HIF-1alpha via endoplasmic reticulum stress rather than a rise in intracellular calcium. J cell Physiol 215, 708-714 (2008).

30) Bakhshi, J., Weinstein, L., Poksay, K.S., Nishinaga, B., Bredesen, D.E. & Rao, R.V. Coupling endoplasmic reticulum stress to the cell death program in mouse melanoma cells: effect of curcumin. Apoptosis 13, 904-914 (2008).

31) Williams, J.A., Hou, Y., Ni, H.M. & Ding, W.X. Role of intracellular calcium in proteasome inhibitor-induced endoplasmic reticulum stress, autophagy, and cell death. Pharm Res 30, 2279-2289 (2013).

32) Rorsman, P., Braun, M. & Zhang, Q. Regulation of calcium in pancreatic α- and β-cells in health and disease. Cell Calcium 51, 300-308 (2012).

33) Tu, M.K., Levin, J.B., Hamilton, A.M. & Borodinsky, L.N. Calcium signaling in skeletal muscle development, maintenance and regeneration. Cell Calcium 59, 91-97 (2016)

34) Wittkopp, N., Huntzinger, E., Weiler, C., Saulière, J., Schmidt, S., Sonawane, M. & Izaurralde, E. Nonsense-mediated mRNA decay effectors are essential for zebrafish embryonic development and survival. Mol Cell Biol. 29, 3517-3528 (2009).

35) Tarpey, P.S., Raymond, F.L., Nguyen, L.S., Rodriguez, J., Hackett, A., Vandeleur, L., Smith, R., Shoulbridge, C., Edkins, S., Stevens, C., O'Meara, S., Tofts, C., Barthorpe, S., Buck, G., Cole, J., Halliday, K., Hills, K., Jones, D., Mironenko, T., Perry, J., Varian, J., West, S., Widaa, S., Teague, J., Dicks, E., Butler, A., Menzies, A., Richardson, D., Jenkinson, A., Shepherd, R., Raine, K., Moon, J., Luo, Y., Parnau, J., Bhat, S., Gardner, A., Corbett, M., Brooks, D., Thomas, P., Parkinson-Lawrence, E., Porteous, M., Warner, J., Sanderson, T., Pearson, P., Simensen, R., Skinner, C., Hoganson, G., Superneau, D., Wooster, R., Bobrow, M., Turner, G., Stevenson, R., Schwartz, C., Futreal, P., Srivastava, A., Stratton, M. & Gecz, J. Mutations in UPF3B, a member of the nonsense-mediated mRNA decay complex, cause syndromic and nonsyndromic mental retardation. Nat Genet. 39, 1127-1133 (2007).

36) Nguyen, L.S., Kim, H.G., Rosenfeld, J.A., Shen, Y., Gusella, J.F., Lacassie, Y., Layman, L.C., Shaffer, L.G. & Gécz, J. Contribution of copy number variants involving nonsense-mediated mRNA decay pathway genes to neuro-developmental disorders. Hum Mol Genet. 22, 1816-1825 (2013).

37) Addington, A.M., Gauthier, J., Piton, A., Hamdan, F.F., Raymond, A., Gogtay, N., Miller, R., Tossell, J., Bakalar, J., Inoff-Germain, G., Gochman, P., Long, R., Rapoport, J.L. & Rouleau, G.A. A novel frameshift mutation in UPF3B identified in brothers affected with childhood onset schizophrenia and autism spectrum disorders. Mol Psychiatry. 16, 238-239 (2011).

38) Laumonnier, F., Shoubridge, C., Antar, C., Nguyen, L.S., Van Esch, H., Kleefstra, T., Briault, S., Fryns, J.P., Hamel, B., Chelly, J., Ropers, H.H., Ronce, N., Blesson, S., Moraine, C., Gécz, J. & Raynaud, M. Mutations of the UPF3B gene, which encodes a protein widely expressed in neurons, are associated with nonspecific mental retardation with or without autism. Mol Psychiatry. 15, 767-776 (2010).

39) Jolly, L.A., Homan, C.C., Jacob, R., Barry, S. & Gécz, J. The UPF3B gene, implicated in intellectual disability, autism, ADHD and childhood onset schizophrenia regulates neural progenitor cell behaviour and neuronal outgrowth. Hum Mol Genet. 22, 4673-4687 (2013).

40) Xu, X., Zhang, L., Tong, P., Xun, G., Su, W., Xiong, Z., Zhu, T., Zheng, Y., Luo, S., Pan, Y., Xia, K. & Hu, Z. Exome sequencing identifies UPF3B as the causative gene for a Chinese non-syndrome mental retardation pedigree. Clin Genet. 83, 560–564 (2013).

41) Long, A.A., Mahapatra, C.T., Woodruff, E.A., Rohrbough, J., Leung, H.T., Shino, S., An, L., Doerge, R.W., Metzstein, M.M., Pak, W.L. & Broadie, K. The nonsense-mediated decay pathway maintains synapse architecture and synaptic vesicle cycle efficacy. J Cell Sci. 123, 3303-3315 (2010).

42) Giorgi, C., Yeo, G.W., Stone, M.E., Katz, D.B., Burge, C., Turrigiano, G. & Moore, M.J. The EJC factor eIF4AIII modulates synaptic strength and neuronal protein expression. Cell. 130, 179-191 (2007).

43) Colak, D., Ji, S.J., Porse, B.T. & Jaffrey, S.R. Regulation of axon guidance by compartmentalized nonsense-mediated mRNA decay. Cell. 153, 1252-1265 (2013).

44) Eom, T., Zhang, C., Wang, H., Lay, K., Fak, J., Noebels, J.L. & Darnell, R.B. NOVA-dependent regulation of cryptic NMD exons controls synaptic protein levels after seizure. Elife. 2, e00178 (2013).

45) Regehr, W.G,. Carey, M.R. & Best, A.R. Activity-dependent regulation of synapses by retrograde messengers. Neuron 63, 154-170 (2009).

46) Zucker, R.S. Calcium- and activity-dependent synaptic plasticity. Curr Opin Neurobiol 9, 305-313 (1999).

47) Wong, R.O. & Ghosh, A. Activity-dependent regulation of dendritic growth and patterning. Nat Rev Neurosci 3, 803-812 (2002).

48) Martinowich, K., Hattori, D., Wu, H., Fouse, S., He, F., Hu, Y., Fan, G. & Sun, Y.E. DNA methylation-related chromatin remodeling in activity-dependent BDNF gene regulation. Science 302, 890-893 (2003).

49) Giorgi, C. & Moore, M.J. The nuclear nurture and cytoplasmic nature of localized mRNPs. Semin Cell Dev Biol 18, 186-193 (2007).

50) Bramham, C.R., Worley, P.F., Moore, M.J. & Guzowski, J.F. The immediate early gene Arc/Arg3.1. Regulation, mechanisms, and function. J Neurosci 28, 11760-11767 (2008).

51) Hai, T., Wolfgang, C.D., Marsee, D.K., Allen, A.E. & Sivaprasad, U. ATF3 and stress responses. Gene Expr 7, 321-335 (1999).

52) Buganim, Y., Madar, S., Rais, Y., Pomeraniec, L., Harel, E., Solomon, H., Kalo, E., Goldstein, I., Brosh, R., Haimov, O., Avivi, C., Polak-Charcon, S., Goldfinger, N., Barshack, I. & Rotter, V. Transcriptional activity of ATF3 in the stromal compartment of tumors promotes cancer progression. Carcinogenesis 32, 1749-1757 (2011).

53) Kim, K.H., Park, B., Rhee, D.K. & Pyo, S. Acrylamide induces senescence in macrophages through a process involving ATF3, ROS, p38/JNK, and a telomerase-independent pathway. Chem Res Toxicol 28, 71-86 (2015).

54) Lu, D., Wolfgang, C.D. & Hai, T. Activating transcription factor 3, a stress-inducible gene, suppresses Ras-stimulated tumorigenesis. J Biol Chem 281, 10473-10481 (2006).

55) Yan, C., Lu, D., Hai, T. & Boyd, D.D. Activating transcription factor 3, a stress sensor, activates p53 by blocking its ubiquitination. EMBO J 24, 2425-2435 (2005).

56) Maréchal, A. & Zou, L. DNA damage sensing by the ATM and ATR kinases. Cold Spring Harb Perspect Biol 5, doi: 10.1101/cshperspect.a012716 (2013).

57) Liu, P., Cheng, H., Roberts, T.M. & Zhao, J.J. Targeting the phosphoinositide 3-kinase pathway in cancer. Nat Rev Drug Discov 8, 627-644 (2009).

58) Rodier, F., Coppe, J.P., Patil, C.K., Hoeijmakers, W.A., Munoz, D.P., Raza, S.R., Freund, A., Campeau, E., Davalos, A.R. & Campisi, J. Persistent DNA damage signaling triggers senescence-associated inflammatory cytokine secretion. Nat Cell Biol 11, 973-979 (2009).

59) Reinhardt, H.C., Aslanian, A.S., Lees, J.A. & Yaffe, M.B. p53-deficient cells rely on ATM- and ATR-mediated checkpoint signaling through the p38MAPK/MK2 pathway for survival after DNA damage. Cancer Cell 11, 175-189 (2007).

60) Reinhardt, H.C. Hasskamp, P., Schmeddling, I., Morandell, S., van Vugt, M.A., Wang, X., Linding, R., Ong, S.E., Weaver, D., Carr, S.A. & Yaffe, M.B. DNA damage activates a spatially distinct late cytoplasmic cell-cycle checkpoint network controlled by MK2-mediated RNA stabilization. Mol Cell 40, 34-49 (2010).

61) Gao, D., Bambang, I.F., Putti, T.C., Lee, Y.K., Richardson, D.R. & Zhang, D. ERp29 induces breast cancer cell growth arrest and survival through modulation of activation of p38 and upregulation of ER stress protein p58IPK. Lab Invest 92, 200-213 (2012).

62) Jiang, Q., Li, F., Shi, K., Wu, P., An, J., Yang, Y. & Xu, C. Involvement of p38 in signal switching from autophagy to apoptosis via the PERK/eIF2α/ATF4 axis in selenite-treated NB4 cells. Cell Death Dis 5, e1270 (2014).

63) Chang, B.D., Swift, M.E., Shen, M., Fang, J., Broude, E.V. & Roninson, I.B. Molecular determinants of terminal growth arrest induced in tumor cells by a chemotherapeutic agent. Proc Natl Acad Sci USA 99, 389-394 (2002).

64) Kim, K.H., Park, B., Rhee, D.K. & Pyo, S. Acrylamide induces senescence in macrophages through a process involving ATF3, ROS, p38/JNK, and a telomerase-independent pathway. Chem Res Toxicol 28, 71-86 (2015).

65) Lu, D., Wolfgang, C.D. & Hai, T. Activating transcription factor 3, a stress-inducible gene, suppresses Ras-stimulated tumorigenesis. J Biol Chem 281, 10473-10481 (2006).

66) Yan, C., Lu, D., Hai, T. & Boyd, D.D. Activating transcription factor 3, a stress sensor, activates p53 by blocking its ubiquitination. EMBO J 24, 2425-2435 (2005).

67) Davalos, A.R., Coppe, J.P., Campisi, J. & Desprez, P.Y. Senescent cells as a source of inflammatory factors for tumor progression. Cancer Metastasis Rev 29, 273-283 (2010).

68) Mendell, J.T., Sharifi, N.A., Meyers, J.L., Martinez-Murillo, F. & Dietz, H.C. Nonsense surveillance regulates expression of diverse classes of mammalian transcripts and mutes genomic noise. Nat Genet 36, 1073-1078 (2004).

69) Hanahan, D. & Weinberg, R.A. Hallmarks of cancer: the next generation. Cell 144, 646-674 (2011).

70) Zarabun, T. & Han, J. Activation and signaling of the p38 MAP kinase pathway. Cell Res 15, 11-18 (2005).

71) Baird, T.D. & Wek, R.C. Eukaryotic initiation factor 2 phosphorylation and translational control in metabolism. Adv Nutr 3, 307-321 (2012).

72) Wengrod, J., Martin, L., Wang, D., Frischmeyer-Guerrerio, P., Dietz, H.C. & Gardner, L.B. Inhibition of nonsense-mediated RNA decay activates autophagy. Mol Cell Biol. 33, 2128-2135 (2013).

73) Alspach, E., Flanagan, K.C., Luo, X., Ruhland, M.K., Huang, H., Pazolli, E., Donlin, M.J., Marsh, T., Piwnica-Worms, D., Monahan, J., Novack, D.V., McAllister, S.S. & Stewart, S.A. p38MAPK plays a cruicial role in stromal-mediated tumorigenesis. Cancer Discov 4, 716-729 (2014).

74) Alimbetov, D., Davis, T., Brook, A.J., Cox, L.S., Faragher, R.G., Nurgozhin, T., Zhumadilov, Z. & Kipling, D. Suppression of the senescence-associated secretory phenotype (SASP) in human fibroblasts using small molecule inhibitors of p38 MAP kinase and MK2. Biogerontology 17, 305-315 (2016).

75) Freund, A., Patil, C.K. & Campisi, J. p38MAPK is a novel DNA damage response-independent regulator of the senescence-associated secretory phenotype. EMBO J 30, 1536-1548 (2011).

76) Knapinska, A.M., Gratacos, F.M., Krause, C.D., Hernandez, K., Jensen, A.G., Bradley, J.J., Wu, X., Pestka, S. & Brewer, G. Chaperone Hsp27 modulates AUF1 proteolysis and AU-rich element-mediated mRNA degradation. Mol Cell Biol 31,1419-1431 (2011).

77) Nelson, J.O., Moore, K.A., Chapin, A., Hollien, J. & Metzstein, M.M. Degradation of GADD45 mRNA by nonsense-mediated decay is essential for viability. Elife 5, doi: 10.7554/elife.12876 (2016).

78) Tamura, R.E., de Vasconcellos, J.F., Sarkar, D., Libermann, T.A., Fisher, P.B. & Zerbini, L.F. GADD45 proteins: central players in tumorigenesis. Curr Mol Med 12, 634-651 (2012)

79) Schoenberg, D.R. & Maquat, L.E. Regulation of cytoplasmic mRNA decay. Nat Rev Genet 13, 246-259 (2012).